



**Design Issues for Helmet-Mounted
Display Systems for Rotary-Wing
Aviation**

By

**Clarence E. Rash
William E. McLean
John C. Mora
Melissa H. Ledford**

Aircrew Health and Performance Division

and

**Ben T. Mozo
Joseph R. Licina
B. Joseph McEntire**

Aircrew Protection Division

July 1998

Approved for public release, distribution unlimited.

**U.S. Army Aeromedical Research Laboratory
Fort Rucker, Alabama 36362-0577**

Notice

Qualified requesters

Qualified requesters may obtain copies from the Defense Technical Information Center (DTIC), Cameron Station, Alexandria, Virginia 22314. Orders will be expedited if placed through the librarian or other person designated to request documents from DTIC.

Change of address

Organizations receiving reports from the U.S. Army Aeromedical Research Laboratory on automatic mailing lists should confirm correct address when corresponding about laboratory reports.

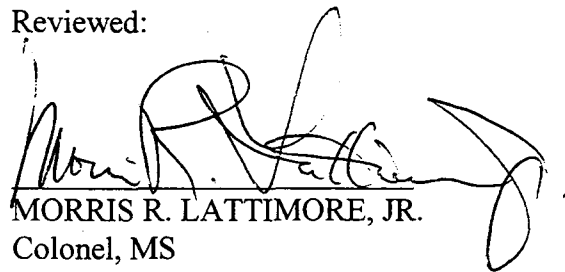
Disposition

Destroy this document when it is no longer needed. Do not return it to the originator.

Disclaimer

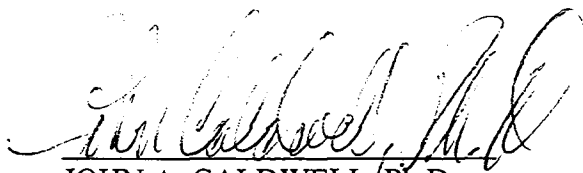
The views, opinions, and/or findings contained in this report are those of the author(s) and should not be construed as an official Department of the Army position, policy, or decision, unless so designated by other official documentation. Citation of trade names in this report does not constitute an official Department of the Army endorsement or approval of the use of such commercial items.

Reviewed:

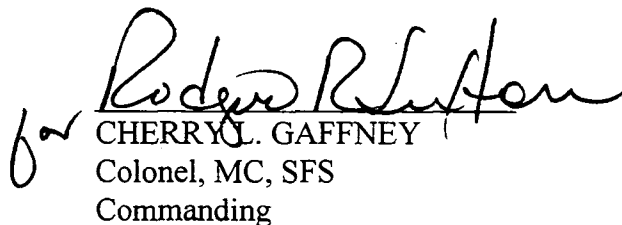


MORRIS R. LATTIMORE, JR.
Colonel, MS
Director, Aircrew Health &
Performance Division

Released for publication:



JOHN A. CALDWELL, Ph.D.
Chairman, Scientific Review
Committee



for
CHERRYL L. GAFFNEY
Colonel, MC, SFS
Commanding

REPORT DOCUMENTATION PAGE				Form Approved OMB No. 0704-0188		
1a. REPORT SECURITY CLASSIFICATION Unclassified			1b. RESTRICTIVE MARKINGS			
2a. SECURITY CLASSIFICATION AUTHORITY			3. DISTRIBUTION / AVAILABILITY OF REPORT Approved for public release, distribution unlimited			
2b. DECLASSIFICATION / DOWNGRADING SCHEDULE						
4. PERFORMING ORGANIZATION REPORT NUMBER(S) USAARL Report No. 98-32			5. MONITORING ORGANIZATION REPORT NUMBER(S)			
6a. NAME OF PERFORMING ORGANIZATION U.S. Army Aeromedical Research Laboratory		6b. OFFICE SYMBOL <i>(If applicable)</i> MCMR-UAD	7a. NAME OF MONITORING ORGANIZATION U.S. Army Medical Research and Materiel Command			
6c. ADDRESS <i>(City, State, and ZIP Code)</i> P.O. Box 620577 Fort Rucker, AL 36362-0577			7b. ADDRESS <i>(City, State, and ZIP Code)</i> Fort Detrick Frederick, MD 21702-5012			
8a. NAME OF FUNDING / SPONSORING ORGANIZATION Aircrew Integrated Systems		8b. OFFICE SYMBOL <i>(If applicable)</i> SFAE-AV-LSE	9. PROCUREMENT INSTRUMENT IDENTIFICATION NUMBER			
8c. ADDRESS <i>(City, State, and ZIP Code)</i> Building 5681 Redstone Arsenal, Alabama 35898			10. SOURCE OF FUNDING NUMBERS			
			PROGRAM ELEMENT NO. 62787A	PROJECT NO. 30162787A879	TASK NO. PB	WORK UNIT ACCESSION NO. 178
11. TITLE <i>(Include Security Classification)</i> (U)Design Issues for Helmet-Mounted Display Systems for Rotary-Wing Aviation						
12. PERSONAL AUTHOR(S) CE Rash, WE McLean, JC Mora, MH Ledford, BT Mozo, JR Licina, & BJ McEntire						
13a. TYPE OF REPORT Final		13b. TIME COVERED FROM TO		14. DATE OF REPORT <i>(Year, Month, Day)</i> 1998 July	15. PAGE COUNT 172	
16. SUPPLEMENTAL NOTATION						
17. COSATI CODES			18. SUBJECT TERMS <i>(Continue on reverse if necessary and identify by block number)</i> Air Warrior, helmet-mounted display(HMD), optical and visual performance, rotary-wing			
FIELD	GROUP	SUB-GROUP				
01	03					
09	05					
19. ABSTRACT <i>(Continue on reverse if necessary and identify by block number)</i> Since the 1970s, the trend in Army aviation has been to rely on helmet-mounted displays (HMDs) to provide the aircrew with pilotage imagery, flight information, and fire control imagery and symbology. This paper is intended to serve as both a checklist and a guide for designers of future integrated helmet and display systems for rotary-wing aircraft. In this paper: 1) salient performance parameters of such systems are identified; 2) recommendations for values of these parameters are suggested, based on past research and the opinions of subject matter experts; 3) an analysis of potential health and safety hazards is provided; 4) a human factors engineering assessment (HFEA) is provided; and 5) lessons learned from previously fielded U.S. Army HMD systems are summarized. However, this paper is not a cookbook for building an integrated helmet and display system.						
20. DISTRIBUTION / AVAILABILITY OF ABSTRACT <input checked="" type="checkbox"/> UNCLASSIFIED/UNLIMITED <input type="checkbox"/> SAME AS RPT. <input type="checkbox"/> DTIC USERS				21. ABSTRACT SECURITY CLASSIFICATION Unclassified		
22a. NAME OF RESPONSIBLE INDIVIDUAL Chief, Science Support Center			22b. TELEPHONE <i>(Include Area Code)</i> (334) 255-6907		22c. OFFICE SYMBOL MCMR-UAX-SI	

Preface

Over the past 30 years, there have been innumerable articles and books which address the design and performance of helmet- and head-mounted display systems. A large portion of this report is the result of a careful and comprehensive analysis of this literature. With the fielding of various military systems, research within this area has accelerated greatly since the mid-1980s. While this report is intended to provide a fairly comprehensive overview of this area of technology and its interface with a human observer, it is not exhaustive. Readers wishing to pursue selected topics in greater detail are directed to the following resources which served as important sources for this report:

- Melzer, J. E., and Moffitt, K. 1997. Head mounted displays: designing for the user. McGraw-Hill, New York.
- A series of proceedings on Helmet- and Head-Mounted Displays, 1989 - 1997. Vol. 1116, 1290, 1695, 2218, 2465, 2735, and 3058. SPIE - The International Society for Optical Engineering, Bellingham, WA.
- Over 125 reports and papers published since 1972 by the U.S. Army Aeromedical Research Laboratory, Fort Rucker, Alabama, dealing with helmet-mounted displays and the Army aviation environment.

Acknowledgments

The authors would like to thank the following individuals for their assistance in the preparation of this paper: Jim Brindle, LME, Warminster, PA; Vic Arnold and Bob Whitcraft, Honeywell, Inc., Minneapolis, MN; Tom Mueller, Camber Corporation, St. Louis, MO; Steve Martin, UES, Fort Rucker; Raj Kausik, Sikorsky, Stratford, CT; Brian Tsou, Air Force Research Laboratory, Wright-Patterson AFB, OH; and Lauren Haworth, Aeroflightdynamics Directorate, Moffett Field, CA.

Table of contents

	<u>Page</u>
Introduction	1
Helmet-Mounted Displays	6
Overview	6
Types	8
Fielded systems	16
Image sources	16
Cathode ray tubes	17
Flat panel technologies	21
Liquid crystal	21
Electroluminescence	23
Light emitting diode	23
Field emission	23
Vacuum fluorescent	24
Plasma	24
Electrochromism	24
Electrophoresis	25
Digital micromirror	25
Lasers	28
Optical designs	28
Determining field-of-view	28
Optical aberrations	30
Chromatic aberration	30
Spherical aberration	31
Distortion	31
Field curvature	31
Types	32
Refractive	32
Catadioptric	32
On- and off-axis designs	36
Pupil and nonpupil forming	39
Partially silvered, dichroic, and holographic combiners	41
Visual coupling	42
Tracking systems	42
Head trackers	43
Eye trackers	45
Alternative tracking technology	46
System lag (delay)	46
Roll compensation	49

Table of contents (continued)

	<u>Page</u>
Vibration	49
Sensor switching	50
Design Issues	52
Optical performance	52
Image quality	52
Contrast	53
Resolution	65
Modulation transfer function (MTF)	67
Distortion	73
Luminous uniformity	75
Field-of-view	75
Visual field	77
Magnification	78
See-through luminous/spectral transmittance	80
Exit pupil	80
Extraneous reflections	81
Monocular/biocular/binocular considerations	82
Monocular issues	82
Biocular/binocular issues	83
Biocular tolerances	84
Partial binocular overlap issues	85
Monochrome vs. color	87
Visual performance	89
Visual acuity	89
Contrast sensitivity	90
Depth perception and stereopsis	93
Visual illusions and spatial disorientation	95
Visual problems	96
Helmet performance	98
Biodynamics	98
Mass and CM	98
Impact attenuation	106
Frangibility	111
Individual fitting systems	112
Retention	116
Stability	117
Visors and visor assemblies	118

Table of contents (continued)

	<u>Page</u>
Acoustical	119
Sound attenuation	123
Speech intelligibility (SI)	124
Operational assessment	125
Weight (mass) of helmet/communications	127
3-D audio	129
Human factors engineering (HFE) issues	129
Manpower and Personnel Integration (MANPRINT) program	129
Manpower and personnel requirements	129
Maintenance	130
Training	130
System safety assessment	131
Health hazard assessment	131
User adjustments	132
Mechanical adjustments	132
Electronic adjustments	133
Optical adjustments	134
Anthropometry	135
Fitting	137
Egress	138
Equipment compatibility	138
Test and evaluation	141
Laboratory	142
In-flight	142
Summary and recommendations	144
References	147
Appendix	171

Table of contents (continued)

List of figures

	<u>Page</u>
1. The AN/AVS-6 Aviator's Night Vision Imaging System (ANVIS)	2
2. The AH-64 Integrated Helmet and Display Sighting System (IHADSS)	2
3. The RAH-66 Helmet Integrated Display Sight System (HIDSS)	3
4. The HIDSS relay optics	3
5. Block diagram of basic Army aviation HMD	6
6. Ishikawa diagram for physical characteristic approach to HMD design	9
7. Ishikawa diagram for performance approach to HMD design	10
8. Partially overlapped FOV with a central binocular region and two monocular regions	12
9. Visual interpretation of the divergent display mode	13
10. Visual interpretation of the convergent display mode	13
11. Visor projection HMD design approach	15
12. Basic diagram of retinal scanning display	15
13. The IHADSS Integrated Helmet Unit (IHU) and Helmet Display Unit (HDU)	17
14. The human eye's photopic and scotopic response	20
15. Diagram of flat panel technologies	21
16. HMD eyepieces: a) Direct view, no see-through, NVG type eyepiece and b) refractive see-through combiner at 45°	33
17. HMD eyepieces: a) Refractive (IHADSS), b) refractive prism combiner, c) catadioptric, and d) catadioptric with prism combiner	34
18. FOV versus eyepiece diameter for different designs	37

Table of contents (continued)
List of figures (continued)

	<u>Page</u>
19. Comparisons between refractive and catadioptric HMDs with and without prism combiners	37
20. Ray trace of 50° x 60° tilted cat ocular	38
21. Optically induced distortion from tilted cat, off-axis HMD design	38
22. MONARC with rotationally symmetrical lens system (folded catadioptric)	39
23. Reflective visor HMD: a) side view and b) top view	40
24. Ray trace of exit pupil formed by a) the center rays and b) the marginal rays for a pupil forming optical device	41
25. Typical magnetic tracker	44
26. AH-64 EO tracker	44
27. High resolution inset in HMD FOV	46
28. Latencies in HMD systems	48
29. Luminance patterns for several combinations of target and background luminance values .	55
30. A cyclical luminance pattern	56
31. Typical gamma curve	57
32. Discrete luminance values of the 16 grey levels of a graphic LCD display	59
33. Typical catadioptric HMD optical design	63
34. Red, green, and blue color triad pixels	66
35. Typical MTF curve	68
36. MTFA	69

Table of contents (continued)
List of figures (continued)

	<u>Page</u>
37. Representative model output for a CRT display using P28 phosphor (70-msec persistence) and having a vertical frame period of 33 msec	71
38. MTF curves for P1 phosphor	72
39. MTF curves for P43 phosphor	72
40. Percent ANVIS distortion as a function of angular position	74
41. Human visual system's binocular FOV	76
42. Binocular visual field for the HIDSS PRU only	79
43. HIDSS ARU monocular visual field (left eye)	79
44. Luning in partial overlap HMDs	87
45. Probability of detecting a small round target luminance against an uniform background luminance	91
46. The relationship between threshold contrast and background luminance for various sized targets	92
47. The relationship between threshold contrast and background luminance for various viewing times	92
48. The human contrast sensitivity function	93
49. Parameters required to fully define helmet system mass properties	100
50. Head anatomical coordinate system	101
51. Engineering descriptions of neck loading	102
52. Frequency distribution of spinal fractures in class A and B survivable crashes by vertebral level	103
53. Vertical center of mass placement as a function of head-supported mass	105

Table of contents (continued)
List of figures (continued)

	<u>Page</u>
54. Allowable head-supported mass as a function of longitudinal center of mass placement .	106
55. Acceleration pulse shapes	109
56. Typical acceleration time history trace	109
57. Theoretical stopping distances for various G levels	110
58. Vector limits for HMD breakaway force	112
59. Sling suspension in SPH-4 helmet	115
60. View of a 4-ply TPL™ removed from the foam liner and cloth cover	115
61. USAARL modified yoke harness, used in the SPH-4B, and the HGU-56/P retention system	117
62. Noise level distribution of U.S. Army helicopters with noise exposure levels for aviators while wearing the SPH-4, HGU-56/P and SPH-4B with yellow foam earplugs .	120
63. Communications earplug (CEP) (top) and attached to HGU-56/P helmet (bottom)	121
64. Sound attenuation of the HGU-56/P helmet worn alone, with spectacles and with CB mask	122
65. Noise level distribution of U.S. Army helicopters with noise exposure levels for aviators while wearing the HGU-56/P alone, with spectacles and the CB mask	124
66. Speech intelligibility verses speech level in UH-60 noise for three devices	126
67. Speech intelligibility improvement for hearing impaired aviators when compared with normal aviators at 95% confidence interval using SPH-4.	126
68. Percent of weight of components in the prototype Comanche helmet	128
69. A frontal view of an Apache aviator wearing a full ALSE ensemble with M-43 mask . . .	139
70. An aviator in the Apache front seat with the IHADSS HDU attached	139

Table of contents (continued)

List of tables

	<u>Page</u>
1. Summary of current rotary-wing HMD programs	5
2. HMD subsystem physical characteristics	8
3. HMD performance figures-of-merit	11
4. Comparison of operating characteristics of miniature CRT tubes	18
5. Phosphor characteristics	19
6. FP technology advantages and disadvantages	26
7. CRT display system FOMs	51
8. FPD FOMs	53
9. Shades of grey (SOG) and corresponding contrast ratios	58
10. Michelson contrast, contrast ratio, and SOG values for an HMD design	64
11. Summary of expressions for resolution in discrete displays	67
12. Summary of binocular optical tolerance limits	85
13. Apache aviator reports of visual complaints during and after flight	97
14. Impact attenuation maximum G thresholds	107
15. Helmet fitting systems	114
16. Results of midpoint and final questionnaire assessments (15 subjects)	127
17. Mass of the CEP and helmet communications components	128
18. An order of precedence for satisfying system safety concerns	131
19. Head anthropometry parameters	136

Table of contents (continued)

List of tables

	<u>Page</u>
20. Recommended FPD image source evaluation program	142
21. Recommended integrated HMD test parameters	143
22. Recommended in-flight HFEA areas	144

Introduction

Since the 1970s, the trend in Army aviation has been to rely increasingly on helmet-mounted display (HMD) devices or systems to provide the aircrew with pilotage imagery, flight information, and fire control imagery and symbology. The first such system was the AN/PVS-5 series night vision goggle (NVG), circa 1973. This system was the aviation version of the SU-50, the earliest HMD used by the infantry (McLean et al., 1997). It consisted of 2nd generation image intensification (I²) devices “hung” on the existing flight helmet. By 1989, the AN/PVS-5 had been replaced by the AN/AVS-6 Aviator’s Night Vision Imaging System (ANVIS) (Figure 1), the first I² HMD designed specifically for Army aviation use. ANVIS is a passive, binocular, 3rd generation I² system and has improved sensitivity and resolution over the 2nd generation I² tubes. ANVIS is attached to current Army helmets, e.g., SPH-4B and HGU-56/P, using specially designed mounting brackets. The recent addition of symbology to the standard ANVIS has produced the AN/AVS-7 head-up display (HUD) (Nicholson and Troxel, 1996). A history of I² HMDs in Army aviation is given by McLean et al. (1997). [Note: There is some disagreement among leaders in the field of HMD research and development as to whether or not ANVIS and its predecessor, the AN/PVS -5 NVG, are “true” HMDs. However, for the purpose of this paper, the authors assert that these systems do meet the basic definition of an HMD and do perform the same functions as more prototypical HMDs.]

When the AH-64 Apache attack helicopter was fielded in the early 1980s, the head-mounted I² sensors in NVGs were replaced as the imagery source by a forward-looking infrared (FLIR) sensor, the Pilot’s Night Vision System (PNVS), mounted on the nose of the aircraft. Imagery from this sensor is displayed on a miniature 1-inch diameter cathode ray tube (CRT) and optically relayed to the eye. This system is known as the Integrated Helmet and Display Sighting System (IHADSS) (Figure 2). It is a monocular system, presenting imagery to the right eye only. The IHADSS was the first integrated HMD, where the helmet, head tracker, and display were designed as a single system. The success of IHADSS in Army aviation has greatly influenced and contributed to the proliferation of HMD programs (Rash and Martin, 1988).

Currently, the Army is developing the RAH-66 Comanche reconnaissance helicopter. This aircraft will utilize a partially overlapped biocular HMD, known as the Helmet Integrated Display Sight System (HIDSS) (Figure 3). It consists of an aircraft retained unit (ARU) and a pilot retained unit (PRU). The PRU is the basic helmet with visor assembly. The ARU is a front piece consisting of two image sources and optical relays attached to a mounting bracket (Figure 4). The HIDSS development and validation phase design, which uses two miniature, 1-inch, CRTs as image sources, provides a 30° (V) by 52° (H) field-of-view (FOV) with a 17° overlap region. However, miniature displays based on flat panel (FP) technologies [e.g., liquid crystal (LC) and electroluminescence (EL)] will very likely replace the CRTs in subsequent program phases.

The trend for increasing reliance on HMDs in aviation, as well as in other sectors of the Army, will continue. The U.S. Army Night Vision and Electronic Sensor Directorate (NVESD), Fort Belvoir, Virginia, is developing an HMD under the Advanced Helicopter Pilotage (AHP) program (Perconti, 1997). The AHP HMD is biocular, providing the same imagery to each eye. Its two optical channels each provide a 40° monocular circular FOV. When mounted on a helmet, the system provides a 30° (V) x 50° (H) total FOV with a 30° binocular overlap region.

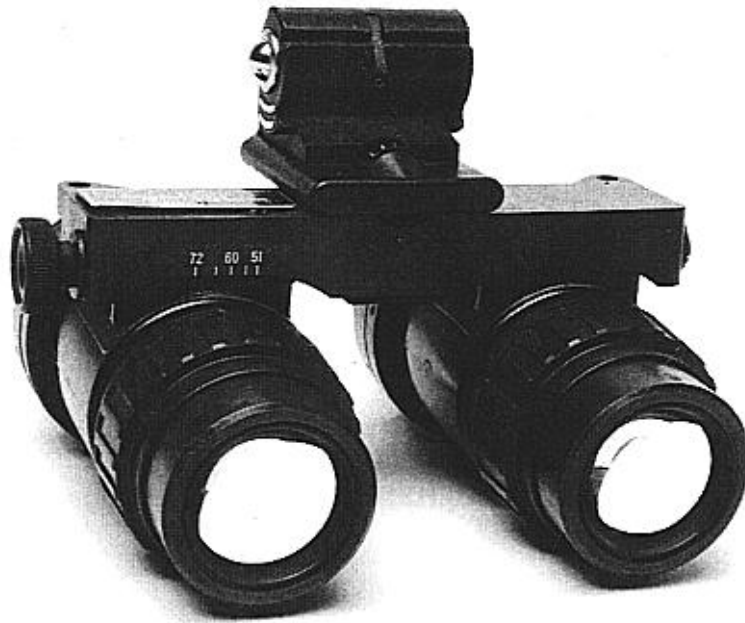


Figure 1. The AN/AVS-6 Aviator's Night Vision Imaging System (ANVIS).



Figure 2. The AH-64 Integrated Helmet and Display Sighting System (IHADSS).



Figure 3. The RAH-66 Helmet Integrated Display Sight System (HIDSS).

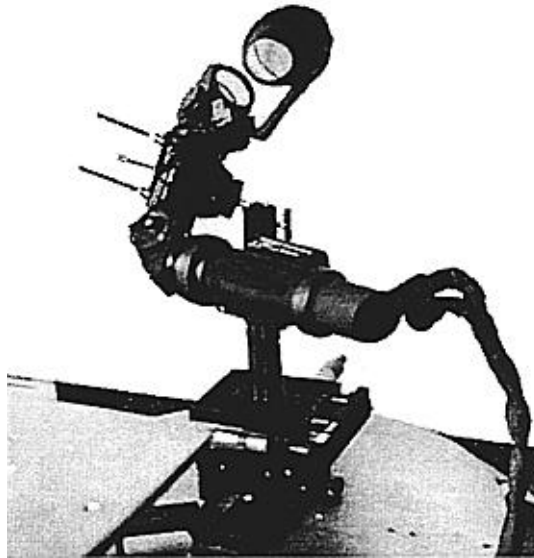


Figure 4. The HIDSS relay optics.

The United States and the United Kingdom of Great Britain and Northern Ireland have collaborated on the Covert Night/Day Operations for Rotorcraft (CONDOR) program. CONDOR is a research platform for demonstrating advanced visionics concepts and includes a variable FOV HMD based on high resolution miniature active matrix liquid crystal displays (AMLCDs) (Kanahele and Buckanin, 1996).

The U.S. Army and the Defense Advanced Research Projects Agency (DARPA) have funded a number of additional aviation HMD concepts based on FP technologies (Girolamo, Rash, and Gilroy, 1997). These include the Miniature Flat Panel for Aviation (MFP/A) program which has as its goal the investigation of using miniature FP technology displays in the development of an HMD for use in rotary-wing aircraft and the Aircrew Integrated Helmet System (AIHS) Comanche Compatibility program which has as its goal the development of an HMD design using the Helmet Gear Unit No. 56/P (HGU-56/P) flight helmet as the platform. A partial summary of current rotary-wing HMD programs (both fielded and under development) by Belt et al. (1997) is provided in Table 1. An excellent attempt to develop a taxonomy and philosophy of HMD systems has been made by Brindle, Marano-Goyco, and Tihansky (1995).

This paper is intended to serve as both a checklist and a guide for designers of such future integrated helmet and display systems for rotary-wing aircraft. In this paper: 1) salient performance parameters of such systems are identified; 2) recommendations for values of these parameters are suggested, based on past research and the opinions of subject matter experts; 3) an analysis of potential health and safety hazards is provided; 4) a human factors engineering assessment (HFEA) is provided; and 5) lessons learned from previously fielded U.S. Army HMD systems are summarized. However, this paper is not a cookbook for building an integrated helmet and display system. The design of such a system is strongly dependent on its purpose, user requirements, and the environment within which it is intended to operate.

For Army aviation, the purpose of the HMD is to assist the aviator in the performance of various missions. Each type of mission requires the aviator to perform a certain number of complex tasks. The performance of these tasks is impacted by aviator skills and capabilities (user properties), and by the characteristics of the HMD. The operational environment may include high speed, low level flight, during low illumination and/or adverse weather conditions. Eggleston (1997) developed a model which maps aviator tasks (e.g., navigation, unmasking maneuver, etc.), user properties (e.g., perception, organization, etc.), and HMD characteristics (e.g., FOV, resolution, etc.) for specific missions and mission elements. This type of analysis is essential in ensuring an optimal HMD design which meets the needs of the aviator and the mission.

In summary, the design specifications for any system must be guided by these criteria convolved with hardware limitations, human performance strengths and weaknesses, and good human factors engineering practices. [Note: This paper does not tackle the complex, and still unresolved, issue of HMD imagery information content, which includes the selection of types and quantity of data to be presented, the symbols used, or their placement within the displayed imagery. Interested readers may find information in these areas in Craig, Marshall, and Jordan (1997), Drewery, Davy, and Dudfield (1997), and Murray (1997).]

Table 1.
Summary of current rotary-wing HMD programs.

Highlights	ANVIS	IHADSS	IHDSS	MFP/A	AVS/CONDOR	AIHS-H	AIHS-K
Vehicle	Rotorcraft	AH-64 Apache ⁽¹⁾	RAH-66 Comanche	Rotorcraft	Rotorcraft	RAH-66 Comanche	RAH-66 Comanche
Program Type	Production	Production	EMD	R&D	R&D	P ³ I	P ³ I
Mass	2.2 kg ⁽²⁾	1.8 kg	2.6 kg	---	---	---	---
CM longit.	30 mm ⁽²⁾	20 mm	34 mm	---	---	---	---
CM vertical	37 mm ⁽²⁾	27 mm	48.4 mm	---	---	---	---
Helmet	All	Custom	Custom	HGU-56P	HGU-56P	HGU-56P	HGU-56P
LLLTV	---	ANVIS	I ²	---	---	ANVIS	ANVIS
FLIR	---	1 st gen	2 nd gen	2 nd gen	2 nd gen	2 nd gen	2 nd gen
Channels	Binocular	Monocular	Biocular	Biocular	Biocular	Biocular	Biocular
FOV	40°	40° x 30°	52° x 30°	50° x 30°	60°-100° x 50°	52° x 30°	52° x 30°
Overlap	40°	N/A	18°	30°	20 to 50°	30°	30°
Exit pupil	---	10 mm	>15 mm	>15 mm	15 mm	>15 mm	>15 mm
Eye relief	15-30 mm	40 mm	>25 mm	>25 mm	>25 mm	>25 mm	>25 mm
Eye clearance	15-30 mm	13 mm	>22 mm	>22 mm	>22 mm	>22 mm	>22 mm
Display	18-mm I ² P22 phosphor	1" CRT P43 phosphor	1" CRT P53 phosphor	1280x1024 AMEL	1280x1024 AMLCD	1280x1024 Flat Panel	1280x1024 Flat Panel
Color	Monochrome	Monochrome	Monochrome	Monochrome	Color	Monochrome	Monochrome
TV lines/pixels	~2000-3000	809	960	960/809/525	960	960	960
Roll compensation	Yes	No	Yes	No	No	Yes	Yes
Electronics	Analog	Analog	Analog	Digital	Digital	Digital	Digital
Modules	---	LRU	SEM-E	6U VME	9U VME	SEM-E	SEM-E
Latency	1.3 msec ⁽³⁾	≤ 17 msec	≤ 66 msec	---	21 msec	≤ 42 msec	≤ 42 msec
Egress	Breakaway	Breakaway	QDC	---	---	QDC	QDC
Sponsor	NVESD	U.S. Army AAH PMO	U.S. Army Comanche PMO	U.S. Army Natick RDE	U.S. Army AATD	U.S. Army ACIS PMO	U.S. Army ACIS PMO
Company	Multiple	Honeywell	Kaiser	Honeywell	Hughes	Honeywell	Kaiser
Start/Duration	1980- present	6/85-present	1/93-present	3/94-present	1/94-present	8/95-present	8/95-present
Progress	25,000 units	1300 units ⁽⁴⁾	3 units	1 unit	---	Passive HMD	Passive HMD

MFP/A- Miniature Flat Panel for Aviation; AVS- Advanced Visionics System; AIHS-H- Aircrew Integrated Helmet System- Honeywell Inc.; AIHS-K- Aircrew Integrated Helmet System-Kaiser Electronics; EMD- Engineering Manufacturing and Development; P³I- Pre-planned Product Improvement; LLLTV- Low Light Level Television; LRU- Line Replaceable Unit; SEM-E- Standard Electronic Module, Format E; VME- Virtual Module European; QDC- Quick Disconnect; AAH- Advanced Attack Helicopter; PMO- Project Manager's Office; AATD- Aviation Applied Technology Directorate; ACIS- Aircrew Integrated Systems; NVESD-Night Vision and Electronic Sensor Directorate.

Notes: (1) Also used on Italy's A-129 Agusta helicopter.

(2) Based on SPH-4B w/ANVIS and battery pack.

(3) Based on phosphor persistence; No measurable electronic delay.

(4) Quantities: AH-64 (807 units), A-129 (87 units), spares (> 400 units) with two HMD's per unit.

Helmet-Mounted Displays

Overview

Melzer and Moffitt (1997) describe an HMD as minimally consisting of “an image source and collimating optics in a head mount.” For the purpose of this paper, we expand this description to include a visual coupling system, which performs the function of slaving head and/or eye positions and motions to one or more aircraft systems. Figure 5 presents the basic Army aviation HMD as a block diagram in which there are four major elements: image source (and associated drive electronics), display optics, helmet, and head/eye tracker. The image source is a display device upon which sensor imagery is produced. These sources typically have been miniature CRTs or I² tubes. Other miniature displays based on FP technologies rapidly are becoming alternate choices. The display optics are used to couple the display imagery to the eye. The optics generally magnify and focus the display image. The helmet, while providing the protection for which it was designed originally, serves additionally as a platform for mounting the image source and display optics. The tracking system couples the head/eye line of sight with that of the pilotage sensor(s) (when mounted off the head) and weapons.

The overall goal of HMDs in Army rotary-wing aviation is to effectively interface the aviator/crewmember with the aircraft and its associated systems, which allows the aviator to acquire and maintain situational awareness (state of knowledge or mental model of the surroundings). The HMD performs one or more of the following functions: (a) To display pilotage or gunnery imagery from I² or FLIR sensors, (b) To present strategical, tactical, and operational data on demand, serving as an information management system, and (c) To sense head/eye position and motion for the purpose of designating targets, directing sensors and weapons, and activating switches (Buchroeder, 1987). In general, well designed HMDs should enhance aviator situational awareness and increase mission effectiveness (Arbak, 1989).

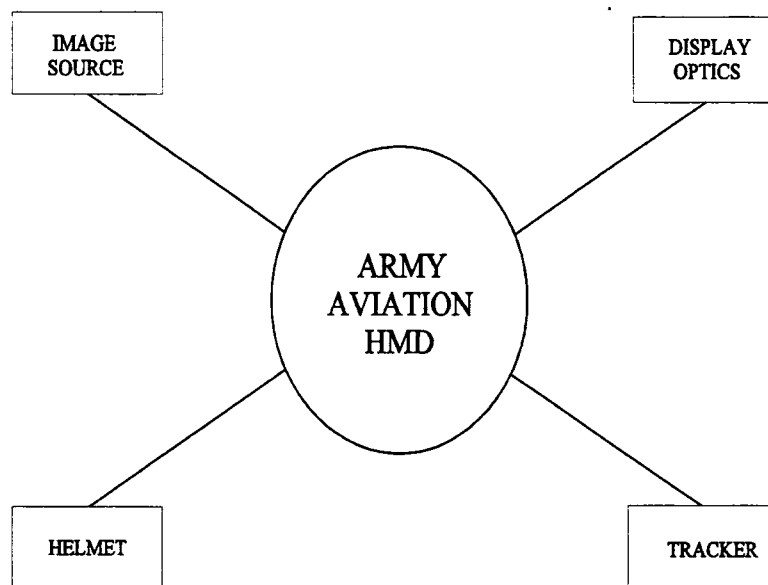


Figure 5. Block diagram of basic Army aviation HMD.

The modern HMD is not a new concept. Its invention has been attributed to Gordon Nash, a British researcher, who explored alternative methods of providing additional information to the aviator in the 1950's (Adam, 1995). Marshall (1989) traces the concept of using the helmet as a platform for a fire control (weapon aiming) back to 1916, when Albert Bacon Pratt developed and received patents for an integrated gun helmet, perhaps the very first helmet-mounted sight (HMS). This concept was revisited in the Helmet Sight System (HSS) used in the U.S. Army's AH-1 Cobra attack helicopter in the 1970's. Task and Kocian (1995) cite the U.S. Navy's Visual Target Acquisition System (VTAS), developed in the 1960's, as the first fully operational visually coupled sighting system. [However, the system was abandoned due to lack of sufficient missile fire control technology.] For Army aviation, the AN/PVS-5 NVG was the first pilotage imagery HMD (first tested in 1973), and the IHADSS was the first integrated HMD (fielded since 1985).

Simply, an HMD projects head-directed sensor imagery and/or fire control symbology onto the eye, usually superimposed over a see-through view of the outside world. As such, HMDs offer the potential for enhanced situation awareness and effectiveness. However, their design and implementation are not without problems and limitations. Virtually every HMD, concept or fielded system, suffers from one or more deficiencies, such as high head-supported weight, center of mass (CM) off-sets, inadequate exit pupil, limited FOV, low brightness, low contrast, limited resolution, fitting problems, and low user acceptance (Cameron, 1997; Naor, Arnon, and Avnur, 1987). Of the potential problems with HMDs, none are more troublesome than those associated with the interfacing of the system with the human user. The wide variation in head and facial anthropometry makes this a formidable task, requiring HMD designs rich in flexibility and user adjustments.

An HMD designer must develop a system which is capable of satisfying a large number of widely different and often conflicting requirements in a single system. Such design goals include but are not limited to the following (Lewis, 1979):

- Maximum impact protection
- Maximum acoustical protection
- Maximum speech intelligibility
- Minimum head supported weight
- Minimum bulk
- Minimum CM offset
- Optimum head aiming/tracking accuracy
- Maximum comfort and user acceptance
- Maximum freedom of movement
- Wide FOV
- Minimum obstructions in visual field
- Full color imagery
- Maximum resolution
- High brightness and contrast
- No induced sensory illusions
- Hazard free
- Maximum crashworthiness
- 24-hour, all weather operation
- Minimum training requirements
- Low maintenance
- Low design cost and minimum schedule

From this abridged list of requirements, it becomes apparent that the design of an HMD requires the careful consideration of a multitude of physical parameters and performance factors. This results in two different design approaches. The first emphasizes careful analysis and control of the individual subsystems' physical characteristics. The identified subsystems are those in the basic description given earlier: image source, display optics, helmet, and tracking system. This approach is presented in Table 2 and as an Ishikawa (Fishbone) diagram (Figure 6). The second approach, which focuses on performance, is presented in Table 3 and Figure 7. In the latter approach, which allows for subsystem interaction, physical characteristics are replaced by performance figures of merit (FOMs). These FOMs are grouped into natural performance categories: optical system, visual, helmet (with tracking system), and human factors engineering. As expected, there can be considerable overlap both between and within the two approaches. The performance approach (Table 3) is adopted in this paper.

Table 2.
HMD subsystem physical characteristics.

Image source	Display optics	Helmet	Tracking system
Resolution	Luminous efficiency	Weight (mass)	Accuracy
Luminance range	Spectral transmittance	Center of mass	Resolution
Contrast range	Optical eye relief	Visor optical characteristics	Update rate
Chromaticity range	Prismatic deviation	Impact attenuation	Motion box size
Image size	Residual refractive power	Shell tear resistance	Jitter
Static and dynamic modulation transfer functions (MTFs)	Aberrations (Spherical, astigmatic, chromatic)	Fitting system characteristics	
Distortion	Exit pupil size and shape	Anthropometric fitting range	
Weight and size	Distortion	Earphone/earcup characteristics	
Luminance uniformity	Weight and size	HMD breakaway force	
	Field-of-view	Microphone characteristics	
	MTF		
	Extraneous reflections		
	Luminance uniformity		

Types

There are several classification schemes which can be applied to HMDs. These include imagery type, imagery presentation mode, and optical design approach. Strictly speaking, HMDs can produce either real or virtual images. Images are the regions of concentration of light rays originating from the source, called the object (Levi, 1968). When these rays actually intersect, the resulting image is *real*; when only the extensions of the rays intersect, the resulting image is *virtual*. More practically, the image formed by an optical system, e.g., an HMD, is a real image if it is formed outside the optical system, where it falls onto a surface such as a screen or roll of film, and is a virtual image if it is formed within the system, where it is viewed by looking into one end of the system. Examples of real images include those produced by slide and movie

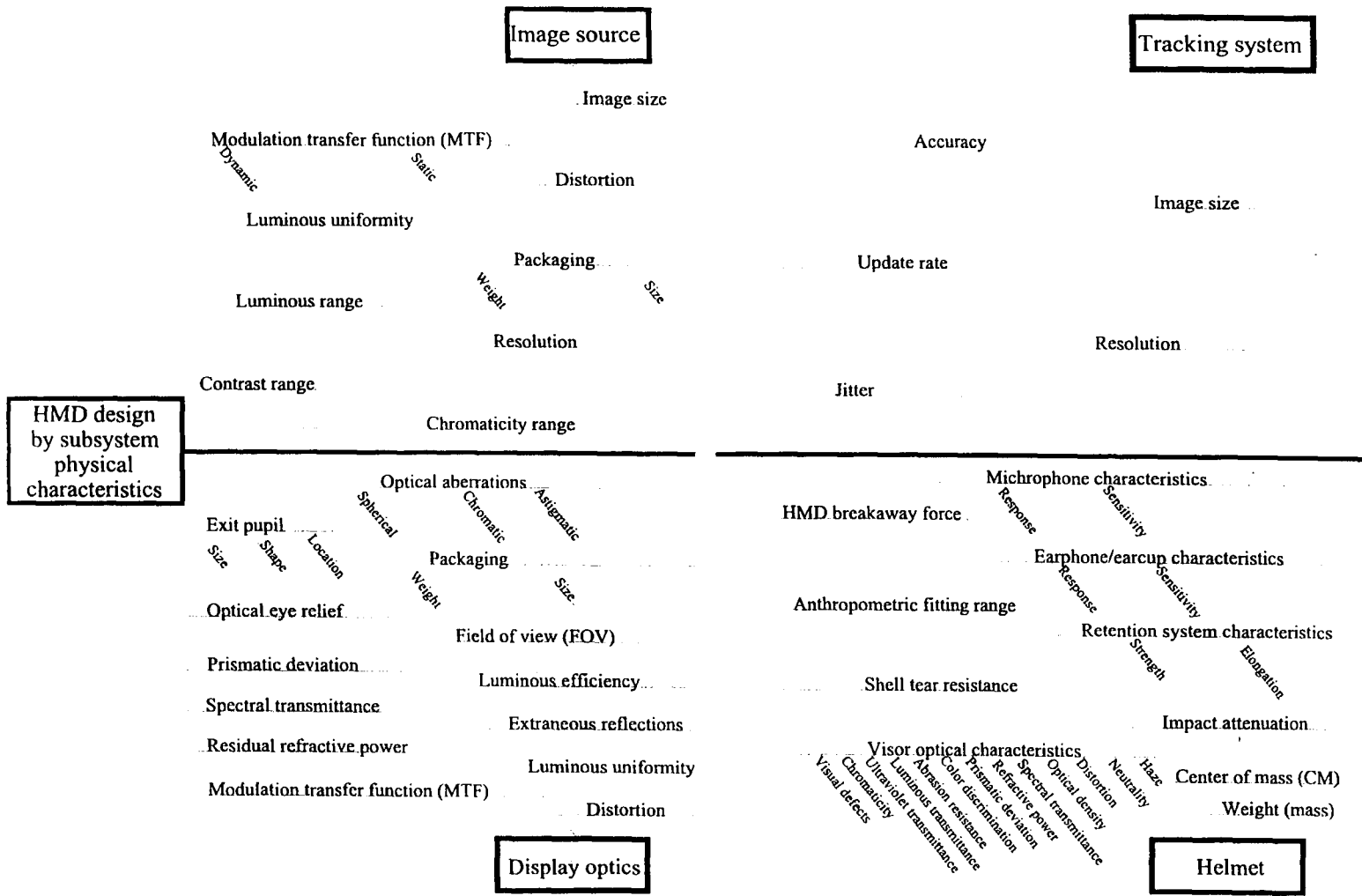


Figure 6. Ishikawa diagram for physical characteristic approach to HMD design.

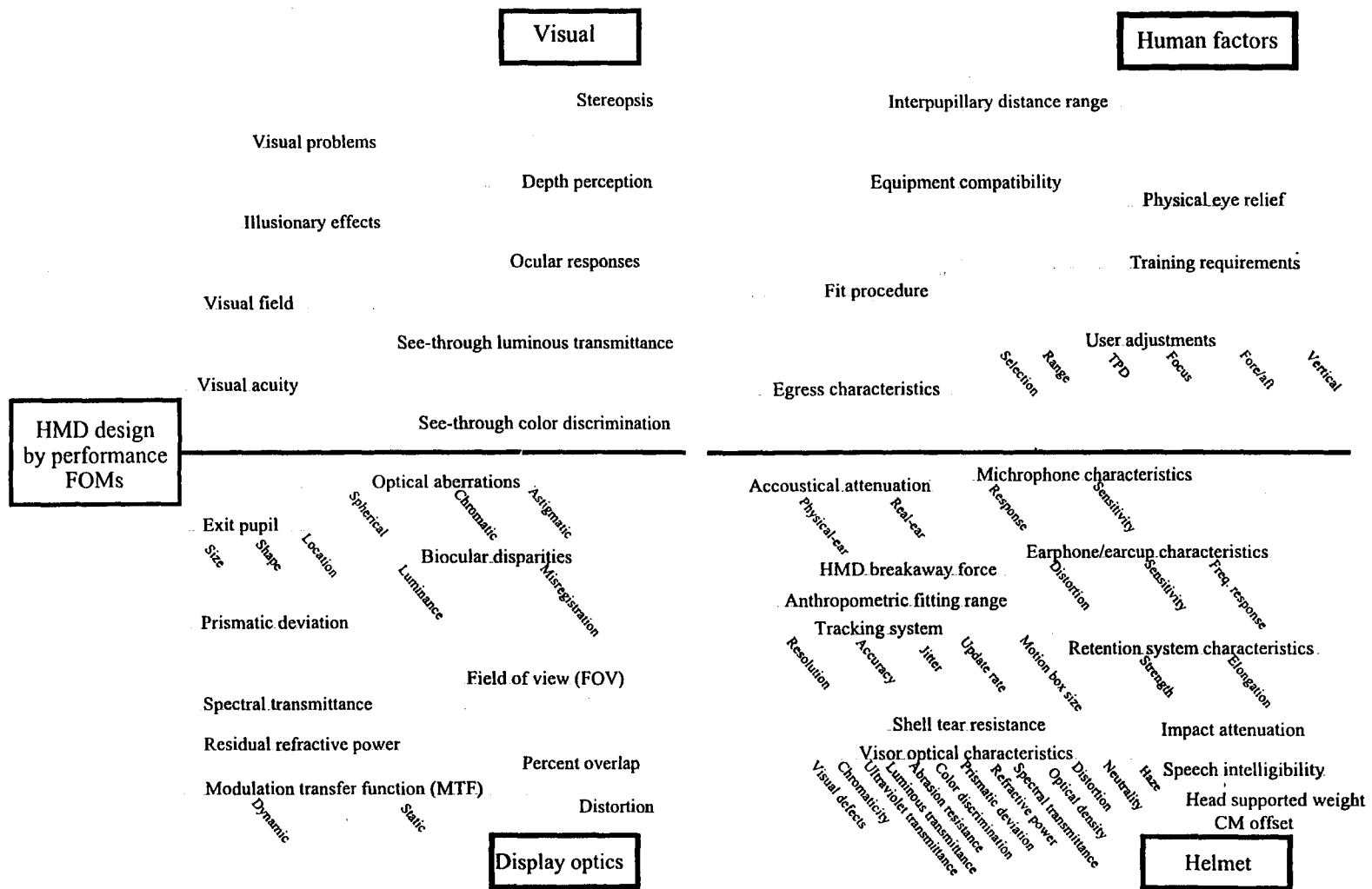


Figure 7. Ishikawa diagram for performance approach to HMD design.

Table 3.
HMD performance figures-of-merit.
 (Rash et al., 1996a; Task and Verona, 1976)

Prismatic deviation	Visual acuity	Head supported weight	Interpupillary distance range
Residual refractive power	Visual field	CM offset	Physical eye relief
FOV	See-through luminous transmittance	Impact attenuation	User adjustments-selection and range
Percent overlap	See-through color discrimination	Shell tear resistance	Equipment compatibility
Extraneous reflections	Ocular responses	Fitting system characteristics	Training requirements
Biocular channel disparities and misregistration	Depth perception and stereopsis	HMD breakaway force	Egress characteristics
Chromatic aberrations	Illusionary effects	Anthropometric fitting range	Fit procedure
Exit pupil size and shape	Visual problems	Visor optical characteristics	
Image overlap		Tracking accuracy	
Static and dynamic MTFs		Tracking resolution	
Distortion		Tracking system update rate	
Spherical/astigmatic aberrations		Tracking system motion box size	
		Tracking system jitter	
		Earphone/earcup characteristics	
		Real-ear attenuation	
		Physical-ear attenuation	
		Speech intelligibility	

projectors, captured on film by a camera, and formed on the retina by the direct viewing of an object. Examples of virtual images include those produced by eyeglasses, telescopes, and microscopes (Kingslake,1983). However, real image HMD designs are rare. They would be direct view systems requiring the image source (e.g., a miniature LC display) to be located in front of the eye(s) at the typical reading distance of the eye. All fielded aviation HMDs are virtual image systems.

Virtual image displays offer several advantages (Seeman et al., 1992). At near optical infinity, virtual images theoretically allow the eye to relax (reducing visual fatigue) and provide easier accommodation for older aviators. By providing a virtual image, a greater number of aviators can use the system without the use of corrective optics (but not all) (Seeman et al., 1992). The collimated image also reduces effects of vibration producing retinal blur.

Shontz and Trumm (1969) categorize HMDs based on the mode by which the imagery is presented to the eyes. They define three categories: One eye, occluded; one eye, see-through; and two eye, see-through. In the one eye, occluded type, imagery is presented to only one eye, to which the real world is blocked, with the remaining eye viewing only the real world. The one eye, see-through type, while still providing imagery to one eye, allows both eyes to view the real

world. [Note: The optics in front of the imagery eye will filter the real world to a lesser or greater degree.] The AH-64 IHADSS is an example of this type. In the two eye, see-through type, imagery is presented to both eyes, and the real world also is viewed by both eyes. The RAH-66 HIDSS is an example of this type.

Another classification scheme, which parallels the three types described above, uses the terms monocular, biocular, and binocular. These terms refer to the presentation of the imagery by the HMD. For this paper, monocular means the HMD imagery is viewed by a single eye; biocular means the HMD provides two visual images from a single sensor, i.e., each eye sees exactly the same image from the same perspective; binocular means the HMD provides two visual images from two sensors displaced in space. [Note: A binocular HMD can use a single sensor, if the sensor is somehow manipulated to provide two different perspectives of the object scene.] A biocular HMD may use one or two image sources, but must have two optical channels. A binocular HMD must have separate image sources (one for each eye) and two optical channels.

Typically, binocular HMDs fully overlap the images in each eye. In such HMDs, the FOV is limited to the FOV of the display optics. However, in order to achieve larger FOVs, recent HMD designs partially overlap the images from two optical channels. This results in a partially overlapped FOV consisting of a central binocular region (seen by both eyes) and two monocular flanking regions (each seen by one eye only) (Figure 8). Such overlapping schemes can be implemented by either divergent or convergent overlap designs. In a divergent design, the right eye sees the central overlap region and the right monocular region, and the left eye sees the central overlap region and the left monocular region (Figure 9). In a convergent design, the right eye sees the central overlap region and the left monocular region, and the left eye sees the central overlap region and the right monocular region (Figure 10). IHADSS is an example of a monocular HMD; ANVIS is an example of a 100% overlapped binocular HMD; and the CRT-based HIDSS design is divergent and has an overlap of approximately 30% (based on a 17° overlap region within the 52° horizontal FOV).

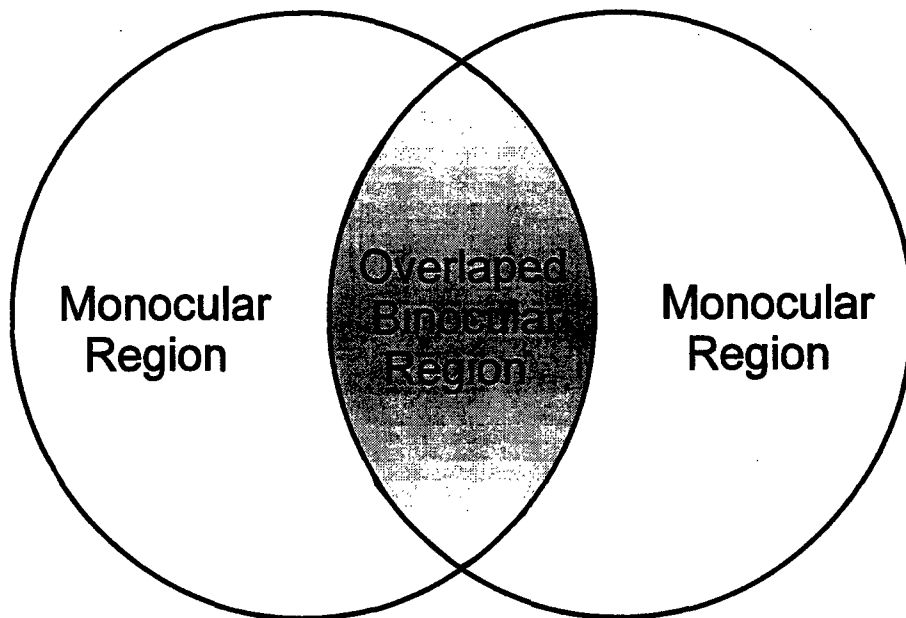


Figure 8. Partially overlapped FOV with a central binocular region and two monocular regions.

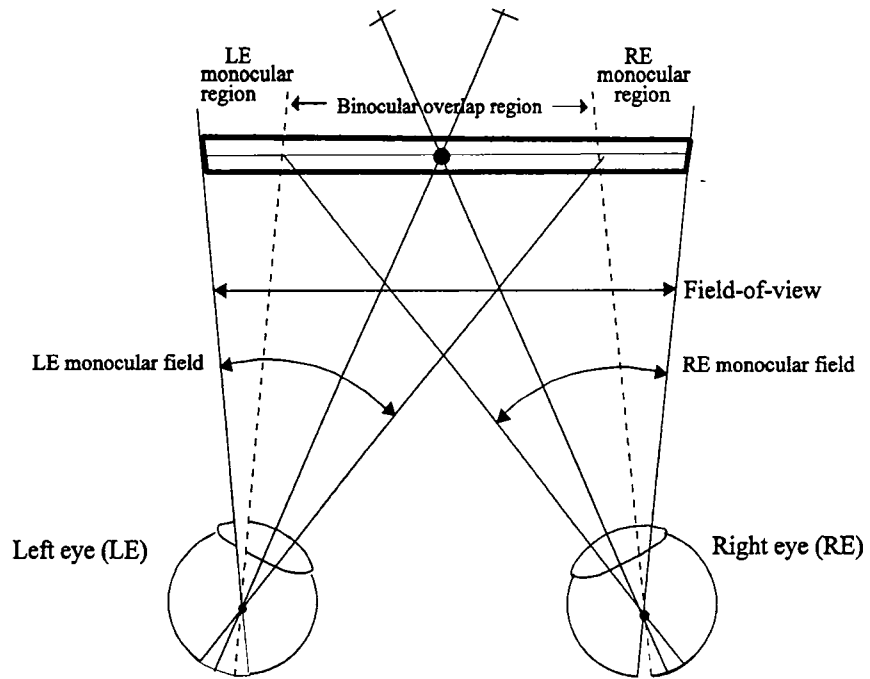


Figure 9. Visual interpretation of the divergent display mode.

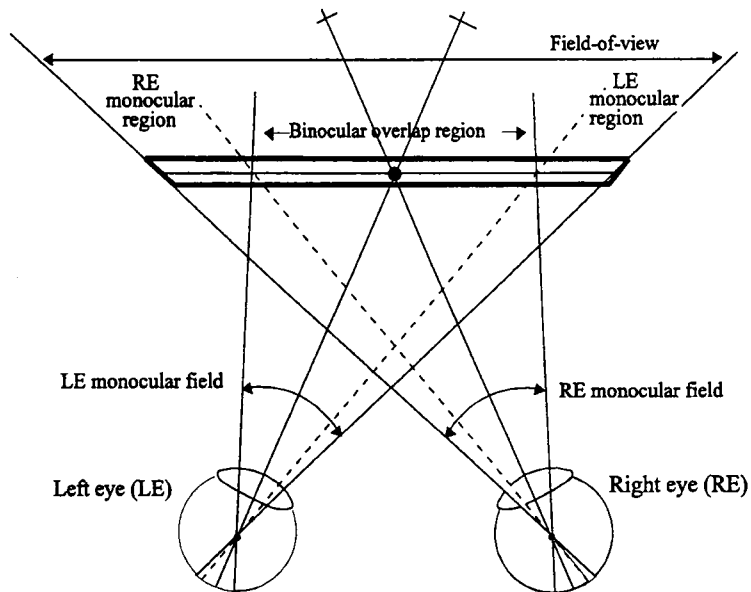


Figure 10. Visual interpretation of the convergent display mode.

Classifying HMDs by optical design is even more convoluted. The simpler and more predominate types use optical designs based on reflective and refractive elements. A standard characteristic of these designs is the presence of a final partially reflective element(s) positioned in front of the aviator's eye(s) (Wood, 1992). These elements are called "combiners," as they combine the see-through image of the real world with the reflected image of the HMD image source. Reflective/refractive optics designs will be discussed in detail in a following section.

Another type is based on a visor projection design (e.g., Cameron and Steward, 1994). A simple diagram of this design approach is presented in Figure 11. The image source(s) is usually mounted to the side of the helmet, and the image is relayed optically so as to be projected onto the visor where it is reflected back into the aviator's eye(s). The advantages of visor projection HMDs include lower weight, improved CM, increased eye relief, and maximum unobstructed visual field. A major deficiency is image degradation which can result in a high vibration environment. Also, this design requires that the visor be able to be placed consistently at the same position.

Another approach, which again allows for low weight and provides a compact design is one using holographic optical elements (Vos and Brandt, 1990). A holographic combiner is used to merge the standard combiner function with the collimation function usually performed by an additional refractive optical element. This merging implies that the holographic combiner acquires optical power, hence the term power combiner (Wood, 1992). In some designs, the visor serves as the combiner, with a holographic coating on the visor substrate. Using the visor as the combiner offers the additional advantage of being able to obtain wider FOVs. Disadvantages of this approach include the problem of preventing humidity and temperature effects from degrading the holograms and the poor optical quality of standard visor materials, such as polycarbonate, which are used as the holographic substrate.

The most recent entry into HMD design approaches is the use of lasers which scan an image directly unto the retina of the user's eye (Johnston and Willey, 1995). Figure 12 provides a diagram of the basic retinal scanning approach. This approach eliminates the need for a CRT or FP image source, improving both weight and CM. Other cited advantages of this system include diffraction (and aberration) limited resolution, small volume (for monochromatic), full color capability, and high brightness potential. Disadvantages, at least potentially, include scanning complexity, susceptibility to high vibration environments (as in Army aviation), limited exit pupil size, and safety concerns.

Regardless of the actual optical approach used, an Army aviation HMD also must include an image source, a head/eye tracker (if sensor is remotely located), and a helmet platform. At one time, the traditional approach was to integrate the optics and image source into a subsystem which was then mounted onto an existing helmet (Melzer and Larkin, 1987). This add-on approach was used with ANVIS. As one might expect, attaching one subsystem to another subsystem may not produce the optimal design. Instead, an integrated approach in which all elements of the HMD are designed in concert generally will result in the best and most functional overall design. The IHADSS is the first product of the integrated approach. However, care must be taken not to assume that an integrated approach is one which always will produce a single HMD configuration. In fact, the various missions, and the conditions under which they must be completed, are so different, that a single HMD design, while optimal for one set of conditions, may be significantly deficient for other mission scenarios. A solution to this problem may be a modular approach (Bull, 1990), where the HMD system consists of a base mounting unit (e.g., helmet platform), and interchangeable modules are attached, each for a specific set of mission requirements. This modular approach can be effective as long as an integrated approach is used which does not compromise the basic requirements of any subsystem. For example, the helmet,

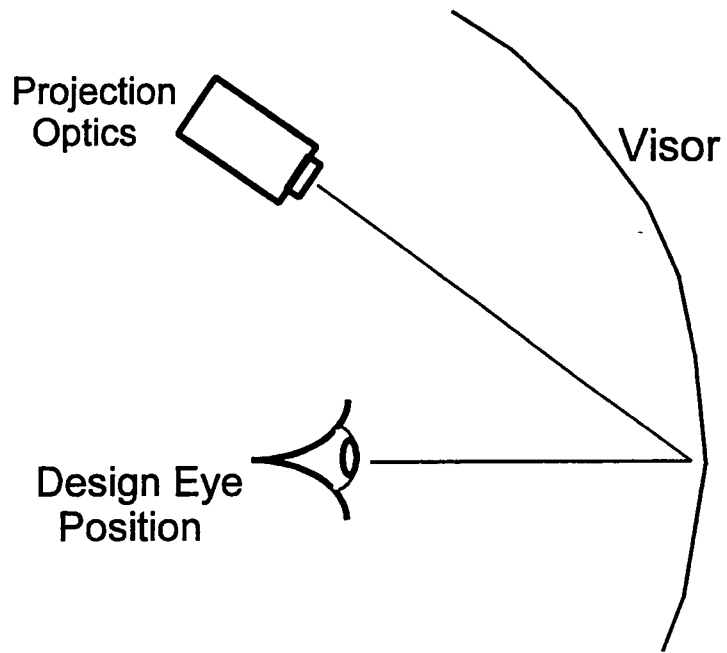


Figure 11. Visor projection HMD design approach.

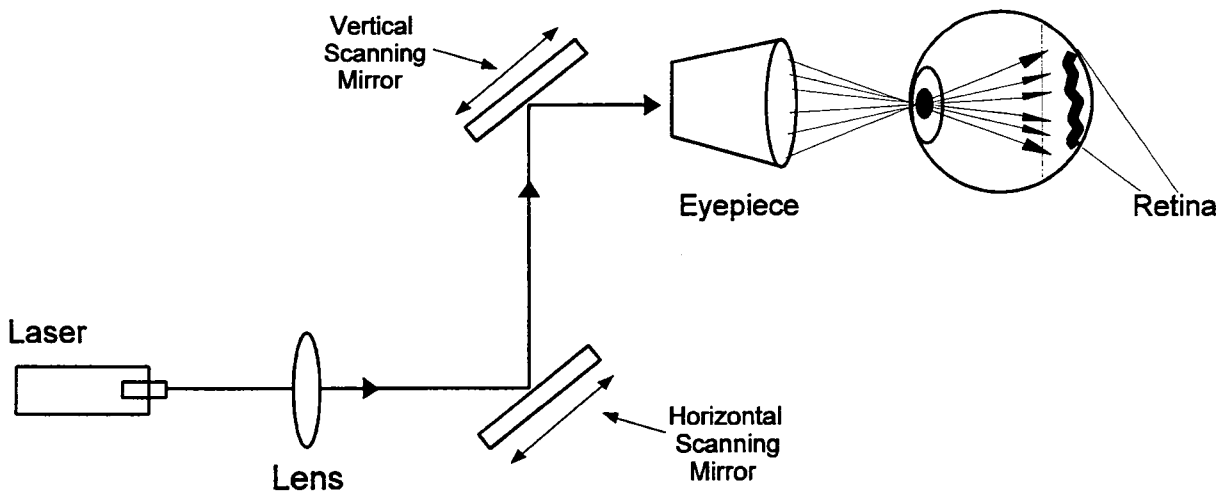


Figure 12. Basic diagram of retinal scanning display (adapted from Proctor, 1996).

while now being used as a platform to attach optics, must still serve its primary function of providing impact, visual, and acoustical protection.

Fielded systems

To date, two HMD systems have been fielded in U.S. Army aviation, the ANVIS and the IHADSS. These systems are vastly different in design and implementation. ANVIS is a combined sensor/display optics package which mounts onto existing aviator helmets by means of a visor assembly mounting bracket. The ANVIS is binocular (100% overlap) and uses 3rd generation I² sensors, which being head-mounted do not require an additional head tracking system. Typical ANVIS optical characteristics (for procurements prior to December 1996) include: a focus range of 28 cm (11 inches) to infinity, unity (1x) magnification, 27-mm effective focal length objective (f/1.2), 27-mm effective focal length eyepiece lens, resolution of greater than 0.82 cycles/milliradian (cy/mr), minimum 2000x brightness gain (3000x for newer versions), -6 to +2 diopter eyepiece focus adjustment, and a 52-72 mm interpupillary distance (IPD) adjustment. The ANVIS housing can be flipped up or down and has a 10-G breakaway feature. A tilt adjustment of approximately 8° is provided. There is a minimum vertical and fore/aft adjustment range of 16 mm. They operate off of one lithium or two "AA" batteries. A dual battery pack is Velcro™ mounted on the rear of the helmet to improve the CM. A summary of ANVIS optical and electro-optical (EO) specifications is presented in Table 1. Additional summaries of ANVIS performance characteristics are provided by McLean et al. (1997); Harding et al. (1996a) DeVilbiss, Ercoline, and Antonio (1994); Brickner (1989); and Verona and Rash (1989).

IHADSS is a monocular design with imagery provided to the right eye only. Where ANVIS integrates the I² sensors into the HMD, IHADSS depends on a FLIR sensor located on the nose of the aircraft. The IHADSS HMD consists of a helmet, visor housing with visor (clear and tinted are provided), miniature CRT image source, head tracker, and display optics. Lead sulfide detectors, mounted on the helmet, are part of the EO head tracking system which slaves the nose-mounted FLIR to the aviator's head motion. The headborne components of IHADSS are called the integrated helmet unit (IHU) and the combination of the CRT and display optics is called the helmet display unit (HDU) (Figure 13). The last element in the HDU optics is a combiner (beamsplitter) which reflects the HMD imagery into the aviator's eye. The combiner is a multilayer dichroic filter on a neutral density glass substrate which has its reflective characteristics maximized for the P43 phosphor used in the CRT.

IHADSS performance specifications include a 30° (V) x 40° (H) FOV, unity (1x) magnification, a 10-mm exit pupil, a nominal ± 3 diopters optical focus range, and a 10-mm optical eye relief. A summary of IHADSS optical and EO specifications is presented in Table 1. Additional summaries of IHADSS performance are provided by Harding et al. (1996a); Harding et al. (1995); Rash, Verona, and Crowley (1990); and Rash and Martin (1987a).

Image sources

In a typical aviation scenario, an external scene is acquired by a sensor, converted into an electrical signal, reproduced on a display, and then relayed optically to the eye(s). Within our definition of an HMD, the display which first reproduces the scene imagery, prior to relaying it to the eye, is referred to as the image source. In the IHADSS, the image source is a miniature, 1-inch diameter, CRT. When the concept of HMDs was first seriously pursued, the CRT was the only established display technology available. CRTs have remained the display of choice due to their attributes of low cost, easy availability, dependability, and good image quality. However, CRTs, even miniature ones, have inherent drawbacks which include weight, size (primarily



Figure 13. The IHADSS Integrated Helmet Unit (IHU) and Helmet Display Unit (HDU).

depth), power requirements, high anode voltage, and heat generation. And, it is only due to these deficiencies that a new class of display technologies has been able to gain a foothold. These new technologies are collectively referred to as FP technologies, due to their flat display surface and thin physical profile. Displays based on FP technologies offer characteristics which counter the deficiencies of CRT displays. Flat panel displays (FPDs) have a greatly reduced physical profile, low power and voltage requirements, low heat output, and low weight. All of these characteristics make them very desirable for aviation use where space, weight, and power are at a premium. While types of image sources are not limited to CRTs and FP technologies, these are the most likely candidates for near-future systems (excluding I² systems).

Cathode ray tubes

CRTs generate images by modulating the intensity of a scanning electron beam striking a phosphor coated surface. The electron beam, focusing coils, deflection plates, and phosphor are encapsulated in a glass envelope (tube). CRTs provide a bandwidth and resolution (limited) which are compatible with the eye's requirements for high quality imagery. They use simple scanning schemes, consist of few parts, provide full-color capability, have long life, and are versatile in the types of information they can present (Lehrer, 1985).

It was only natural that the CRT was selected as the image source for the first integrated aviation HMD, the IHADSS. However, for CRT displays to be head-mounted, their size and weight had to be reduced. The result was the development of miniature (\leq 1-inch diameter) CRTs. Tubes with $\frac{1}{2}$ -, $\frac{3}{4}$ -, and 1-inch diameters have been developed. Typical performance characteristics for these tubes (Levinsohn and Mason, 1997) are presented in Table 4. Comparison of these characteristics shows that the 1-inch tube offers the best raster imagery resolution and luminance. The CRT's peak raster luminance is important since it must suffer transmission and scatter losses during relay to the eye where the delivered luminance is most critical. Its resolution defines the fidelity of the details in the imaged scene.

Table 4.
Comparison of operating characteristics of miniature CRT tubes.
 (Levinsohn and Mason, 1997)

	1-inch CRT	1/2-inch CRT	1/4-inch CRT
Useable face plate	19 mm dia	17.5 mm dia	11.5 mm dia
Final anode voltage	13 kV	12 kV	8.5 kV
Deflection sensitivity	1.29 A/cm	1.14 A/cm	1.5 A/cm
Face plate	Fiber optic plano concave	Fiber optic plano concave	Fiber optic plano concave
Phosphor	P53	P53	P53
Raster peak luminance	3000 fL	1500 fL	1500 fL
Stroke peak luminance	5000 fL	10000 fL	5000 fL
Raster line width	20 μm	30 μm	25 μm
Stroke line width	25 μm	30 μm	30 μm
Mass	75g excluding leads	60g excluding leads	45g excluding leads
Dimensions	104 mm x 26.5 mm diameter	90 mm x 22.5 mm diameter	75 mm x 16.5 mm diameter

However, all of the parameters of a CRT contribute to the resulting image quality. Certain parameters are weighted more than others in their contribution. These include phosphor efficiency and persistence, and electron beam spot size. Adequate luminance and contrast (ratio of luminances in bright and dim areas of the display) require efficient phosphors; good resolution depends on a small spot size; and adequate reproduction of dynamic imagery requires a short phosphor persistence.

Adequate luminance and contrast ratios are a function of anode voltage, beam current, and phosphor luminous efficiency. Increasing anode voltage increases luminance, which can improve available contrast. Anode voltages in miniature CRTs now are as high as 13 kilovolts (kv). [Note: Achieving increased luminance by increasing anode voltage is limited by safety considerations which include radiation concerns and rapid high voltage disconnect during egress.] Increasing anode voltage results in increased beam current. For a given phosphor, the higher the beam current for a given spot size, the greater the luminance output. Similarly, for a given beam current, the greater the phosphor luminous efficiency, the greater the luminance output. CRT phosphor efficiencies, defined as the ratio of the luminous energy output to the electron beam energy input, range from 1-20%. [Efficiency values vary somewhat as a function of high voltage and spot size.] Luminance, also, is affected by beam writing speed, with slower speeds generating higher luminances. Miniature CRTs have demonstrated the capability of generating luminances > 6000 fL in stroke mode and > 3000 fL in raster mode.

Contrast is an important FOM which is tied to the ability of the human visual system to detect the luminance difference between two adjacent areas. A number of definitions and associated equations are used to express measures of contrast, e.g., contrast, contrast ratio, contrast modulation, etc. (Klymenko et al., 1997). In analog displays, such as CRTs, the range of contrast available is often expressed using the artificial concept of shades of grey (SOGs). SOGs are luminance steps which differ by a defined amount. They are by convention typically defined as differing by the square-root-of-two (approximately 1.414). In miniature CRTs for aviation, a minimum of 6 SOGs is considered acceptable for pilotage imagery. [This last statement is based on IHADSS experience.]

The selection of a CRT phosphor is based on those phosphor characteristics which impact the application the most. The phosphor characteristics generally of greatest interest are luminous efficiency, spectral distribution, and persistence. Fielded ANVIS use the P20 (older) or P22-Green (newer - adopted for environmental concerns over cadmium in the P20) phosphors; IHADSS uses the P43 (which is being fielded for ANVIS use also) and the HIDSS currently uses the P53. A summary of characteristics for these phosphors is given in Table 5.

Table 5.
Phosphor characteristics.
(EIA Tube Engineering Advisory Council, 1980)

	P20 (Zn,Cd,Sr,Ca) ANVIS	P22-Green (Zn,Sr,Cd,Al) ANVIS	P43 (Cd,Os,Tb) IHADSS	P53 (Mg,Cd,Tb) HIDSS
Luminous efficiency	18.7%	12.4%	10.2%	6.3%
Persistence	Medium 3 msec	Medium 3 msec	Medium 1.3 msec	Medium 6.7 msec
Spectral distribution	Broad band 495 to 672 nm 560 nm peak	Broad band 495 to 660 nm 530 nm peak	Narrow band 540 to 560 nm 543 nm peak	Narrowband 540 to 560nm 546 nm peak
Color	Green/Green-yellow	Green/Green-yellow	Green-yellow	Green-yellow

Note: Most phosphors have several formulations which can result in differing persistence, peaks, and efficiencies.

The spectral distribution of a phosphor is important in transferring display luminance to the eye. The eye's photopic (daytime, >1 fL) response peaks at approximately 555 nanometers (nm), which is in the green region of the visible spectrum (Figure 14). [The eye's nighttime (scotopic response) peaks at approximately 507 nm.] It is not coincidental that all of the phosphors mentioned so far as being used in CRTs have a green or greenish yellow color.

The persistence of a phosphor, defined here as the time required for a phosphor's luminance output to fall to 10% of maximum, is the major factor in the dynamic or temporal response of a CRT. In the military aviation environment, the temporal response of the imaging system (sensor, display, and associated electronics) is especially critical in pilotage and target acquisition tasks (Rash and Verona, 1987). The loss of temporal response results in degraded modulation contrast at all spatial frequencies (with greater losses at higher frequencies) (Rash and Becher, 1982).

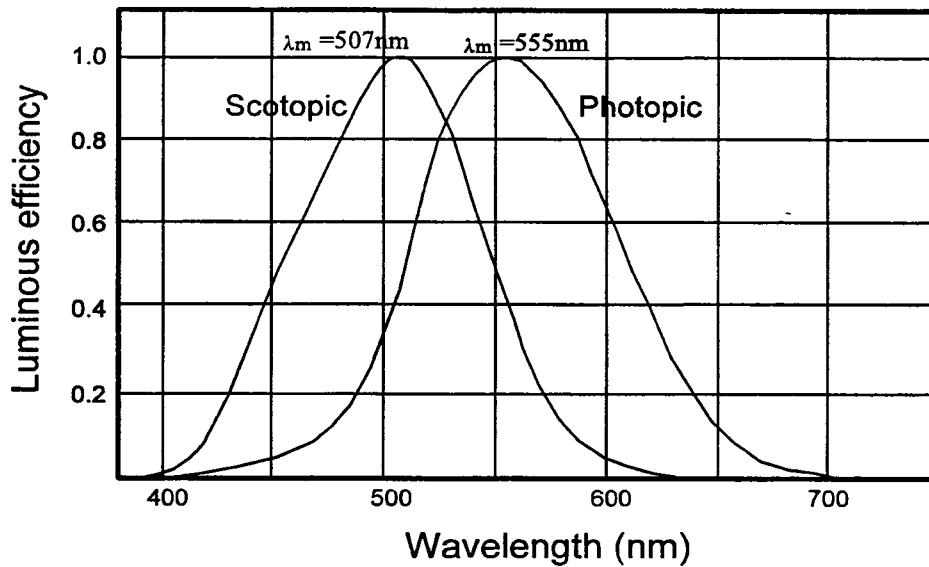


Figure 14. The human eye's photopic and scotopic response.

This loss of modulation transfer can severely degrade user visual performance. When modulation contrast degrades below a certain threshold, targets begin to blend with the background and the aviator loses the ability to discriminate targets from their backgrounds; aviators may fail to see tree branches and gunners may mistake tanks for trucks. This issue actually manifested itself during the early development of the IHADSS. Initially, the P1 phosphor with its high luminance potential was selected for the CRTs. P1 has a persistence of 24 msec. Early flights with this phosphor resulted in a minor mishap when imagery of tree branches smeared due to relative motion of the aircraft. Replacing P1 with the P43 phosphor (1.3 msec persistence) solved this problem. The HIDSS uses the P53 phosphor with a 6.7 msec persistence. However, Beasley et al. (1995) showed that the five-fold difference over the P43's 1.3 msec persistence produced only minor degradation in MTF performance.

In HMDs where the image source is a CRT, it is the CRT's resolution which is often the limiting resolution of the system. The HMD's resolution delineates the smallest size target which can be displayed. CRTs have both a vertical and horizontal resolution. The horizontal resolution is defined primarily by the bandwidth of the electronics and the spot size. Vertical resolution is usually of greater interest and is defined mostly by the beam diameter and the spreading of light when the beam strikes the phosphor, which defines the spot size (and line width). CRT resolution is usually expressed as the number of raster lines per display height, the line width, the spot diameter, or by the MTF (Lehrer, 1985). Identified years ago as a good FOM for CRT display image quality (Verona et al., 1979), the MTF recently has become the defining resolution specification for new HMDs. There are several methods which historically have been used to obtain MTF curves. These include the subjective techniques of shrinking raster, line width, and TV limiting resolution; and the objective techniques of discrete frequency, half power width, and Fast Fourier Transform (FFT). Verona (1992) provides an excellent comparison of these techniques.

A detailed discussion of miniature CRT performance can be found in Task and Kocian (1995).

Flat panel technologies

There are a number of FP technologies which are available for use as miniature image sources in aviation HMDs (Figure 15). The size, weight, and power advantages of displays based on these technologies have brought them under consideration as replacement image sources by HMD designers. The DARPA have funded a number of programs which have a goal of developing and integrating FP display technologies into HMD and other Army systems (Girolamo, Rash, and Gilroy, 1997). Aviation programs benefitting from this investment include: (a) The Miniature Flat Panel HMD for Aviation program, to investigate the concept of using FP technology in the development of an HMD for use in rotary-wing aircraft; (b) the AIHS Comanche Compatibility program, to develop an HMD design using the HGU-56/P helmet shell that gives the RAH-66 Comanche program an alternate system which capitalizes on recent display technology advancements; and (c) the CONDOR program, to develop a research HMD tool for investigating the impact of various display parameters on performance.

FP technologies generally are classed as emissive or nonemissive. Emissive displays produce their own light; nonemissive displays operate by the transmission and/or reflection of an external light source. A brief description of each of the major FP technologies follows:

Liquid crystal

The most widely known flat panel display technology is that of liquid crystals. LCDs are nonemissive displays. They produce images by modulating ambient light, which can be reflected light or transmitted light from a secondary, external source (e.g., a backlight). The mechanism by which modulation is achieved is the application of an electric field across a liquid crystal material which has both liquid and crystalline properties. The LC material is sandwiched between layers of glass and a set of polarizers. By applying an electric field, the LC can be caused to act as a light valve.

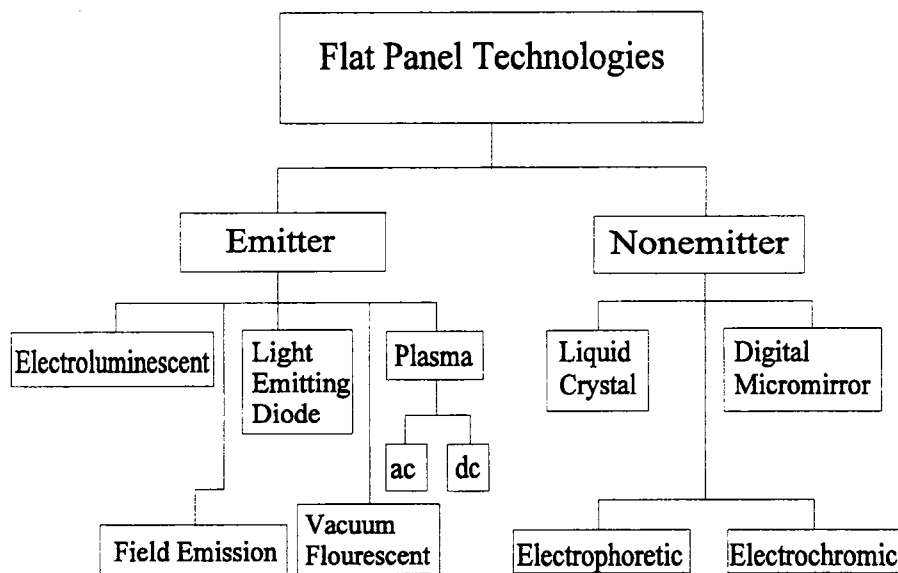


Figure 15. Diagram of flat panel technologies.

LCDs exist in several configurations. These include the twisted nematic (TN), the modulated twisted nematic (MTN), the optical mode interference (OMI) effect, and the super twisted nematic (STN). These differ primarily by the EO effect the crystal exhibits. The liquid crystal cell is constructed using two glass plates which are coated with a transparent conducting material. Between the plates, a thin layer of polyimide is applied. This layer is rubbed in one direction causing the LC molecules to align parallel to the rubbing direction. Polarizers are placed on the outside of each glass plate with the direction of polarization parallel to the rubbing direction. Application of a drive voltage affects the polarization of the LC material, and hence the transmission/reflection characteristics of the cell.

Two active areas of research in LCDs are the development and testing of ferroelectric and the polymer dispersed (reflective cholesteric) LCDs. Ferroelectric LCDs (FELCDs) utilize intrinsic polarization, meaning these LC molecules have a positive or negative polarity in their natural state, even without the application of an external electric field. This attribute gives FELCDs certain characteristics such as high operating speed, wide viewing angle, and inherent (no power) memory (Patel and Werner, 1992). Polymer dispersed LC technology is based on a concept called nematic curvilinear aligned phase (NCAP), in which the nematic LC material is microencapsulated in a transparent polymer. Polymer dispersed LCDs do not use polarizers and employ plastic film substrates rather than glass (Castellano, 1992). This technology does not require a backlight, is bistable, and has full grey scale memory (Yaniv, 1995).

LCDs also can be grouped according to the method by which the individual picture elements (pixels) are activated (or addressed). The two commonly used addressing modes are passive matrix and active matrix. In passive matrix LCDs (PMLCDs), pixels are defined by the intersection of a pair of vertical and horizontal electrodes. Voltages applied to any selected pair causes the LC material at the intersection to respond. AMLCDs employ an array of individual pixels, each controlled by an electronic switch (Tannas, 1985). The most successful active matrix approach to addressing pixels uses thin film transistors (TFTs). In this approach, a TFT and a capacitor are used to switch each LC cell on and off.

LCDs can be monochrome or full color. Monochrome LCDs usually use a backlight consisting of one or more fluorescent lamps, a reflector, and a diffuser. Less frequently used is a backlight where the light source is an electroluminescent panel. [See following section.] Approaches to achieving color LCDs are numerous and increasing every day. One approach is similar to the additive color method employed in modern CRT displays. In this approach, pixels are composed of three or more color subpixels. By activating combinations of these subpixels and controlling the transmission through each, a relatively large color gamut can be achieved.

Backlighting is an important issue with LCDs and even more important for HMD designs based on LCDs. In general, backlights must be efficient (> 40 lumens/watt), produce high luminance ($> 20,000$ fL) (critical due to the pore through-put of LCDs), have high luminance uniformity ($< 20\%$ variation), have long life ($> 30,000$ hours), and have a wide dimming range ($> 5000:1$) (Allen et al., 1995). Research is ongoing to achieve and/or exceed these requirements for military aviation applications (Altadonna, 1996; Jiang, 1996; Kalmanask and Sundraresan, 1996). For HMDs, two options are possible: (a) The backlight is physically located away from the LCD, i.e., elsewhere in the aircraft or (b) a miniature backlight must be used. Mounting the backlight in the aircraft places additional luminance requirements on the backlight and the aircraft designers, since space, weight, and power demands must be addressed. Integrating the backlight with the display requires the development of subminiature (< 2 " diagonal) backlights capable of the requirements cited above. Several manufacturers currently provide fluorescent backlights with diagonal measurements of approximately 0.8" and 1.6". Currently, these lights provide only moderate luminance values which are inadequate for HMDs during daytime use.

The most common backlight source is the cold-cathode fluorescent tube (CCFT). The four parameters which define their operation are the minimum discharge voltage, operating voltage, frequency, and tube current (Ward, 1992). The minimum discharge voltage (which is developed by the inverter and increases with tube age) is the minimum voltage needed to fire the tube near the end of its life. The voltage across the tube during normal operation and drawing normal current is the operating voltage. Tubes operate on an alternating current (AC) voltage at some frequency usually near 30 kHz. The most important parameter in determining the tube brightness is the tube current, expressed as the nominal root-mean-square (rms) current.

Alternative, potentially high brightness, backlights based on field emission displays (FEDs) and light emitting diodes (LEDs) are being investigated. LED backlights have been in use for monochrome transfective LCDs for some time (Bernard, 1996). However, currently available LEDs do not have the luminous efficiency to replace CCFTs in most LCD applications. Recent improvements in efficiencies and the investigation of more exotic materials, such as organic LEDs, are improving their potential. If current luminous efficiency and manufacturing problems can be overcome, the packaging problem for backlight in LCDs for HMDs may be solved.

Electroluminescence

Electroluminescent displays generally have a layer of phosphor material sandwiched between two layers of a transparent dielectric (insulator) material which is activated by an electric field. Pixels are formed by patterning the phosphor into dots. EL displays are either AC or direct current (DC) driven and also can be classified as powder or thin/thick film. The two most prevalent EL display types are direct current thick film EL (DCTFEL) and alternating current thin film EL (ACTFEL). Active matrix EL (AMEL), which uses active matrix addressing, can provide reasonably high luminance, contrast, and speed. All EL displays are emissive in nature (Castellano, 1992).

EL displays are available as monochrome, limited color, or full color. Color is achieved either by classic filtering techniques of color-by-white or by patterned phosphors similar to those used in conventional CRTs. EL panels of uniform layers of phosphor sometimes are used as backlights for LC displays.

Light emitting diode

Light emitting diode displays are emissive displays composed of multiple LEDs arranged in various configurations which can range from a single status indicator lamp to large area x-y addressable arrays. The individual LEDs operate on the principle of semiconductor physics where electrical energy is converted into light energy by the mechanism of electroluminescence at the diode junction. Light energy is produced when this junction is forward biased by an applied voltage. The LED's light output is a relatively narrow spectral band and often is considered monochromatic (single color) and identified by a dominant wavelength. The "color" of the LED is a function of the semiconductor material, and, for the visible spectrum, includes green, yellow, red, and blue (Tannas, 1985; Castellano, 1992).

LED displays typically are monochrome, but the use of subminiature LEDs in red-green-blue (RGB) configurations can provide full color.

Field emission

FEDs are emissive displays. They consist of a matrix of miniature electron sources which emit the electrons through the process of field emission. Field emission is the emission of

electrons from the surface of a metallic conductor into a vacuum under the influence of a strong electric field. Light is produced when the electrons strike a phosphor screen (Cathey, 1995; Gray, 1993). [Note: This process also is referred to as cold emission.] FEDs can be classified by their geometry: point, wedge, or thin film edge. Each geometry has its own advantages and disadvantages. FEDs are driven by addressing a matrix of row and column electrodes. Full grey scale monochrome and full color displays have been developed.

Vacuum fluorescent

Vacuum fluorescent displays (VFDs) are flat vacuum tube devices that use a filament wire, control grid structure, and phosphor-coated anode. They operate by heating the filament to emit electrons which then are accelerated past the control grid and strike the phosphor anode, producing light. They are emissive displays. VFDs typically are used in small dot matrix or segmented displays. VFDs can be classified by their anode configuration: single matrix, multiple matrix, and active matrix. The single matrix configuration uses one anode and is the simplest design. The multiple matrix configuration uses multiple anodes which allow the duty cycle of the display to be increased. Active matrix configurations also have multiple anodes but have switching elements at each anode (Nakamura and Mohri, 1995).

VFDs are widely used in automotive applications. They primarily are used to present text and graphics. Monochrome and multicolor displays are available, with full color possible as more efficient blue phosphors are developed. They have little potential for HMD applications.

Plasma

Plasma (gas discharge) displays are emissive in nature and produce light when an electric field is applied across an envelope containing a gas. The gas atoms are ionized, and photons (light) are emitted when the atoms return to their ground state. A plasma display is an array of miniature gas discharge lamps, similar to fluorescent lamps. Images are produced by controlling the intensity and/or duration of each lamp's discharge currents.

Plasma flat panel displays can be classified according to whether the applied voltages are alternating current or direct current; however, there is a hybrid AC-DC plasma display. Plasma displays also can be classified by the method used to update the information on the display. The methods are known as memory and refresh.

Initially, plasma displays were only monochrome and light emission was orange, green, yellow, or red, dependent upon gas type. Full color has been achieved by placing phosphors in the plasma panel and then exciting those phosphors with ultraviolet light from the plasma. Plasma displays are currently the only choice if the display application requires direct view, full color, large-screen, and video rate capable displays. Currently, these FPDs are candidates for HMD use.

Electrochromism

Electrochromism (EC) is a change in light absorption (color change) as a result of a reversible chemical reaction which occurs in accordance with Faraday's Law of electrolysis (Tannas, 1985). The pixels act as little batteries which are charged and discharged. These displays possess excellent color contrast between "on" and "off" pixels and do not have to be refreshed. EC displays are low power, nonemissive displays. Disadvantages include poor resolution, limited color range, high cost, and addressing problems (Warszawski, 1993).

Electrophoresis

Electrophoretic (EP) displays are passive (nonemissive) displays whose technology is based on the movement of charged particles (of one color) in a colloidal-suspension (of a second color) under the influence of an electric field. The application of the electric field changes the absorption or transmission of light through the solution. Usually, color contrast is achieved through the use of dyes in the solution. When a DC field is applied to the suspended dye, the particles of the dye migrate to the surface of a transparent conductor which acts as the screen. The surface takes on the color of the particles. When the electric field is removed (or reversed), the dye particles are dispersed back into the suspending liquid, and the surface takes on the color of the suspending liquid. EP displays offer the desirable features of large area, wide viewing angle, and long memory without the need of a power supply (Castellano, 1992; Tannas, 1985; Toyama et al., 1994).

Digital micromirror

The digital micromirror device (DMD) display is a matrix where each pixel is a very small square mirror on the order of 10-20 microns. Each mirror pixel is suspended above two electrodes driven by complementary drive signals. The mirrors are suspended between posts by a very thin torsion hinge attached to opposite (diagonal) corners of the mirror. When no signal voltage is applied, the mirror is in its flat state. The application of a drive signal causes the mirror to tilt one way or the other. The mirror tilt is typically 10 degrees. These two conditions (actually three, since the tilt can be in two directions) correspond to "on" and "off" pixel states. Images are formed by using the mirrors to reflect light. DMDs are used in projection displays and offer potentially significant advantages in size, weight, and luminance capability over other types of projection systems (Critchley et al., 1995; Sampson, 1994).

Further detailed descriptions of these technologies can be found in Tannas (1985), Clark (1992), and Biberman and Tsou (1991).

While overcoming the weight, size, power, and heat generation deficiencies of CRTs, each FP technology offers advantages and disadvantages. These are summarized in Table 6.

A survey of existing FP technologies (Harding et al., 1996b) to identify those promising the most potential for Army aviation use concluded that AMLCD, EL, and plasma were the most commercially available technologies. LCDs, by far, are the most mature of the FP technologies and, therefore, the most likely candidate for aviation applications. In fact, AMLCDs have been selected by the Comanche program for both its panel- and head-mounted displays. In November 1997, it was decided to replace the miniature CRTs in the HIDSS with AMLCDs.

Considerable effort has been put into establishing criteria for the use of AMLCDs in U.S. military aircraft. A draft standard for such use (Hopper et al., 1994) has been prepared which addresses both the engineering and visual performance issues of these displays. However, this standard does not address those performance issues inherent solely to miniature displays considered for use in HMDs.

The growing requirement for alternate image sources to CRTs for HMD designs has helped to drive the development of miniaturized FPDs. Typical physical goals for such devices are 20 mm x 20 mm (~ 3/4" x 3/4") area, 15 mm depth, and <25 grams mass (Worboys et al., 1994). In addition to these desirable size and mass (weight) characteristics, miniature displays must be adaptable to see-through systems and have sufficient resolution and luminance. The image source size dimensions (~28 mm diagonally) are loosely dictated by the FOV (25° to 50°), eye

Table 6.
FP technology advantages and disadvantages.

Technology	Advantages	Disadvantages
AMLCD	<ol style="list-style-type: none"> 1. Full color 2. Superior image quality 3. Video speed for general viewing 	<ol style="list-style-type: none"> 1. Limited viewing angle 2. Requires backlighting 3. Lacks sufficient video speed for military applications
Passive LCD	<ol style="list-style-type: none"> 1. Low cost 2. Simple design 	<ol style="list-style-type: none"> 1. Reduced resolution 2. Slow response
Electroluminescent	<ol style="list-style-type: none"> 1. Very rugged 2. High resolution 3. Wide viewing angle 4. Long life 	<ol style="list-style-type: none"> 1. Limited brightness 2. Full color not available 3. Inefficient drive scheme
Plasma	<ol style="list-style-type: none"> 1. Large life 2. High luminance 	<ol style="list-style-type: none"> 1. Affected by electromagnetic fields
Field emission	<ol style="list-style-type: none"> 1. High luminance 2. High energy efficiency 	<ol style="list-style-type: none"> 1. Questionable reliability 2. Higher voltages required 3. Production problems
Digital micromirror	<ol style="list-style-type: none"> 1. High luminance for projection 2. Reduced flicker 	<ol style="list-style-type: none"> 1. Temporal artifacts 2. Artifacts, both temporal and spatial
Light emitting diode	<ol style="list-style-type: none"> 1. Low cost 	<ol style="list-style-type: none"> 1. Lack of full color 2. High power requirement
Electrochromic	<ol style="list-style-type: none"> 1. High contrast 	<ol style="list-style-type: none"> 1. Addressing techniques 2. Low pixel addressing speed
Electrophoretic	<ol style="list-style-type: none"> 1. Low power requirement 	<ol style="list-style-type: none"> 1. Suspensions are complex and hard to reproduce 2. Low pixel addressing speed
Vacuum fluorescent	<ol style="list-style-type: none"> 1. High luminance 2. Wide viewing angle 	<ol style="list-style-type: none"> 1. Limited resolution

relief distance (> 25 mm), and exit pupil size (~ 10 to 15 mm). Strangely, if the image source is significantly smaller or larger, the physical packaging of the display and its optics become unacceptably large (Ferrin, 1997).

Resolution for FP displays is defined as the highest spatial frequency which can be presented. It is usually expressed as the number of picture elements (pixels) in both the horizontal and vertical directions. Typical resolution values are 640 (H) x 480 (V), 1024 (V) x 768 (H), and

1280 (H) x 1024 (V). An important concern when selecting the resolution of pixelated image sources is to ensure that when viewed by the eye through the display optics, individual pixels are not resolvable (Ferrin, 1997). Such a situation would lower image quality and be found objectionable to the viewer. Based on the human eye's minimum resolution of 1 arcminute, an HMD with a field of view of 40° should not have less than 2400 pixels in either dimension (3400 pixels, if the Kell factor is applicable to discrete displays and considered). Currently, this is an unobtainable requirement. Displays with 1280 pixels (in one dimension) are currently state of the art. Even neglecting the Kell factor, this resolution would limit the FOV to approximately 20°. However, one method to overcoming this problem is the use of diffusion or defocusing screens over the image source. This "softens" the image, making it more visually acceptable. One study (Harding et al., 1997), which investigated threshold visual acuity with a number of LCD FPDs, found that a diffusing screen did not reduce acuity and may have helped by filtering out unwanted high spatial frequency noise.

In a see-through HMD design, the HMD image is viewed against the background of the outside world, which can take on a wide range of luminance values. These values range from that of a moonless, clear night sky (0.00001 fL) to that of a sunlit white cloud (10,000 fL). The image source must have high enough luminance to provide (after losses through the optics which can be as high as 80%) sufficient contrast (SOGs) to allow adequate vision for successful completion of all mission tasks. Current commercially available miniature FP image sources are limited to luminances of only slightly better than 200 fL.

There are two leading candidate FP technologies for the miniature image sources needed for Army aviation: AMEL and AMLCD. As with all FP displays, these two display types do not have a mature and reliable manufacturing history, do not provide for insufficient symbology luminance, and have limited distortion correction schemes (Belt et al., 1997). AMELs additionally suffer from insufficient video luminance; AMLCDs (because of their low structure transmission) require extremely high backlight luminances and have insufficient temporal response for presenting the dynamic imagery required for the military rotary-wing environment.

A FP technology display which has recently gained considerable attention because it offers CRT-like characteristics in a thin, flat package is the FED (Jones and Jones, 1995). FEDs are considered by some HMD designers to be the best of both worlds and a hands-down choice for future aviation applications. Their potential performance advantages include very low power requirements, wide viewing angle, excellent resolution, and high contrast (>100:1); and they can withstand the harsh aviation environment, including temperature and vibration requirements. However, FED displays have yet to meet their full potential, still attempting to overcome problems with high density patterning, switching voltages, luminance uniformity, driver electronics, production, reliability, and others (Jones et al., 1996; Giri, 1995.). While considered as the most promising display technology for advanced cockpit applications (Marticello and Hopper, 1996), for now, FEDs will have to settle for being the "holy grail" of image sources.

An excellent bibliography for the technical characteristics of currently available miniature FP image sources is provided by Ferrin (1997). The FP manufacturing community is actively seeking to expand the performance of current displays. Through these efforts, these displays are slowly overcoming the limitations briefly described here. It is imperative that HMD developers maintain awareness of such improvements. The authors have found the two major sources of information on FP development and HMD design to be the annual conferences held by the Society of Information Display (SID), Santa Ana, California, and by the Society of Photo-Optical Instrumentation Engineers (SPIE), Bellingham, Washington.

Lasers

A novel imaging source, which has recently gained recognition as having a potential for application to HMDs, is the laser. Lasers as image generators have been designed and investigated on a large physical scale (Bohannon, 1997). Based on projection, these devices produce imagery on a screen using the basic scanning method of CRTs. Rather than an electron beam, a laser beam is scanned in two dimensions, with the beam intensity modulated at every pixel. If scanned at frequencies of 60 Hz or greater, a flicker-free image which the eye can see is produced. Laser projectors are claimed to produce images with: sufficient luminance, color gamut, and color saturation.

An image source based on the scanning laser which generates an image directly onto the retina of the eye has been proposed for HMD application (Proctor, 1996; Johnston and Willey, 1995; Kollin, 1993) (Figure 12). One version of this device, called the Virtual Retinal Display, has been developed at the Human Interface Technology Laboratory, University of Washington, Seattle, Washington. Its basic principle is the same as used in the scanning laser ophthalmoscope (Webb, Hughes, and Delori, 1987). A laser (or three lasers for color) is intensity modulated as it is scanned vertically and horizontally. An optical interface is used to project the scanning beam onto the retina. The exit pupil of the optics is designed to be coplanar with the entrance pupil of the eye. The eye's natural focusing then forms the image on the retina. It is claimed that the device will be able to provide high (diffraction limited) resolution, high luminance, and monochromatic or color imagery within the small weight and volume requirements of HMD designs. Disadvantages, at least potentially, include scanning complexity, susceptibility to degradation in high vibration environments (as in Army aviation), limited exit pupil size, and safety concerns.

Optical designs

The basic purpose of the optical designs for helmet and head mounted devices is to focus small image sources to provide a specific field of view to the viewer with sufficient eye clearance for spectacles and protective masks, and sufficient size eye box to compensate for pupil displacements from eye movement, vibration, and head/helmet slippage. To achieve these objectives, a series of calculations are required to determine the sizes of key HMD elements, particularly the diameter of the last optical power element(s) of the eyepiece for a given set of HMD characteristics. The sizes of the HMD elements will primarily determine the ultimate weight. This exercise will start first with a direct view system such as NVG with no see-through provision, the refractive, on-axis (such as IHADSS), and the on-axis catadioptric designs with see-through vision. The first order eyepiece calculations for the off-axis designs are unique to the particular design, and are beyond the scope of this exercise. However, they will be discussed later on in this section.

Determining FOV

The focal length of the eyepiece is selected based on the size of the image source (real or virtual) to obtain a particular FOV. This general relationship between optical focal length and FOV can be approximated by the following equation, assuming the image is focused at infinity:

$$f = [0.5 d / \tan (0.5 \text{ FOV})] \quad \text{Equation 1}$$

where f = eyepiece focal length (linear units such as inches, millimeters),
 d = diameter or dimension of the display (linear units), and
 FOV = field of view in degrees.

Example: What is the approximate eyepiece focal length to obtain a 40° FOV with an 18-mm display?

$$f = [0.5 \times 18 / \tan (0.5 \times 40)] = 9 / \tan (20) = 24.73 \text{ mm}$$

Note that increasing the image source size will increase the FOV for a given focal length and vice versa. Methods to optically increase the size of the display will be discussed in the pupil versus nonpupil forming optical system section.

The diameter of the last optical element in an eyepiece design will also determine the maximum eye clearance distance to retain the full FOV. The physical limits for the eyepiece diameters are determined by the focal lengths. As the eyepiece diameter increases for a given focal length, the contribution from optical distortions will also increase, which will usually require more optical elements (more weight) to compensate for the aberrations and distortions. Although the eyepiece for the ANVIS is referred to optically as a simple magnifier, there are five refractive elements in the present design. The relationship between the lens focal length and its entrance or exit aperture (clear optical diameter) is the $f/\#$, which is expressed as the ratio of the lens focal length to its diameter:

$$f/\# = F/d \tag{Equation 2}$$

where F = focal length and d = diameter of lens in the focal length units.

The maximum practical $f/\#$ for an eyepiece is $f/\#$ 1.0. The $f/\#$ for the ANVIS objective lens is $f/\#$ 1.2. Typical fast camera lenses are $f/\#$ 1.4. For this discussion, we will use an $f/\#$ limit of 1.2. For the above eyepiece focal length example, the diameter of the 24.73 mm focal length lens with an $f/\#$ 1.2 would be 20.6 mm (24.73/1.2). For a nonsee-through system such as a typical NVG, the lens diameter then can be used to compute the maximum eye clearance distance to obtain the maximum FOV. For an imaging system with a beamsplitter (combiner) to provide see-through vision, determining the maximum eye clearance distance for a specific eyepiece diameter becomes a little more complex, but will be illustrated and plotted in later graphs.

Additional requirements for an HMD include sufficient eye clearances for spectacles and protective masks and lateral eye displacements (function of the size of the exit pupil) without reducing the FOV of the display. Eye clearance is measured from the apex of the cornea to the last optical or mechanical obstruction such as the lens mount or edge of the combiner. With on-axis viewing, the pupil is located approximately 3 mm behind the apex of the cornea. The size of the typical pupil viewing a night display is less than 5 mm. To retain the FOV of the display with increasing eye clearance distances or vertex distances and lateral displacements, the diameter of the last optical element with power has to increase, which increases weight and may exceed the $f/\#$ limits. For a direct view, nonsee-through design, the minimum eyepiece diameter without vignetting with eye alignment along the optical axis can be calculated by using the tangent function:

$$d = 2 (d_{ec} + 3) [\tan (0.5)(\text{FOV})] + d_{ep} \tag{Equation 3}$$

where d_{ec} = eye clearance in millimeters, which includes the vertex distance and mechanical obstructions and d_{ep} = exit pupil diameter in millimeters.

For a direct view nonpupil forming system, mounted on a stable platform, and with sufficient mechanical adjustments for fore-aft, vertical, IPD, and tilt, such as the ANVIS, the effective exit pupil diameter can be smaller than for a pupil forming system. For example, IHADSS HDU has a 10-mm exit pupil, the specification for the HIDSS is 15 mm on axis and 12 mm for peripheral rays, where ANVIS is specified as 7 mm. Using Equation 3, the eye clearance in millimeters can be calculated from the previous diameter calculation (20.6 mm) and 40 degree FOV, assuming an d_{ep} value of 7.

$$20.6 = 2(d_{ec} + 3)[\tan (0.5)(40)] + 7$$

$$2 d_{ec} + 6 = (20.6-7)/\tan 20$$

$$d_{ec} = [(13.6/0.364) - 6]/2$$

$$d_{ec} = 15.7 \text{ mm}$$

Later in this section, we will show that a protective mask without a blower will require an eye clearance of approximately 30 mm. Therefore, the optical designer typically begins with the eye clearance requirement and exit pupil size, and works backwards to determine the display size for a given FOV. To demonstrate the importance and contribution of the eye clearance on FOV, recalculating the above equation with an eye clearance of 30 mm and the eyepiece and exit pupil the same, the FOV is reduced to 23.3 degrees. Similarly, to obtain a 40 degree FOV with 30 mm of eye clearance, the diameter of the eyepiece would be 31.0 mm. Also note that reducing the exit pupil size reduces the eyepiece diameter the same amount. With angular eye movements, the eye is displaced perpendicular to the optical axis and will require the optical exit pupil to be located ideally approximately 2 to 3 mm behind the pupil of the eye, particularly for pupil forming imaging systems (Shenker, 1987).

The primary purpose of this first order optical exercise was to show how the variables of FOV, exit pupil size, eye clearance, image source size, and $f/\#$ interact with the simplest of optical designs for a flat display with nonsee-through vision. When see-through vision is desired with an added combiner, the calculations become more complex, but can be solved with multiple trigonometry steps. The optical designer can also increase the FOV for a given eyepiece focal length by using a concave display or image plane, inducing barrel distortion for the objective lens and neutralizing the barrel distortion with an equivalent pincushion distortion for the eyepiece. This technique is used for ANVIS. Graphs of the diameter of the eyepiece for the various HMD designs will be shown in the next section for comparison purposes.

Optical aberrations

In addition to just focusing or collimating the display, additional optical elements are usually required to compensate for chromatic and spherical aberrations, distortion, field of curvature, etc. Because the additional elements add undesirable mass to electro-optical devices, a short discussion of these optical characteristics will be included (Smith, 1990).

Chromatic aberration

All lens elements with refractive power act like a prism by refracting (bending) wavelengths of different colors by slightly different amounts. To compensate for this and to reduce the rainbow effects from the lens elements, the optical designer uses lenses in pairs (usually fused), opposite in lens power with different refractive characteristics (index of refraction and dispersion). These lenses are called achromats. Other methods to reduce chromatic aberrations are to (a) use narrow band light sources or phosphors, (b) use spectral filters that block and narrow the wavelength range of the display, and (c) to reflect select wavelengths with dichroic combiners or beamsplitters.

Spherical aberration

The curvatures of the front and back surfaces of most optical lenses are spherical, to both reduce cost and optimize surface quality and fidelity. To maximize the bending power of a lens with the least weight, the front and back lens curvatures would be similar in shape, but curved in opposite directions (double convex). However, the spherical curvatures in the double convex form induce additional lens power as the rays enter the lens away from the optical center for a given angle of incidence. The characteristics of eyepiece spherical aberrations to the observer when viewing a resolution chart in the middle of the FOV would provide clear vision when the eye is positioned on the optical axis, but blurred vision as the viewer moves their eye perpendicular away from the optical axis, or vice versa, depending on the focus of the eyepiece.

To minimize spherical aberrations with spherical surface lenses, the optical designer could use a combination of achromatic lenses and changes in lens curvatures. A simpler optical design to reduce spherical aberrations can be obtained using aspheric lenses. Instead of spherical surfaces, an aspheric lens has surface curvatures that deviate from a spherical surface such as being parabolic in shape. The parabolic curvature would reduce the increasing lens power with increasing lateral distances from the optical axis towards the edges of the lens. Unfortunately, producing custom aspheric lens designs usually requires either a molding process or diamond turning. The molding process for quality lenses is expensive unless the volume is high, and diamond turning limits the materials and the smoothness of the lens surface. Therefore, aspheric surfaces for optical designs have been limited to either high volume camera lenses (Polaroid Land™ camera) or expensive small production items (Hubble telescope components).

Distortion

The ideal optical design will project the image from the display to the viewer without altering the shape of the image. Common optical distortions are referred to as pincushion, barrel, trapezoidal, or a combination of shapes from square images. In addition to the common optical distortions, shear and “S” distortions of straight line images may occur with EO systems with coherent fiber-optic bundle components. Pincushion and barrel image distortions are common with “on-axis” optical designs. Trapezoidal distortions occur with “off-axis” designs. These distortions can be corrected either optically and/or electronically for HMDs. NVGs use only optical distortion corrective methods. Optical corrections increase the number of optical elements and weight. Electronic corrections can be analog for CRT displays, without any additional delays in the signal processing. Digital distortion correction can be applied to both CRTs and to discrete element displays such as LCDs and ELs. Digital processing may induce a possible image delay. However, required distortion corrections, particularly the electronic method, may reduce resolution or cause the resolution to vary across the display.

Field curvature

Field curvature induces changes in the refractive power from the center to the edges of the display. The effect is similar to spherical aberrations, except the center and edges of the display would have different focal distances. The center could be clear and the edges blurred, or vice versa, depending on the focus of the eyepiece. Field curvature can be compensated for by using additional lenses or curving the face of the display. With NVGs, the fiber-optic inverter of the image intensifier tube has a concave surface to reduce field curvature. For the IHADSS, a plano concave lens is placed on the plano CRT faceplate, which optically curves the image from a flat CRT faceplate.

Types

There are a number of HMD optical design types. Figures 16 and 17 show the ray trace differences between the various simplified eyepiece designs. For comparison purposes, the drawings of each eyepiece type design are equally scaled. The full scaled drawings used 30-mm eye clearances and 5-mm exit pupils to obtain a vertical FOV of 40°.

Refractive

The simplest NVG, HUD, and HMD use refractive, on-axis eyepiece optics. Examples are the ANVIS (Figure 16a) with no see-through vision and a reflex HUD (Figure 16b) with a 45° angle combiner and see-through vision. The see-through vision is provided with a partial reflective beam splitter or plano combiner. IHADSS HDU (Figure 17a), which is an HMD with see-through vision in the AH-64 aircraft for night pilotage, tilts the combiner to 38° from the last optical lens to improve eye relief. Refractive optical designs use lenses for imaging. The IHADSS HDU provides imagery and symbology from remote sensors, where the two night imaging sensors (I² tubes) are contained in the ANVIS. The primary advantage of the refractive design with a plano combiner is the high percent luminance transfer from the display to the eye. The primary disadvantages for refractive HMDs with see-through vision are excessive weight with limited fields of view and eye clearance.

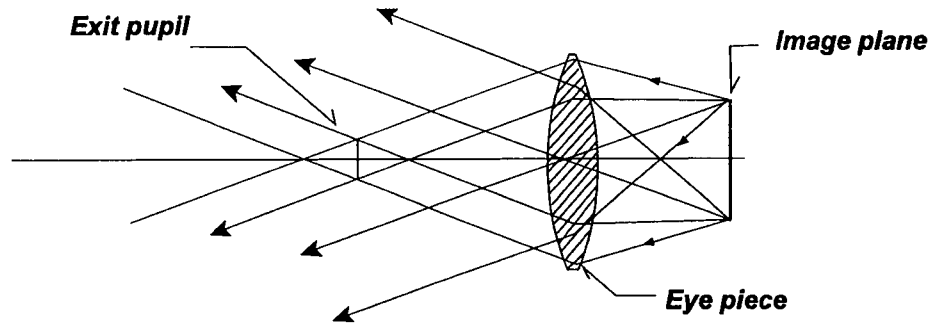
The ANVIS eyepiece is a simple well corrected magnifier with no see-through vision. Other NVG designs such as the Eagle Eye™ or the Cat's Eyes™ use prism combiners for see-through vision with I², but the see-through combiners with intensifier tubes have been used primarily by fixed-wing fighter type aircraft with HUDs. These see-through plano combiners are enclosed or sandwiched between two prisms which, when combined, form a plano refractive media with minimal prismatic deviation. The purpose of the prism combiners is to increase the combiner stability and increase the eye clearances for a given FOV and eyepiece diameter. Figure 17b shows a prism combiner using the IHADSS design. The prism combiners can also be used with power reflective combiners. Figure 17c shows a catadioptric eyepiece design without the prism combiner and Figure 17d with a prism combiner.

Catadioptric

Catadioptric optical designs use curved reflective mirrors with or without lenses for imaging (Figures 17c and d). The primary advantage of catadioptric designs is larger diameter optics with less weight and without induced chromatic aberrations. By coating transmissive curved surfaces with partial reflective materials to provide see-through vision, the beam splitter is referred to as a power combiner. Figure 17d shows the catadioptric design with a prism combiner to increase the eye clearance for a given FOV. The primary disadvantages are reduced luminance transfer from the display for a given percent see-through vision compared to refractive systems. Extraneous reflections have also been a problem area. The catadioptric designs can obtain slightly larger fields of view for a given eye clearance compared to refractive systems. Catadioptric designs have not been used in significant numbers for production HMDs at present, but have been used in a few HUDs (example OH-58D pilot display unit (PDU) for Stinger missiles).

Figure 18 shows comparison plots of the eyepiece diameters versus FOV for the refractive nonsee-through versus the various see-through HMD designs without prism combiners. The differences between the refractive and IHADSS HMDs are only in the angle of the combiner to the eyepiece and central ray to the eye. The refractive see-through HMD (Figure 16b) uses a

**Direct View - No See-through
Non pupil forming**



**Refractive - 45° Combiner
Conventional Head-up Display**

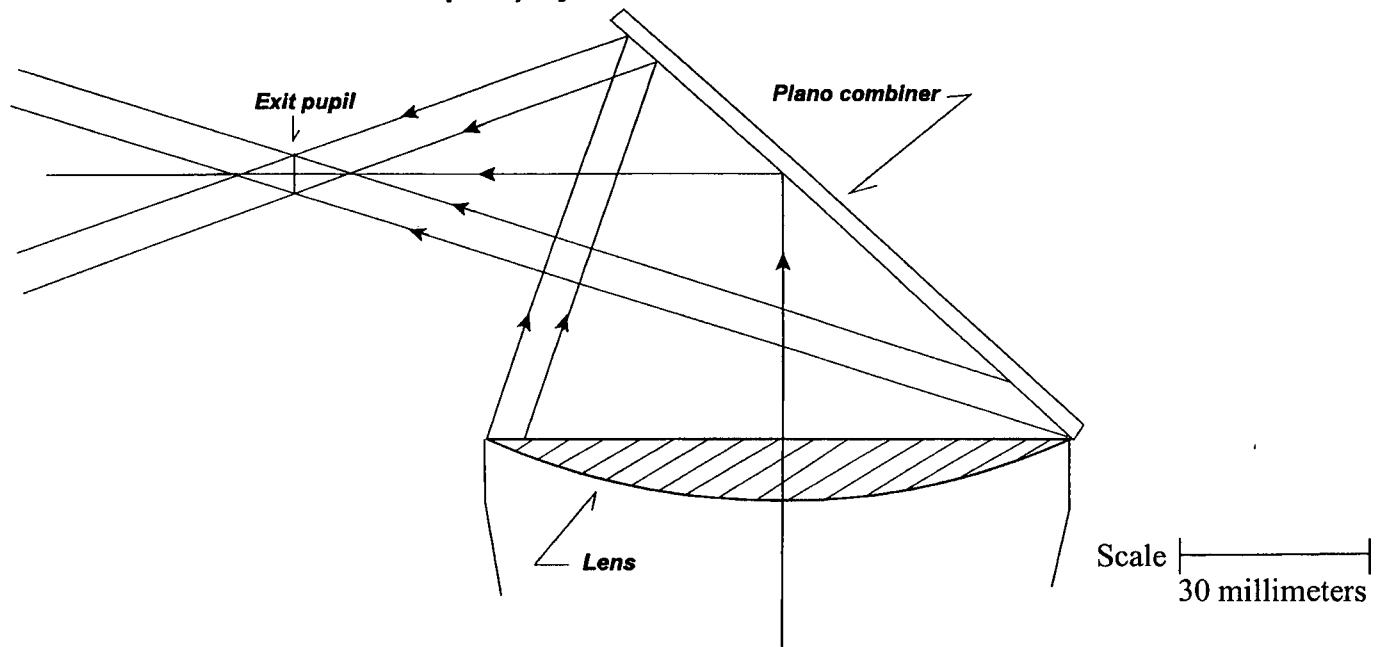


Figure 16. HMD eyepieces: a) Direct view, no see-through, NVG type eyepiece and b) refractive see-through combiner at 45°.

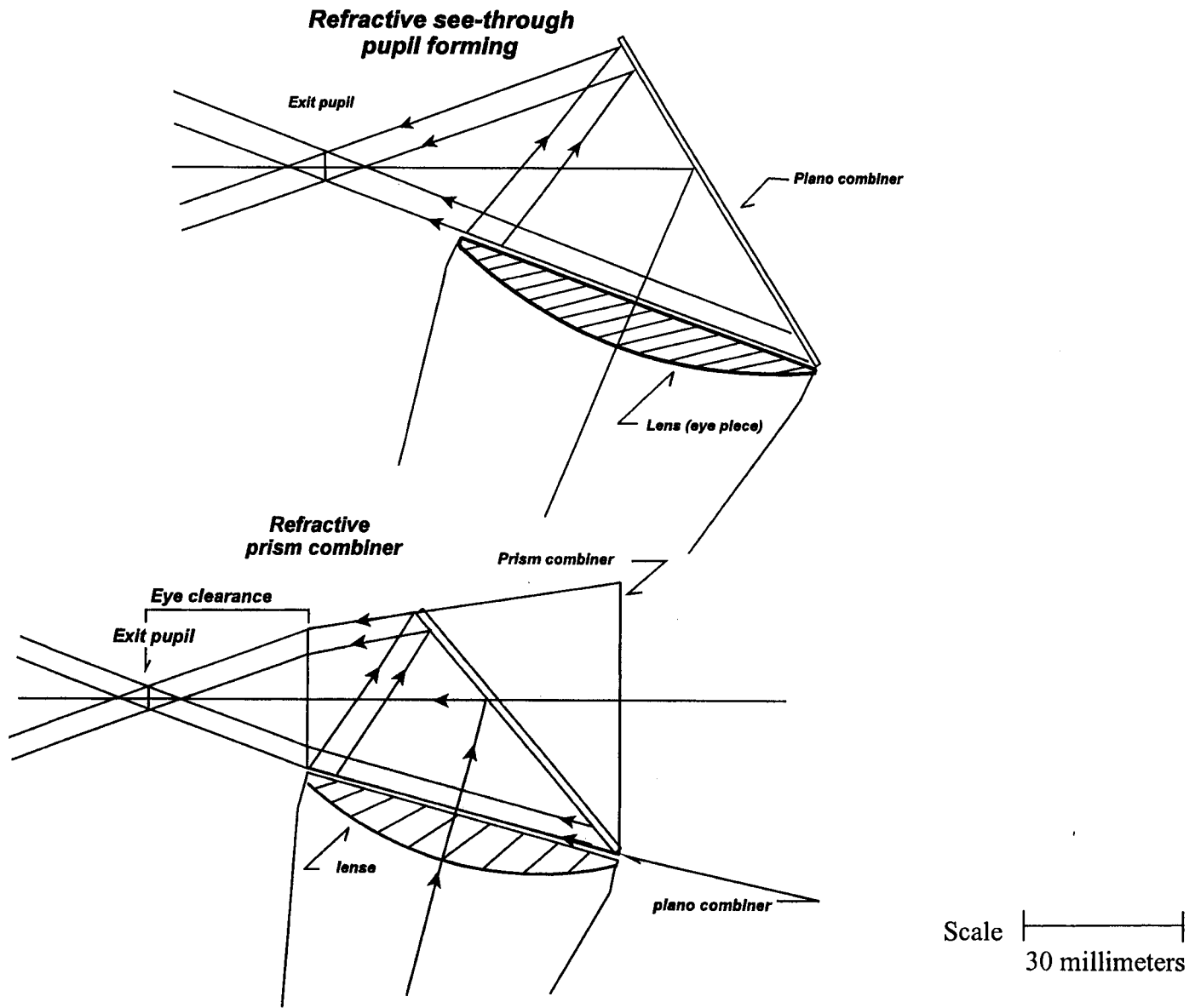
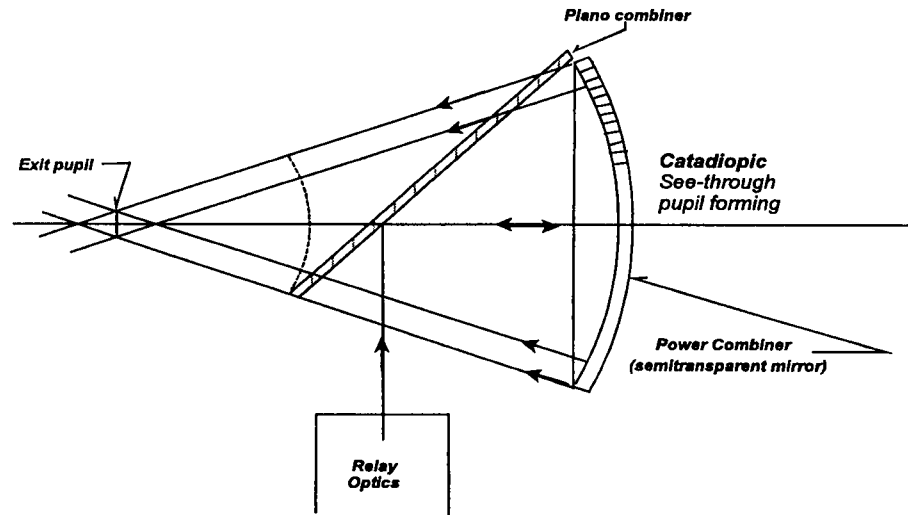
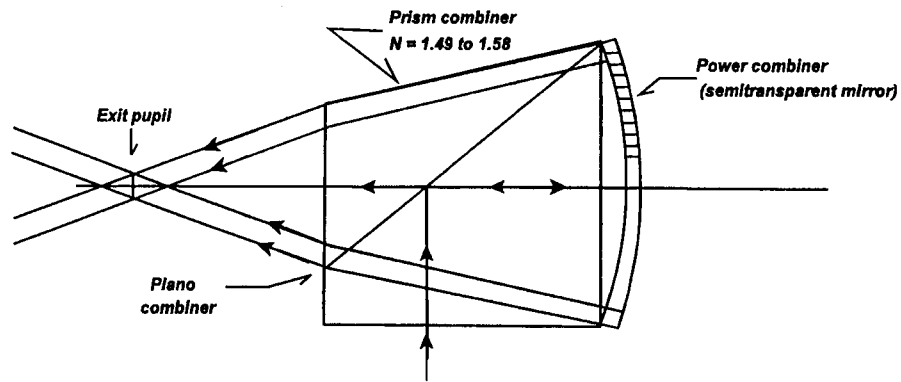


Figure 17. HMD eyepieces: a) Refractive (IHADSS), b) refractive prism combiner, c) catadioptric, and d) catadioptric with prism combiner.



Catadioptric Prism Combiner



Scale |—————|
30 millimeters

Figure 17. (continued)

constant 45° combiner angle for all FOVs, where the IHADSS HMD (Figure 17a) adjusts the lower FOV limit ray to run parallel with the eyepiece to minimize its diameter. The estimated 60-mm diameter eyepiece limit is based on mechanical considerations for the smaller IPD ranges and overlapped HMD FOVs.

Figure 19 graphs and compares the effects on the eyepiece diameter with and without prism combiners for the IHADSS and catadioptric designs. A high index of refraction plastic material (polycarbonate) was selected for the prism combiners ($n = 1.58$) for calculation purposes to obtain the maximum effect. Other materials could be selected for the prism combiners for the particular properties of the material such as lower weight and manufacturing qualities. Note that the surfaces closest and farthest from the eye of the prism combiners are parallel surfaces for the see-through vision. Without parallel surfaces, unwanted prismatic deviations or refractive powers would be induced. The prism combiner is actually more like a cube beam splitter, except the alignment of the beamsplitter does not have to be 45° to the central ray.

On- and off-axis designs

On-axis optical designs align the optical centers of each optical element, or slightly displace one of the elements which can be rotated to achieve vertical and horizontal alignment for binocular designs such as binoculars. The IHADSS and the ANVIS refractive designs use on-axis alignment. The on-axis, see-through catadioptric designs include power and plano combiners. Off-axis catadioptric systems are usually referred to as reflective off-axis systems and may or may not require plano combiners. As the off-axis angle to the power combiner increases, the induced distortions and aberrations increase rapidly (Buchroeder, 1987). An example of a modest off-axis catadioptric design with a plano combiner is shown in Figure 20 (Droessler and Rotier, 1989; Rotier, 1989). This catadioptric design achieves a 50° x 60° FOV with a 10-exit pupil and 30-mm eye relief (measured from plano combiner intercept to apex of eye along primary line of sight). However, note the optical complexity with 11 refractive elements and 3 reflective surfaces with very complex coatings for both eyepiece reflective surfaces to maximize see-through and display transmissions. The modest trapezoidal distortion of 7.5% (Figure 21) will be aligned with the power combiner. Another promising HMD is the Monolithic Afocal Relay Combiner (MONARC), which is an off-axis, rotationally symmetrical lens system with modest FOV potential, but excellent see-through approach (Figure 22). However, for any of the off-axis binocular systems, the distortions will have to be corrected to achieve point for point image alignment throughout the FOV.

The primary advantage of the off-axis reflective HMD design is that it provides the highest potential percent luminance transfer from the display with the most see-through vision and increased eye clearances for a given FOV. The primary disadvantages are very complex optical designs, shape distortions, and low structural integrity and stability of the reflective surface. Figure 23 shows the conceptual drawings (top and side view) of an off-axis HMD using the visor as the eyepiece. Note the locations of the aerial images, which are shown for the left eye. The location of the relay optics will be either on top of the helmet, or below, where both locations have undesirable characteristics such as a high center of mass, or produce lower obstructions to unaided vision. Also, note that the head seems to get in the way with the optics or relay image. Again, there have been prototypes and a few HUDs, but no production off-axis reflective HMDs. Where there are no provisions for electronic distortion correction, as found with NVGs, the off-axis designs become unacceptable from the keystone or trapezoidal type distortions.

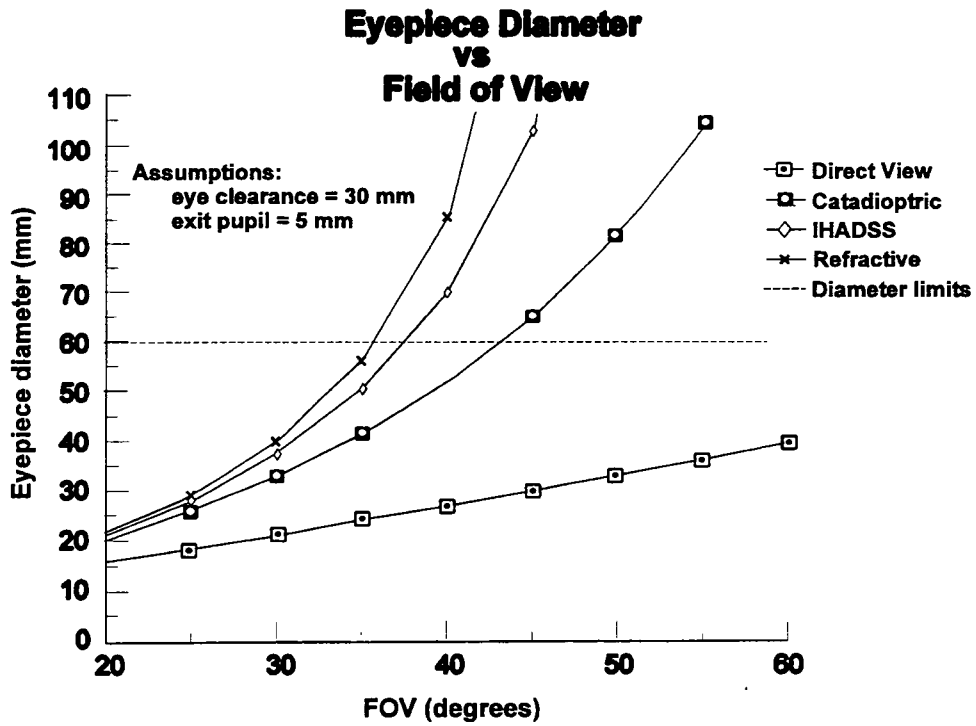


Figure 18. FOV versus eyepiece diameter for different designs.

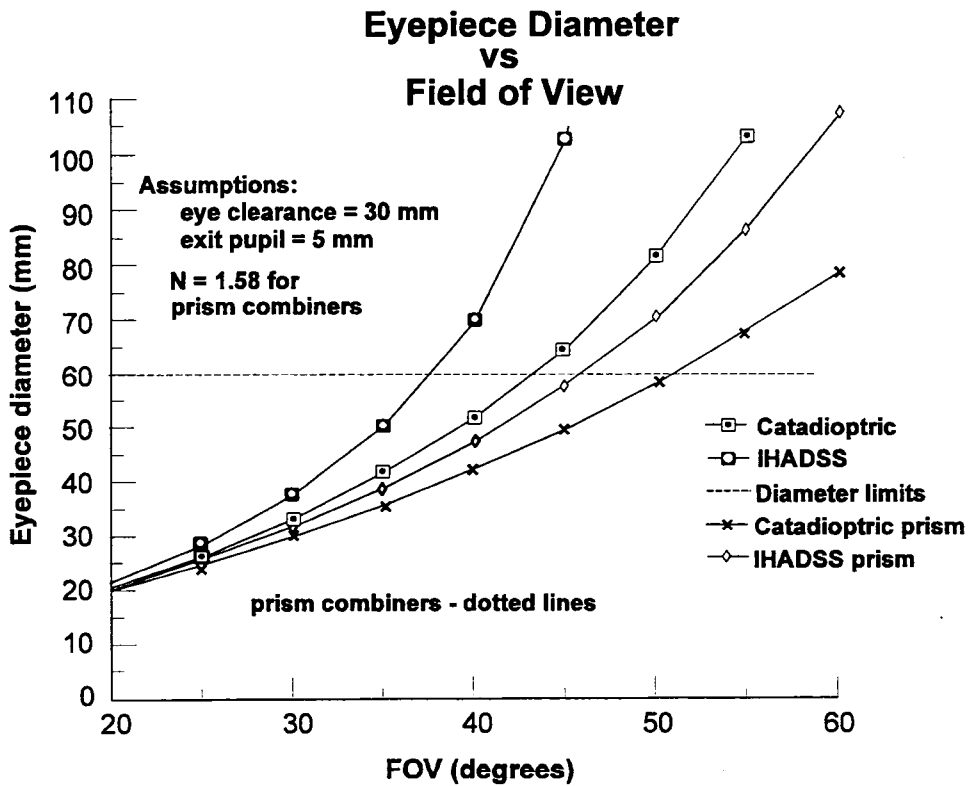


Figure 19. Comparisons between refractive and catadioptric HMDs with and without prism combiners.

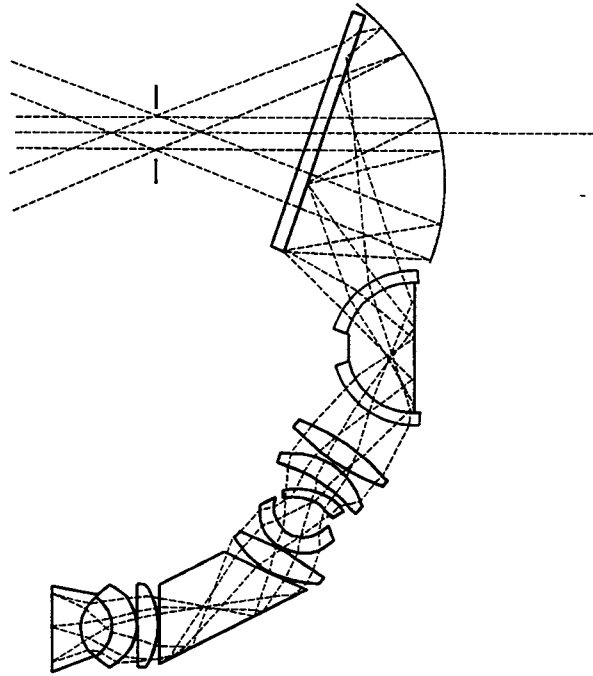


Figure 20. Ray trace of 50° x 60° tilted cat ocular (Droessler and Rotier, 1989).

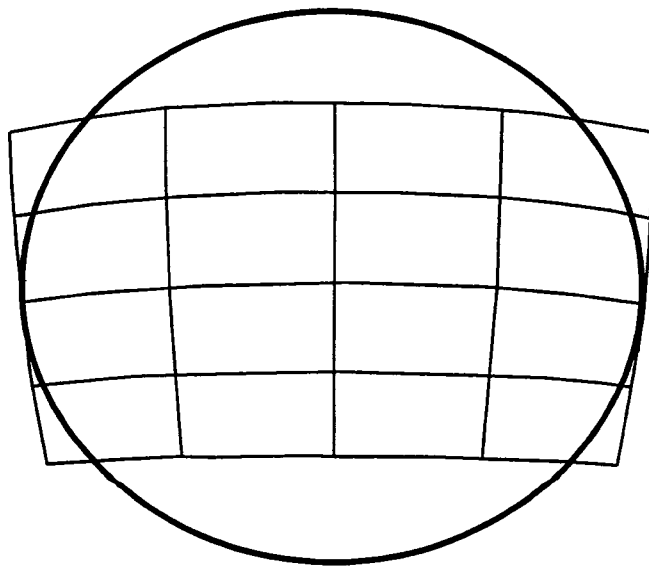


Figure 21. Optically induced distortion from tilted cat, off-axis HMD design.

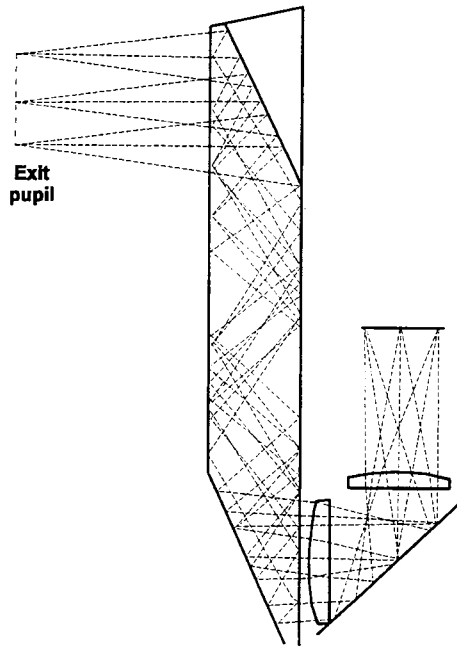


Figure 22. MONARC with rotationally symmetrical lens system (folded catadioptric).

Pupil and nonpupil forming

A nonpupil forming virtual display uses a simple eyepiece to collimate or focus a real image source. An example is NVG where eyepieces focus the 18-mm phosphor screens to produce a 40° FOV. The display size, eyepiece focal length, eye clearance, exit pupil diameter, and $f/\#$ define the FOV relationships similar to viewing through a knot hole (Figure 16a). A method to increase the apparent size of a display up to approximately 2x is with a coherent fiber-optic taper placed on the display. This approach based on a 1.5x taper was used with the Advanced I² program to obtain a 60° NVG FOV from the 18-mm diameter intensifier tubes. The disadvantages of the expanding taper are a slightly increased weight compared to the 40° FOV ANVIS and reduced light transmissions. However, without the taper, the increased tube diameter (from 18 mm to 27 mm) needed to obtain the same 60° FOV would weigh much more than the 18-mm tube with the 1.5x taper, but would not have a reduction in light transmission.

A pupil forming system has the same basic optical design as a compound microscope or telescope. Other common examples are rifle scopes, periscopes, and binoculars. For the pupil forming system, the eyepieces collimate virtual images that are formed using relay optics. The primary purpose of the relay optics is to magnify the real image with the eyepiece providing additional magnification. Relay optics can also transport and invert the image as in the case of a periscope. The pupil forming system forms a real exit pupil that can be imaged with a translucent screen. Unlike the knot hole analogy for the nonpupil forming device, the pupil forming system requires the pupil of the eye to be positioned within a specific area to obtain the full FOV. If the eye is moved closer than the exit pupil, the FOV will actually decrease. Also, if the eye is moved laterally outside the exit pupil, the complete display disappears where the nonpupil forming system merely vignettes the FOV in the opposite direction of lateral movement outside the exit pupil. The exit pupil for a pupil forming system is defined by the optical ray trace and is shown in Figure 24a for the center of the FOV and Figure 24b for the edge of the FOV. Note also the field lens, which is used to channel the aerial image to the eyepiece and adjust the eye clearance.

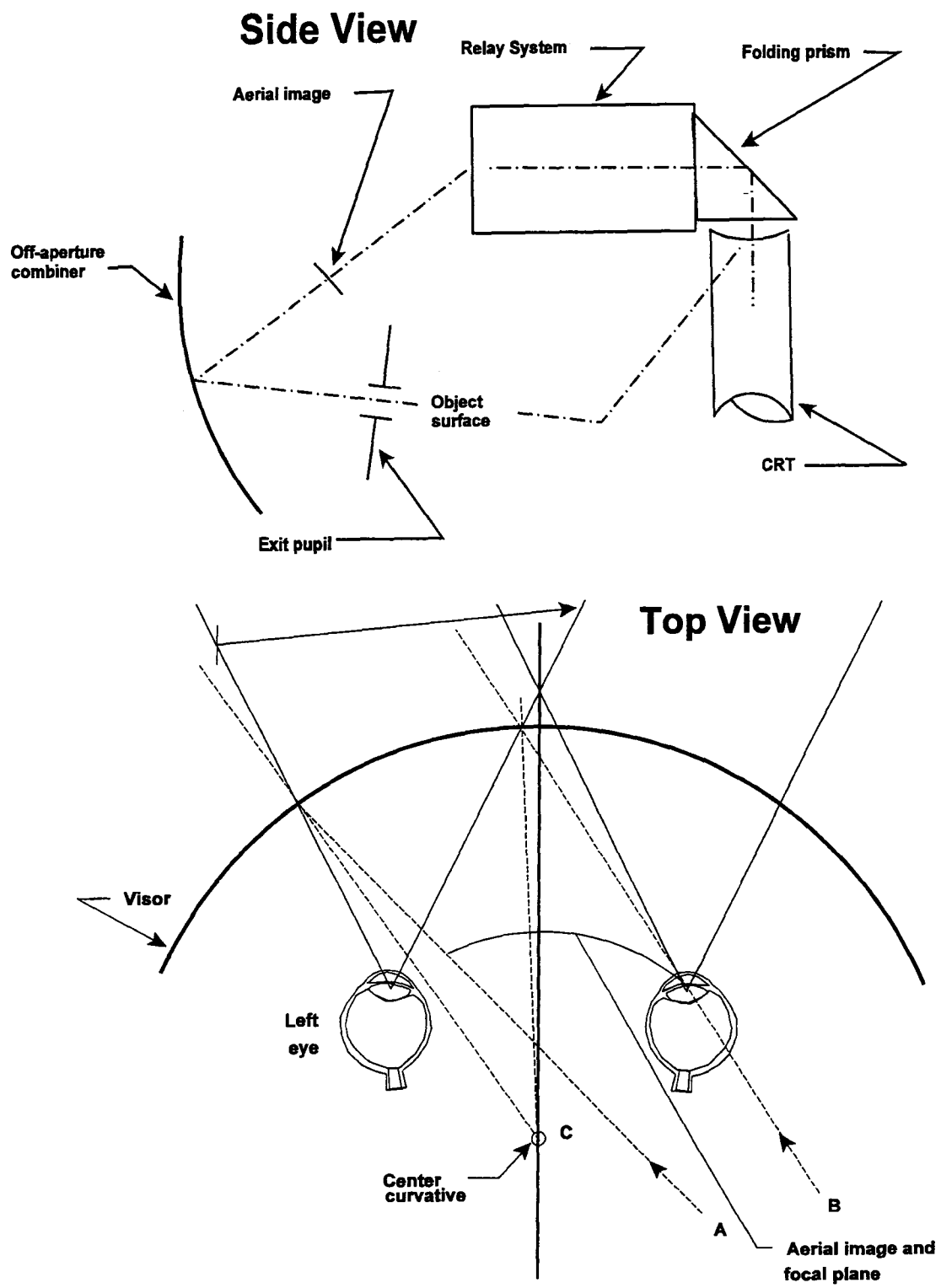


Figure 23. Reflective visor HMD: a) side view and b) top view (Skenker, 1987).

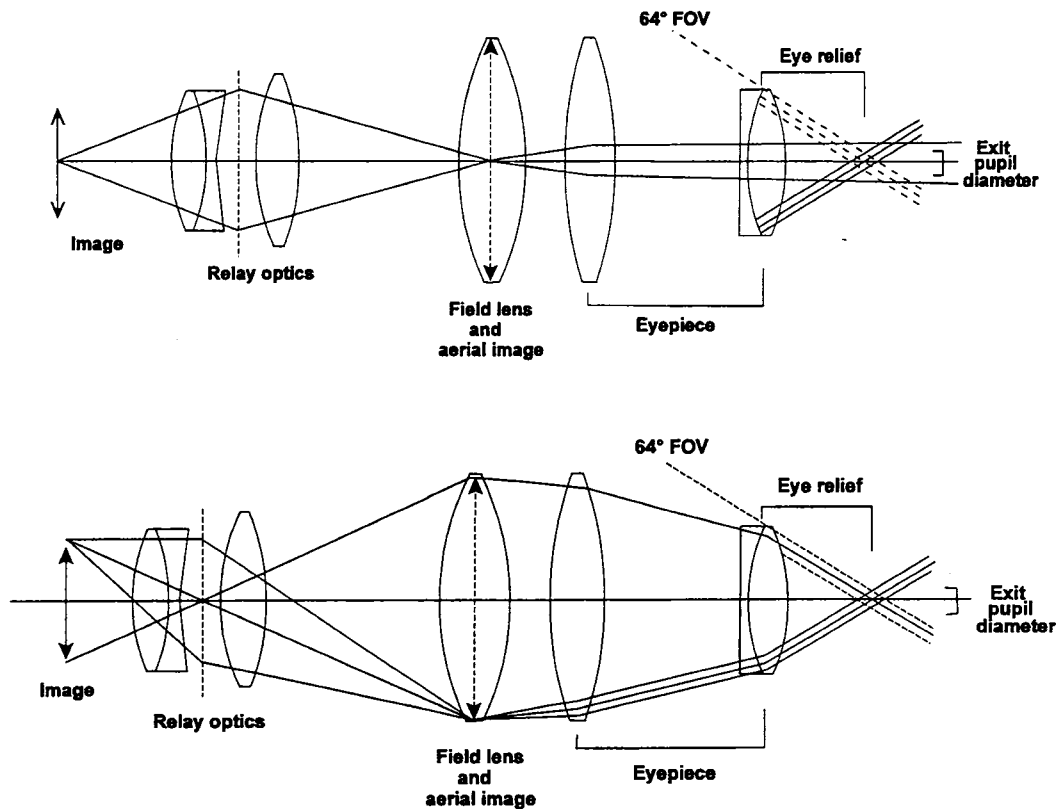


Figure 24. Ray trace of exit pupil formed by a) the center rays and b) the marginal rays for a pupil forming optical device.

The relay optics of pupil forming devices usually are determined after the type eyepiece design, FOV, optical length, exit pupil diameter, and eye clearance values have been defined. To minimize the size and weight of the relay optics, the designer will attempt to use the shortest optical path possible within mechanical constraints.

Partially silvered, dichroic, and holographic combiners

Partially silvered combiners are broadband reflectors of the visible wavelengths. The advantages of partially silvered combiners are minimal effects on color transmittance of the image source or see-through vision. Increasing the reflectance of the combiners increases the luminance transfer from the display, but proportionally reduces the see-through transmittance. The sum of the display transfer and see-through vision for partially silvered mirrors is always less than 100%.

Dichroic combiners reflect the primary wavelengths of the display and transmit the other visible wavelengths. When using narrow band phosphors such as P43 phosphors, the sum of the percent luminance transfer from the display and the percent see-through vision can be greater than 100%. The primary disadvantage of a dichroic combiner is the effects of color perception with see-through vision. Typically, the wavelengths optimized for reflection by the combiner are also one of the wavelengths of head-down displays.

Holographic combiners are essentially diffraction gratings for use with monochromatic or very narrow band light. The primary advantages of a holographic combiner are: a) it has a high luminance transmittance and see-through vision; and b) the apparent shape and tilt of the holographic reflective surface do not have to conform to the normal equal angles for incidence and reflection. Thereby, the shape of the combiner may take the form of a visor. However, the quality of the image is degraded as the tilt angle of the final reflective surface deviates from the normal equal angles for incidence and reflection (Buchroeder, 1987). The holographic combiner typically is shown as a visor type eyepiece which was discussed in the off-axis HMD section. Some of the disadvantages of holographic combiners are durability and reproducibility concerns; see-through vision is also altered in color and light scattering characteristics.

The holographic combiner sandwiched in a visor has been the goal of many programs to produce wide FOV, luminance efficient, high resolution, and cosmetically pleasing helmet mounted displays for aviation. However, this technological approach basically defies the laws of optics. The off-axis power combiner hologram in a visor basically requires a top location for the display and relay optics. As previously stated, this top location for the relay optics and the display places the head borne CM in an undesirable location and the upper head room area is the least available for modern scout and attack aircraft.

Visual coupling

One HMD enhancement to mission effectiveness is the providing of video imagery used for pilotage (most effective during night and foul weather missions). This pilotage imagery is generated from sensors. These sensors can either be head/helmet-mounted, as with ANVIS, or aircraft-mounted, as with the FLIR on the AH-64 Apache. With head-mounted sensors, the resulting imagery is inherently correlated with the direction of head line-of-sight. However, to obtain this spatial correlation for aircraft-mounted sensors, it is necessary to slave the sensor to head motion; the sensor must be "visually coupled" to the head. [It should be noted that true line-of-sight is defined by eye gaze direction as well as head direction.] To accomplish this task, a head/eye tracking system is incorporated into the HMD (Figure 5). This visual coupling also provides the capability to point (aim) fire control systems (weapons). Visual coupling takes advantage of the natural psycho-motor skills of the aviator (Brindle, 1996).

Tracking systems

The fundamental concept of a visually coupled system (VCS) is that the line-of-sight-direction of the aviator is continuously monitored and any change is replicated in the line-of-sight-direction of the (aircraft-mounted) sensor (Task and Kocian, 1995). The subsystem which detects these changes in head/eye position is called a tracking system (or tracker). As hinted at before, tracking systems may detect only head position (and are called head trackers), may detect only eye position (and are called eye trackers), or may be a combination (providing both eye and head position tracking). Currently, military VCSs use only head trackers to direct pilotage/targeting sensors and weaponry. More sophisticated HMDs, which may wish to use eye movement to control switches or position of imagery insets, may incorporate eye trackers.

Tracking systems with helmet-mounted components must minimize the additional weight, volume, and packaging impacts on the HMD. This is best achieved by using an integrated approach in the HMD design (Thomas, 1989). The various subsystems, e.g., the helmet, optics, etc., still perform their basic functions with minimal compromise to these functions and those of other subsystems. Tracking components which must be helmet-mounted can be modular (add-on), but integrated approaches allow for the imbedding of these components into the helmet shell, thereby optimizing the HMD packaging.

Head trackers

The simplest type of tracking is head tracking, where the position of the head pointing direction is constantly measured. Four major head tracking technologies are currently available: Magnetic, EO, acoustical (ultrasonic), and mechanical. Magnetic head tracking systems (HTSs) have rapidly become the tracking system of choice for HMDs. This is due to their high accuracy and extremely low impact on HMD (and aircraft) weight, size, and packaging. They also can provide tracking in 6 degrees of freedom. Magnetic trackers can be AC or DC. Each uses a transmitter attached to the aircraft and a receiver attached to the helmet (Figure 25). The transmitter fills the cockpit with a magnetic field. Through the measurement of the magnetic field strength at the receiver, the position and orientation of the head can be determined (Cameron, Trythall, and Barton, 1995). The major drawback to magnetic trackers has been their susceptibility to distortion by conducting metallic objects in the cockpit. This has been overcome partially by pre-mapping the magnetic field of the cockpit, a one time, but complicated, calibration (unless the cockpit is modified). Problems with magnetic trackers have included a limited motion box (volume through which the head can move and the tracker perform effectively), noise, jitter, and poor dynamic response. Recently, major advancements in AC magnetic trackers have produced a "very robust metal tolerant" system which overcomes many previous problems (Hericks, Parise, and Wier, 1996). Continuing advances in integrated chip technology have advanced magnetic (and other) tracking systems through the development of high speed digital signal processors (Murry, 1995).

There are several approaches to EO head trackers. These range from the use of video cameras to infrared beams. The AH-64 Apache uses an EO tracker. It operates using two pair of lead sulfide photodiodes mounted on the helmet. The two infrared sources are mounted behind the aviator's seat (Figure 26). These photodiodes continuously assess their position relative to the sources and, therefore, the position/orientation of the aviator's head line-of-sight. These position data are processed and passed to the AH-64's FLIR sensor gimbal. EO HTSs must be able to operate without interference under combat lighting conditions.

The two remaining types of HTSs, mechanical and acoustical, have not been implemented to any great degree. Mechanical trackers require physical linkages to the helmet, raising obvious safety issues during crash scenarios. Acoustical (ultrasonic) trackers suffer from susceptibility to high frequency background noise and the requirement for demanding high component mounting accuracy during installation (Cameron, Trythall, and Barton, 1995).

Regardless of the technology, an HTS must provide defined measures of accuracy. System parameters include motion box size, pointing angle accuracy, pointing angle resolution, update rate (of tracker, not display), and jitter. The motion box size defines the linear dimensions of the space volume within which the HTS can accurately maintain a valid line-of-sight. The box is referenced to the design eye position of the cockpit. It is desirable that this box provide angular coverage at least equal to that of normal head movement, i.e., $\pm 180^\circ$ in azimuth, $\pm 90^\circ$ in elevation, and $\pm 45^\circ$ in roll (Task and Kocian, 1995). The motion box size for the AH-64 IHADSS is 12 inches forward, 1.5 inches aft, ± 5 inches laterally, and ± 2.5 inches vertically from the design eye position. From a human factors viewpoint, it is important that the motion box be able to accommodate multiple seat positions and aviator posture variances.

Pointing accuracy, also referred to as static accuracy, usually means the performance within the local area of the design eye position and for an angular coverage of $\pm 30^\circ$ in azimuth and

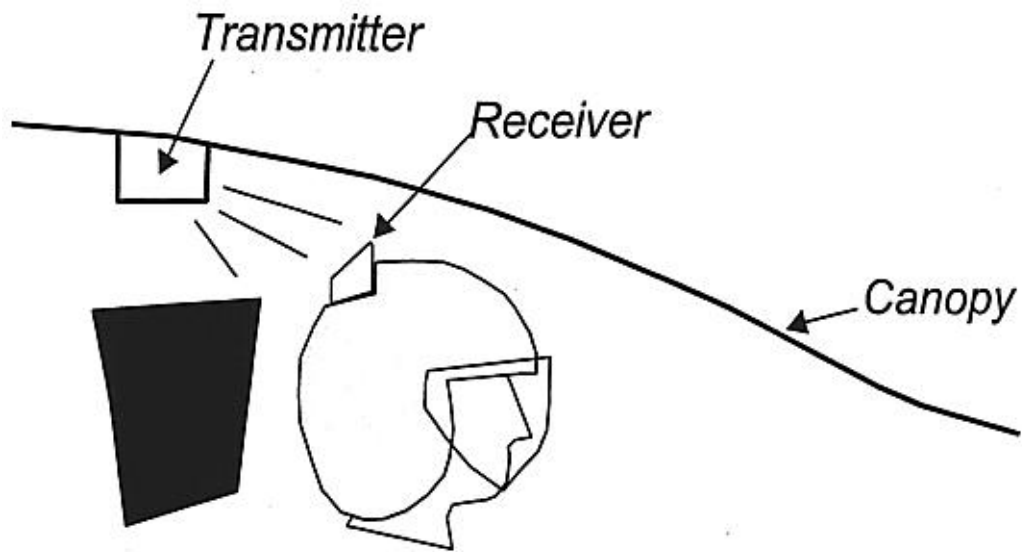


Figure 25. Typical magnetic tracker.

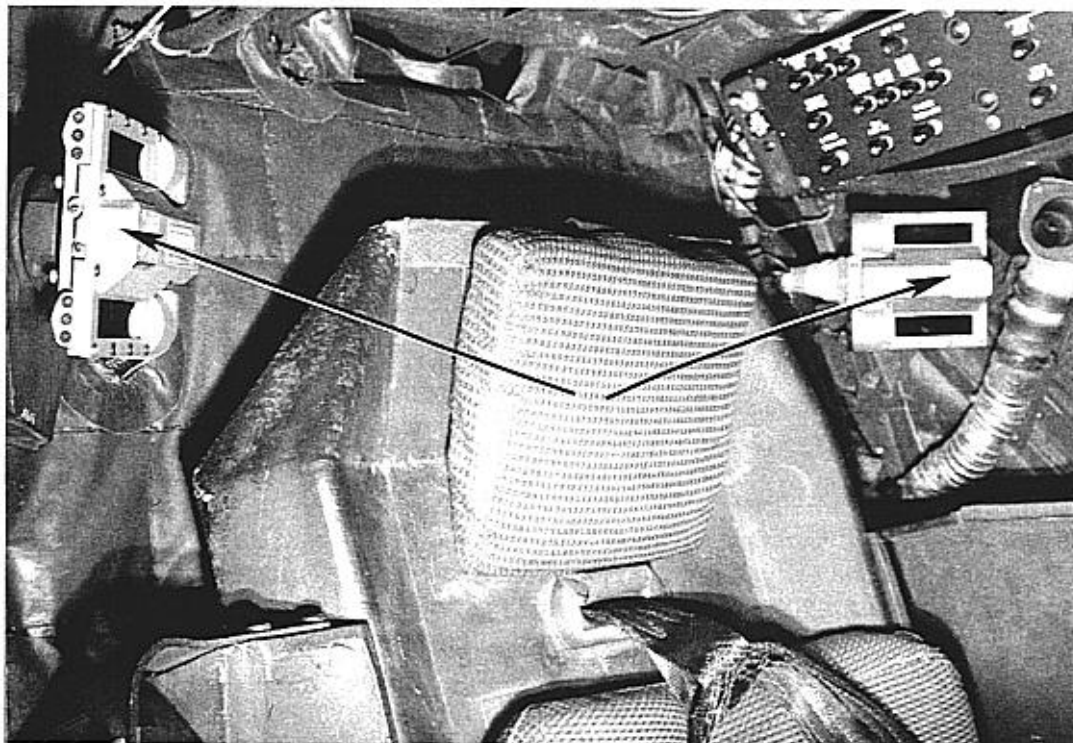


Figure 26. AH-64 EO tracker.

$\pm 70^\circ$ in elevation, i.e., the envelop where the head spends most of its time (Task and Kocian, 1995). In a laboratory setting, current systems can provide excellent static pointing accuracies of 1 to 2 milliradians (mr) (at least in azimuth and elevation, roll accuracy is more difficult to achieve). Measured accuracies in actual aircraft are more typically in the 3 to 4 mr range. Maximum static accuracy is limited by the system's pointing resolution. Pointing resolution refers to the smallest increment in head position (or corresponding line-of-sight angle) which produces a difference in HTS output signal level. One recommendation (Rash et al., 1996a) states that the HTS should be able to resolve changes in head position of at least 1.5 mm along all axes over the full motion box. HTSs also need to provide a specified dynamic accuracy, which pertains to the ability of the tracker to follow head velocities. Dynamic tracking accuracy (excluding static error) should be less than 30 mr/sec.

HTS update rate performance is an often poorly defined parameter. To be useful, update rate must be defined in terms of the sampling rate and the tracking algorithm (Task and Kocian, 1995). Sampling rates of >100 Hz are available. Both IHADSS and HIDSS use a 60 Hz rate. However, if the display update rate is slower than the HTS sampling rate, then these higher rates do not offer an advantage.

Variations in head position output due to vibrations, voltage fluctuations, control system instability, and other unknown sources are collectively called jitter. Techniques to determine the amount of jitter present are extremely system specific.

Eye trackers

When viewing or tracking objects in the real world, a combination of head and eye movements is used. [It is an unnatural act to track or point using the head alone. Normal head and eye coordinated motion begins with the eye executing a saccade towards the object of interest, with velocities and accelerations exceeding those of the associated head motion. Consequently, the eye reaches the object well before the completion of the head motion (Barnes and Sommerville, 1978).] Eye movements are confined to $\pm 20^\circ$ about the head line-of-sight. To replicate this viewing mode, more sophisticated VCSs may augment head tracking with eye tracking. This higher order tracking capability would be required for visual operation of switches, use of high resolution FOV insets, and future advanced optical/visual HMD enhancements. For example, several HMD designs (Fernie, 1995; Barrette, 1992) have explored the concept of creating within the HMD's FOV a small inset area of increased resolution which is slaved to eye movement (Figure 27). Such "area of interest" displays overcome the computational problems of trying to provide high resolution, wide field-of-view imagery in real time. This is achieved by mimicking the eye's design of maximum visual acuity within a central high resolution area (fovea - 2° diameter area) (Robinson and Wetzell, 1989). Such designs would help the long standing conflict between wide FOV and high resolution, currently design tradeoff parameters.

Eye tracking devices must be usable over the range in which the "area of interest" inset can be positioned. They must have sufficient spatial and temporal resolution to accommodate the high velocity and acceleration rates associated with the saccadic movements of the eye, which can be $> 800^\circ/\text{sec}$ and $> 2000^\circ/\text{sec}^2$, respectively. They also must operate over a wide range of illumination levels, pupil sizes, and other physical ocular differences. And, they have to be able to address all these variations, in real time, while ignoring meaningless artifacts (Robinson and Wetzell, 1989).

Eye trackers can be monocular or binocular and can measure movements along both horizontal and vertical axes. There are a number of techniques used in these devices for

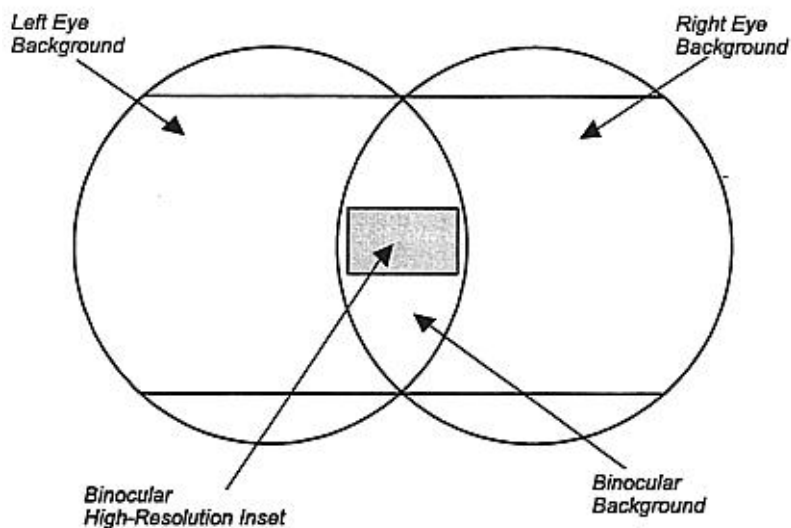


Figure 27. High resolution inset in HMD FOV.

detecting eye movements. These include the use of electrodes to measure minute electrical voltages in eye muscles responsible for eye movements, the detection of Purkinje images formed by reflections from the cornea and lens of the eye (Crane, 1994), the Limbus reflection method using an infrared (IR) LED on the border between the cornea and the sclera of the eye (Onishi et al., 1994), and a method where a coil is attached to the eye and its coupling effect to another stationary coil is measured. However, techniques which are adaptable to HMDs use a principle of reflecting IR energy from an IR LED(s) off the eye back into an IR detector(s). One design uses pulsed IR LEDs to illuminate the orbital field of the eyes. The distribution of the reflected energy, which changes with eye movement, is detected by an array of photodiode detectors (Permobil Medtech, Inc., 1997).

For HMD applications, eye tracking would be used in conjunction with head tracking.

Alternative tracking technology

For the purpose of completeness, an alternative method of slaving off-head sensors and weapons to aviator line-of-sight will be included. This novel, and currently futuristic, method is based on using electroencephalogram (EEG) patterns to control certain functions (McMillan, 1995). One such "brain actuated" control under investigation is based on the concept of recognizing the alpha- and gamma-band EEG patterns which precede certain muscular movements. More complex control applications based on self-regulation of the amplitude of a sensori-motor rhythm known as "mu" have been explored in EEG control of a roll position indicator in a simulator (Wolpaw and McFarland, 1994).

System (lag) delay

For HMDs where the sensor is helmet-mounted, as with ANVIS, the head and sensor are directly coupled and act as one unit. There is no time delay associated with this coupling. However for aircraft-mounted sensor systems, the very presence of a VCS implies that there will be a delay between the real world and its presentation (Tsou, 1993). This delay is present

because the VCS has to calculate the head positions, translate them to sensor motor commands, and route these commands to the sensor gimbal. Then, the gimbal must slew to the new positions and the display must be updated with the new images. If the magnitude of the delay is large enough, several image artifacts may occur: image flicker, simultaneously occurring objects, erroneous dynamic behavior, and/or multiple images (Eggleston, 1997).

The natural question is: How fast should the VCS be in transferring head motion to sensor motion and then presenting the new imagery? Its answer depends strongly on the maximum slew rate of the sensor gimbal. The inability of the sensor to slew at velocities equal to those of the aviator's head will result in significant errors between where the aviator thinks he is looking and where the sensor actually is looking, constituting time delays between the head and sensor lines-of-sight. Medical studies of head motion have shown that normal adults can rotate their heads $\pm 90^\circ$ in azimuth (with neck participation) and -10° to $+25^\circ$ in elevation (without neck participation). These same studies show that peak head velocity is a function of anticipated movement displacement, i.e., the greater the required displacement, the higher the peak velocity, with an upper limit of $352^\circ/\text{sec}$ (Zangemeister and Stark, 1981; Allen and Hebb, 1983). However, these studies were laboratory-based and may not reflect the velocities and accelerations indicative of the helmeted head in military flight scenarios (Rash, Verona, and Crowley, 1990).

In support of the AH-64 Apache, Verona et al. (1986) investigated single pilot head movements in an U.S. Army JUH-1M utility helicopter. In this study, head position data were collected during a simulated mission where four JUH-1M aviators, fitted with prototype IHADSS helmets, were tasked with searching for a threat aircraft while flying a contour (50 to 150 feet above ground level) flight course. These acquired position data were used to construct frequency histograms of azimuth and elevation head velocities. Although velocities as high as $160^\circ/\text{sec}$ to $200^\circ/\text{sec}$ in elevation and azimuth, respectively, were measured, approximately 97% of the velocities were found to fall between a range of $0^\circ/\text{sec}$ to $120^\circ/\text{sec}$. This conclusion supported the design slew rate value of $120^\circ/\text{sec}$ for the AH-64 FLIR sensor. It also lent validity to the complaints attributed to the second AH-64 targeting FLIR (used by copilot/gunner) of being too slow, having a maximum slew capability of only $60^\circ/\text{sec}$. It has been recommended that a $300^\circ/\text{sec}$ slew rate and $5000^\circ/\text{sec}^2$ acceleration is required to minimize delays and artifactual errors (Krieg et al., 1992).

However, VCS lags are not the only delays in the presentation of imagery in HMDs. King (1995) cites three types of time lags which must be considered in HMD use: Display lag, slaving lag, and sensor/weapon feedback lag (Figure 28). Display lag is defined as the display latency relative to the current helmet line-of-sight and includes the update rate of the tracker and the refresh rate of the display. Slaving lag is defined as the latency of the sensor/weapon line-of-sight relative to the helmet line-of-sight. This includes the tracker computational time, data bus rate, and physical slaving of the sensor/weapon. Sensor/weapon feedback lag is the latency involved in getting the slave command to the slaving mechanism (gimbal). King (1995) provides typical values for these three lags as 50, 650, and 150 msec, respectively.

When discussing time delays in HMDs in the display community, it has been customary to use the term "lag" to mean the time between when the head moves and when the presented image changes to reflect this movement. The frequency at which new display image frames are presented (display refresh) is called the update rate. However, other disciplines do not adhere to this format, and it is wise to precisely define all delay times used with HMDs and VCS.

So and Griffin (1995) investigated the effects of lag on head tracking performance using lag times between head movement and target image movement of 0, 40, 80, 120, and 160 msec.

They found that head tracking performance was degraded significantly by lags greater than or equal to 40 msec (in addition to a 40 msec delay in the display system). A similar study (Rogers, Spiker, and Fisher, 1997) which investigated the effect of system lag on continuous head tracking accuracy for a task of positioning a cursor on a stable target found performance effects for lags as short as 20 msec (plus 40 msec display system delay).

The studies cited above, and others (Whiteley, Lusk, and Middendorf, 1990; Boettcher, Schmidt, and Case, 1988; Crane, 1980), suggest that there is some uncertainty in maximum allowable time delays, ranging from 40 to 300 msec, depending on task and system. Wildzunas, Barron, and Wiley (1996) utilized a NUH-60 Blackhawk simulator to investigate the delay issue under a more realistic military aviation scenario. They tested delays of 0, 67, 133, 267, 400, and 533 msec. The delays were inserted into the simulator's visual display. However, while more representative of rotary-wing flight, the displays were panel-mounted, not head-mounted. While finding some performance effects for delays less than or equal to 267 msec, consistently significant effects were found for the 400 and 533 msec delays.

Data show that lags, attributed to the display and VCS, must be minimized. Strategies to achieve this include improved engineering designs, faster processing chip technology, and the use of predictive algorithms (Nelson et al., 1995; So and Griffin, 1992). Failure to achieve an acceptable maximum lag value has been shown to degrade visual tracking performance, introduce image artifacts, and sometimes promote motion sickness (Moffit, 1997; Kalawsky, 1993; Biocca, 1992).

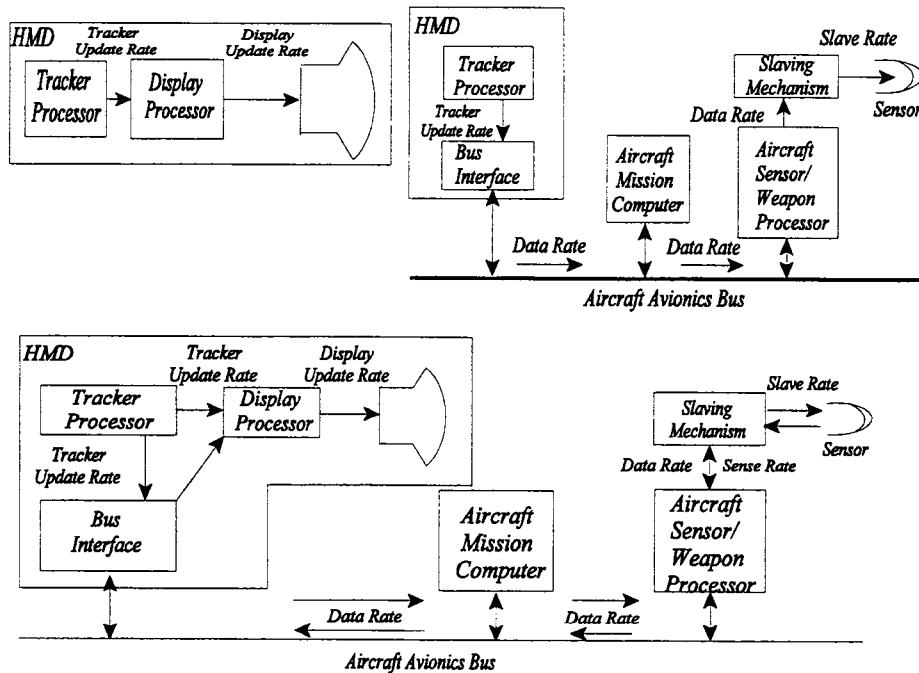


Figure 28. Latencies in HMD systems (King, 1995).

Roll compensation

Some tracking systems provide only head azimuth and elevation information, as does the AH-64 Apache head tracker. However, there has been a growing interest in providing 3-axis information, with head roll added. The Comanche plans to provide this capability. The addition of roll information provides the capability of keeping the imagery aligned with the aircraft structure (Task and Kocian, 1995). The availability of roll compensation is considered to be an advantage and should reduce workload. After all, the human visual system acts this way, and roll compensation is intrinsic to all HMDs with helmet-mounted sensors, such as with ANVIS. In see-through HMDs, where the imagery or symbology is used for daytime flights, roll compensation will prevent misregistration between the imagery or orientation symbology with the outside world. Also, as wider FOV HMDs are developed, the displayed imagery becomes more compelling and may require roll compensation (Haworth, 1997). However, Apache aviators informally state that they would not like the addition of roll compensation. Their argument being they are more interested in aircraft roll with respect to the horizon, than the visual effect of head roll. To maintain this awareness with roll compensation, additional symbology would have to be added.

Roll compensation can be accomplished by roll stabilizing the sensor, a mechanical challenge. More likely, it will be accomplished in image processing, which introduces an additional time delay. If accomplished electronically, other problems will arise. When a rectangular image is rotated, the corners will be clipped, causing a loss of FOV. In addition, unless compensated, information from the attitude indicator would be confusing.

In an investigation of weapon aiming performance, Michael, Jardine, and Goom (1978) concluded that any rotary-wing aircraft maneuver which caused the HMD sighting image to roll resulted in considerable tracking/aiming performance degradation, independent of flight experience.

Vibration

Helicopters vibrate and any aviator will tell you that is an understatement. This vibration affects both the aircraft and the aviator. Human response to this vibration has been a more difficult problem to understand and solve than that with the aircraft (Hart, 1988). The effects of vibration manifest themselves as retinal blur, which degrades visual performance, and as physiological effects, whose resulting degradation is not fully understood (Biberman and Tsou, 1991). Rotary-wing aircraft differ in their vibrational frequencies and amplitudes and these vibrations are triaxial in nature. However, in general they have a frequency range in all axes of 0.5-100 Hz. However, specific frequencies of significant amplitude are associated with the revolution rates of the rotor, gears, engines, and other mechanical components (Boff and Lincoln, 1988). The largest amplitude frequency occurs at the main rotor blade frequency multiplied by the number of blades. Other frequencies having significant amplitude include the main rotor frequency (~7 Hz); twice, eight, and twelve times the main rotor frequency, tail rotor frequency (~32 Hz), twice the tail rotor frequency, and the tail rotor shaft frequency (~37 Hz). These vibrations are transmitted to the head through the seat and restraint systems (peak transmission, 3-8 Hz). This vibration is typically in the vertical and pitch axes and are affected by posture, body size, and add-on masses, such as helmets). However, the transfer function of these vibrations to the eye is not straightforward. The activity of the vestibulo-ocular reflex stabilizes some of the vibrational transfer, mostly low frequency. However, visual performance degradation still will be present. To further complicate this scenario, the vibrational transfer function to the helmet and HMD is different from that to the eye. While the general influencing factors are the same, e.g., posture, body size, etc, the helmet/HMD mass is also a factor. The result is a very complex frequency

and amplitude relationship between the eye and the HMD imagery, which results in relative motion between the imagery and the eye (Wells and Griffin, 1984).

Viewing collimated (infinity focused) HMD imagery should in theory eliminate nonangular vibration effects on visual performance. However, investigations of visual performance with HMDs under the relative motion between the display and the eye due to vibration have shown a number of effects. At frequencies below 10 Hz, reading information off the HMD is more difficult than reading off panel-mounted displays (Furness, 1981), up to tenfold at some frequencies. In an investigation of reading HMD symbology numerals, numerals which could be read correctly in 0.4 second while stationary on the ground required 1.0 second in flight (Wells and Griffin, 1987a). This will result not only in increased error but also increased reaction time.

Since HMDs are used also as weapon aiming systems, similar performance effects might be expected. Aircraft vibration (and voluntary head movements) causes reflexive eye responses. Again, the vestibulo-ocular reflex is to induce eye movement opposing the head movement, thus stabilizing the eye to the outside world (Barnes and Sommerville, 1978). However, if the target has a velocity component in the axis of the vibration or head movement, these induced eye movements are undesirable and can produce tracking error. Indeed, numerous studies (Verona, Johnson, and Jones, 1979; and Wells and Griffin, 1987b,c) have shown that tracking error increases significantly in vibrational environments. However, Butler, Maday, and Blanchard (1987) showed that the greatest of such errors occurred for vibrations in the x-axis, followed by the z-axis, followed by the y-axis. For the rotary-wing environment, this is somewhat beneficial in that z-axis vibration dominates with little x-axis vibration.

To overcome these vibration induced degradations in visual performance, one can take the basic engineering approach of reducing the amplitude of the identified vibration frequencies. Another approach is to utilize active image stabilization techniques (Wells and Haas, 1992). One such technique, adaptive noise-cancellation, acts as a low pass filter, passing low frequency voluntary head motions, while dampening unwanted higher vibrations (Velger, Merhav, and Grunwald, 1986). A less attractive approach recommends increasing the size of the alphanumeric characters, thereby reducing the effects of vibration (Lewis and Griffin, 1979). However, this will increase clutter or reduce the amount of information which can be displayed.

One final point regarding vibration: Most HMD designs are exit pupil forming systems. They can, in a very loose analogy, be compared to knotholes in a fence. To have an unobstructed view, you must put, and keep, your eye in the knothole. The exit pupil is the HMD's knothole. To prevent vignetting of the full image, the aviator must keep his eye within the exit pupil. If the exit pupil is large enough, additional vibrational effects can be ignored. However, if the exit pupil is small, then the eye may move out of it under the influence of vibration.

Sensor switching

The current version of the Comanche HIDSS expects to provide both I² and FLIR imagery. While the final decision on whether the I² sensor(s) will be aircraft- or head-mounted is yet to be made, the current HIDSS design is based on all sensors being mounted on the aircraft. If at a later date, a decision is made to mount the I² sensor(s) on the helmet, then aviators will be in a situation where they will be switching back and forth between sensor imagery originating from two different perspectives (Rash, Verona, and Crowley, 1990). The human's basic visual sensors are his/her eyes. Prior to encountering aircraft-mounted sensors, his experience in perception and interpretation of visual information has been referenced to the eye's position on the head. When flying the Apache, the imagery often is from the FLIR sensor. This sensor is located on the nose of the aircraft and is approximately 10 feet forward and 3 feet below the aviator's design

position. This exocentric positioning of the imagery source can introduce problems of apparent motion, parallax, and incorrect distance estimation (Brickner, 1989). However, this mode of sensor location does offer the advantage of allowing the aviator to have an unobstructed view of the area directly in front of and under the aircraft. This “see-through” capability is very useful when landing must be made in cluttered or unfamiliar landing areas.

If the Comanche decides to mount the I² sensor exocentrically on the nose, collocated near the FLIR sensor, then the displaying of both imageries on the HIDSS will not introduce any human factors problems other than those just cited. [Remotely locating the I² sensor will affect resolution, system lag, and contrast.] However, if the FLIR remains exocentrically located and the I² sensor(s) is integrated into the HIDSS, then additional issues associated with mixed sensor location modes and the resulting switching of visual reference points must be considered. One study (Armbrust et al., 1993) looking at these potential issues was conducted using the AH-64 with its exocentrically located FLIR and several HMDs with integrated I² sensors. Aviators were tasked with performing a set of standard maneuvers (i.e., precision hover, lateral hover, rearward hover, deceleration, and pirouette). At designated points during each maneuver, the aviators were required to switch from one sensor to the other. For the hover maneuvers, the switch occurred at the maneuver midpoint. For the deceleration maneuver, the switch occurred immediately after the start of the deceleration. For the pirouette, switches were required every 90°. The direction of the switch (from aircraft nose to head and vice versa) was counterbalanced across subjects. The objective of this study (phase) was to investigate the effects of switching sensor perspective on measured performance and subjective aviator workload. Measured performance was based on monitoring of drift, altitude, and heading data. Aviator workload was measured by the Subjective Workload Technique (SWAT) (Armstrong Aerospace Medical Research Laboratory, 1989). The study found significant degradation in performance for all maneuvers, regardless of direction of switching. SWAT scores indicated higher workloads associated with sensor switching. Over 80% of the aviators reported that targets appeared to be at different distances as a result of switching, targets in the I² imagery appearing closer than in the FLIR imagery. Over a third (37%) of the aviators reported apparent changes in attitude or flight path when switching; three-fourths (75%) stated that switching caused disorientation in one or more of the maneuvers due to switching. And, of most concern, should be the fact that one-half (50%) had to transfer controls to the safety pilot during one of the maneuvers. All of the aviators in the study stated that sensor switching increased workload. In view of these results, careful consideration should be given to HMD designs which require the user to switch between noncollocated sensor sources.

In a related study (Rabin and Wiley, 1994) investigating transitory effects on visual acuity due to potential luminance differences when switching from FLIR and I² imagery, a significant reduction in letter recognition was found during the first second after switching from simulated FLIR to simulated ANVIS imagery when the FLIR luminance was >10 fL. This effect was associated with the luminance imbalance between the two imageries. It was recommended that engineering safeguards to minimize luminance shifts be implemented in HMDs which will be used to display both FLIR and I² imagery.

In summary, VCSs are used as head control systems for aircraft-mounted imagery sensors and fire control systems. They make use of the natural physiological action of head and eye motion which is associated with human perception and reaction to the environment (Shirachi, Monk, and Black, 1978). They operate by providing accurate and responsive tracking of the head (and/or eye). They must operate over a sufficiently large volume (motion box) to allow for the normal range of head movements and must track these movements accurately and with minimum delay (Barrette, 1992).

Design Issues

The performance approach to group HMD system and subsystem issues into performance categories. These are: Optical system, visual, helmet, and human factors engineering. The issues under each category are discussed in terms of how various HMD parameters relate to corresponding human sensory or structural parameters, and how they interact to limit or enhance aviator performance.

Optical performance

In most HMD designs, an image source (e.g., CRT, LCD, etc.) creates on its face a reproduction of the outside scene. This reproduced image then is relayed through a set of optical elements (relay optics) producing a final image which is viewed by the eye. The former image on the image source has certain characteristics. The relay optics have a transfer function which modifies these characteristics in producing the final image. When the aviator dons the HMD, there are both system characteristics (e.g., FOV, magnification, see-through transmittance, etc) and image characteristics (relating to image quality) which define the usefulness of the HMD in helping the aviator perform the mission. The optical performance of an HMD can be evaluated using two approaches. The first addresses the physical characteristics of the HMD and its imagery. The second addresses the perceived performance with regard to the human user.

Image quality

Farrell and Booth (1984) define image quality as the extent to which a displayed image duplicates the information contained in the original scene in a form suitable for viewing and interpreting. [It should be noted that near-IR and IR images are not normally viewed images.] To the user, image quality determines his ability to recognize and interpret information. For our purpose, we shall confine our discussion to the system's final image, which is defined by the image source and display optics. Numerous image quality FOMs have been developed and used to evaluate the physical quality of the image produced on a display with the goal of gauging user performance with the display. Task (1979) provides an excellent summary of a number of FOMs which commonly are used for evaluating image quality in CRTs. These are listed in Table 7, categorized as geometric, electronic, and photometric.

Table 7.
CRT display system FOMs.

Geometric	Electronic	Photometric
Viewing distance Display size Aspect ratio Number of scan lines Interlace ratio Scan line spacing Linearity	Bandwidth Dynamic range Signal to noise ratio Frame rate	Luminance Grey shades Contrast ratio Halation Ambient illuminance Color Resolution Spot size and shape MTF Luminance uniformity Gamma

FP technologies are being used as alternate HMD image sources. Klymenko et al. (1997) have categorized FOMs for FPDs into four domains: spatial, spectral, luminance, and temporal (Table 8). These image domains parallel analogous human visual performance domains. The spatial domain includes those display parameters associated with angular view (subtense) of the user and coincide with the user's visual acuity and spatial sensitivity. The spectral domain consists of those parameters associated with the user's visual sensitivity to color (wavelength). The luminance domain encompasses those display parameters identified with the overall sensitivity of the user to illumination levels. The temporal domain addresses display parameters associated with the observer's sensitivity to changing levels of light intensity. [Baron (1994) adds two additional domains: depth (3D) and noise.]

Table 8.
FPD FOMs.

Spatial	Spectral	Luminance	Temporal
Pixel resolution (H x V) Pixel size and shape Pixel pitch Subpixel configuration Number of defective (sub)pixels	Spectral distribution Color gamut Chromaticity	Peak luminance Luminance range Grey levels Contrast (ratio) Uniformity Viewing angle Reflectance ratio Halation	Refresh rate Update rate Pixel on/off response rates

In general, these FOMs can be used for image quality evaluation for HMDs since the final image is that of the source image modified by the transfer function of the relay optics. However, there are a few additional FOMs which relate to the system as a whole. The FOMs selected for discussion here are not all inclusive but represent the most critical ones needed to effectively evaluate image quality. However, even for simple HMDs, these FOMs can fail to allow a user to judge between two competitive designs which significantly differ in scope and function (Baron, 1994).

In the following FOM discussions, the FOM will be developed in relationship to the overall HMD design. The interrelationship between FOMs will be discussed. In addition, the operational values of the FOM for the currently fielded ANVIS and IHADSS, and in-development HIDSS HMDs will be provided along with recommendations for minimum or maximum specifications.

Contrast

Contrast refers to the difference in luminance between two (usually) adjacent areas. There is often confusion associated with this term due to the multiple FOMs used to express contrast (Klymenko et al., 1997). Contrast, contrast ratio, and modulation contrast are three of the more common formulations of luminance contrast. Further confusion may result from the terminology, because different names are used for the two luminances involved in the definitions. Sometimes the luminances are identified according to their relative values and, therefore, labeled as the *maximum* luminance (L_{max}) and *minimum* luminance (L_{min}). However, if the area at one luminance value is much smaller than the area at the second luminance, the luminance of the smaller area sometimes is referred to as the *target* luminance (L_t), and the luminance of the larger area is referred to as the *background* luminance (L_b). The more common mathematical expressions for luminance contrast include:

$$C = (L_t - L_b) / L_b \quad \text{for } L_t > L_b \quad (\text{Contrast}) \quad \text{Equation 4a}$$

$$= (L_b - L_t) / L_b \quad \text{for } L_t < L_b \quad \text{Equation 4b}$$

$$= (L_{\max} - L_{\min}) / L_{\min} = (L_{\max} / L_{\min}) - 1 \quad \text{Equation 4c}$$

$$C_r = L_t / L_b \quad \text{for } L_t > L_b \quad (\text{Contrast ratio}) \quad \text{Equation 5a}$$

$$= L_b / L_t \quad \text{for } L_t < L_b \quad \text{Equation 5b}$$

$$= L_{\max} / L_{\min} \quad \text{Equation 5c}$$

$$\text{and } C_m = (L_{\max} - L_{\min}) / (L_{\max} + L_{\min}) \quad (\text{Modulation contrast}) \quad \text{Equation 6a}$$

$$= |(L_t - L_b)| / (L_t + L_b) \quad \text{Equation 6b}$$

In the preceding equations, modern conventions are adopted which preclude negative contrast values. [Classical work with the concept of contrast did not concern itself with which had the larger luminance value, the target or the background and, therefore, allowed negative contrast values (Blackwell and Blackwell, 1971); Blackwell, 1946.] The values for contrast as calculated by Equations 4a and 4c can range from 0 to ∞ for bright targets and from 0 to 1 for dark targets (Equation 4b). The values for contrast ratio (Equations 5a-c) can range from 1 to ∞ . Modulation contrast (Equations 6a-b), also known as Michelson contrast, is the preferred metric for cyclical targets such as sine waves and square waves. It can range in value from 0 to 1, and is sometimes given as the corresponding percentage from 0 to 100. Conversions between the various mathematical expressions for contrast can be performed through algebraic manipulation of the equations or through the use of nomographs (Farrell and Booth, 1984). Some of the conversion equations are:

$$C_r = (1 + C_m) / (1 - C_m), \quad \text{Equation 7}$$

$$C_m = (C_r - 1) / (C_r + 1), \quad \text{Equation 8}$$

$$C = (2 C_m) / (1 - C_m) \quad \text{for bright targets,} \quad \text{Equation 9}$$

$$\text{and } C = (2 C_m) / (1 + C_m) \quad \text{for dark targets.} \quad \text{Equation 10}$$

It may be instructive to examine a number of typical luminance patterns for which the contrast figures of merit could be applied and calculate the various contrast values. The patterns in Figure 29 each consist of a small circular area at a given luminance, which will be referred to as the *target*, surrounded by a larger area at a lower luminance value, which will be referred to as the *background*. The luminances of the targets and backgrounds will be labeled L_t and L_b , respectively. Assume, as in Figure 29a, luminance values of 100 fL and 20 fL for the target and background luminances, respectively. Contrast for a target brighter than its background, as defined by Equation 4a, is calculated as follows:

$$C = (L_t - L_b) / L_b = (100 - 20) / 20 = 80 / 20 = 4$$

Equation 4c would produce the same value. However, applying Equations 5a or 5c for contrast ratio results in the following:

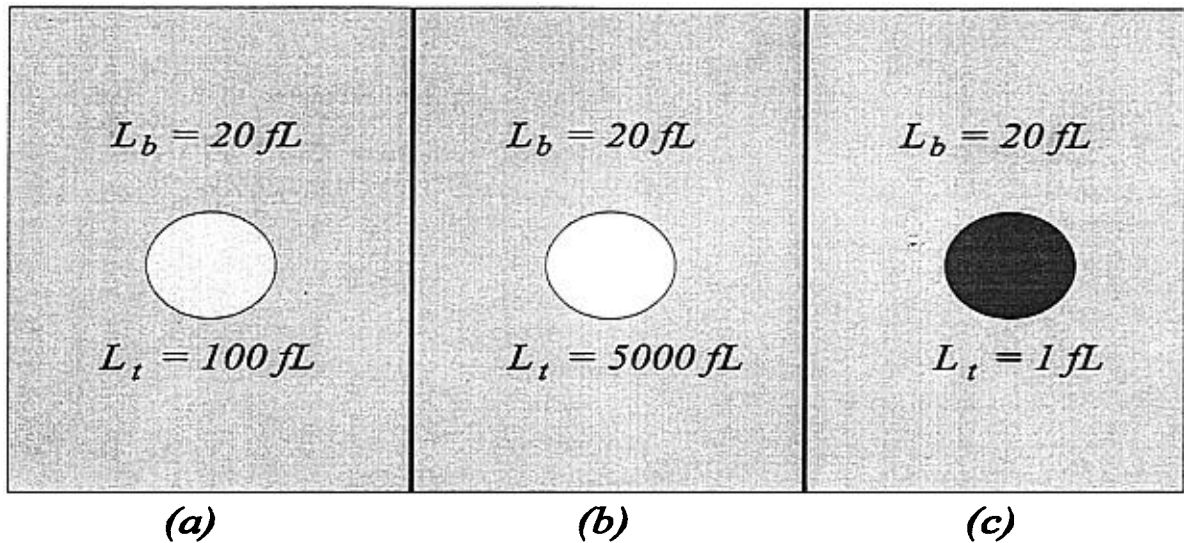


Figure 29. Luminance patterns for several combinations of target and background luminance values.

$$C_r = L_t / L_b = L_{\max} / L_{\min} = 100/20 = 5$$

Assume, now, that the target luminance becomes significantly larger, 5000 fL for example, but with the same background value (Figure 29b). The contrast value using Equations 4a and 4c would be:

$$C = (5000 - 20) / 20 = 249$$

The contrast ratio using Equations 5a or 5c take the value:

$$C_r = 5000/20 = 250$$

Further increases in the value of the target luminance would continue to produce larger values for contrast as defined by Equations 4a and 4c and contrast ratio as defined by Equations 5a and 5c. Note that as L_{\max} (or L_t) becomes significantly greater than L_{\min} (or L_b), the contrast values of Equation 4a and 4c approach the contrast ratio values of Equations 5a and 5c. This can easily be seen by rearranging Equation 4a into the following form:

$$C = (L_t / L_b) - 1 \quad \text{Equation 11}$$

As the ratio of L_t / L_b increases, the significance of subtracting the value of 1 becomes meaningless and Equation 11 takes the form of Equation 5a, that of contrast ratio.

By comparison, if, as in Figure 29c, the target luminance (1 fL) is lower than the background luminance ($L_t < L_b$), the calculated value for contrast (Equation 4b) is:

$$C = (L_b - L_t) / L_b = (20 - 1) / 20 = 19/20 = 0.95$$

and, the calculated value for contrast ratio (Equations 5b and 5c) is:

$$C_r = L_b / L_t = L_{\max} / L_{\min} = 20/1 = 20.$$

Note: The equation for contrast ratio is defined always by the ratio of the greater luminance to the lesser luminance.

Values for modulation contrast for the luminance patterns of Figure 29 generally are not used. However, consider the luminance pattern in Figure 30. This pattern consists of a series of light and dark bars. While values for contrast and contrast ratio can be calculated, the concept of contrast for such a cyclical pattern is best defined by the modulation contrast (Equations 6a and 6b).

For the luminance values in Figure 30, the value of the modulation contrast becomes:

$$C_m = (L_{\max} - L_{\min}) / (L_{\max} + L_{\min})$$

$$= (50 - 10) / (50 + 10) = 40 / 60 = 0.66$$

In summary, for any given luminance pattern consisting of two different luminance values, a number of different contrast figures of merit can be calculated. For luminance patterns which are cyclical, the modulation contrast figure of merit is preferred. However, since algebraic

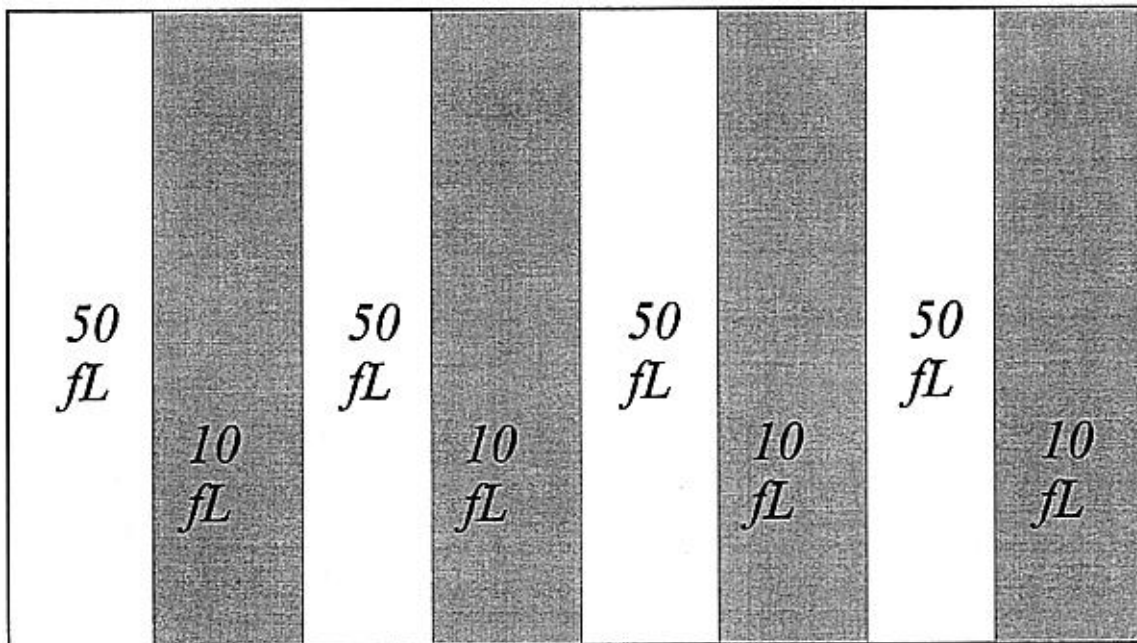


Figure 30. A cyclical luminance pattern.

manipulation can be used to convert between the various contrast figures of merit, perhaps the most important step in presenting any contrast value is to clearly define the selected figure of merit.

Available contrast depends on the luminance range of the display. The range from minimum to maximum luminance values that the display can produce is referred to as its dynamic range. For CRT displays the luminance range often is characterized by measuring and plotting the luminance of an arbitrary area of the display as a function of the voltage on the anode of the CRT, which controls the electron beam current. Figure 31 shows a typical light output vs.

voltage curve, which is called a “gamma curve.” The continuous nature of this curve illustrates the analog nature of this type of display. This analog characteristic has led to an often used, but often misunderstood, method of describing an analog display’s dynamic range (Tannas, 1985). This descriptor for the luminance dynamic range within a scene reproduced on a CRT display is the number of SOG.

SOG are luminance steps which differ by a defined amount. They are by convention typically defined as differing by the square-root-of-two (approximately 1.414). For example, if the lowest (minimum) luminance value within a scene is 10 fL, then the next square-root-of-two grey shade would be 10 multiplied by 1.414 or 14.14 fL. The next grey shade, if present, would be 14.14 multiplied by 1.414 or 20.0 fL, and so on. Therefore, a scene having 10 and 20 fL as its minimum and maximum luminance values, respectively, would have a dynamic range of 3 shades of grey (10, 14, and 20 fL). Its contrast ratio (C_r) would be 20/10 or 2.0.

For a linear system, which CRTs are considered to be over most of their dynamic luminance range, there is a straightforward relationship between the number of shades of grey and the contrast ratio. This relationship is:

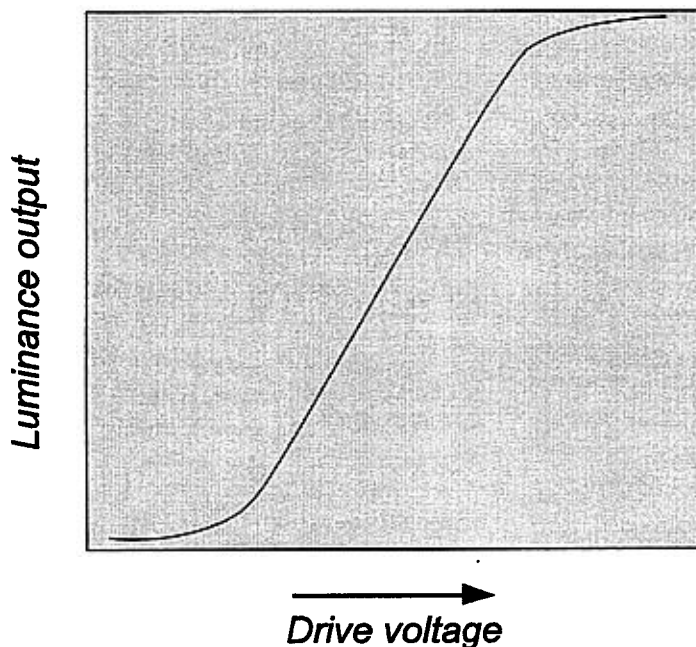


Figure 31. Typical gamma curve.

$$\text{Number of SOG} = [\log(C_r) / \log(\sqrt{2})] + 1$$

Equation 12

The addition of the 1 takes into account the first luminance level (grey shade). This can be illustrated by considering the number of SOG in a scene which is of uniform luminance, i.e., the minimum and maximum luminances are the same. For this special case, the contrast ratio is 1/1 or 1, and using Equation 12:

$$\begin{aligned} \text{Number of SOG} &= \log(C_r) / \log(\sqrt{2}) + 1 \\ &= \log(1) / 0.1505 + 1 \\ &= 0 / 0.1505 + 1 = 0 + 1 \\ &= 1, \end{aligned}$$

which means that a scene of uniform luminance has one grey shade. Table 9 shows SOG and corresponding contrast ratios.

Table 9.
Shades of grey (SOG) and corresponding contrast ratios.

Shades of grey	1	2	3	4	4.5	8	16
Contrast ratio	1.00	1.41	2.00	2.83	3.40	11.3	181

It is worth noting that the square-root-two choice as the unit of the grey shade scale does not imply that the threshold for the human eye requires two luminances to differ by a ratio of 1.4 in order to reach a “just noticeable difference (jnd).” In fact, for targets of a wide range of spatial frequencies, the human eye can detect differences in luminances which are several times smaller than the square-root-of-two unit. The consistent use of square-root-of-two differences instead of empirical jnds is a practical compromise between an engineering and a psychophysics philosophy.

Square-root-of-two SOG have been used historically for CRTs, which have enjoyed a position of preeminence as the choice for given display applications for decades. However, within the past few years, the FPD technologies have begun to gain a significant share of the display application market. Displays based on these various flat panel technologies differ greatly in the mechanism by which the luminance patterns are produced, and all of the mechanisms differ from that of CRTs. In addition, FPDs differ from conventional CRT displays in that most flat panel displays are digital with respect to the signals which control the resulting images. (Note: There are FPD designs which are capable of continuous luminance values, as well as CRTs which accept digital images.) As a result, usually, luminance values for flat panel displays are not continuously variable but can take on only certain discrete values. Figure 32 graphs the 16 available luminance values, the grey levels, of a typical graphic LCD. A difference between analog and digital displays is the way in which the incoming signal (usually a voltage) can change. In analog displays, the input signal voltage can vary continuously (i.e., can take on any value in the range) and, therefore, so can the output signal; i.e., the luminance. However, for most digital displays, e.g., FPDs, the input signal voltage takes on certain discrete values, thus, the output luminance also can take on only certain discrete values. In other words, the luminance output of a digital flat panel display is quantized as shown in Figure 32. Discrete luminance values of the 16 grey levels of a graphic LCD measured in our laboratory, where minimum and maximum values were 3.6 cd/m² (1.05 fL) and 44.6 cd/m² (13.0 fL), respectively, give a contrast ratio of 12.4.

Confusion can occur when the term grey shades, historically used to express the number of discriminable luminance levels in the dynamic luminance range of analog CRT displays, is applied to digital FPDs. Since these displays, in most cases, can produce only certain luminance values, it is reasonable to count the total number of possible luminance steps and use this number as a figure of merit. However, this number should be referred to as “grey steps” or “grey levels,” not “grey shades.” For example, a given LCD may be specified by its manufacturer as having 64 grey levels. The uninitiated may misinterpret this as 64 shades of grey, which is incorrect. It’s true meaning is that the display is capable of producing 64 different electronic signal levels between, and including, the minimum and maximum values, which generally implies 64 luminance levels. If one insisted on using a SOG figure of merit for discrete displays, it would appropriately depend on the value of the 1st and 64th levels.

LCD Flat Panel Display

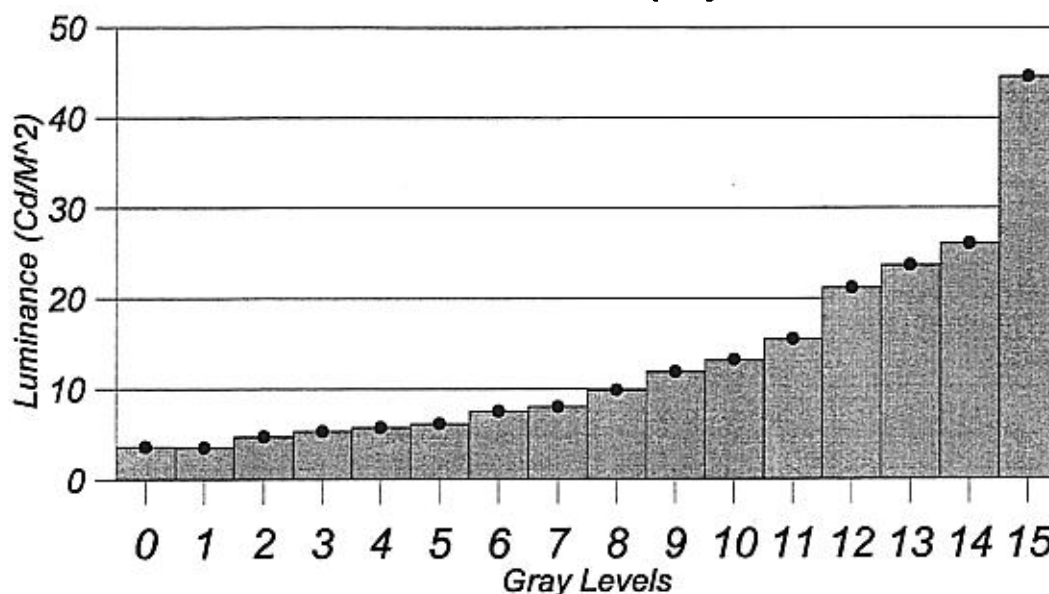


Figure 32. Discrete luminance values of the 16 grey levels of a graphic LCD display.

This is not advisable as misinformation can easily result from confusing grey shades and grey levels. Consider the 16 grey level specification of the LCD flat panel display, whose luminance levels are shown in Figure 32. If this 16 grey level specification is misinterpreted as 16 grey shades, a contrast ratio of 181.0 would be falsely implied as shown by Table 9. If, instead, we conversely use the LCD's available contrast ratio of 12.4 to compute a SOG, an appropriate figure of merit only for analog systems, we get a value of only 8.3, which is less than the 16 grey levels of the display. (It should be noted here that since SOG is assumed to refer to discriminable luminance levels in analog displays, there is a further question as to whether the 16 discrete grey levels adequately sample the range in terms of discriminable luminance levels.) To reiterate, for analog displays, a SOG specification is computed from the contrast ratio consisting of the minimum and maximum luminances. To actually produce a contrast ratio of 181.0 (equivalent to 16 SOG if it were an analog display), the LCD display in Figure 32 would need a maximum luminance of 651.6 cd/m² if its minimum luminance was 3.6 cd/m².

To avoid confusion, one should limit some figures of merit to either discrete or analog displays. Contrast ratio, computed from maximum and minimum luminance, is applicable to both. The concept of SOG is most appropriate for analog displays and can be computed from contrast ratio. The number of grey levels is most appropriate for displays with discrete luminance steps, but additional information on how these grey levels sample the luminance range needs to be specified.

Other contrast figures of merits may still be applicable to FPDs. However, in some cases they have been adapted to conform to the unique characteristics of these displays. For example, because of the discrete nature of FPDs, where the image is formed by the collective turning on or off of an array of pixels, the concept of contrast ratio is redefined to indicate the difference in luminance between a pixel that is fully "on" and one that is "off" (Castellano, 1992). The equation for pixel contrast ratio is:

$$C_r = (\text{Luminance of ON pixel})/(\text{Luminance of OFF pixel}) \quad \text{Equation 13}$$

It can be argued that this pixel contrast ratio is a more important figure of merit for discrete displays. Unfortunately, the value of this figure of merit as cited by manufacturers is intrinsic in nature, that is, it is the contrast value in the absence of ambient lighting effects. The value of this figure of merit which is of real importance is the value which the user will actually encounter. This value depends not only on the ambient lighting level, but also on the reflective and diffusive properties of the display surface (Karim, 1992). Additional factors may need to be taken into consideration. An example is the dependence of luminance on the viewing angle where a liquid crystal display's luminance output given by a manufacturer may only be reliable for a very limited viewing cone. Here the luminance and contrast need to be further specified as a function of viewing angle. On the other hand, the propensity of manufacturers sometimes to define "additional" figures of merit which put their products in the best light must always be kept in mind.

The term grey scale is used to refer to the luminance values available on a display. (The term as used usually includes available color as well as luminance per se.) Grey scales can be analog or digital. The display may produce a continuous range of luminances, described by the shades of grey concept; or, it may only produce discrete luminance values referred to as grey steps or grey levels. The analog case is well specified by the SOG figure of merit and more compactly by the maximum contrast ratio of the dynamic range. Also the gamma function succinctly describes the transformation from luminance data (signal voltage) to displayed image luminance. (The MTF additionally describes the display's operating performance in transferring contrast data to transient voltage beam differences over different spatial scales.) In an analog image, easily applicable image processing techniques, such as contrast enhancement algorithms, are available to reassign the grey levels to improve the visibility of the image information when the displayed image is poorly suited to human vision. (The techniques are easily applicable because they often simply transform one continuous function into another, where computer control over 256 levels is considered as approximating a continuous function for all practical purposes.) Poor images in need of image processing often occur in unnatural images, such as thermal images, and artificial images, such as computer generated magnetic resonance medical images. Since only certain discrete luminance levels are available in the digital case, the description of the grey scale and its effect on perception is not as simple and straightforward as in the analog case. One would like to know if there is a simple function which can describe the luminance scale; but one would also like to know how the function is sampled. A problem is, many image enhancement techniques may not be as effective if the discrete sampling of the dynamic range is poor. For example, consider an infrared sensor generated image presented on an LCD with a small number of discrete grey levels. A contrast enhancement algorithm in reassigning pixel luminances must pick the nearest available discrete grey level and so could inadvertently camouflage targets by making them indistinguishable from adjacent background. Also the original image might contain spurious edges because neighboring pixel luminance values which would normally be close and appear as a smooth spatial luminance gradient become widely separated in luminance due to the available discrete levels, thus producing quantization noise.

Color contrast While the ability to discriminate between two luminance values has been the major point of emphasis, images where the background and target have the same luminances can still be discerned by color differences (chromatic contrast). These equal luminance chromatic contrasts are less distinct in terms of visual acuity than luminance contrasts, but can be very visible under certain conditions (Kaiser, Herzberg, and Boynton, 1971).

The sensation of color is dependent not only on the spectral characteristics of the target being viewed, but also on the target's context and the ambient illumination (Godfrey, 1982). The sensation of color can be decomposed into three dimensions: hue, saturation, and brightness. Hue refers to what is normally meant by color, the subjective "blue, green, or red" appearance.

Saturation refers to color purity and is related to the amount of neutral white light that is mixed with the color. Brightness refers to the perceived intensity of the light.

The appearance of color can be affected greatly by the color of adjacent areas, especially if one area is surrounded by the other. A color area will appear brighter, or less grey, if surrounded by a sufficiently large and relatively darker area, but will appear dimmer, or more grey, if surrounded by a relatively lighter area (IES, 1984). To further complicate matters, hues, saturations, and brightnesses may all undergo shifts in their values.

The use of color in displays increases the information capacity of displays and the natural appearance of the images. CRTs can be monochrome (usually black and white) or color. Color CRTs use three electron beams to individually excite red, blue, and green phosphors on the face of the CRT. By using the three primary colors and the continuous control of the intensity of each beam, a CRT display can provide "full color" images. Likewise, FPDs can be monochrome or color. Many flat panel displays that produce color images are still classified as monochrome because these displays provide one color for the characters or symbols and the second color is reserved for the background, (i.e., all of the information is limited to a single color). An example is the classic orange-on-black plasma discharge display, where the images are orange plasma characters against a background colored by a green electroluminescent backlight (Castellano, 1992).

Full color capability has been achieved within the last several years in most all of the flat panel technologies, including liquid crystal, electroluminescent, light emitting diode, field emission, and plasma displays. Even some of the lesser technologies, such as vacuum fluorescence, can provide multicolor capability. Research and development on improving color quality in flat panels is ongoing. Figures of merit describing the contrast and color generating capacities of displays are an ongoing area of development.

Figures of merit defining color contrast are more complicated than those presented previously where the contrast refers only to differences in luminance. Color contrast metrics must include differences in chromaticities as well as luminance. And, it is not as straightforward to transform chromatic differences into jnds in a perceived color space. This is due to a number of reasons. One, color is perceptually a multidimensional variable. The chromatic aspect, or hue, is qualitative and two dimensional, consisting of a blue-yellow axis and a red-green axis. Additionally, the dimensions of saturation and brightness, as well as other factors such as the size and shape of a stimulus, affect the perceived color and perceived color differences. The nature of the stimulus, whether it is a surface color, reflected off a surface, or a self-luminous color, as present in a display, will affect the perceived color space in complex ways. Delineating the nature of perceived color space has been an active area of research with a vast literature (Widdel and Post, 1992).

As a consequence, there is no universally accepted formulation for color contrast. One figure of merit combining contrast due to both luminance and color, known as the discrimination index (ID), was developed by Calves and Brun (1978). The ID is defined as the linear distance between two points (representing the two stimuli) in a photolorimetric space. In such a space, each stimulus is represented by three coordinates (U, V, log L). The U and V coordinates are color coordinates defined by the CIE 1960 chromaticity diagram. The third coordinate, log L, is the base ten logarithm of the stimulus luminance. [A concise discussion of the discrimination index is presented in Rash, Monroe and Verona (1981).] The distance between two points (stimuli) is the ID and is expressed as:

$$ID = \left[\left(\frac{\log(L_1/L_2)}{0.15} \right)^2 + \left(\frac{[(\Delta U)^2 + (\Delta V)^2]^{1/2}}{0.027} \right)^2 \right]^{1/2} \quad \text{Equation 14}$$

where L_1 and L_2 refer to the luminances of the two stimuli, and (ΔU) and (ΔV) refer to the distances between the colors of the two stimuli in the 1960 CIE two dimensional color coordinate space.

A more recent figure of merit, ΔE (Lippert, 1986; Post, 1983), combining luminance and color differences into a single overall metric for contrast, has been provisionally recommended for colors which present only an impression of light, unrelated to context, only recently by the International Organization for Standardization (ISO, 1987) for colored symbols on a colored background. It is defined as follows:

$$\Delta E = \left[(155 \Delta L/L_{Max})^2 + (367 \Delta u')^2 + (167 \Delta v')^2 \right]^{1/2} \quad \text{Equation 15}$$

where the differential values (Δ) refer to the luminance (L) and chromaticity (u' , v') differences between symbol and background and L_{max} refers to the maximum luminance of either symbol or background. Developing the appropriate figure of merit to describe the color contrast capacities of displays is an ongoing area of development (Widdel and Post, 1992).

Contrast and HMDs. This discussion has been general in nature. It is applicable to panel-mounted as well as helmet-mounted displays. However, HMDs introduce additional contrast issues. For example, in IHADSS, the sensor imagery is superimposed over the see-through view of the real world. Although see-through HMD designs are effective and have proven successful, they are subject to contrast attenuation from the ambient illumination. The image contrast as seen through the display optics is degraded by the superimposed outside image from the see-through component which transmits the ambient background luminance. This effect is very significant during daytime flight when ambient illumination is highest.

A typical HMD optical design in a simulated cockpit scenario is shown in Figure 33. The relay optics consist of two combiners, one plano and one spherical. Light from the ambient scene passes through the aircraft canopy, helmet visor, both combiners, and then enters the eye. Simultaneously, light from an image source such as a CRT partially reflects first off of the plano combiner and then off of the spherical combiner, and then is transmitted back through the plano combiner into the eye. The resulting image is a combination of the modified ambient (outside) scene and CRT images. Nominal values for the transmittances and reflectances of the various optical media are: 70% canopy transmittance; 85% and 18% transmittance for a clear and shaded visor, respectively; 70% transmittance (ambient towards the eye); 70% reflectance (CRT luminance back towards the eye) for the spherical combiner, 60% transmittance (ambient towards the eye) and 40% reflectance (CRT luminance) for the plano combiner. An analysis of this design shows that approximately 17% of the luminance from the CRT image (and CRT optics) and approximately 25% of the ambient scene luminance reaches the eye for the clear visor (5% for the shaded visor).

Ambient scene luminances vary greatly over a 24-hour period. They can range from 0.001 fL under moonless, clear starlight conditions to 10,000 fL for bright daylight. Daytime luminances begin at approximately 300 fL. The image source used in Figure 33 is a miniature CRT. Depending on viewing time, day versus night, luminance values provided by the CRT and its associated optics can be selectively ranged from 100 fL (for night use) to an optimistic 1600 fL (for day use). A luminance of 800 fL may be a more typical daytime value.

Image contrast during night operations is usually not a problem. However, the use of HMDs for daytime imagery (versus for symbology) is not well defined. Based on the design in Figure 33 and the nominal values provided, Table 10 provides the theoretical values for Michelson contrast (C_m , Eq. 6a and 6b), contrast ratio (C_r , Eq. 5a), and shades of grey (SOG, Eq. 12) for various combinations of visors, ambient scene luminances, and CRT display luminances. In these equations, the ambient luminance reaching the eye assumes the role of the background luminance and the sum of the CRT and background luminances reaching the eye assumes the role of the target luminance. Note that for the purpose of these calculations, the background luminance is a combination of the light reaching the eye due to both the ambient and the CRT luminances. See Appendix for a sample calculation of Michelson contrast, contrast ratio, and shades of grey values for the set of conditions for viewing an 800 fL CRT against a 3,000 fL ambient scene using both clear and shaded visors.

Several obvious trends are present in the data of Table 10. These are: (1) for a given ambient background luminance, increasing the CRT display luminance increases contrast; (2) for a given CRT display luminance, increasing ambient background luminance decreases contrast; and (3) for a given set of CRT display and ambient background luminances, the use of a shaded visor over a clear visor increases contrast.

Contrast requirements. Once appropriate figures of merit have been established for quantifying contrast, an obvious question is what are their recommended values. Unfortunately, there is no single value or set of values, for minimum contrast requirements. The amount of contrast required to perform a task on a display depends on numerous factors. These factors include the type of visual task (e.g., rapid target detection or status indicators), the viewing environment (e.g., ambient light level, presence of glare sources, the size and distance of the display, etc.), the nature of the displayed information (e.g., text, symbology, video, graphics), and the other display characteristics (such as screen resolution, blur and sharpness, jitter, color, pixel geometry, etc.).

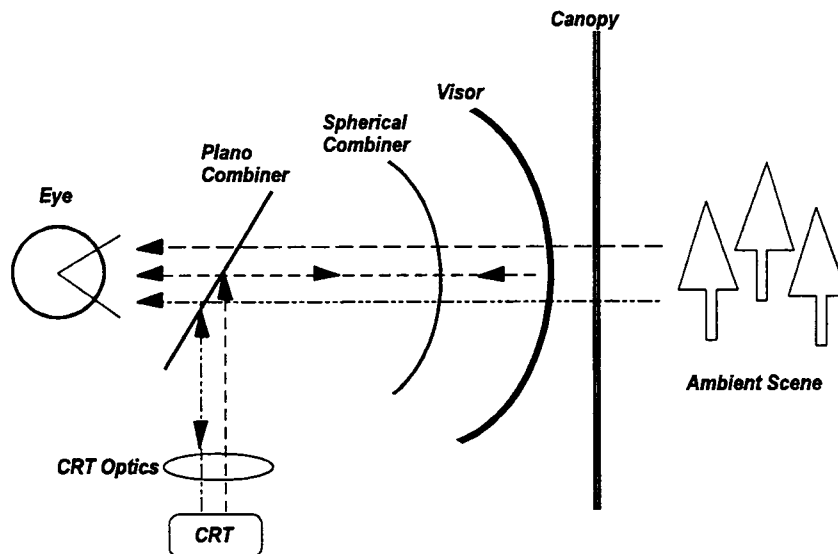


Figure 33. Typical catadioptric HMD optical design.

Table 10.

Michelson contrast, contrast ratio, and SOG values for an HMD design.

	Ambient luminance					
	3,000 fL		1,000 fL		300 fL	
Display luminance	Clear visor	Shaded visor	Clear visor	Shaded visor	Clear visor	Shaded visor
100 fL	$C_m = 0.01$ $C_r = 1.02$ SOG= 1.06	$C_m = 0.05$ $C_r = 1.11$ SOG= 1.29	$C_m = 0.03$ $C_r = 1.07$ SOG= 1.19	$C_m = 0.14$ $C_r = 1.32$ SOG= 1.80	$C_m = 0.10$ $C_r = 1.22$ SOG= 1.59	$C_m = 0.35$ $C_r = 2.06$ SOG= 3.09
400 fL	$C_m = 0.04$ $C_r = 1.09$ SOG= 1.25	$C_m = 0.17$ $C_r = 1.42$ SOG= 2.02	$C_m = 0.12$ $C_r = 1.27$ SOG= 1.69	$C_m = 0.39$ $C_r = 2.27$ SOG= 3.37	$C_m = 0.32$ $C_r = 1.90$ SOG= 2.85	$C_m = 0.68$ $C_r = 5.23$ SOG= 5.79
800 fL	$C_m = 0.08$ $C_r = 1.18$ SOG= 1.48	$C_m = 0.30$ $C_r = 1.85$ SOG= 2.77	$C_m = 0.21$ $C_r = 1.54$ SOG= 2.25	$C_m = 0.56$ $C_r = 3.54$ SOG= 4.66	$C_m = 0.47$ $C_r = 2.79$ SOG= 3.97	$C_m = 0.81$ $C_r = 9.45$ SOG= 7.50
1600 fL	$C_m = 0.15$ $C_r = 1.36$ SOG= 1.89	$C_m = 0.46$ $C_r = 2.69$ SOG= 3.87	$C_m = 0.35$ $C_r = 2.08$ SOG= 3.11	$C_m = 0.72$ $C_r = 6.07$ SOG= 6.22	$C_m = 0.64$ $C_r = 4.58$ SOG= 5.40	$C_m = 0.89$ $C_r = 17.91$ SOG= 9.35

Despite the inability to establish a single set of contrast requirements, a considerable amount of research has gone into determining requirements for viewing and interpreting information in various display scenarios (Farrell and Booth, 1984; Masterman, Johnson and Silverstein, 1990; Silverstein, 1989). For example, for text to be legible on a directly viewed display, it is recommended that the modulation contrast for small characters (between 10 and 20 arc minutes) displayed on a monochrome CRT should be at least that defined by the equation:

$$C_m = 0.3 + [0.07 * (20 - S)], \quad \text{Equation 16}$$

where S is the vertical size of the character set, in minutes of arc (Human Factors Society, 1988). This equation is based on studies by Crook, Hanson, and Weisz (1954) and Shurtleff and Wuersch (1979). Consider, for example, characters 17 arcminute in size. Equation 16 specifies a minimum contrast modulation of 0.5 (contrast ratio of 3 to 1). However, in practice, a modulation value of 0.75 (contrast ratio of 7 to 1) is recommended. So, if the background luminance is 3.3 fL, then the character luminance should be at least 10.0 fL.

Fortunately, even with the absence of well defined minimum contrast values, several rules of thumb can be applied. For displayed text, the above recommendation of a minimum contrast ratio value of 3:1, with 7:1 as the preferred value, can be used in benign viewing conditions. For displayed video, a minimum of 6 SOG is recommended.

The recommendations above generally apply to direct view monochromatic displays. Contrast recommendations for color displays are even more difficult to develop. Snyder (1980) reported that, while a number of studies have produced a large amount of data on color discrimination, most of these data are "threshold measurements which are not easily extrapolated to suprathreshold tasks, such as legibility." Some recent studies have attempted to address this

deficiency (Imbeau et al., 1989; Lovasik, Matthews, and Kergoat, 1989; Pastoor, 1990; Travis et al., 1992), but fall short of definitive recommendations.

In applications where direct view displays are supplemented or replaced by helmet-mounted displays, the task of defining minimum contrast values is further complicated by optical and EO design considerations. The U.S. Army's most current HMD program is the HIDSS, being designed for use in the RAH-66 Comanche helicopter. The current version of this design is similar to that of Figure 33. The HIDSS specification for contrast and shades of grey, as available at the eye, addresses high ambient daylight (up to 10,000 fL background luminance) requirements. A contrast value (Equation 4a) of > 4.66 with a minimum of 6 shades of grey is required. This contrast value of 4.66 is equivalent to a C_r value of 5.66 which corresponds to 6 SOG. For day symbology, the contrast ratio is required to equal or exceed a value of 1.5:1 for a 3000 fL background and equal to or exceed 7:1 for a background of 100 fL; both values are based on the use of a tinted visor. For nighttime viewing of sensor imagery, a minimum contrast ratio value of 11.2 which corresponds to 8 SOG is required.

Resolution

The most frequently asked HMD design question is "How much resolution must the system have?" Resolution refers to the amount of information (detail) which can be presented. This will define the fidelity of the image. Spatial resolution is, perhaps, the most important parameter in determining the image quality of a display system. An HMD's resolution delineates the smallest size target which can be displayed. An image's resolution usually is given as the number of vertical and horizontal pixels which can be presented.

In HMDs using CRTs as the image source, the CRT's resolution is the limiting resolution of the system. The CRT's horizontal resolution is defined primarily by the bandwidth of the electronics and the spot size. Vertical resolution is usually of greater interest and is defined mostly by the beam current diameter and the spreading of light when the beam strikes the phosphor, which defines the spot size (and line width). CRT vertical resolution is usually expressed as the number of raster lines per display height. However, a more meaningful number is the raster line width, the smaller the line width, the better the resolution. From Table 4, it can be seen that 20 μm is the current limit on line width in miniature CRTs. Task and Kocian (1995) have expressed the opinion that CRT electron designs will continue to improve for specific applications.

In discrete displays such as FPDs, resolution is given as the number of horizontal by vertical pixels. These numbers depend on the size of the display, pixel size, spacing between pixels, and pixel shape (Snyder, 1985). Typical resolution values are 640 (H) x 480 (V), 1024 (V) x 768 (H), and 1280 (H) x 1024 (V). This expression for pixelated resolution can be converted into other formats using a number of equations given in Table 11 (Task, 1997). Some complications can arise when dealing with color FPDs. In such displays, a color pixel may consist of several (sub)pixels (red, green and blue). Depending on the subpixel arrangement, the color pixel count can be different for the horizontal and vertical directions. In the example in Figure 34 (Task, 1997), where each color pixel consists of elongated red, green, and blue subpixels positioned in rows of triads, the color pixel count in the horizontal direction would be one-third of the (sub)pixel count in that direction, but the color pixel count would be the same as the (sub)pixel count in the vertical direction.

The pixel output for current FLIR sensors suggest a FP pixel resolution of greater than 1355 (H) x 960 (V) (Belt et al., 1997). While some research and development programs are

developing miniature FPDs with resolutions as high as 2560 (H) x 2048 (V) (Girolamo, Rash, and Gilroy, 1997), current availability appears to be limited to 1280 (H) x 1024 (V).

In any optical imaging system, we want the eye to be the limiting resolution factor. At an adaptation level of 100 fL, the eye can detect approximately 1.72 cy/mr (which equates to 20/20 vision). Ideally, the HMD should match or exceed this value. A more realistic, but still optimistic, goal for HMD resolution in the central area of vision is 0.91 cy/mr, with values between 0.39 and 0.77 cy/mr being acceptable (Seeman et al., 1992). Rash et al. (1996a) cite monocular vertical and horizontal resolution specifications for a display background luminance of less than 10 fL as greater than or equal to 0.7 cy/mr (20/50 Snellen equivalent) for high contrast targets in the center of the monocular FOV and greater than or equal to 0.57 cy/mr (20/60 Snellen equivalent) at 0.75 distances from the center to the edge of the FOV.

The resolution (resolving power) of ANVIS and other I² devices usually is expressed in angular units (cy/mr). [For the individual I² tubes, a linear unit of “line pairs per millimeter (lp/mm)” is used to separate the optical characteristics of the objective and eyepiece lenses from the resolution of the intensifier tubes themselves. A minimum ANVIS value is 36 lp/mm.] Optimal I² resolution is obtained under high light level conditions with high contrast targets. Resolution decreases with light level because of the proportional decrease in luminance output below the automatic brightness control level and increase in the noise in the intensified image. Omnibus I and II ANVIS tubes have a resolution of 0.86 cy/mr at moonlight illumination levels and 0.55 cy/mr at starlight levels.

The IHADSS, unlike ANVIS, does not have an integrated sensor, but uses imagery provided by the nose-mounted FLIR, where target angular subtense is confounded by the target’s emission characteristics. Rash, Verona, and Crowley (1990) and Greene (1988) report that an upper bound resolution value is approximately 0.57 cy/mr (20/60 Snellen).

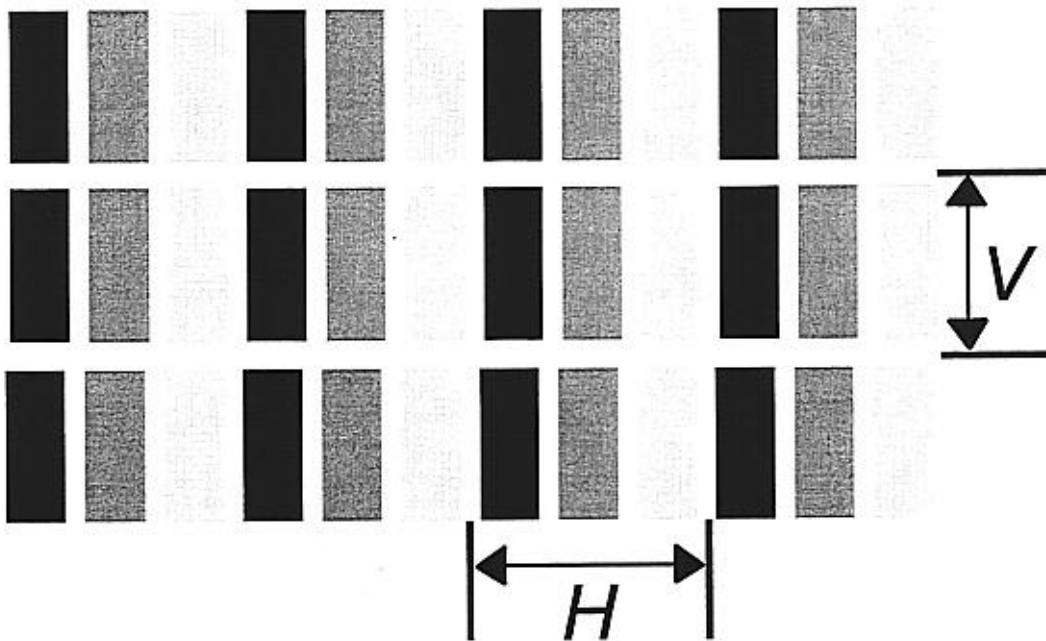


Figure 34. Red, green, and blue color triad pixels (Task, 1997).

Table 11.
Summary of expressions for resolution in discrete displays.
(Task, 1997)

Equation	Units	Visual limit
Res = Total pixels	pixels	not applicable
Res = (N/FOV)	pixels/degree	60 pixels/degree
Res = (N/2 FOV)	cycles/degree	30 cycles/degree
Res = (8.74 · N/FOV)	cycles/milliradian	1.72 cycles/milliradian
Res = (FOV/N)	degrees/pixel	0.0167 degree
Res = (60 · FOV/N)	arcminutes/pixel	1 arcminute
Res = (17.5 · FOV/N)	milliradian/pixel	0.291 milliradian

N = Number of pixels in a given direction; FOV = Field-of-view

In a following discussion of FOV, it is stated that the aviation community, if asked, will request an HMD which provides the largest FOV with the highest resolution. If the sensor can provide only a certain number of pixels, then an inverse relationship between resolution and FOV will result. As previously mentioned, several HMD designs (Fernie, 1995; Barrette, 1992) have explored achieving larger FOVs by uniquely distributing the available sensor pixels on the HMD. The basic concept is to create within the HMD's FOV a small inset area of increased resolution which is slaved to eye movement. Such "area of interest" displays mimic the eye's design of maximum visual acuity within a central high resolution area (fovea) (Robinson and Wetzel, 1989). This and similar approaches could help the long standing conflict between wide FOV and high resolution, currently design tradeoff parameters.

Modulation transfer function (MTF)

Expressing resolution only in terms of the number of scan lines or addressable pixels is not a meaningful approach. It is more effective to quantify how modulation is transferred through the HMD as a function of spatial frequency. A plot of such a transfer is called a MTF curve. Since any scene theoretically can be resolved into a set of spatial frequencies, it is possible to use a system's MTF to determine image degradation through the system. If the system is linear, the system MTF can be obtained by convolving (multiplying) the MTFs of the system's individual components.

There are several methods which historically have been used to obtain MTF curves. These include the subjective techniques of shrinking raster, line width, and TV limiting resolution; and the objectives techniques of discrete frequency, half power width, and FFT. All of these techniques have been employed to measure CRTs. Verona's (1992) comparison of these techniques shows that considerable variation exists across these techniques, with the discrete frequency technique being the most dependable. However, this technique, which requires the measurement of modulation contrast at multiple discrete frequencies, is very time consuming. Most automated MTF measuring systems are based on an FFT of a line spread function. [For an

MTF to validly describe a system, the response of the system must be uniform through the field-of-view (homogeneous) and in all directions (isotropic), and the response must be independent of input signals (Cornsweet, 1970). CRT displays approximate all of these conditions except one; those that are anisotropic. CRT imagery has continuous horizontal sampling but discrete vertical sampling. This implies that two MTFs, one vertical and one horizontal, are required to completely describe the system. However, the horizontal MTF is the more commonly measured and presented FOM.]

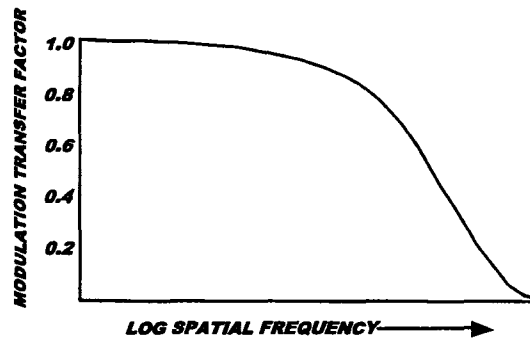


Figure 35. Typical MTF curve.

A CRT display's MTF curve typically is a monotonic function, maximum at the lowest spatial frequency present (determined by the display width) and decreasing to zero at the limiting highest spatial frequency of the display (Figure 35). A CRT display's MTF is defined by a number of factors: Scan rate, spot size, phosphor persistence, bandwidth, and drive level (luminance output). Investigations of the effects of these factors for currently used miniature CRTs can be found in Rash and Becher (1982) and Beasley et al. (1995).

Whether or not the MTF is a meaningful FOM for FPDs is still a point of contention within the HMD community. Biberman and Tsou (1991) state that there is no "quantitatively useful" metric for measuring FP technologies which can be related to the MTF. However, Infante (1993) provides the following explicit MTF expression for discrete displays:

$$MTF(u) = \left| \frac{\sin \pi \sqrt{FF} x_p u}{\pi \sqrt{FF} x_p u} \right| = \left| \frac{\sin \pi x_a u}{\pi x_a u} \right| \quad \text{Equation 17}$$

where x_p is the pixel pitch, FF is the fill factor, and x_a is the active pixel size. This expression is based on the Fourier transform of the following line spread function $f(x)$:

$$f(x) = 1, \text{ when } -\frac{x_a}{2} \leq x \leq \frac{x_a}{2}, \text{ and } = 0 \quad \text{elsewhere.}$$

Other discussions of the application of MTF to discrete displays include Barten (1993, 1991), Feltz (1990), and Beaton (1988). Nelson and Cox (1992) have developed a rather comprehensive image quality model for HMDs. It is a linear systems model which can accommodate

component MTFs for I² tubes (and optics), charge coupled device (CCD) cameras, LCD or CRT image sources, display relay optics, and electronic processing, predicting a final system MTF, which then is convolved with the contrast sensitivity function of the human eye. The model is intended as a design tradeoff tool for HMD designers. At this time, however, the model does not incorporate the temporal parameters.

Folding in the eyes response is important in assessing the “information transfer” a viewer can achieve. One image quality FOM based on taking the human visual system in consideration is the MTF area (MTFA). The MTFA was developed by Charman and Olin (1965) and is pictured in Figure 36. The MTFA is the area bounded by the display system’s MTF and the detection threshold curve for the human eye. Theoretically, the greater the MTFA, the greater the information perceived by the eye. The crossover point of the system MTF and the detection threshold curve defines the highest spatial frequency that can be detected (limiting resolution).

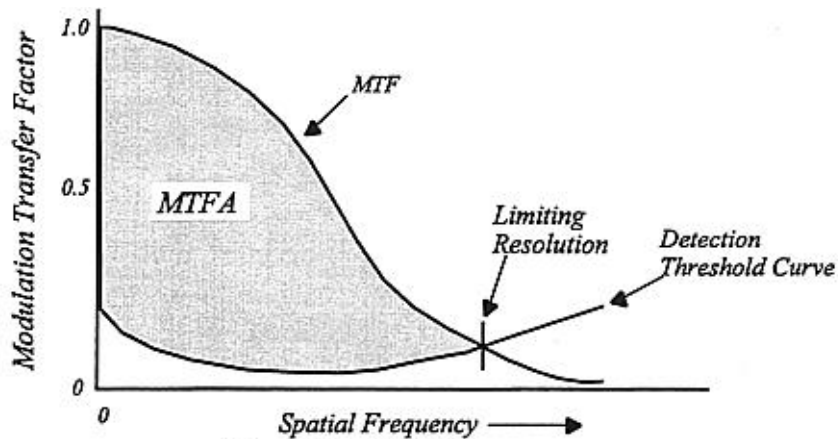


Figure 36. MTFA.

The MTFA, however, oversimplifies visual task performance and violates certain mathematical principles. Because of this oversimplification, other image quality metrics have been pursued. Of recent significance is the work of Peter Barten (1993, 1991) and the "Square-root integral" (SQRI) assessment method.

The SQRI is given by

$$SQRI = \int \sqrt{(M(u)/M_t(u))} \frac{du}{u} \quad \text{Equation 18}$$

where $M(u)$ is the MTF of the display, $M_t(u)$ is the visual contrast threshold curve, and u is spatial frequency per unit angle at the eye of the observer. The integration extends over the range from 0 to maximum spatial frequency. As with the MTFA, this equation takes into consideration the spatial frequency description of the display and the human visual system. Good agreement has been found between the SQRI and subjective measures of image quality (Barten, 1993, 1991; Westerink & Roufs, 1989).

What has not been emphasized so far is that most MTF curves encountered are static MTFs, i.e., the modulation in the scene is not changing. However, while static targets relative to the ground do exist on the battlefield, in the aviation environment, relative motion obviously is the

more prevalent condition. In addition to the relative target-aircraft motion, when VCSs are used, sensor gimbal jitter and head motion are present. When motion is present, the temporal characteristics of the scene modulation interact with those of the imaging system (e.g., scan rate and phosphor persistence for CRTs) and the transfer of modulation from the scene to the final display image can be degraded.

Phosphor persistence is an important display parameter affecting temporal response in CRT displays. Excessive persistence reduces modulation contrast and causes a reduction of grey scale in a dynamic environment where there is relative motion between the target and the imaging system (Rash and Becher, 1983). Persistence effects can cause the loss of one or more grey steps. This may not be a concern at low spatial frequencies, where there may be multiple grey steps. But, where there is only enough modulation contrast to provide one or two grey steps under static conditions, the loss of even one grey step at high spatial frequencies would be significant.

This effect is well demonstrated in the history of the IHADSS. A P1 phosphor initially was selected to satisfy the high luminance daytime symbology requirement. After initial flight tests, the CRT phosphor was changed to the shorter persistence (1.2 msec) P43 phosphor because of reported image smearing. Test pilots reported tree branches seemed to disappear as pilots moved their heads in search of obstacles and targets. It was determined the longer persistence (24 msec) of the P1 phosphor was responsible for the phenomenon (Rash, Verona, and Crowley, 1990).

From this incident, it has become self-evident that to effectively assess a display's capability to faithfully reproduce real world scenes, it is necessary to measure its dynamic response as well as its static response. Modulation transfer for a static image can be quite different from that achieved for a dynamic image (resulting from relative velocities). A preliminary model which describes a family of MTF curves, with a separate curve for different values of relative velocity, has been developed for CRT displays by Rash and Becher (1983). The model predicts reductions in MTF resulting from the interaction of target/scene relative motion and the display's temporal characteristics of scan rate and phosphor persistence. Representative model output for a CRT display using P28 phosphor (70 msec persistence) and having a vertical frame period of 33 msec is shown in Figure 37. Using a sinusoidal counterphase modulation technique developed by Verona et al. (1994) (and based on prior visual sciences testing), the dynamic MTFs for P1 and P43 phosphors were measured by Beasley et al. (1995) as a function of temporal frequency. The resulting curves, presented in Figures 38 and 39, validate the smearing effect found in early IHADSS test flights.

The degradation in image contrast due to temporal factors is not limited to CRT displays. AMLCDs are currently the leading FP display and are frequently used to present moving imagery (Bitzakidis, 1994). The liquid crystal molecules require a finite time to reorient themselves when the pixel is changing. This is a physical limitation. A response time of 20 - 100 msec is typical. This value is defined by the pixel access time (relatively short, ~65 μ sec), crystal's response speed, and other LCD physical properties such as the dependence of cell capacitance on drive voltage and temperature (Bitzakidis, 1994; Leroux, 1989).

In a similar fashion to CRT phosphor response, the slow transition between luminance values will degrade modulation transfer in dynamic images on AMLCDs. Consider the example of a black vertical bar moving across a white background where the luminance changes are completed after addressing the pixels twice (Bitzakidis, 1994). The display pixels can be categorized as:

- 1) Background pixels, which remain white for two fields.
- 2) Overlap-area pixels between the presentations of the bar at different fields, which remain black for two fields.
- 3) Pixels which change from white to black (the leading edge of the bar).
- 4) Pixels which change from black to white (the trailing edge of the bar).

The leading edge of the bar will appear dark grey, since the transition from white to black will be incomplete. The area behind the trailing edge suffers also. It will be a light grey due to the incomplete transition from black to white. The overall effect is that of a low-pass filter. Motion blur will result with a loss of high frequency detail. The magnitude of the effect increases with speed.

Rabin and Wiley (1995) compared visual performance between CRT and liquid crystal displays for high rates of image presentations and found a significant difference, which was attributed to the display response speed. The study involved a target detection task for various horizontal target velocities presented on the IHADSS (using a P43 phosphor image source) and an AMLCD HMD developed by Honeywell, Inc., Minneapolis, Minnesota. Target recognition (contrast sensitivity) was found to be degraded for the AMLCD HMD for the three highest velocities tested (4.4-17.6 deg/sec).

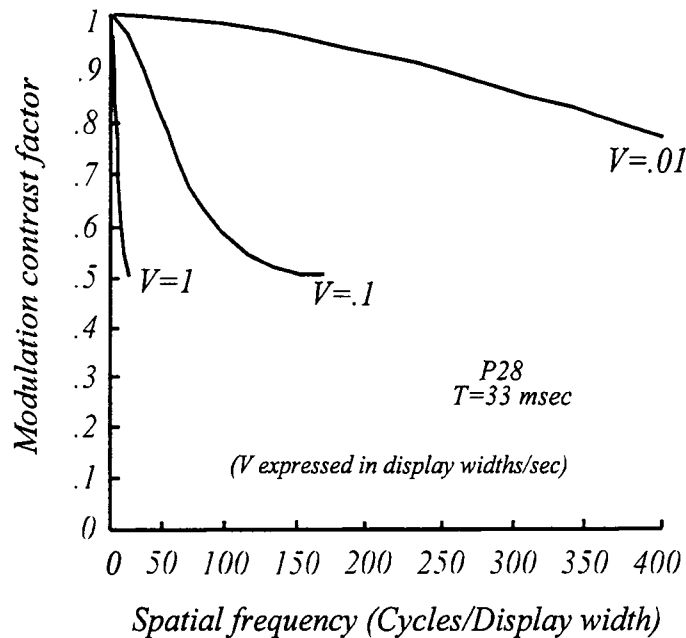


Figure 37. Representative model output for a CRT display using P28 phosphor (70-msec persistence) and having a vertical frame rate of 33 msec (Rash and Becher,1983).

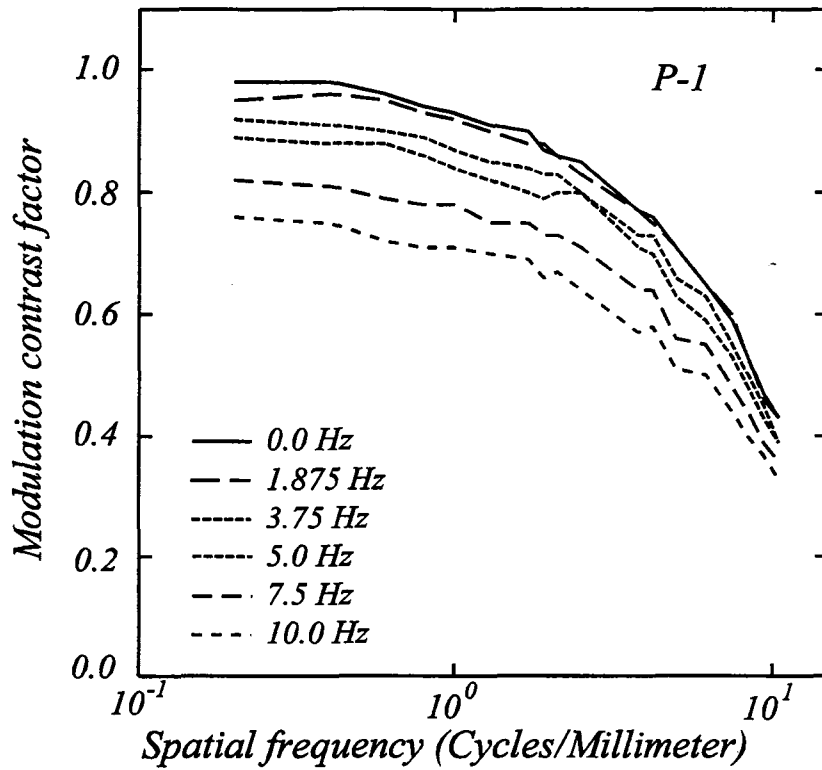


Figure 38. MTF curves for P1 phosphor (Beasley et al., 1995).

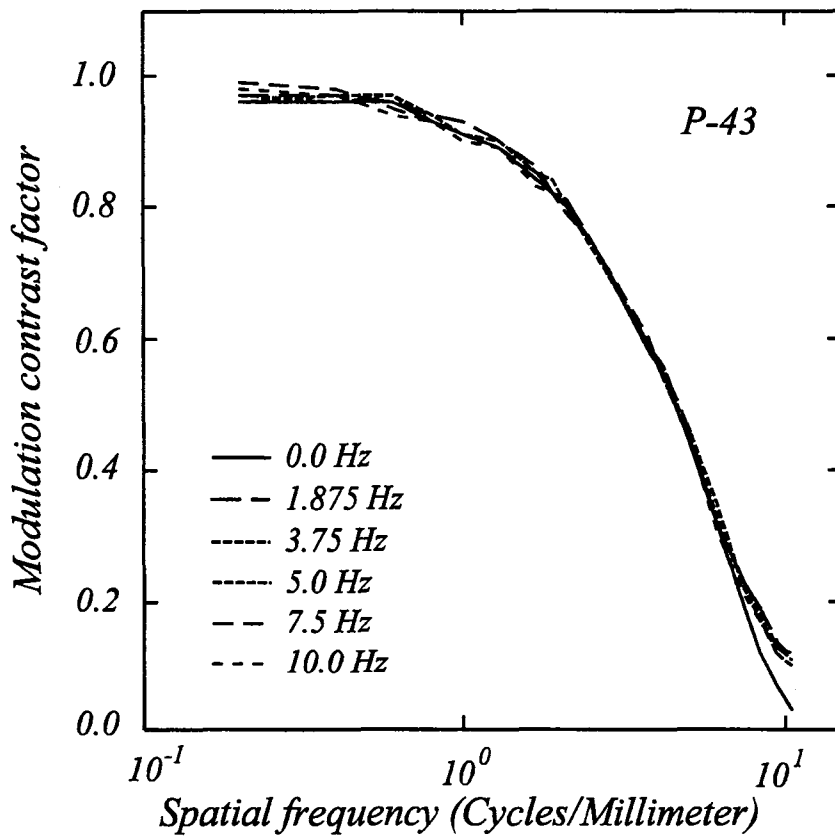


Figure 39. MTF curves for P43 phosphor (Beasley et al., 1995).

In conclusion, the dynamic response of a display and its interaction with other imaging system components is a critical area of concern. Therefore, it is necessary to be able to measure the dynamic MTF of such systems. Current wisdom is that pixel persistence (10%) values greater than 5 msec can lead to image blurring in dynamic head-tracked applications (Nelson, 1996).

Distortion

Distortion can be defined as any difference in the apparent geometry of the outside scene as viewed on or through the display. Sources of distortion in the display image include the image source and display optics (with combiner). For see-through designs, the combiner introduces distortion into the image of the outside scene. Distortion can exist outside the display itself, such as that caused by the aircraft windscreen. In current I² designs, e.g., ANVIS, the fiberoptic inverter is the primary source of distortion. Wells and Haas (1992) suggest that additional distortion can be induced in HMDs using CRTs as image sources. This distortion is perceptual and relates to a change in the shape of a raster-scanned picture on the retina during rapid eye movements (Crookes, 1957), such as those inherent in head-coupled systems.

Distortion in CRTs is rather easily minimized through the use of external correction circuitry. The CRT image also can be predistorted to allow for distortion induced in the display optics. FP image sources generally are considered to be distortion free, with the display optics being the source of any distortion present in HMDs using these sources. FP images also can be predistorted to correct for the display optics. However, this will require at least one additional frame of latency (Nelson, 1994).

In ANVIS, the optical system can produce barrel or pincushion distortion and the fiber-optic inverter can cause shear and gross (or "S") distortion. Shear distortion in fiber optic bundles causes discrete lateral displacements and is known also as incoherency. "S" distortion is due to the residual effect of the twist used to invert the image, which causes a straight line input to produce an "S" shape (Task, Hartman, and Zobel, 1993). Distortion requirements for ANVIS are cited in MIL-A-49425 (CR) and limit total distortion to 4%. Distortion for ANVIS typically is given as a function of angular position across the tube. Sample data from a single tube are presented in Figure 40 (Harding et al., 1996a).

As a historical note, in 1988, when AN/PVS-5's were still the most common I² system, a number of reports from National Guard units surfaced regarding "depression" and "hump" illusions during approaches and landings (Markey, 1988). Suspect goggles were obtained and tested. The final conclusion was that the distortion criteria were not sufficiently stringent. Based on testing, a recommendation was made to tighten both shear and "S" distortion specifications. Distortion requirements generally apply to single tubes. However, distortion differences between tubes in a pair of NVGs are more important. In fact, care should be taken to match tubes in pairs based on other characteristics; e.g, luminance, as well as distortion.

In Crowley's (1991) investigation of visual illusions with night vision devices, he cites examples of where aviators reported having the illusion of landing in a hole or depression when approaching a flat landing sight. Aviators also reported that normal scanning head movement with some pairs of ANVIS caused the illusion of trees bending.

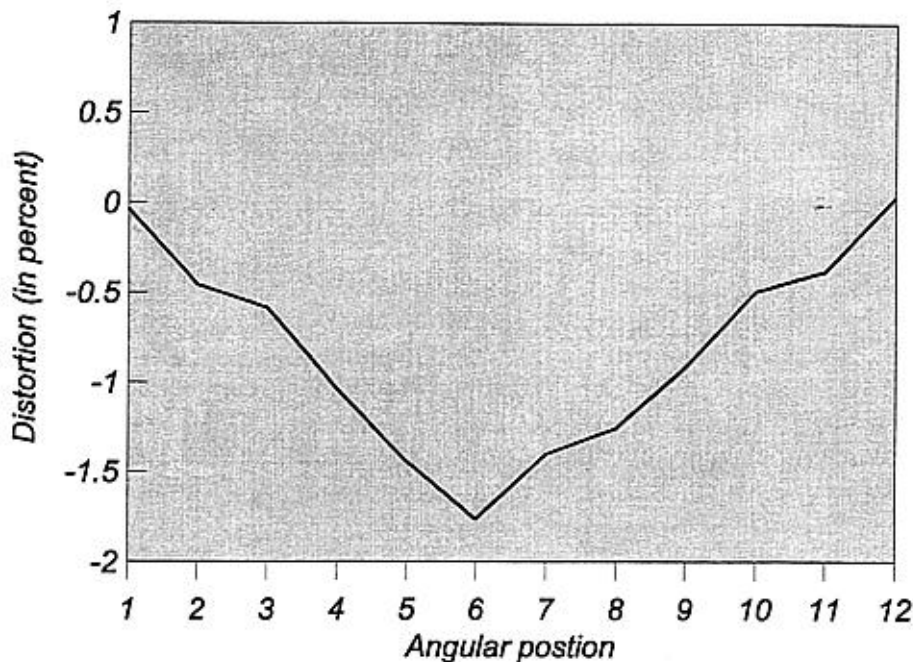


Figure 40. Percent ANVIS distortion as a function of angular position.

In general, for monocular, as well as for biocular/binocular, optical systems with fully overlapped fields of view, an overall 4% distortion value has usually been considered acceptable. That is, a deviation in image mapping towards the periphery of the display could be off by 4%, providing the deviation is gradual with no noticeable irregular waviness of vertical or horizontal lines. For a projected display with a 40-degree circular field-of-view and 4% distortion, this would mean an object at the edge of the visible FOV could appear at 40×1.04 (41.6° pincushion distortion) or $40/1.04$ (38.5° barrel distortion). For binocular displays, differences in distortion between the images presented to the two eyes are more serious than the amount of distortion (Farrell and Booth, 1984.) Distortion is better tolerated in static images than in moving images, and therefore is of increased concern in HMDs.

Biocular/binocular HMDs having overlapping symbology will have to meet head-up display specifications of 1 milliradian or less difference between the right and left image channels for symbology within the binocular overlapped area if the symbology is seen by both eyes. Otherwise, diplopia and/or eye strain will be induced. However, with see-through vision, this criterion can not be met when viewing at less than 60 meters due to eye convergence (McLean and Smith, 1987).

When imagery is used with a minimum see-through requirement, the maximum displacement between the right and left image points within the biocular/binocular region should not exceed 3 milliradians (0.3 prism diopter) for vertical, 1 milliradian (0.1 prism diopter) for divergence, and 5 milliradians (0.5 prism diopter) for convergence.

Distortion can be particularly important in aviation. For example, the apparent velocity of a target having a relative motion will change in proportion to the magnitude of the distortion (Fischer, 1997).

Luminance uniformity

Variation in luminance across a display image can be distracting (Farrell and Booth, 1984). Luminance uniformity across an image is best described by its absence or nonuniformity (Snyder, 1980). Three important types of nonuniformity are: Large area nonuniformity, small area nonuniformity, and edge discontinuity. Large area nonuniformity is a gradual change in luminance from one area of a display to another; e.g., center to edge or edge to edge. Small area nonuniformity refers to pixel to pixel luminance changes over a small portion of the image. Edge discontinuities occur over an extended boundary.

While uniformity requirements are still lacking in the classical literature, one such guidance is that the luminance at any two points within a flat field image shall not vary by more than 20% (Rash et al., 1996a). Farrell and Booth (1984) suggest limiting small and large area nonuniformities to 10% and 50%, respectively. The HIDSS allows a 20% variation from the mean image luminance, which should be based on luminance readings of at least 9 or more equally spaced positions within the image. [In cases where the entire image area is not useable, variation can be based on only that portion which provides acceptable image quality.]

CRTs provide uniformity on the order of 37% (i.e., the luminance of any small area can decrease to 63% of center luminance) (Farrell and Booth, 1984). FP technology displays also should provide reasonably acceptable uniformity. In EL displays, uniformity will be a function of quality control on the deposition of the phosphor. Uniformity in LED displays will depend on the variation in individual LEDs within and across production lots. LCD uniformity (typically <20%) is dependent on cell thickness, molecular alignment, and voltage control (Snyder, 1980). However, many LCD displays suffer from luminance fall-off as a function of viewing angle. The display optics also will affect luminance uniformity, particularly with spectrally tuned combiners.

Field-of-view

FOV, as used here, refers to the display FOV, the horizontal and vertical angles the display image subtends to the eye. In terms of impact on performance, FOV can be considered to be as important as resolution and contrast. During night and foul weather flights with HMDs, the largest amount of visual information available to the aviator is provided via the display imagery. In principle, the larger the FOV, the more information available. The maximum FOV target value would be that currently achieved by the unobstructed human visual system.

The human eye has an instantaneous FOV that is roughly oval and typically measures 120° vertically by 150° horizontally. Considering both eyes together, the overall binocular FOV measures approximately 120° (V) by 200° (H) (Zuckerman, 1954) (Figure 41). The size of the FOV that an HMD is capable of providing is determined by several sensor and display parameters including size, weight, placement, and resolution. Designs achieved so far all provide restricted FOV sizes. As FOVs decrease, head motion becomes greater and increases head and neck muscle fatigue. This also reduces the amount of background information about the area (target) of interest and induce “tunnel vision” (Biberman and Alluisi, 1992).

In ANVIS, the FOV of a single I² tube is a circular 40°. The two tubes have a 100° overlap; hence, the total FOV is also 40°. This FOV size seems small in comparison to that of the unobstructed eye. But, the reduction must be judged in the context of all of the obstructions associated with a cockpit, e.g., armor, glareshield, support structures. Still, the aviator must use continuous head movements in a scanning pattern to help compensate for the limited FOV.

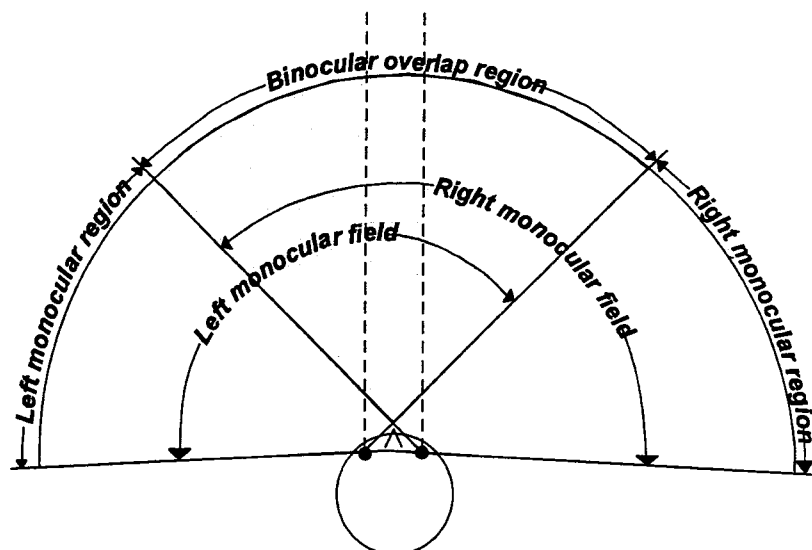


Figure 41. Human visual system's binocular FOV.

The ANVIS 40° FOV is a theoretical value. Even though the ANVIS is not an exit pupil forming system (instead uses a simple magnifier), as the eye backs away, the FOV will decrease. Such situations can occur in use due to improper adjustments, anthropometry, and use of nuclear, biological, and chemical (NBC) protective masks. These losses may not be apparent to the aviator. Kotulak (1992) investigated the in-flight FOV with ANVIS and found: a) ANVIS FOV is typically less than 40° in flight, and b) In-flight ANVIS FOV is reduced mostly due to equipment limitations. The fore-aft adjustment of the ANVIS helmet mount lacks adequate range in the aft direction. Kotulak recommended that a change from a 18-mm to a 25-mm eyepiece would improve the percentage of individuals able to achieve full FOV; this was confirmed by McLean (1995).

The IHADSS provides a 30° (V) by 40° (H) rectangular FOV, presenting an image to the pilot which is equivalent to a 7-foot (diagonal) CRT being viewed from 10 feet away (Berry et al., 1984). Although the monocular HDU design obstructs unaided lateral vision to the lower right, the IHADSS provides an unimpeded external view throughout the range of PNVS movement ($\pm 90^\circ$ azimuth and $+20^\circ$ to -45° elevation). However, the Apache aviator is trained, as with ANVIS, to continuously scan with head movements to compensate for the limited FOV. A potentially disorienting effect occurs when the aviator's head motion exceeds the PNVS range of motion – the image suddenly stops, but head motion continues. This could be misinterpreted by the aviator as a sudden aircraft pitch or yaw in the direction opposite to the head motion.

The IHADSS is designed to present the FLIR sensors's FOV in such a manner that the image on the combiner occupies the same area in front of the eye, resulting in unity magnification. However, to achieve this goal, the aviator must position his eye within the exit pupil of the HDU optics. The major determinant of whether this can be achieved is the physical distance between the eye and the edge of the HDU optical barrel. Variations in head and facial anthropometry greatly influence the ability of the aviator to comfortably obtain a full FOV. Some aviators report discomfort due to pressure against the zygomatic arch (cheekbone) (Rash and Martin, 1987a) and many report difficulty in seeing all of the symbology (Hale and Piccione, 1990). As with ANVIS, the interposition of NBC protective masks and spectacles increases the eye-HDU distance, potentially reducing the likelihood that the full FOV will be achieved (Rash and Martin, 1987b; McLean and Rash, 1984). Improper adjustment of the HDU/helmet attachment bracket and combiner also can result in FOV loss.

A number of studies have been conducted in an attempt to understand the role of FOV in pilotage and targeting tasks. Sandor and Leger (1991) looked at tracking with two restricted FOVs (20° and 70°). They found that tracking performance appeared to be “moderately” impaired for both FOVs. Further investigation on FOV targeting effects found negative impacts on coordinated head and eye movements (Venturino and Wells, 1990) and reinforced decreased tracking performance with decreasing FOV size (Kenyon and Kneller, 1992; Wells and Venturino, 1989). Kasper et al. (1997) also examined the effect of restricted FOVs on rotary-wing aviator head movement and found that aviators respond to such restrictions by making significant changes in head movement patterns. These changes consist of shifts in the center of the aviator’s horizontal scan patterns and movements through larger angles of azimuth. They also concluded that these pattern shifts are highly individualized and change as the restrictions on FOV change. This work was an extension of Haworth et al. (1996) which looked at FOV effects on flight performance, aircraft handling, and visual cue rating.

Perhaps the most important FOV study to rotary-wing aviation is the Center for Night Vision and Electro-Optics, Fort Belvoir, VA, investigation of the tradeoff between FOV and resolution (Greene, 1988). In this study, five aviators using binocular simulation goggles, performed terrain flights in an AH-1S Cobra helicopter. Seven combinations of FOV (40° circular to 60° x 75°), resolutions (20/20 to 20/70), and overlap percentages (50% to 100%) were studied. They reported the lowest and fastest terrain flights were achieved using the 40° - 20/60 - 100% and 40° - 20/40 - 100% conditions, with the aviators preferring the wider (60°) condition. However, the author did not feel that the results justified increasing FOV without also increasing resolution.

In spite of this research, the question of how large a FOV is required still has not been fully answered. Aviators want it to be as large as possible. HMD designers must perform tradeoffs between FOV, resolution, weight, size, and cost. The task of determining FOV required for flying is not a simple one. Obviously, the selected FOV should reflect the aircraft’s mission, providing optimal visual search performance, object recognition, and spatial orientation (Lohman and Weisz, 1989). Therefore, first the minimal FOV required is highly task dependent. Consider the different sensory cues used for high-speed flight across a desert floor (narrow FOV) versus a confined-area hovering turn (wide FOV). Second, the FOV required to maintain orientation depends on workload. A small attitude indicator bar (or cue), occupying only a few degrees on the display image, does not provide much information to the peripheral retina, which normally mediates visual information regarding orientation in the environment (Gillingham and Wolf, 1985). Acquiring this orientation information from the central (foveal) vision requires more concentration and renders the pilot susceptible to disorientation should his attention be diverted to other cockpit tasks for even a brief period. Third, with HMDs such as the IHADSS and HIDSS, any reduction in the FOV also may deprive the pilot of critical flight symbology.

Seeman et al. (1992) recommend an instantaneous FOV of 50° (V) by 100° (H) for flight tasks involving control of airspeed, altitude, and vertical speed. This estimate does not include considerations for other flight tasks, such as hover. Current HMD programs are striving to produce FOVs of 60° or larger. However, even a 90° FOV does not provide all the visual cues available to the naked eye (Hart and Brickner, 1989). Both Haworth et al. (1996) and Edwards et al. (1997) found that performance gains could be tied to increasing FOVs up to about 60°, where performance seems to encounter a ceiling effect. This raises the question as to whether increased FOV designs are worth the tradeoff costs.

Visual field

The term visual field refers to the unaided, unobstructed look-under/look-around ability to see the outside world. Effective and safe operation in the cockpit is in most cases dependent on

the extent of the physical space visible to the aviator's unaided eyes. It is especially important that caution and warning lights be visible, along with other instruments, in order to be able to perform tasks such as tuning radios. In an HMD, the available visual field can be impacted by the helmet, image source and the display optics. Visual field can be further reduced when NBC devices and/or oxygen masks are worn. The unaided visual field should allow for quick and easy viewing of critical cockpit instruments without excessive head movement.

The unobstructed human binocular visual field covers approximately 120° vertically by 200° horizontally. Just the wearing of a protective helmet alone can cause significant reductions in visual field, almost all in the upper vertical region. The placement of display optics obscures large portions of the central visual field. The IHADSS with its monocular HDU introduces less field obstruction than might be expected due to the overlapping of the monocular fields of the left and right eye. Measurements on the HIDSS (Harding et al, 1998) reveal that the PRU alone produces field losses similar to the HGU-56/P helmet (Figure 42). And when the ARU (with baffles used to reduce extraneous reflections) is added, the monocular field losses shown in Figure 43 are present. Binocular blind spots which may exist were not measured. However, RAH-66 simulator pilots detected only minimal presence of such areas.

The ANVIS provides limited look-under capability, allowing viewing of instruments and maps. This capability is what drove the development of the ANVIS to replace the full-face AN/PVS-5 NVG.

It is obvious that display FOV and available unaided visual field are inversely related. And, monocular HMDs, such as the IHADSS, provide a greater visual field than biocular HMDs. IHADSS aviators anecdotically report that they prefer to retain the visual field provided in the left eye available due to the monocular IHADSS design.

It must be reemphasized that the additional requirement to wear NBC masks will further reduce the available unaided visual field as well as the FOV. Such effects due to the XM-40 mask were documented by Rash and McLean (1983) where losses in both monocular and binocular fields were found.

Magnification

System magnification results in the images of objects subtending different visual angles than the objects themselves. It generally is accepted that imagery used for pilotage should be one-to-one with the sensor FOV. Magnification can result in disorientation and inaccurate distance and velocity estimations. These effects could have dire consequences during landings and formation flying. All current HMDs use unity magnification.

However, Apache aviators have reported a perceived magnification in the IHADSS imagery. Hart and Brickner (1989) and Bennett and Hart (1987) cite aviator's reports of objects appearing larger and closer than they actually are. However, Hale and Piccione (1990) report that 65% of Apache aviators (n = 52) surveyed state that objects appear to be smaller and farther away than they actually are. Responses to follow-up questions indicated that these effects were present only when viewing FLIR imagery and not when viewing only collimated symbology. During the early history of IHADSS, it was found that some aviators electronically reduced the raster image in an attempt to achieve the full FOV. However, aviator comments imply that the reported misperceptions occurred even when the system was verified as having 1:1 magnification.

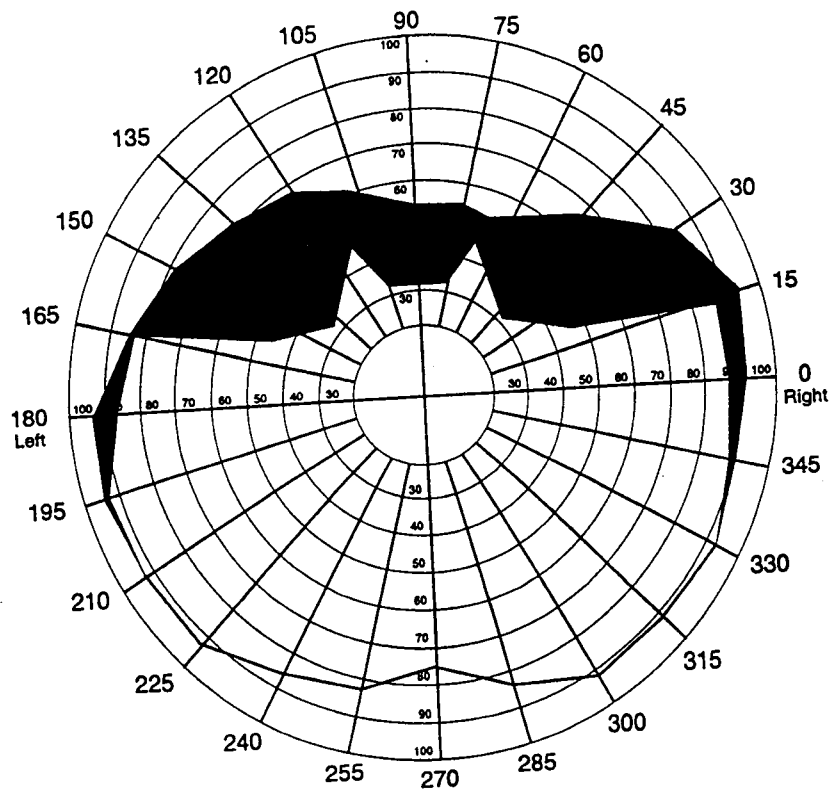


Figure 42. Binocular visual field for the HIDSS PRU only.

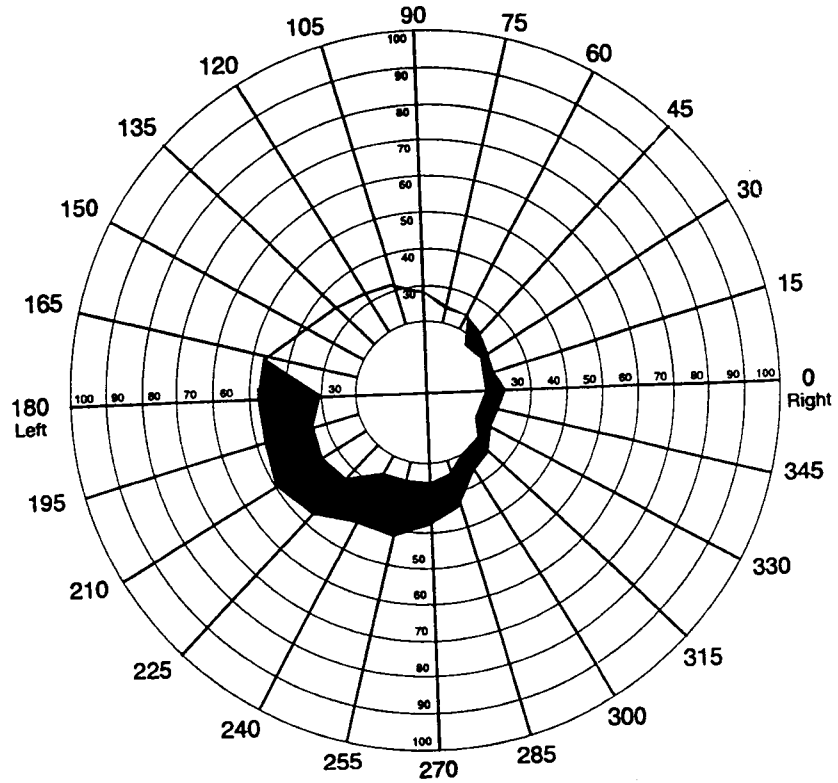


Figure 43. HIDSS ARU binocular visual field (left eye shifted due to PRU redonning).

Magnification is used in targeting with head-down systems. However, in general, using high magnification with the narrow FOV used for targeting would be undesirable because of head jitter and aviator disorientation (Tsou, 1993). In a simulator study (Peterson, King, and Hilgendorf, 1977), it has been shown that a 7:1 change in magnification (from 20° to 3°) can be tolerated.

See-through luminous/spectral transmittance

Aviation HMD designs, except for ANVIS, use a beamsplitter (combiner) to present sensor imagery while allowing limited see-through vision to the outside world. This see-through capability requires that attention be paid to the luminous and spectral characteristics of the combiner. A certain percentage of the luminance of the background must be transmitted, however, high ambient background luminances must be attenuated to provide sufficient imagery contrast (Cohen, 1979). This problem was discussed in a previous section, Contrast.

Since the combiner overlays the sensor image onto that of the outside world, interference may occur (Wells and Haas, 1992). This interference may affect the perception of information within the HMD imagery and/or the external scene. Luminance contrast can be reduced and spectral deviations may be introduced due to the combiner's characteristics. To achieve higher contrast, the combiner often is designed to attenuate the external background luminance and to be highly reflective for the peak wavelength of the monochromatic image source. Reducing combiner transmittance has been shown to be effective in increasing HMD imagery contrast in the Apache (Rash, McLean, and Monroe, 1981). The spectral effects on symbology contrast were modeled by Rash, Monroe, and Verona (1981) using the spectral transmittance and reflectance of the IHADSS combiner, emission of P43, and various variegated backgrounds.

It must also be noted that the HMD system usually incorporates one or more visors. These visors are depended upon to assist in the achievement of sufficient contrast values in high ambient luminance environments and must be considered when designing the combiner's transmittance characteristics. While visors used for sun and wind protection usually will be spectrally neutral, some visors are designed to provide protection from directed energy sources, e.g., lasers, and will have spectrally selective transmittance characteristics. [For further discussion, see upcoming section, Visors and visor assemblies.]

Exit pupil

The exit pupil (or Ramsden disk) of an (pupil forming) HMD is the area in space where all the light rays pass; however, it often is pictured as a two-dimensional hole. To obtain the full FOV, the viewing eye must be located at (within) the exit pupil. Conversely, if the eye is totally outside of the exit pupil, none of the FOV is visible. As the viewer moves back from the exit pupil, the FOV will decrease. [The eye has an entrance pupil; when the exit pupil of the HMD is larger than the entrance pupil of the eye, the eye can move around without loss of retinal illumination or FOV (Self, 1986).] The main advantage of an exit pupil forming system is the use of the extra optical path length to form fit the HMD to the head (Task, 1997).

The exit pupil has three characteristics: Size, shape, and location. Within the limitation of other design confounds, e.g., size, weight, complexity, and cost, the exit pupil should be as large as possible. IHADSS has a circular 10-mm diameter exit pupil. The HIDSS exit pupil also is circular but with a 15-mm diameter. While systems with exit pupils with diameters as large as 20 mm have been built, 10 to 15 mm is the typical value (Task, Kocian, and Brindle, 1980). Tsou (1993) suggests that the minimum exit pupil size should include the eye pupil (~ 3 mm), an allowance for eye movements that scan across the FOV (~ 5 mm), and an allowance for helmet

slippage (± 3 mm). This would set a minimum exit pupil diameter of 14 mm. Since the exit pupil is the image of an aperture stop in the optical system, the shape of the exit pupil is generally circular and, therefore, its size is given as a diameter.

The exit pupil is located at a distance called the optical eye relief, defined as the distance from the last optical element to the exit pupil. This term has caused some confusion. What is of critical importance in HMDs is the actual physical distance from the plane of the last physical element to the exit pupil, a distance called the physical eye relief or the eye clearance distance. This distance should be sufficient to allow use of corrective spectacles, NBC protective masks, and oxygen mask, as well as, accommodate the wide variations in head and facial anthropometry. This has been a continuous problem with the IHADSS, where the optical eye relief value (10 mm) is greater than the actual eye clearance distance. This is due to the required diameter of the HDU objective lens and the bulk of the barrel housing. To overcome the incompatibility of spectacles with the small physical eye relief of the IHADSS, the Army has investigated the use of contact lenses (Bachman, 1988; Lattimore and Cornum, 1992; Lattimore, 1990). While citing a number of physiological, biochemical and clinical issues associated with contact wear and the lack of reliable bifocal capability, the studies did conclude that contact lenses may provide a partial solution to HMD eye relief problems.

Extraneous reflections

Extraneous reflections also are known as ghost images. If no recognizable images result, the effect generally is called veiling glare. They can be defined as unwanted or stray light in an optical image. They can have a number of sources (Farrell and Booth, 1984) which include interreflections from optical surfaces, reflections from support structures inside the display, and optical surface defects such as fingerprints and dirt. Since most of the optical elements are polished and curvilinear, images of bright external sources, such as the sun, can be present with sufficient brightness to be extremely troublesome (Kingslake, 1983).

The primary method for reducing ghost images is the application of antireflection coatings. Baffles and light blocks also are used.

In HMD optical designs which are only partially enclosed, such as the IHADSS and HIDSS, the open combiner(s) serve as excellent surfaces to collect dirt and oils. In the real world environment, such open designs are natural casualties of continuing handling with contaminated hands. The fingerprints and the resulting veiling glare will degrade image contrast (Coleman, 1947). Visors used as part of the HMD optical design also can be major sources for extraneous reflections (Task, 1997). This comes about because visors have two surfaces, only one of which (the inner) are used as part of the optical path. A measure of the effect of such a ghost image is given by the following equation (Task, 1997):

$$G_r = R_1 / (T_1^2 \cdot R_2) \quad \text{Equation 19}$$

where G_r = image to ghost ratio; R_1 = reflection coefficient of the first (inner) surface; R_2 = reflection coefficient of the second (outer) surface; and T_1 = transmission coefficient of the visor material and inner surface. A more robust but more complicated method for quantifying ghost images from external light sources such as the sun can be found in Rash et al. (1996a).

A number of extraneous reflections have been reported with the CRT based HIDSS (Harding et al., 1997). A partial solution to this problem has been to install rubber baffles over the combiners.

Monocular/biocular/binocular considerations

HMDs can be classified as monocular, biocular, and binocular. These terms refer to the presentation of the imagery by the HMD. As previously defined, monocular means the HMD imagery is viewed by a single eye; biocular means the HMD provides two visual images from a single sensor, i.e., each eye sees exactly the same image from the same perspective; binocular means the HMD provides two visual images from two sensors displaced in space. [Note: A binocular HMD can use a single sensor, if the sensor is somehow manipulated to provide two different perspectives of the object scene.] A biocular HMD may use one or two image sources, but must have two optical channels. A binocular HMD must have separate image sources (one for each eye) and two optical channels.

Monocular issues

The AH-64 IHADSS is a monocular design, providing imagery to the right eye only. The ANVIS is a binocular design, with two sensors providing imagery to the separate eyes. The HIDSS design is a partial binocular divergent design with an overlap of approximately 30% (based on a 17° overlap region within the 52° horizontal FOV).

Monocular HMDs generally have smaller packaging, lighter weight, and lower design costs. Their smaller packaging permit them to be placed closer to the head, causing less reduction in visual field (Laycock and Chorley, 1980). Their drawbacks include FOV limitations, small exit pupil, the potential for binocular rivalry, eye dominance problems, increased workload, and reduced reaction time (Conticelli and Fujiwara, 1964). The reduced FOV [30° (V) x 40° (H) for the IHADSS] results in the need for increased head movements. The small exit pupil size requires the display to be very close to the eye and requires a very stable head/HMD interface. Binocular rivalry causes viewing conflicts between the aided eye viewing the display imagery and the unaided eye viewing the outside world. [Rivalry would be a greater concern in monocular systems where one eye was totally occluded. Such is not the case for IHADSS, where the display eye has see-through capability.] When rivalry does exist, studies have shown that target recognition and visual performance in general decreases (Hershberger and Guerin, 1975). Eye dominance may influence visual performance, of critical interest if the monocular HMD design does not allow for user preference (such as in the IHADSS where the display is always mounted on the right eye).

The IHADSS has been in use since its full fielding in June 1985. The IHADSS monocular design requires the aviator to switch his visual processing from the aided to unaided eye. Apache training has the highest failure rate for rated student aviators transitioning into a complex aircraft (Cornum, Caldwell, and Ludwick, 1993). It is a 7-phase training program with the most difficult being the “bag phase” when aviators fly in an enclosed cockpit using only the imagery provided on the IHADSS. Cornum, Caldwell, and Ludwick (1993) conducted a study of 140 Apache student aviators in order to determine factors which might be used to predict course success or failure. The use of a monocular display and the remoteness of the FLIR sensor were not identified as potential factors. However, many aviators were unable to overcome “bag” sickness, a type of simulator sickness, which manifested itself during the “bag” phase. It was unclear whether the use of the HMD was related to this problem.

When Hale and Piccione (1990) performed an aviator assessment of the IHADSS, they found evidence of increased workload, visual and mental fatigue, and stress. They found that as a mission progressed, aviators experienced increased difficulty in switching between eyes for visual input. Aviators reported having to resort to extreme actions, such as closing one eye, to

either suppress or produce attention switching. Aviators, also, reported visual fatigue from the display “brightness” in the aided eye.

To help understand the visual processing with monocular HMDs, Caldwell et al. (1991) compared the performance of rated Apache aviators to other Army aviators on visual tasks involving monocular imagery presentation. Each aviator was given a task presented monocularly to the right eye, a task presented monocularly to the left eye, and a task presented to both eyes simultaneously in a dichoptic task. Results indicated no performance difference between groups for the dichoptic task, but indicated better performance with the Apache aviators for the monocular left eye task. Also, there was a trend for the Apache aviators to perform better on the monocular right eye task. The ability of the Apache aviators to perform better on the dichoptic task was contrary to what was expected. However, the improved monocular performance seems to indicate that aviators trained on monocular HMDs are capable of performing single-eye tasks better than aviators who use binocular vision while flying.

During the first years of fielding the Apache, the training failure rate was high (~10%), and eye dominance was suggested as a probable cause. McLean (1990) correlated data on 16 Apache aviators for multiple eye dominance tests. Results showed little correlation between tests. This was explained by the rationale that eye dominance itself is not a singularly defined concept and is task dependent. Also, data failed to show any before and after effects on eye dominance due to PNVS training.

The one-eye, see-through design of the IHADSS has the potential of one last problem. The design produces a differential dark and light adaptation in the two eyes (Shontz and Trumm, 1969). Such conditions could bring rise to an effect known as the Pulfrich phenomenon, a depth illusion for laterally moving objects caused by image delay to the darker adapted eye. The Pulfrich phenomenon has not been documented with the IHADSS.

Biocular/binocular issues

As previously discussed, perhaps the greatest disadvantage of monocular HMDs is their reduced FOVs. It is well documented that reduced FOVs degrade many visual tasks (Kenyon and Keller, 1992; Osgood and Wells, 1991). In HMD designs, the size (diameter) of the relay optics limits the available FOV. To provide larger FOVs, designers have adopted a method of partially overlapping the FOVs of two optical channels. This results in a larger, partially overlapped FOV consisting of a central binocular region (seen by both eyes) and two monocular flanking regions (each seen by one eye only) (Figure 8). Such overlapping schemes can be implemented by either divergent or convergent overlap designs. In a divergent design, the right eye sees the central overlap region and the right monocular region, and the left eye sees the central overlap region and the left monocular region (Figure 9). In a convergent design, the right eye sees the central overlap region and the left monocular region, and the left eye sees the central overlap region and the right monocular region (Figure 10). As an example, the Comanche HIDSS design is divergent and has an overlap of approximately 30% (based on a 17° overlap region within the 52° horizontal FOV).

It generally is agreed that most visual capabilities, e.g., detection, discrimination, recognition, etc., are improved when two eyes are used, as compared to one (Rabin, 1995; Home, 1984; Campbell and Green, 1965). Using this logic and the FOV argument, current HMD designs are two-eye designs. If an HMD is a two-eye design, there are a number of parameters which must be considered. These include IPD, image alignment between the two eyes, and luminance balance (Task and Kocian, 1995). Failure to pay proper attention to these and corresponding issues can result in retinal rivalry, eye strain, fatigue, and, if severe enough, diplopia.

Humans view scenes binocularly. Typically, an adult male's eyes are located 55-73 mm apart with the eyes' lines-of-sight converged to an angle that matches their accommodation distance. Because of this configuration, each eye sees a slightly different view (perspective) of the same scene, which provides depth perception and stereopsis. Biocular/binocular HMDs, while providing imagery to both eyes, can depart from this natural arrangement in several ways (National Research Council, 1997). Biocular HMDs use a single sensor to present the same image of the scene to both eyes, but lacking the disparity in perspective to provide stereopsis. ANVIS is a straight forward binocular display, using two input sensors separated by a distance to provide separate images to the two eyes. HIDSS is a biocular system. But, since the FLIR sensor FOV is larger than the display optics FOV, the HIDSS presents approximately two-thirds of the sensor FOV to each eye, resulting in a display FOV that matches the sensor FOV, but consists of two monocular regions and a central region seen by both eyes.

Biocular tolerances

Having two optical channels presents the opportunity to have disparities (mismatches) between the imagery presented to the two eyes. These disparities can be alignment errors or optical image differences. Alignment errors reflect lack of parallelism of the two optical axes and can be vertical, horizontal, and/or rotational. Optical image differences can be in contrast, distortion, size (magnification), and/or luminance (Self, 1986). These errors will exist. The question is what magnitude of disparity can be tolerated before performance noticeably degrades. These permissible differences are referred to as the optical tolerance limits for the HMD design.

Self (1986) provides a review of optical tolerance studies conducted and standards developed before 1986. The results of the review are summarized in Table 12. Also included in Table 12 are more recent tolerance recommendations. It is important to note that users will have varying sensitivities to these tolerances.

Fusion, which is the human visual system's ability to perceive the two images presented as one, is somewhat tolerate. Therefore, some misalignment can be present. Such tolerance limits are not well defined, as can be seen from the wide variation in values in Table 12. Also, it is expected that tolerance limits will vary among individuals and decrease with exposure, fatigue, and hypoxia. The first signs of having exceeded tolerance limits will most likely manifest themselves in the onset of visual fatigue, eye strain, and headaches.

An all encompassing discussion of binocular tolerance limits can be found in Melzer and Moffitt (1997).

Special consideration must be given to HMD designs using partial overlap. For partial overlapped HMDs, such as the HIDSS, image alignment is of greater criticality for certain parameters. Failure to limit magnification differences in the two optical channels can create considerable disparity effects, depending on the percentage of the overlap, the greater the overlap region, the lesser magnification which can be tolerated (Melzer and Moffitt, 1989; Self, 1986). Distortion induced disparities also will be more pronounced in partial overlapped HMD designs.

Table 12.
Summary of binocular optical tolerance limits.
 (Self, 1986)

Vertical misalignment	Horizontal misalignment (Convergence)	Horizontal misalignment (Divergence)	Rotational difference	Magnification difference	Luminance difference
8 arcminutes (2.3 mr) (Jacobs, 1943)	22.5 arcminutes (6.5 mr) (Jacobs, 1943)	7.5 arcminutes (2.2 mr) (Jacobs, 1943)	10 arcminutes (Gold, 1971)	2% (MIL-Handbook-141, Defense Supply Agency, 1962)	10% (MIL-Handbook-141, Defense Supply Agency, 1962)
14 arcminutes (4.1 mr) (Harvey, 1970)	28 arcminutes (8.1 mr) (Harvey, 1970)	14 arcminutes (4.1 mr) (Harvey, 1970)	2° (MIL-A-49425, 1989)	2% (MIL-STD-1472C, 1981)	3% (U.S. Navy, 1966)
17 arcminutes (4.9 mr) (MIL-Hand-141, 1962)	2 arcminutes (0.6 mr) (U.S. Navy, 1966)	4 arcminutes (1.2 mr) (U.S. Navy, 1966)	29 arcminutes (Farrell and Booth, 1984)	< 5% (MIL-STD-1472C, 1981)	5% MIL-STD-1472C, 1981
2 arcminutes (0.6 mr) (U.S. Navy, 1966)	8.8 arcminutes (2.6 mr) (Genco, 1983)	3.4 arcminutes (1 mr) (Gold, 1971)		< 0.8% (Farrell and Booth, 1984)	< 50% (Farrell and Booth, 1984)
3.4 arcminutes (1 mr) (Gold and Hyman, 1970)	8.6 arcminutes (2.5 mr) (Gold, 1971)	4.1 arcminutes (1.2 mr) (Genco, 1983)		0.28% (Gold, 1971)	15% (Lippert, 1990)
19 arcminutes (5.5 mr) (Lippert, 1990)	2.7° (47.1 mr) (Farrell and Booth, 1984)	3.4 arcminutes (1 mr) (Gold and Hyman, 1970)		10% (MIL-A-49425, 1989)	
3.4 arcminutes (1 mr) (Gold, 1971)					

Note: Caution should be used in applying these values since they are based on studies of various optical devices and under different test conditions.

Partial binocular overlap issues

The implementation of partial overlap to achieve larger FOVs brings with it certain additional concerns. Fragmentation of the FOV, luning, and changes in target detection capability can occur in HMDs employing partial overlap (Klymenko et al., 1994a,b,c). If both eyes see the identical full image in a binocular HMD, what is known as a full overlap FOV, then the overall FOV is limited to the size of each of the monocular fields. If for design reasons, the

size of the monocular fields are at a maximum and can not be increased without incurring unacceptable costs such as reduced spatial resolution, or increased size and weight of the optics, then the size of the full overlap FOV may not be sufficient.

Partial overlap is a way to increase the HMD's FOV, without increasing the size of the two monocular fields. In such a case, the new wider FOV consists of three regions---a central binocular overlap region seen by both eyes and two flanking monocular regions, each seen by only one eye (Figure 8). There are perceptual consequences for displaying the FOV to the human visual system in this unusual way. These perceptual effects have been a concern to the aviation community because of the potential loss of visual information and the visual discomfort (Edgar et al., 1991; Kruk and Longridge, 1984; Landau, 1990; Alam et al., 1992; Melzer and Moffitt, 1989).

First, whereas the full overlap FOV consists of one contiguous binocular region, the partial overlap FOV consists of three regions, distinguished by how each stimulates the visual system. This can result in the visual fragmentation of the three regions into three phenomenally separate areas, separated by the binocular overlap borders. Since this is a non-veridical perception of what is in reality a continuous visual world, visual misinterpretations may result.

Second, luning may occur in the FOV of partial overlap displays. This is a temporally varying subjective darkening of the flanking monocular regions, most pronounced near the binocular overlap borders (Figure 44). This phenomenon, like visual fragmentation, is due to the nature of the dichoptic stimulation of the monocular regions, meaning that each eye is receiving dissimilar stimulation in corresponding locations, instead of the similar stimulation of normal unaided vision. In this situation, dichoptic competition occurs. Here, the monocular region of the FOV presents a portion of the visual world to one eye and the black background, rather than the visual world, to the other eye. This results in various forms of binocular rivalry, where these inputs compete for awareness, with the inputs of each eye alternating in suppressing the input of the other eye. Phenomenally, this is experienced as the darkening effect of luning, which is most prevalent when the eye receiving the wrong image of the black background dominates and suppresses the eye receiving the right image of the visual world.

Third, this competing visual input can result in less detectable targets in the monocular regions of the partial overlap FOV (Klymenko et al., 1994c). Melzer and Moffitt (1997) have proposed blurring the binocular edges or putting in dark contour lines to separate the binocular and monocular regions to alleviate the detrimental visual effects. In dichoptic competition, sharper edges are stronger competitors than smooth edges (Kaufman, 1963). The blurring works by weakening the competitive dichoptic strength of the wrong image, and the placement of dark contours works by enhancing the strength of the right image. Klymenko et al. (1994d) have confirmed that the placement of contours reduces luning.

A remaining issue is the choice of whether the partial overlap should be convergent or divergent (Figures 9 and 10). [In the convergent design, the right monocular image is presented to the left eye, and vice versa; in the divergent design, the right monocular image is presented to the right eye and the left monocular image is presented to the left eye.] Klymenko et al. (1994d) have found that there is less luning in convergent FOVs compared to divergent FOVs, and, while luning is reduced by the placement of dark contours in both cases, the convergent FOV still induces less luning. Klymenko et. al (1994a) found more fragmentation in divergent than in

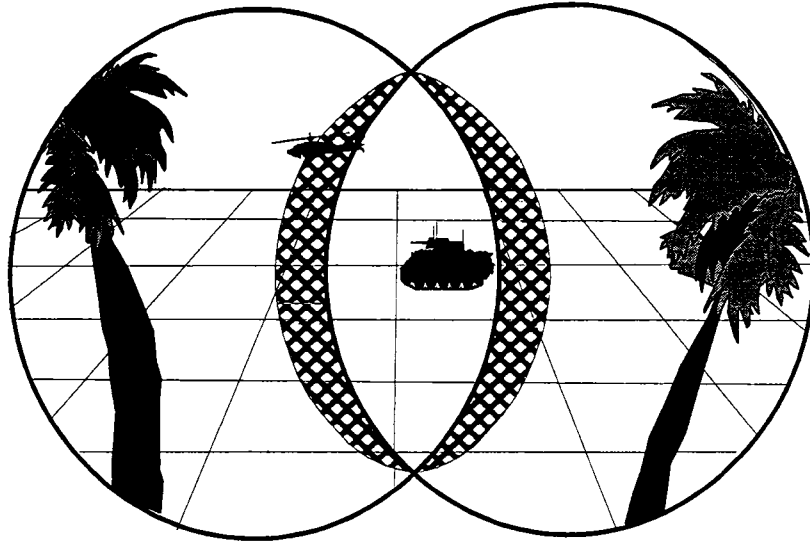


Figure 44. Luning in partial overlap HMDs.

convergent displays, and in displays with smaller as opposed to larger binocular overlap regions. This increased luning and fragmentation of divergent displays also affects target visibility, where Klymenko et al. (1994c) found that targets were less detectable in divergent than in convergent displays, and less detectable in both of these than in full overlap displays. The differences in target visibility, thought small in terms of the contrast required to detect the target, were systematic and significant.

In view of these issues, it generally is recommended that full overlap be implemented wherever unless the increased FOV provided by partial overlap is essential (Kalawsky, 1993).

Monochrome vs. color

All fielded HMDs in Army aviation are monochromatic (having no variation in hue). ANVIS and IHADSS are green on black. Color HMDs have not been fielded to date due mostly to their high cost and weight; color displays also require resolution and luminance tradeoffs. Also, the use of color image sources increases the complexity of the relay optics design since a polychromatic design must be used. However, these factors have not decreased their desirability to the user. This desirability lies in the fact that color is a very conspicuous attribute of objects. Color can facilitate three functions: Serve as the actual work object, support cognitive functions, and to assist in spatial orientation (Spengelink and Besuijen, 1996). Overall, color has the potential to reduce workload and improve visual performance.

The “color” of monochrome CRT and I² displays is defined primarily by the choice of phosphor. And, the choice of phosphor is defined primarily by luminous efficiency. Approaches to achieving color LCDs are numerous and increasing every day. One approach is similar to the additive color method employed in modern CRT displays. In this approach, pixels are composed of three or more color subpixels. By activating combinations of these subpixels and controlling the transmission through each, a relatively large color gamut can be achieved. The most

promising near-term LCD color technology is subtractive-color. AMEL displays can provide limited or full color, achieved either by classic filtering techniques of color-by-white or by patterned phosphors similar to those used in conventional CRTs.

A number of studies have expounded on the positive impact of color on performance. In one of the more comprehensive studies, DeMars (1975) concluded that, for certain applications, accuracy, decision time, and workload capability were enhanced with the use of color. However, Davidoff (1991) and Dudfield (1991) found that the actual significance of color far outweighed its perceived importance. An investigation (Spengelink and Besuijen, 1996) of whether the use of color, and the resulting available chromatic contrast, could help improve performance in the presence of low luminance contrast concluded that only under special conditions was there an additive effect, and, in general, chromatic contrast cannot be substituted for luminance contrast. Rabin (1996a) compared Snellen and vernier acuity, contrast sensitivity, peripheral target detection, and flicker detection for simulated green ($x = 0.331$, $y = 0.618$) and orange ($x = 0.531$, $y = 0.468$) phosphors. For central visual tasks, no differences were found. However, peripheral target detection was found to be enhanced for the green phosphor.

Efforts to develop color HMDs date back at least to the 1970s (Post et al., 1994) at which time Hughes Aircraft under the direction of the U.S. Air Force Armstrong Laboratory, Wright-Patterson AFB, Ohio, produced a monocular display around a miniature, 1-inch, P45 CRT which used a rotating filter to provide field-sequential color. Since this effort, a number of other attempts based on multiple image source technologies and methods have been made with only limited success. However, the most promising approach to providing full color in an HMD is based still on field-sequential color, with its looming field breakup problem. Post, Monnier, and Calhoun (1997) have recently looked at this problem and developed a model for predicting whether this breakup will be visible for a given set of viewing conditions.

It has been suggested that full color HMDs may not be necessary in some applications, and that, through the use of limited color displays, the cost and complexity of color HMDs may be reduced while maintaining the advantages of color. Reinhart and Post (1996) conducted a study looking at the merits and human factors of two-primary color AMLCDs in helmet sighting systems. One of their conclusions was that such a design could prove beneficial in an aviation HMD application.

Besides cost, weight, and complexity drawbacks to the implementation of color HMDs, additional issues are present. The luminous efficiency of the eye is a function of wavelength and adaptation state. For example, at photopic levels of illumination, the eye is most efficient at 555 nm, requiring at other wavelengths more energy to perceive the same brightness. Therefore, care must be taken in multiple color display designs to ensure isoluminance (Laycock and Chorley, 1980). Also, it has been found that larger size symbols are required to ensure that both detail and color can be perceived when color is selected over black and white (DeMars, 1975).

One final issue for this section is the chromatic aftereffects reported with I² devices. This problem first was raised in the early 1970s (Glick and Moser, 1974). This afterimage phenomenon was reported by U.S. Army aviators using NVG for night flights. It was initially, and incorrectly, called "brown eye syndrome." The reported visual problem was that aviators experienced only brown and white color vision for a few minutes following NVG flight. Glick and Moser (1974) investigated this report and concluded that the aviator's eyes were adapting to the monochromatic green output of the NVGs. When such adaptation occurs, two phenomena may be experienced. The first is a "positive" afterimage seen when looking at a dark background; this afterimage will be the same color as the adapting color. The second is a "negative" afterimage seen when a lighter background is viewed. In this case, the afterimage

will take on the compliment color, which is brown for the NVG green. The final conclusion was that this phenomenon was a normal physiological response and was not a concern. A later investigation (Moffitt, Rogers, and Cicinelli, 1988) looked at the possible confounding which might occur when aviators must view color cockpit displays intermittently during prolonged NVG use. Their findings suggested degraded identification of green and white colors on such displays, requiring increased luminance levels.

Visual performance

The discussions of physical FOMs above did not attempt to relate the measured values to the visual performance of the user. However, in some cases, it was appropriate to provide limited comments on the impact of the FOMs on user visual performance. In the following sections, system performance as a function of user visual performance is explored in greater depth. The eye has its own transfer function which must be considered when the display image is viewed. Previously, the FOMs for displays were categorized into four domains: Spatial, spectral, luminance, and temporal (Table 8). These image domains parallel analogous human visual performance domains. The spatial domain includes those display parameters associated with angular view (subtense) of the user and coincide with user's visual acuity and spatial sensitivity. The spectral domain consists of those parameters associated with the user's visual sensitivity to color (wavelength). The luminance domain encompasses those display parameters identified with the overall sensitivity of the user to illumination levels. The temporal domain addresses display parameters associated with the observer's sensitivity to changing levels of light intensity.

The human eye has an extraordinary visual capability. It can perceive light within the spectral region of 0.38 μm (violet) to 0.78 μm (red). It consists of a central region, containing cone detectors, which provides detail and color perception (decreasing with decreasing cone density away from the center, fovea); and a peripheral region, containing rod detectors, which provides black and white perception and motion detection. The maximum sensitivity of the cones is about 555 nm and is 507 nm for the rods. The eye has 10 decades of dynamic sensitivity, which usually are divided into three ranges: Photopic (day), mesopic (twilight), and scotopic (night) (Bohm and Schraner, 1990). Adaptation to these varying levels is achieved through the changing pupil diameter from 2.5 to 8.3 mm. The temporal integration time of the eye is about 200 msec. Its resolution capability (for sine waves) is better than 1.72 cy/mr. However, these characteristics vary with age and viewing conditions.

Visual acuity

Visual acuity is a measure of the ability to resolve fine detail. Snellen visual acuity commonly is used and is expressed as a comparison of the distance at which a given set of letters is correctly read to the distance at which the letters would be read by someone with clinically normal vision. A value of 20/80 indicates an individual reads letters at 20 feet that normally can be read at 80 feet. Normal visual acuity is 20/20. Visual acuity, as measured through imaging systems, is a subjective measure of the user's visual performance using these systems. The acquisition is a primary performance task. For this task, a reduced acuity value implies the user would achieve acquisition at closer distances. The accepted high contrast acuity value for 2nd and 3rd I² systems are 20/60 and 20/40, respectively (Rash, Verona, and Crowley, 1990). However, providing an acuity value for thermal (FLIR) systems is difficult since the parameter of target angular subtense is confounded by the emission characteristics of the target. However, for comparison purposes, Snellen visual acuity with the AH-64 PNVS/THADSS is cited as being 20/60 (Greene, 1988).

It is well known that visual acuity with I^2 decreases with decreasing night sky illumination (Kotulak and Rash, 1992; Wiley, 1989a; Vollmerhausen, Nash, and Gillespie, 1988). Rabin (1996b) explored the source of this decrease and determined the limiting factor to be the contrast attenuation in the I^2 devices.

Contrast sensitivity

The human visual system's ability to discern information from a displayed image is limited by its capacity to perceive differences in luminance within the image. These luminance contrasts demarcate the available pattern information of the image. Discounting color and temporal differences, image information is conveyed primarily by patterned contrast. Thus the information that can be conveyed by a display to a human observer is fundamentally limited by the human ability to perceive contrast. Different magnitudes of contrast are required to perceive different images. For example, the image of a large sharply demarcated object may require less contrast than the image of a small blurry object. If the contrast in an image is too low, i.e., below the visual threshold for detecting contrast, the displayed information will not be perceived. To make appropriate use of the figures of merit describing image quality in terms of contrast, one must characterize the human limitations in detecting contrast. The ultimate goal is to ensure an appropriate match between the contrast in the image conveying the displayed information and the human perceiver's ability to use that contrast.

The smallest magnitude of contrast that can be detected is a jnd between two luminances. A "jnd" is a threshold value that is typically defined as some percentage of the time that a stimulus is correctly detected, often arbitrarily set at 75%. In other words, a jnd of contrast is the threshold magnitude of the luminance difference between two areas that is required to just detect that difference. In order to understand the relevance of the luminances of a display in terms of human perception, the dynamic range of a display, the difference between the maximum and minimum luminances, can be defined, or scaled, in terms of the number of jnds within that range. The number of jnds from minimum to maximum luminance gives us the luminance range in human threshold units (Schuchard, 1990).

The threshold contrast detection characteristics of the human visual system have been quantified in a number of different experiments (IES, 1984). Examples of data are shown in Figures 45-47. A typical plot of a probability function for detecting a small round test target, for different luminances of the target, against a constant uniform luminance background is given in Figure 45 as a function of the contrast between the target and the background. The plot shows that the probability of "seeing" the target increases from zero until the contrast between target and background reaches 1.0, where the target can be detected 100% of the time. [This is a typical threshold curve with an ogival (monotonically increasing s-shaped) region between perfect visual performance and chance performance, where the threshold point is defined as one of the values on the curve, usually the 75% correct point for a yes/no detection paradigm.] The contrast threshold value is affected by many factors, including, for example, target size, background luminance, and viewing duration as shown in Figures 46 and 47. Threshold contrast decreases with increasing size and with increasing background luminance as shown in Figure 46, where target size is held constant.

An efficient way of characterizing the contrast threshold responses of the human visual system is the contrast sensitivity function shown in Figure 48, where "contrast" refers to modulation contrast. This plots contrast threshold values as a function of target spatial frequency. Spatial frequency refers to the number of a periodic pattern's repetitions, or cycles, within a unit length. [This unit length is typically expressed as a degree of visual angle when the perceiver is emphasized or as a display width when the image is emphasized.] Contrast

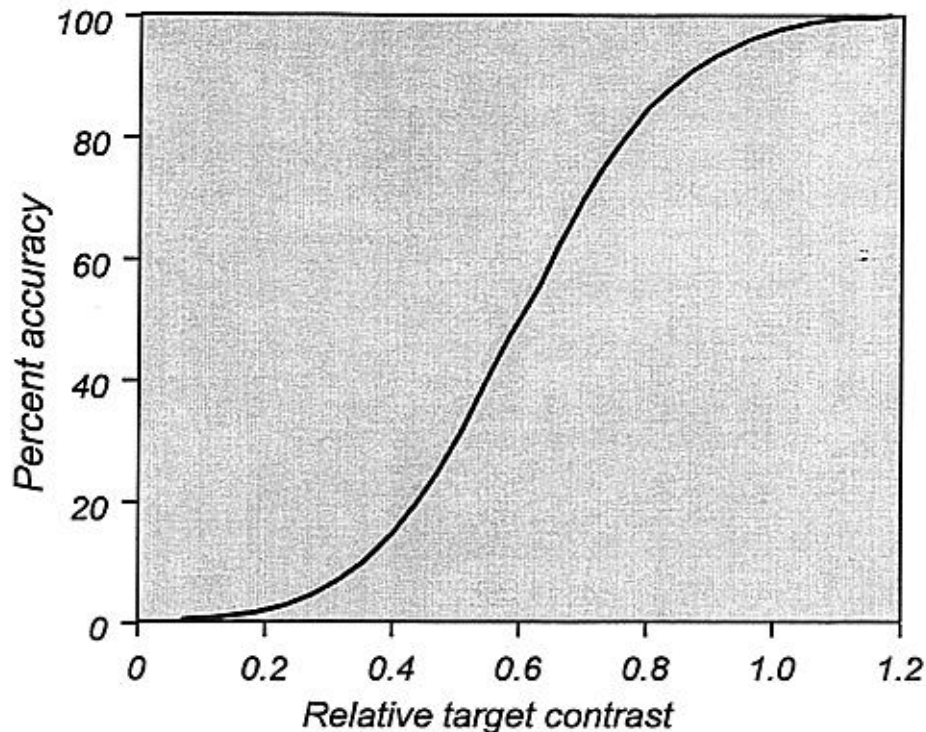


Figure 45. Probability of detecting a small round target luminance against an uniform background luminance (IES, 1984).

sensitivity (on the vertical axis) is the reciprocal of the contrast threshold. The curve indicates that the human visual system is maximally sensitive, i.e., requires the least contrast to detect the pattern's presence, for patterns with a spatial frequency somewhere between 2 and 5 cycles per degree of visual angle. Sensitivity drops off for lower and for higher spatial frequency targets. Sine wave targets smaller or larger than the optimum size need more contrast to be seen.

Sine wave gratings are typically used as the stimulus in generating human contrast sensitivity functions because the mathematical tools available (Fourier analysis and linear systems theory) allow one to generalize the results to a wide range of imaging conditions. [It also allows one conceptually to integrate the human perceiver component into a description of the total imaging context.] The human contrast sensitivity curve essentially describes the ability of the human visual system to perceive luminance differences for different gradients of luminance change across an image in one orientation. For example contrast detection threshold is dependent on whether the stimulus is a thin, sharp edge, i.e., a high spatial frequency stimulus with a sharp gradient in luminance, or a blurry edge, i.e., a low spatial frequency stimulus with a slow gradient, or an intermediate edge, to which the visual system is maximally sensitive. As previously discussed, the analogous function for display devices is the MTF, a contrast based figure of merit describing image quality in terms of a display's efficiency in converting voltage (scene contrast data) into displayed image contrast for different spatial frequencies. The human contrast sensitivity curve can likewise be considered as the visual system's efficiency curve in transmitting a physical stimulus contrast into a perception. Image display scientists have theorized and researched the question of how to mathematically combine the human and the display's contrast transmission efficiency curves in order to predict the suitability of a display's capacity to present contrast in terms of the human's ability to perceive it (Snyder, 1980). These include the MTF and SQRI discussed previously.

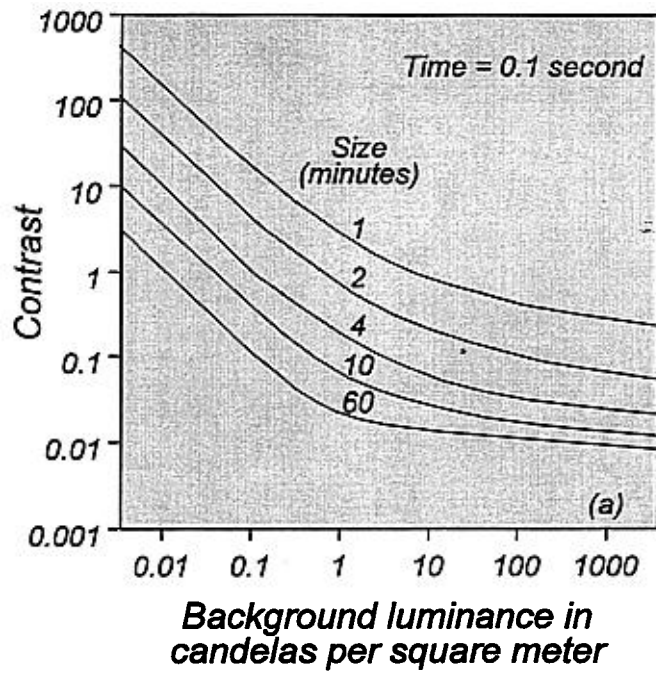


Figure 46. The relationship between threshold contrast and background luminance for various sized targets (IES, 1984).

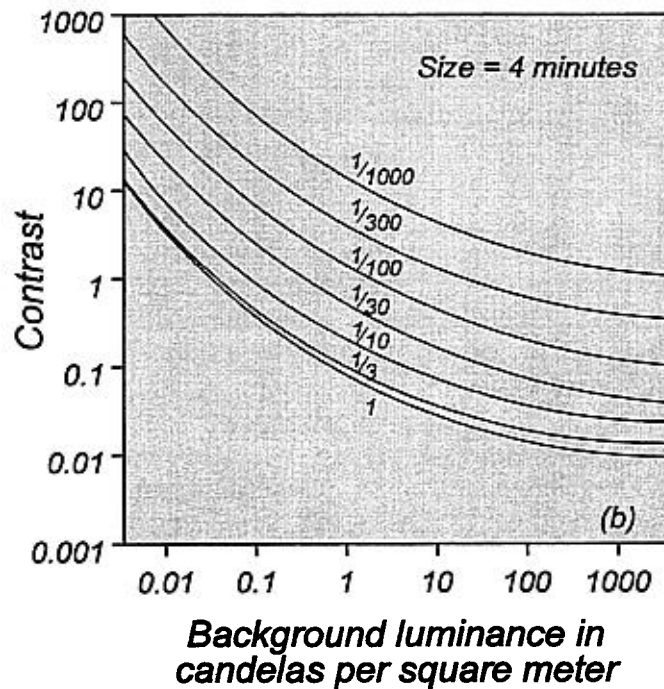


Figure 47. The relationship between threshold contrast and background luminance for various viewing times (IES, 1984).

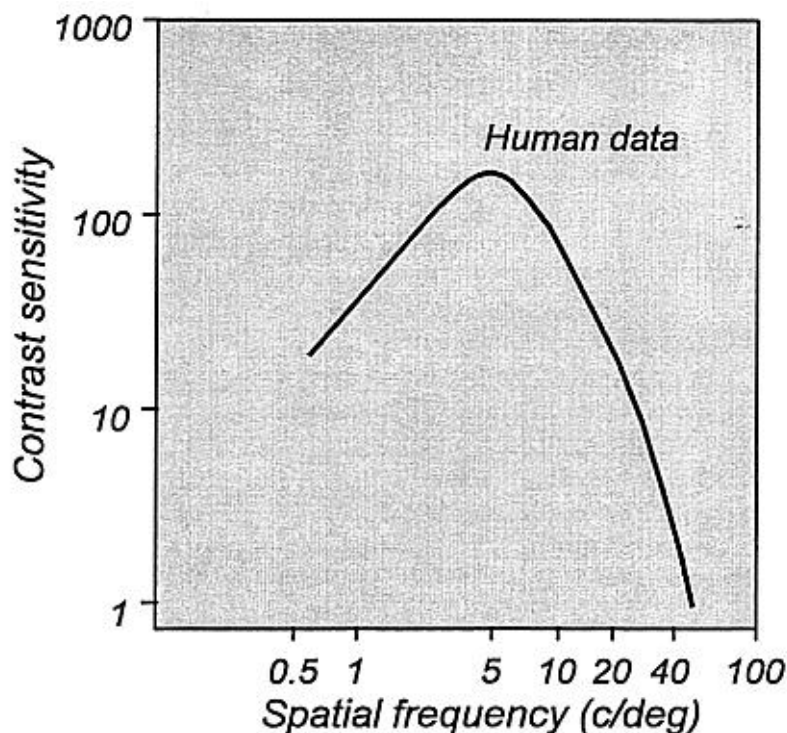


Figure 48. The human contrast sensitivity function.

Depth perception and stereopsis

Depth perception is the ability to estimate absolute distances between an object and the observer or the relative distances between two objects (i.e., which is closer). The cues for depth perception may be monocular and/or binocular. Stereopsis is only a binocular perception and is the results of the two retinae viewing slightly different images of the same object. The differences in the images occur due to the different location of the right and left eyes or the separation between the eyes.

Monocular cues for depth perception include geometric perspective, retinal image size, overlapping contours, shading or shadows, aerial perspective, motion parallax, etc. For Army aviation, motion parallax is considered the most important cue for depth perception (TC1-204). Closer objects appear to move more rapidly than distant objects with increasing displacements from the aircraft line of flight. Another form of motion parallax is referred to as optical flow or streaming.

Stereopsis is a binocular depth perception cue, requiring two slightly laterally displaced inputs for the eyes and sensors. Thresholds for stereopsis have been reported from 1.6 to 24 arcseconds, which is the difference in the eye convergence angles between two objects. For aviators, the passing value for stereopsis with the Armed Forces Vision Tester (AFVT) is 24 arcseconds (group D).

Depth perception and stereopsis with I² devices have been investigated in several studies. Investigators have used laboratory and field settings with various targets consisting of poles, panels, LEDs, and circles. The primary instruments and principles used were (1) a modified Howard-Dolman apparatus where two objects were aligned by the observer or one object was

reported in front of another object with the objects positioned by the investigator and (2) the AFVT which collimates rows of five circles with one of the five circles positioned in front of the other four circles in a row. The AFVT stereo test begins with 83 arcseconds of disparity, decreasing to 19 arcseconds.

Wiley et al. (1976) evaluated depth perception and stereopsis for the unaided eye and with the first fielded NVGs (AN/PVS-5) in both field and laboratory procedures using a modified Howard-Dolman apparatus in the laboratory at 20 feet and the same principle in the field with viewing distances from 200 to 2000 feet. The laboratory Howard-Dolman apparatus consists of two poles where the observer or the experimenter moves one pole to align in depth with a fixed pole, or the observer reports whether one pole is in front of the other with decreasing separation distances. For the field study, the targets were panels (3:1, height to width) and varied in height from 1.75 feet at 200 feet and 17.5 feet at 2000 feet to keep the target size in angular degrees constant. In the laboratory, the unaided photopic binocular threshold for stereo vision was 5 arcseconds and the NVG binocular threshold was approximately 18 arcseconds or similar to monocular unaided vision. Therefore, the conclusion that depth perception was degraded with NVGs implied that there was little or no stereopsis with NVGs. It is interesting to note that in the field study, the unaided monocular threshold was equal to or better than binocular depth perception at any of the tested distances from 200 to 2000 feet, and the NVG stereo threshold, although worse than the unaided thresholds in the field, was better than the unaided stereo threshold obtained in the laboratory.

In another study, Wilkinson and Bradley (1990) found that stereo vision with NVGs was fairly constant over illumination levels at approximately 20 arcseconds. Foyle and Kaiser (1991) evaluated depth perception estimations from 20 to 200 feet with four helicopter pilots for day unaided, night unaided, AN/PVS-5, ANVIS, and PNVIS. Plots of this data suggest greater variability between subjects than between viewing conditions.

Most of the depth perception studies with night imaging systems have used the Howard-Dolman principle of reporting one of two targets closer or the observer adjusting one target to equal the distance of a fixed target. The thresholds have been reported as standard deviations, average error, and/or constant errors. Larson (1985), using 34 subjects, found no correlations among the different scoring methods for the Howard-Dolman device, and concluded that it did not measure stereo acuity thresholds.

For flight physicals, the AFVT is used to determine if a pilot has at least a certain level of stereopsis. In comparing different soft bifocal contact lenses, Morse and Reese (1997) measured stereopsis with ANVIS and the AFVT. Light attenuating filters were placed over the ANVIS to simulate approximately 1/4 moon illumination. Stereo acuity was less through ANVIS compared to unaided stereo vision for a given contact lens or with spectacles at photopic light levels, but was definitely present except with monovision contact lenses for the low add group.

Sheehy and Wilkinson (1989) reported two cases where the pilots experienced a temporary loss of stereopsis after the use of NVGs. To test this possibility, the investigators used 12 subjects and measured stereo acuity with a Howard-Dolman apparatus with green LEDs and lateral phorias with the AFVT before and after NVG training flights. They found no significant difference in stereo acuity, but a slight shift towards exophoria after NVG use. The authors concluded that misadjustment of the IPD with a change in convergence demand was the probable cause for the temporary affects on stereo acuity.

The Integrated Night Vision Imaging System (INVIS) program attempted to design a night vision I² system with lower weight and improved center of mass for fixed-wing aircraft. The

objective lenses and intensifier tubes were placed on the side of the helmet with a separation approximately 4 times wider than the average separation between the eyes. This wider than normal sensor separation induced a phenomenon called "hyperstereopsis," which is characterized by intermediate and near objects appearing distorted and closer than normal. The ground would appear to slope upwards towards the observer and appear closer beneath the aircraft than normal. On initial concept flights in an TH-1 helicopter (modified AH-1S Surrogate trainer for the PNVS) at Fort Belvoir, Virginia, pilots found the hyperstereopsis and sensor placement on the sides of the helmet shortcomings (major deficiencies) during terrain flight. The vertical supports in the canopy always seemed to be in the FOV with any head movement, and under starlight conditions, the pilots rated the hyperstereo system unsafe and terminated the study except for demonstration rides (Kimberly and Mueck, 1992).

A hyperstereopsis study was conducted at Fort Rucker, using an "eagle eye" NVG with a 2 to 1 increase in IPD, the Honeywell INVIS with 4 to 1 increase in separation, a standard ANVIS, and the FLIR as seen from the front seat in an AH-64 Apache (Armbrust et al., 1993). The results showed no difference in flight performance among the different night imaging combinations. However, the pilots' subjective responses indicated they preferred the ANVIS. Aviators also reported they did not like switching from I² to FLIR imagery during landing phases, primarily because of the poor resolution of the FLIR compared to the I² devices.

In a recent study, Crowley et al.(1997) compared the differences in 13 Army aviators' ability to judge and maintain height above terrain using binocular unaided day vision, 40-degree FOV day vision, ANVIS monocular night time, ANVIS binocular night time, and FLIR (PNVS) monocular night time. Aircraft type was an AH-1 Cobra equipped with an Apache FLIR and extensive data collection capability (radar altimeter). Instrument information or flight symbology on the FLIR image for altitude was removed. The results showed that subjects performed poorly when asked to provide absolute altitude estimates under any condition, but were more consistent in estimating changes in altitude. Performance with the FLIR was consistently worse than with the other viewing conditions. The authors attributed the more variable results with the FLIR to poorer resolution and changing thermal conditions over the 1½ year data collection period.

In summary, stereopsis with night imaging devices does not seem to provide any significant additional depth perception information over the strong monocular cues such as motion parallax for helicopter flight. The successful use of the monocular IHADSS in the AH-64 Apache helicopter implies that sufficient depth estimations for pilotage can be obtained with normal flight training with monocular as well as binocular night imaging systems.

Visual illusions and spatial disorientation

Spatial disorientation (SD) is defined by Benson (1978) as "the situation occurring when the aviator fails to sense correctly the position, motion, or attitude of his aircraft or of himself within the fixed coordinate system provided by the surface of the earth and the gravitational vertical." Often included in the definition of SD is Vymwy-Jones' (1988) clause: "the erroneous perception of the aviator's own position, motion, or attitude to his aircraft, or of his aircraft relative to another aircraft." In addition, contact with an obstacle known to be present, but erroneously judged to be sufficiently separated from the aircraft is included as SD.

One might infer that flight with current night vision devices would induce some SD due to their limitations of reduced FOV, decreased resolution, reduced depth perception, and lack of color vision, as compared to unaided vision. However, at terrain altitudes at night, the aviator has essentially no FOV, resolution, depth perception, or color vision with the dark adapted eye,

and could not survive in modern warfare without these night vision devices. Training and improved technology are required to reduce the necessary risks associated with night and adverse weather flying.

In many respects, visual illusions could be considered one of the primary causes of spatial disorientation with night vision devices (Crowley, 1991). Crowley conducted a survey soliciting information from 223 individuals on sensory effects or illusions that aviators had experienced with night vision systems. Frequently reported illusions were misjudgments of drift, clearance, height above the terrain, and attitude. Also reported were illusions due to external lights, and disturbed depth perception. The difference in the incidents and types of illusions were similar for both I² devices and the monocular IHADSS, although the sample size for the Apache pilots was small (n = 21). The illumination levels reported when illusions occurred with I² devices were below 24% moon, or less, for 36% of the illusion incidents, with lower percentages for incidents with increasing illumination. It would be easy to infer that low illumination was a causal factor, where actually the reverse is true. Illumination below 24% moon occurs 70% of the time for flights beginning 1 hour after sunset and lasting 4 hours. This is the typical Army NVG training mission. The most frequently cited methods to compensate for the illusions were to transfer the controls to the other pilot, use other aircrew to crosscheck visually, and to increase visual scan.

From 1987 to 1995, 37% of the 291 NVG accidents involved spatial disorientation (McLean et al., 1997). An analysis of SD accidents of U.S. Army helicopters from 1987 to 1995 found the following results: The types of SD events for night aided flights, listed by frequency of occurrence, were: (1) Flight into the ground (28%), (2) drift descent in hover (27%), (3) recirculation (brownout, whiteout, etc.) (22%), inadvertent entry to instrument meteorological conditions (8%), and (4) flight over water (3%) (Braithwaite, et al., 1997; Durnford et al., 1996). These percentages of SD occurrences were similar for all accidents except the rate for accidents with I² devices and FLIR were higher than for day flight. However, it should be noted that all U.S. Army night aided flights occur at 100 feet above ground level (AGL) or less except when transitioning to and from the primary airfields. This low altitude reduces reaction time and increases the risks compared to day and night general flight profiles. The 1987-1995 SD study (Braithwaite, et al., 1997) also found that very few illusions actually caused SD accidents.

Recommended approaches to reducing SD accidents listed in importance are improved crew coordination, better scanning, height audio warning, hover lock, drift indicator, et al.

Visual problems

The use of HMDs increases visual workload and, very likely, raises stress levels among users. After several years of fielding the AH-64 Apache, a survey of Apache aviators (Hale and Piccione, 1990) documented reports of physical fatigue and headaches following flights using the monocular IHADSS HMD. This followed anecdotal reports of similar problems from instructor pilots at Fort Rucker, Alabama. Hale and Piccione (1990) cited as possible causes: binocular rivalry, narrow FOV, poor depth perception, inadequate eye relief, and overall system discomfort. To investigate potential concerns of long-term medical effects of using the IHADSS, the U.S. Army Aeromedical Research Laboratory (USAARL), Fort Rucker, Alabama, conducted a three-part study (Behar et al., 1990). The first part was a written questionnaire which served the purpose of documenting visual problems experienced by the local Fort Rucker, Alabama, Apache aviator community. The second part was a clinical and laboratory evaluation of the refractive and visual status of a sample of these aviators. The third part was an assessment of the diopter focus settings used by aviators in the field environment. Since the IHADSS is designed to have the virtual imagery appear at optical infinity, incorrect diopter focus settings could, in theory, lead to visual fatigue and related visual problems.

A total of 58 Apache aviator questionnaires were completed. More than 80% of the sample aviators reported at least one visual complaint associated with flying or after flying with the IHADSS. A summary of complaints is provided in Table 13 (Behar et al., 1990). The most common complaint (51%) was that of “visual discomfort” during flight. Approximately a third of the aviators reported occasional headaches, and about 20% reported blurred vision and/or disorientation while flying. The percentage of aviators reporting headache and blurred vision after flying remained about the same, while the percentage of those experiencing disorientation after flying decreased to 5%.

The clinical and laboratory evaluation of the refractive and visual status of 10 aviators found no statistical correlation between visual performance and visual complaints. There were no significant differences found between right and left eye performance. There was evidence of mild incipient presbyopia in a majority of the aviators, but this was within expectations for the sample age range. Binocular ocular motility for the sample was found to be lower than expected. But, in summary, the study concluded there was no significant variation from normal performance values noted.

The diopter focus settings of 20 Apache aviators (11 students and 9 instructor pilots) were measured in the aircraft following their normal preflight setup. Nine were measured under nighttime illumination conditions and 10 under daytime conditions. A range in focus settings of 0 to -5.25 diopters (mean of -2.28 diopters) was obtained. It was concluded that the required positive accommodation by the eye to offset these negative focus settings was a likely source of headaches and visual discomfort during and following long flights. No correlation was found between the focus settings and aviator age or experience; nor were there differences between instructor pilots and students, or day versus night.

Table 13.
Apache aviator reports of visual complaints during and after flight.
(Behar et al., 1990)

Complaint	During flight			After flight		
	Never	Sometimes	Always	Never	Sometimes	Always
Visual discomfort	49 %	51 %	--	70 %	28 %	2 %
Headache	65 %	35 %	--	67 %	32 %	2 %
Double vision	86 %	12 %	2%	89 %	9 %	2 %
Blurred vision	79 %	21 %	--	72 %	24 %	3 %
Disorientation	81 %	19 %	--	95 %	5 %	--
Afterimages	NA	NA	NA	79 %	19 %	2 %

In another survey (Crowley, 1991) of 242 aviators flying either ANVIS (rotary- and fixed-wing) or IHADSS, a very small percentage of the rotary-wing ANVIS users (n = 212) reported physiological effects to include eyestrain (3%), headache (2%), motion sickness/vomiting (2%), postflight blurred vision (1%), and dizziness (1%); only 5% of Apache aviators (n = 21) reported any visual problems (that of dark adaptation effects).

The move towards two-eyed (binocular) wide FOV HMDs may result in adverse visual effects if care is not taken in their design. Mon-Williams, Wann, and Rushton (1995) point out that conflicts between accommodation and vergence, focal error, and prismatic errors may result

in "unstable binocular vision." As previously discussed, failure to maintain strict binocular alignment may introduce serious performance problems.

Currently, HMDs intended for use in the Army aviation community are required to provide some measure of look-under, look-around, and/or look-through capability. However, future HMD designs may employ full-immersion displays in the form of virtual reality display systems. There is considerable ongoing effort in investigating a phenomenon known as "cybersickness" associated with such systems. Cybersickness is similar to simulator sickness in that symptoms of motion sickness (e.g., nausea, sweating, pallor, etc.) can result from a lack of correlation between visual and vestibular sensory inputs. Of course, in an actual aircraft, both inputs are present. However, if imagery has a significant delay in its presentation due to long lag times and slow update rates, cybersickness can manifest itself (Melzer and Moffitt, 1997; Kalawsky, 1993; Hettinger and Riccio, 1992). Even greater concerns have been voiced regarding possible damage to the vestibulo-ocular reflex due to HMD use, manifesting in flashback episodes (Melzer and Moffitt, 1997; Strauss, 1995).

Helmet performance

The role of the basic helmet historically has been to provide protection. This role has not changed but has been expanded. While initially providing impact protection, the helmet's protective role has grown to include hearing and eye protection. Now, the helmet is expected to serve additionally as a platform for mounting a display. However, this new function must not compromise the helmet's primary requirement to provide protection.

To design an integrated HMD which can meet both the old and new requirements, several helmet parameters and associated factors must be considered. These include the biodynamic characteristics of mass and CM, impact attenuation, the design issue of HMD frangibility (breakaway capability), the fitting system; acoustical protection and communication issues; and eye protection from particulate matter as well as sun glare and directed energy (e.g., lasers).

Biodynamics

Helicopter aircrew helmets are becoming more sophisticated with increased mission requirements and their use as platforms for HMDs. This increase results in additional mass being supported on the aircrew's head, often with an asymmetrical CM. The functional requirements of the helicopter pilot helmet have grown considerably. Traditional helmet functions include head impact protection and service as a mounting platform for communication systems, hearing protection, eye protective visors, and on occasion, oxygen systems. Increases in threats and operational capabilities demand the helmet also serve as a mounting platform for such systems as weapon targeting, night vision or image intensification devices, flight symbology displays, chemical defense masks, and nuclear flash protection. These requirements demand more complex mounting devices on the helmet and, ultimately, result in increased system weights and potentially less than optimal CM location. Ultimately, there is a limit to how much mass can be supported by the aircrew without increasing the fatigue rates and neck injury risk in accidents.

Mass and CM

The mass of flight helmets has been a concern since "hard shell" helmets first appeared in the 1950s. These helmets were introduced to provide increased head protection during a crash, but at a significant weight increase over the previously worn cloth caps. The total head supported mass increased from 0.5 kg for the leather or cloth cap to 1.5 kg for early hard shell helmets, which

included noise-attenuating earcups, earphones, microphone, and integral, adjustable visors. The hard shell helmet, lined with polystyrene foam, provided an order of magnitude improvement in impact protection.

In the 1980s, the introduction of various visual enhancement devices further increased the mass to 3 kg for the standard Army SPH-4 flight helmet equipped with the AN/PVS-5 NVG. The increased mass of this helmet system is believed to have a detrimental effect on pilot performance due to neck muscle strain and fatigue and to increase the risk of severe neck injury in crashes. The disadvantages of increased helmet mass, however, are offset by the enhanced visual capability for night flying and increased weapons aiming capability offered by helmet-mounted image intensification devices and other helmet-mounted displays. In order to permit the use of 3-kg helmets without overloading the neck in severe crashes, the U.S. Army's Night Vision Laboratory (currently NVESD), Fort Belvoir, Virginia, developed a spring-loaded, ball-socket mount which permits the latest generation night vision device (AN/AVS-6) to break free during a crash. The 0.6-kg NVG device was designed to break free of the helmet at a goggle deceleration of 10 to 15 times the acceleration of gravity (G) (Military specification, MIL-A-49425 (CR), 1989). Although this approach may offer one solution to the problem of increased head-supported mass in Army aviation, little is known about the dynamic behavior of this device in a crash or of the physical limitations of the human neck to support these masses.

In an initial attempt to define a safe limit on flight helmet mass for the Army, USAARL in 1982 proposed a limit of 1.8 kg (3.96 lb) during the development of the AH-64 Apache IHADSS helmet. The helmet system subsequently developed met this mass limitation while providing the desired platform for the HMD and the required acoustical and impact protection. Nonetheless, the SPH-4 helmet with NVG attached used for night operations in all other Army helicopters continued to exceed the proposed 1.8-kg limit by more than a full kilogram. Although there have been anecdotal reports from aviators complaining of considerable discomfort with this system, particularly after long missions, the effects on pilot performance of bearing this much mass has never been systematically studied. Furthermore, the dynamic consequences of crashing with head-borne masses approximating 3 kg remain largely speculative.

Historically, helmet mass and CM requirements have been nonexistent or vague. These requirements often were written loosely and based on existing designs. Language in helmet development specifications often resembled “. . . the helmet CM must be located as close to the head CM as possible,” “. . . lighter and CM no worse than current helmet systems,” “. . . provide ease of head movement,” and “. . . (have) reduced bulkiness.” These requirements provided little guidance to the design teams and could not be quantitatively evaluated.

Seven parameters are required to define the mass properties of helmet systems. As illustrated in Figure 49, these include mass, the center of mass position along three orthogonal axes, and the mass moment of inertia about the three respective axes. The coordinate system used by the Army aviation community is based on the head anatomical coordinate system and is illustrated in Figure 50 (Rash et al., 1996b). The x-axis is defined by the intersection of the mid sagittal and Frankfurt planes with the positive direction anterior of the trignon notch. The y-axis is defined by the intersection of the Frankfurt and frontal planes with the positive y-axis exiting through the left trignon notch. The z-axis is oriented perpendicular to both, the x- and y-axes following the right hand rule.

The rationale for defining aviator helmet mass requirements can be segregated into three areas: Aircrew health, operational effectiveness, and user acceptance. Aircrew health can be affected by both short- and long-term exposures of head and neck loadings. Long term exposures are the result of helmet mass and its mass center location in normal flight conditions

(vibration and 1 to 2G flight environment). These effects include discomfort from a sore or stiff neck after normal missions. It is not uncommon to find Army aircrew who admit “off-the-record” that they seek unauthorized treatment for sore neck muscles. Treatments may include heat pads, topical ointments, neck rubs and massages from spouses or masseuses, and chiropractic adjustments.

Short-term exposures may cause neck injuries resulting from inertial loadings. Inertial neck loadings are created in high acceleration, short duration, dynamic crash environments. At high seat accelerations, neck loads are compounded by helmet mass and improper center of mass locations. These neck injuries can be low severity, such as strains and muscle tears, or high severity, such as cervical transections.

Aircraft crash environments also may cause direct and indirect loading injuries to the neck. Direct loading injuries are caused by objects physically striking the neck inflicting tissue damage. Indirect loading neck injuries are caused by the transfer of energy to the neck from a head impact. It is assumed that neither direct nor indirect loading neck injuries are influenced by the mass supported by the head. Thus, these direct and indirect types of neck injuries are not considered in the determination of allowable mass properties for head supported devices.

The mass properties of head supported devices also can affect operational effectiveness by increasing aircrew fatigue. Aircrew operating with high fatigue are less efficient, have lower mental concentration ability, and are more prone to commit mistakes. Little data are available on fatigue effects in rotary-wing environments and are generally based on small sample sizes and limited helmet mass and CM positions.

Helmet stability also is affected by helmet mass and CM placement. High helmet mass and misplaced center of mass locations can result in helmet slippage relative to the aircrew eye location. When helmet-mounted displays or image intensification devices are used, helmet slippage could effectively “blind” the aviator from receiving the desired display information for effective aircraft control.

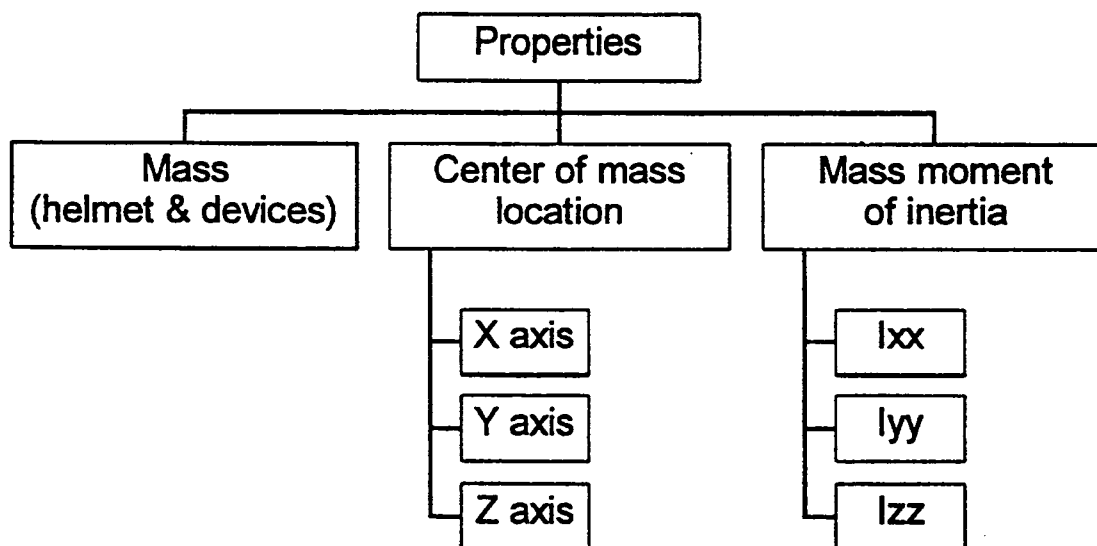


Figure 49. Parameters required to fully define helmet system mass properties.

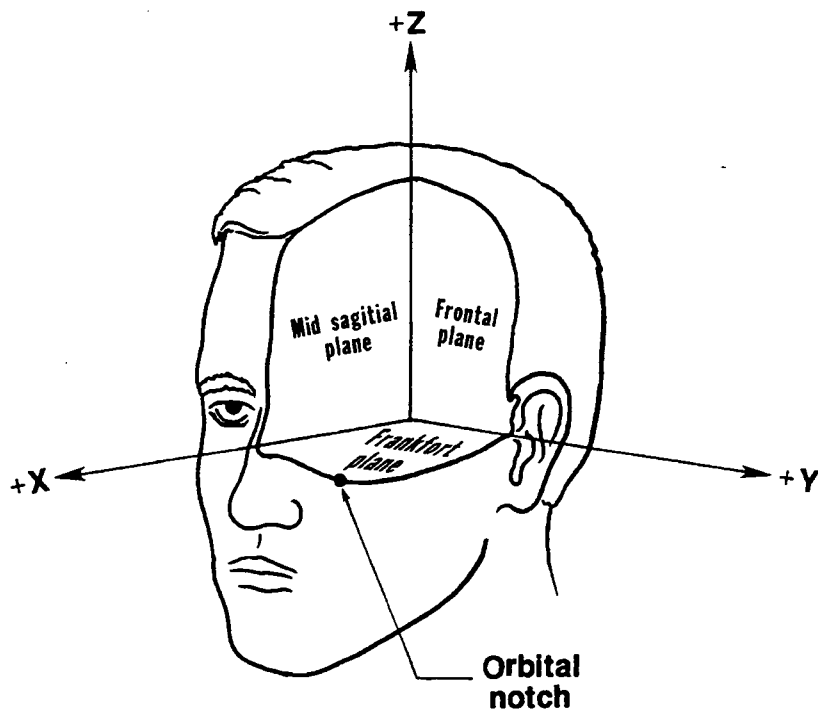


Figure 50. Head anatomical coordinate system.

Another area which can be affected by head-supported mass is user acceptance. The final configuration must be acceptable to the final user prior to fielding to operational units. Failure of a system to receive user acceptance will result in misuse and abuse of the system and failure of the system to achieve its desired operational capability. User acceptability is difficult to define and quantify since each aircrew has a subjective opinion. No data beyond anecdotal data on existing systems have been generated to quantify user acceptance of mass property limits.

The development of the Comanche HIDSS has prompted a continuing effort to develop new head-supported weight and CM requirements. As a result, new recommendations have been developed for total allowable mass and the x- and z-axis CM locations. The recommended allowable mass requirement is based on neck tensile strength; x-axis CM location is based on measured biodynamic responses of aviators wearing various helmet mass and CM combinations; and the z-axis CM is based on maintaining a constant moment about the C7/T1 juncture resulting from the helmet mass and vertical CM position.

It is important to define the mechanisms of neck injury when establishing mass limits on HMDs. McElhanney (1993) provides a good engineering description of neck loadings, which are reproduced in Figure 51. There are two injury mechanisms which are most likely to be affected by the mass properties of HMDs. These are axial tension and forward bending (flexion). Neck extension and neck compression injury mechanisms are not considered to be effected by HMD mass properties. This is based on current helicopter crew seat design requirements which include headrest and load limiting vertical energy absorption capabilities.

Shanahan and Shanahan (1989), in a study of U.S. Army helicopter crash injuries from 1979-1985, found 82 reported spinal fractures. Figure 52 (Shanahan and Shanahan, 1989) illustrates the spinal fracture distribution by vertebral level. The cervical and upper thoracic vertebra with the highest frequency of fracture was the 7th cervical. The lower thoracic and the lumbar region experienced a higher frequency rate, but these injuries are believed due to compression loadings resulting from high vertical impact loads in precrashworthy seat designs. Cervical spine fractures comprise only 1.6% of the 1484 injuries sustained in survivable crashes. The cervical injuries were caused by either acceleration loadings or contact injury. No differentiation between these two injury mechanisms was made.

This review of helicopter crash injury indicates a lack of evidence supporting significant inertial neck injury for Army aviators wearing a 1.5-1.8 kg helmet. In some crashes, heavier helmets of 2.9 kg (including night vision components) have been worn, but the extra 1.1-1.4 kg mass of NVGs and counterbalance weights have broken free from the helmet and relieved the neck of this added loading. The nondocumentation of inertial neck injury does not mean none occurred, but that the accident investigators may have failed to recognize this infrequent injury among the far more obvious contact, crushing, and spinal column injuries in the older, nonload-limiting seats.

An important issue in developing mass and CM recommendations is the factors influencing inertial neck injury. Recent Army helicopter designs incorporate various levels of crashworthiness with specific performance levels for the crewseats. Helicopter crew seats are typically procured to military performance specifications with a 30G longitudinal static load

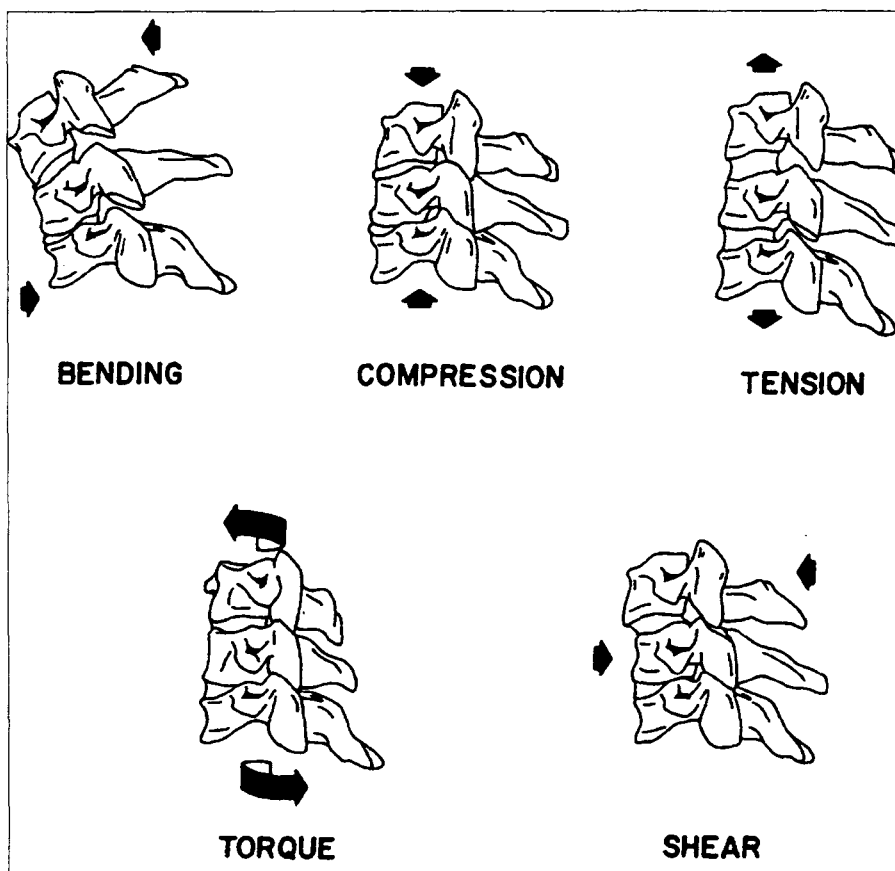


Figure 51. Engineering descriptions of neck loading.

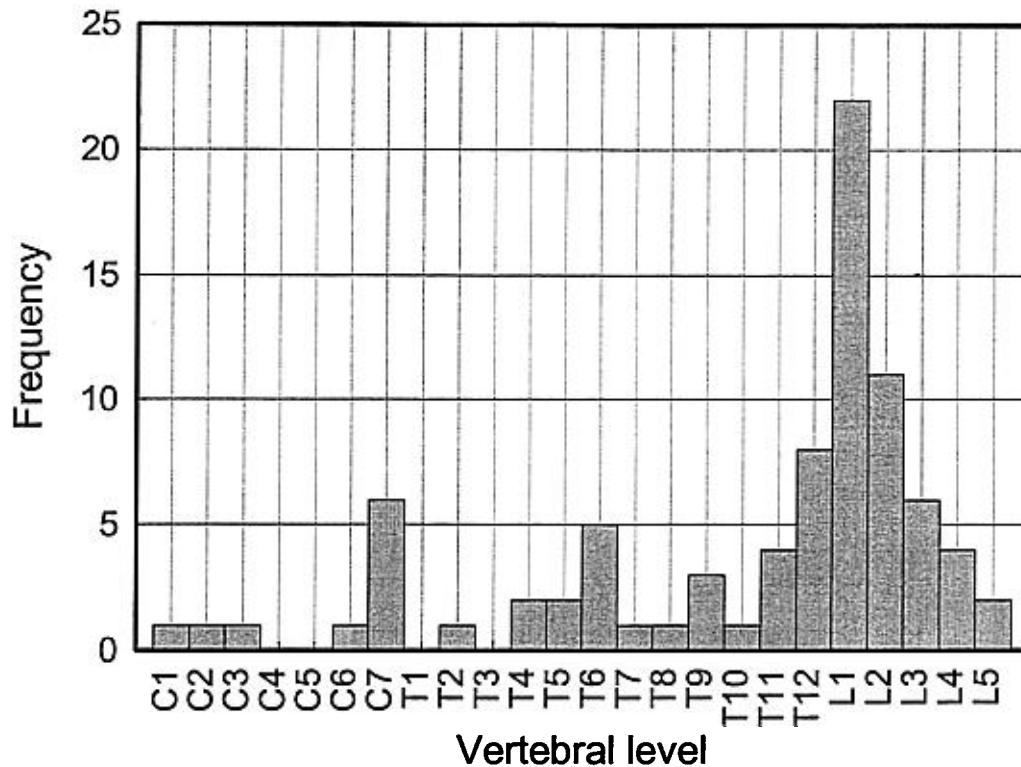


Figure 52. Frequency distribution of spinal fractures in class A and B survivable crashes by vertebral level.

requirement and a vertical energy absorption capability (Military specification, MIL-S-58095(AV), 1986). The 30 G longitudinal requirement is a structural integrity check of the seat and its mounting hardware to provide assurance that the seat will not be ripped from the floor. The vertical energy absorber is a mechanical device which restricts the vertical crashloads experienced by the occupant. The desired vertical load is an average of 14.5 G over the range of seat stroke. Peak loads of 18.3 G have been measured in anthropomorphic test dummies during seat qualification trials (Melvin and Alem, 1985). The worst case condition would be a seat experiencing 30 G longitudinally and stroking with a peak vertical load of 18.3 G. The resultant from these two loading vectors is 35 G directed 31.4 degrees downward from horizontal.

Aircrew restraint systems utilized in Army helicopters are either a traditional 4-point restraint system or a newer 5-point restraint. The primary difference between the two systems is that the 5-point system includes a center tie-down strap to reduce occupant submarining (movement of the pelvis under the lap belt). Dynamic tests with rigid seat structures have indicated a range of possible "dynamic overshoot" (the ratio of measured head or chest acceleration of a test dummy to the input floor or seat acceleration). This increase in acceleration results from harness slack, neck tissue stretch, and upper body compression (by contact with the restraint harness) which allows a relative velocity to be created between the occupant and surrounding structure. The dynamic overshoot value is also dependent on when the shoulder strap inertia reel locks (which is activated by occupant motion). A dynamic overshoot value of 1.5 has been selected as the magnification of seat acceleration to the head acceleration; this is an average value based on dynamic tests of aircrew seats for the UH-60 Black Hawk helicopter.

Neck injury potential is a function of neck strength. Based on a review of military operational experiences (Schall, 1989), automotive accident injuries (Foret-Bruno et al., 1990;

Larder, Twiss, and MacKay, 1985), volunteer (Hearon and Brinkly, 1985; Ewing et al., 1983), cadaver test data (Cheng et al., 1982; Walsh and Kelleher, 1978), animal test data (Clarke et al., 1972), and manikin injury assessment values (Mertz, 1993), a neck tensile strength threshold of 4050 Newtons has been selected as the maximum limit. It is believed that risk of serious neck injuries exist above this limit for the Army aviator population. This value is probably too great for general civilian populations since the Army aviator population is generally are younger and more physically fit.

The determination for maximum allowable head-supported mass is based on Newton's second law, $F = ma$. This equation is used by considering the neck tensile strength threshold of 4050 Newtons and the acceleration environment of 35 G (crashworthy seat performance) with a dynamic overshoot ratio of 1.5. The effective mass acting on the C7/T1 juncture can then be calculated as follows:

$$\begin{aligned}
 F &= ma && \text{Equation 20} \\
 m &= F / a \\
 m &= (4050 \text{ N}) / [(35 \text{ G})(1.5)(9.81 \text{ m/sec}^2)] \\
 m &= 7.86 \text{ kg}
 \end{aligned}$$

The mass acting on the C7/T1 juncture includes the helmet, head, and neck. The total mass of the neck is included in this calculation to be conservative. By subtracting the head mass (4.32 kg) and neck mass (1.04 kg) from the above value, we arrive at the allowable helmet mass for the given impact condition, or

$$\begin{aligned}
 m &= m_{\text{head}} + m_{\text{neck}} + m_{\text{helmet}} && \text{Equation 21} \\
 m_{\text{helmet}} &= m - m_{\text{head}} - m_{\text{neck}} \\
 m_{\text{helmet}} &= 7.86 - 4.32 - 1.04 \\
 m_{\text{helmet}} &= 2.5 \text{ kg}
 \end{aligned}$$

The vertical CM limit is based on a constant mass moment concept acting about the C7/T1 juncture. This rationale allows for greater helmet mass as the vertical CM location moves downward. The C7/T1 juncture was selected as the critical pivot point because it is more frequently injured than upper cervical vertebra in helicopter accidents (Shanahan and Shanahan, 1989). Application of this theory requires selection of a head-supported mass and a vertical CM position to use as a constant mass moment. Lack of empirical data necessitates the selection of the "worst case" fielded helmet system, the AH-1 cobra helmet configuration, to establish an acceptable constant mass moment. This helmet configuration has a mass of 1.74 kg and a vertical CM location of 5.2 cm above the tragion notch. The final variable needed to determine the constant mass moment is the vertical distance between the C7/T1 juncture to the tragion notch (Donelson and Gordon, 1991). A value of 11.94 cm was selected which represents the 95th percentile female and the 85th percentile male neck link measurement.

To determine the constant mass moment, the definition of a mass moment (M) is used: $M = md$. The mass (m) is the helmet mass of 1.74 kg and the distance (d) is the total distance of the helmet vertical CM position above the C7/T1 juncture (i.e., 11.94 cm + 5.2 cm). This is calculated as follows:

$$\begin{aligned}
 M &= md && \text{Equation 22} \\
 M &= (1.74 \text{ kg})(11.94 \text{ cm} + 5.2 \text{ cm}) \\
 M &= 29.8 \text{ kg-cm}
 \end{aligned}$$

This moment value can be used to establish a relationship between the vertical CM position and mass by rearranging the above equation as follows:

$$29.8 \text{ kg-cm} = (m_{\text{helmet}})(11.94 \text{ cm} + Z_{\text{helmet cm}})$$

$$Z_{\text{helmet cm}} = (29.8 \text{ kg-cm} / m_{\text{helmet}}) - 11.94 \text{ cm}$$

Plotting this relationship results in the curve shown in Figure 53. The allowable mass is limited to 2.5 kg as determined above. Additionally, the allowable vertical CM position is limited to 5.2 cm since biodynamic reactions to higher CM locations are unknown. Plotting specific head-supported mass and vertical CM values on the graph allows acceptability assessment.

The longitudinal CM locations of HMDs are believed to have greater effects on aviator fatigue and performance decrements than on crash induced injury. Efforts have been conducted by Butler (1992) to assess these effects by exposing volunteers to controlled helicopter ride environments with various helmet mass and CM configurations. During his study, Butler (1992) measured both physiological and biomechanical responses to the changes in HMD mass properties. The property changes included three masses (2, 3, and 4 kg) and four longitudinal CM positions (-2, 0, 2, and 4 cm) measured relative to the head center of mass. A head supported weight moment of $82.8 \pm 22.8 \text{ N-cm}$, measured about the occipital condyles, was recommended based on changes in head pitch accelerations and posterior neck myoelectric responses. It was also recommended that negative moments be avoided. By using the recommended weight moment, including the tolerance (105.6 N-cm total), this value can be converted into a mass moment relative to the tragon notch and plotted. This relationship is shown in Figure 54. The rearward CM location was limited at -2 cm based on Butler's (1992) recommendation that negative moment be avoided. Mass was limited at 2.5 kg as determined earlier. The forward limit was arbitrarily set at 9.5 cm.

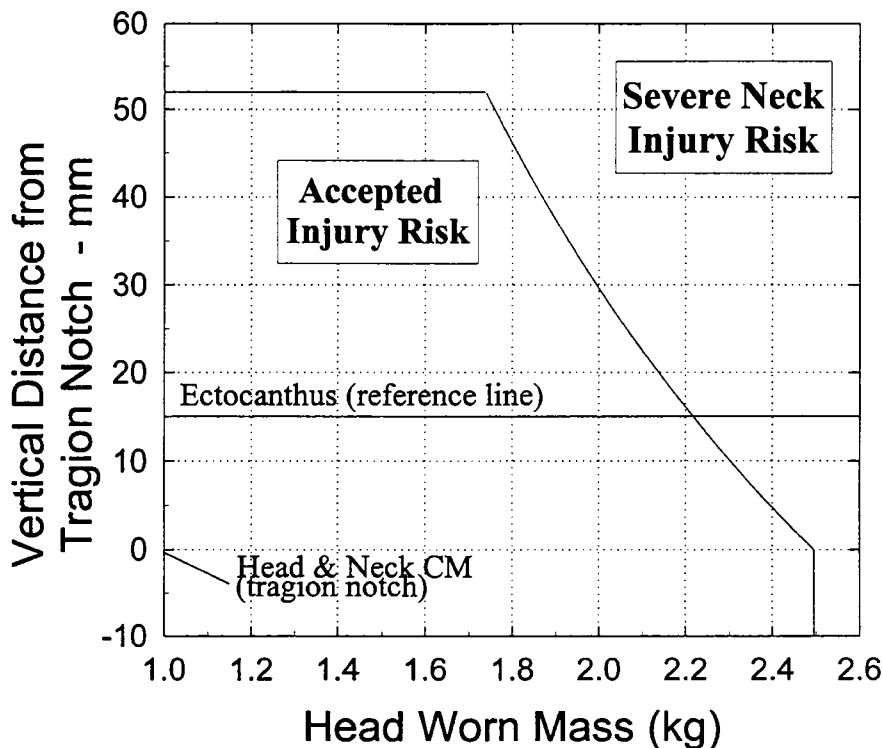


Figure 53. Vertical center of mass placement as a function of head-supported mass.

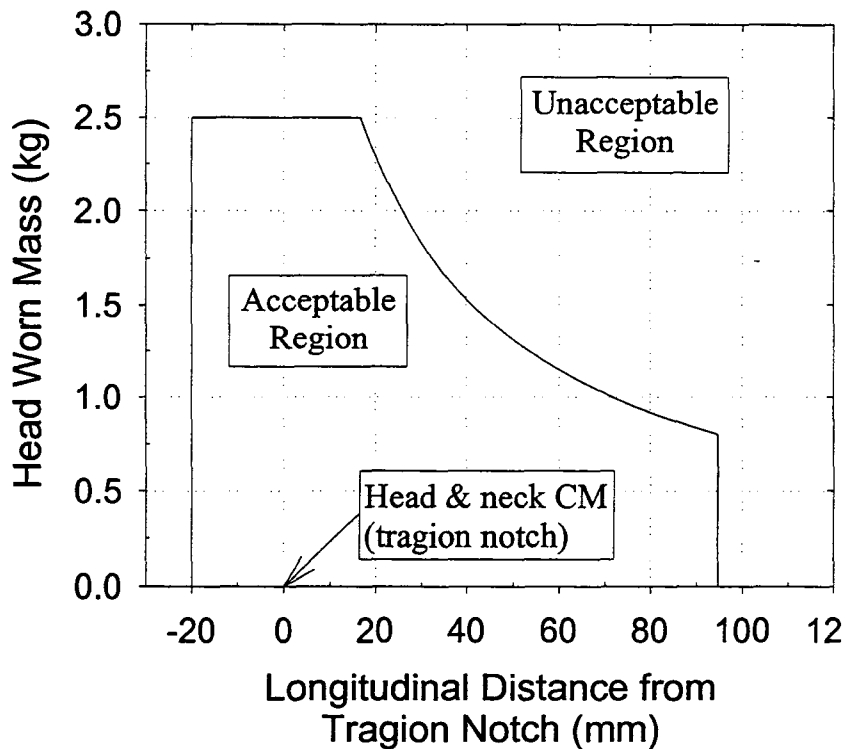


Figure 54. Allowable head-supported mass as a function of longitudinal center of mass placement.

No data have been identified to warrant changing the lateral CM requirements from 1.9 cm off the mid-sagittal plane. Operationally, the IHADSS helmet, which is used in the AH-64 Apache helicopter, possesses an off-sagittal CM position when the monocular HMD is attached. No neck injuries to the occupants involved in mishaps have been attributed to the lateral CM locations. This may be attributed to the breakaway capability of the HDU when exposed to contact forces and acceleration induced inertia loads.

This discussion and the mass and CM requirements presented are based on limited data. Future efforts should be expended to increase the available human tolerance data and subsequently refine or change the presented mass requirements. These efforts should include defining human neck strength to various loading mechanisms, defining user tolerance to mass properties of HMDs, and defining fatigue affects of head-supported mass properties. Epidemiological studies should be conducted to determine the incidence of chronic neck injury among aging and retired aircrew and its correlation to flight experience. In addition, numerical simulations of occupant loads in crash situations should be conducted to validate the presented HMD mass requirements.

Impact attenuation

A primary function of the rotary-wing aviator helmet is head protection during mishaps. Head impact injury is the leading cause of permanent disability and fatality in Army rotary-wing mishaps (Shanahan, 1985). Head impact protection is accomplished by proper helmet design, a design which provides a protective outer shell and sufficient stopping distance between the shell's outer surface and the skull. The purpose of the protective shell is to resist penetration from sharp or jagged impact surfaces and to distribute the load over a greater contact area.

The head impact velocity in survivable helicopter crashes has been estimated at 19.6 feet per second (5.97 meters/sec) through computer simulations and analysis of sled test results. This number is based on the potential flail velocity of the occupant's upper torso (Desjardins et al., 1989).

Human head impact tolerance is an area of continuing research. The USAARL has recommended a test head form threshold of 150 to 175G, depending on the impact location. See Table 14. A review of performance specifications for other helmet applications (i.e., motorcycle, bicycle, equestrian, fixed-wing aviator, etc.) reveals a range of thresholds ranging from 200 up to 400 G. The USAARL recommended value for the headband region (175G) is based on the concussion threshold to linear accelerations, not on skull fracture, fatality, or rotational acceleration thresholds. The USAARL recommended value for the earcup and crown regions (150G) is based on the risk of basilar skull fracture concomitant with impacts to those areas and the high frequency of occurrence in Army helicopter crashes (Shanahan, 1985).

Table 14.
Impact attenuation maximum G thresholds.

Impact location	Impact velocity (m/s)		Drop height (meters)	Maximum G*
	Minimum	Maximum		
Crown	4.88	4.95	1.22	150
Left earcup	5.98	6.05	1.83	150
Right earcup	5.98	6.05	1.83	150
Front	5.98	6.05	1.83	175
Rear	5.98	6.05	1.83	175
Left side	5.98	6.05	1.83	175
Right side	5.98	6.05	1.83	175

Selection of the concussion threshold is based on the threats present in the Army helicopter crash environment. It is possible for helicopter crashes to occur into water, on land, and behind enemy lines. Each scenario possesses unique risks to the aviator who survives the crash but is rendered unconscious due to a head impact. An obvious risk associated with crashes into water is drowning. An unconscious aviator involved in a water impact would be unable to egress the aircraft, resulting in a drowning fatality. The risk of post-crash fire within the Army helicopter community has been reduced significantly through improved fuel system and structural designs, but the risk remains present. Fire can ensue in both ground and water helicopter impacts, severely and fatally wounding individuals. Unconsciousness would prevent an aviator from egressing the wreckage and avoiding exposure to heat and combustion by-products. Finally, there is the risk of crashing into an enemy occupied territory. It is desirable for the aircrew to maintain consciousness in survivable crashes to evade enemy capture and provide assistance to fellow occupants who may have received more serious injuries.

Protective helmet shells have been constructed of various materials. Basically, the shell is constructed of epoxy impregnated fabric. The fabric has been fiberglass (SPH-4), aramid (SPH-4B), aramid and graphite composite (IHADSS), or a polyethaline and graphite composite (HGU-56/P). The U.S. Coast Guard and U.S. Navy have also used helmets constructed with a nylon

fabric (the SPH-4CG and HGU-84/P). All of these fabric materials, when impregnated with epoxy resin and formed into shells, provide good distribution of the impact loads. Shell fracture during impact is a method of energy absorption. This is generally acceptable except when structural integrity is lost and the helmet is unable to provide protection from subsequent impacts, or it departs from the wearer.

Selection of the shell fabric material, number of plies, and resin content affect the shell's weight and its resistance to tear penetration. The USAARL tear penetration test was developed to ensure that advanced technology shell materials don't compromise the functional integrity of resisting penetrating impact surfaces. Fiberglass works well in this test, but requires a large number of layers resulting in a weight penalty. Aramid and graphite, which both have high tensile strength to weight ratios, perform poorly in this test. This test actually places the fabric in shear as opposed to tension. The polyethylene and nylon fabrics perform well in the tear test.

New formulations of woven fabrics are being developed for specific applications and could prove beneficial to aviator helmet construction. Composite sandwiches with honeycomb or other crushable material have been fabricated into helmet shells. These constructions often perform well in impact attenuation, but the fabrication cost and relative low production volume are detrimental to successful implementation.

Helmet design for impact attenuation is based on the laws of physics. To bring a test head form, traveling at an initial velocity of 20 feet per second (6.1 meters per sec), to a stop requires a deceleration. If the deceleration magnitude is not to exceed 175G, sufficient stopping distance must be provided. This required stopping distance is dependent on the acceleration's pulse shape which results from the impact. Three basic pulse shapes are the square, triangular, and half sine pulses. The triangular pulse shape can vary with location of the peak value, with the two extremes having the peak located at the very beginning, a zero rise time, or at the very end, a zero offset time, of the acceleration pulse. These pulse shapes are illustrated in Figure 55. As a comparison, the acceleration time history trace of an Army aviation helmet impact result is provided in Figure 56. Calculation of the required stopping distance for these pulse shapes are based on the following equations (Zimmermann et al., 1989):

$$S = V_0^2 / 2gG \text{ (square pulse)} \quad \text{Equation 23}$$

$$S = (0.7854)(V_0^2) / gG \text{ (half sine pulse)} \quad \text{Equation 24}$$

$$S = V_0^2 / gG \text{ (triangular pulse, symmetrical)} \quad \text{Equation 25}$$

$$S = 2V_0^2 / (96.6)gG \text{ (triangular pulse, zero rise time)} \quad \text{Equation 26}$$

$$S = 4V_0^2 / (96.6)gG \text{ (triangular pulse, zero offset time)} \quad \text{Equation 27}$$

where S is the minimum required stopping distance, V_0 is the initial velocity, g is the gravitation acceleration, and G is the "not to exceed" number of multiples of gravity. For these equations, the required theoretical stopping distances are plotted in Figure 57 for various G levels.

The theoretical stopping distance can be used to help determine the required energy liner thickness used in helmet construction. Additional factors, such as energy liner material efficiency, contact area, and impact surface shapes, must be considered. Material efficiency represents the percentage of useful crush distance available for a given thickness. During the

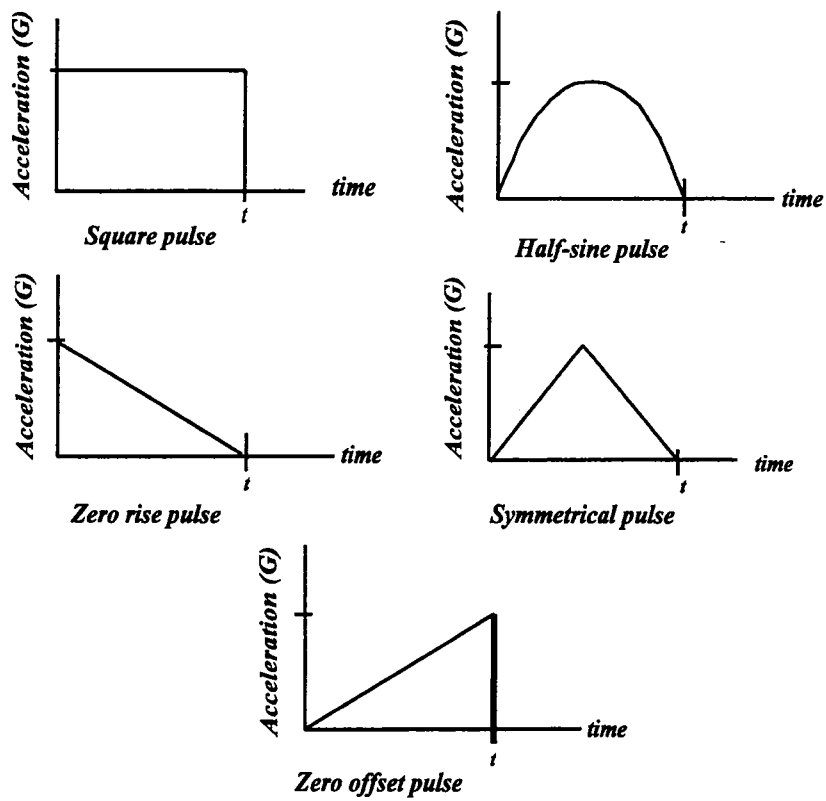


Figure 55. Acceleration pulse shapes.

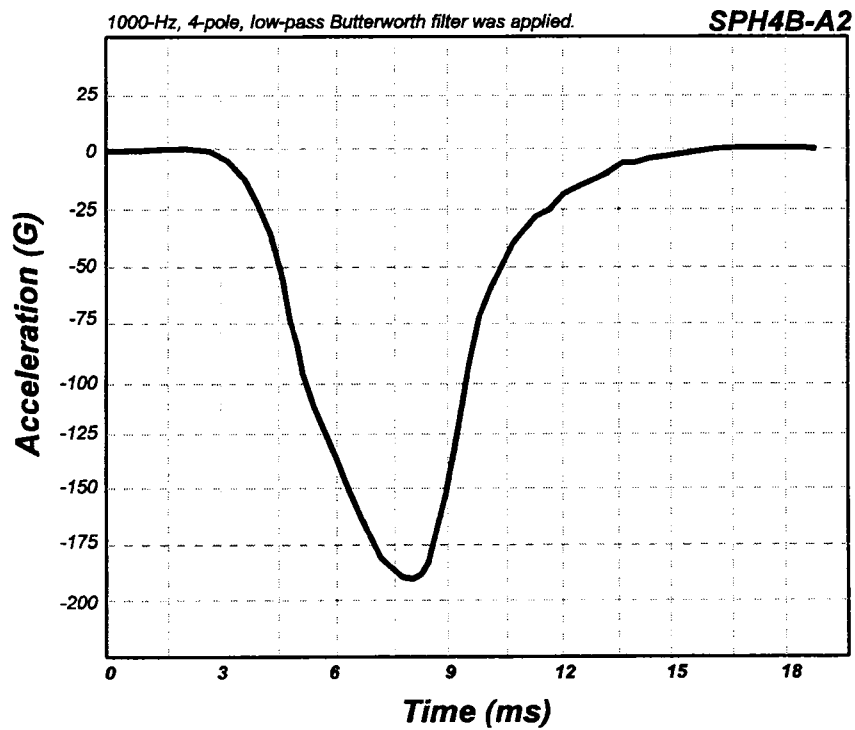


Figure 56. Typical acceleration time history trace.

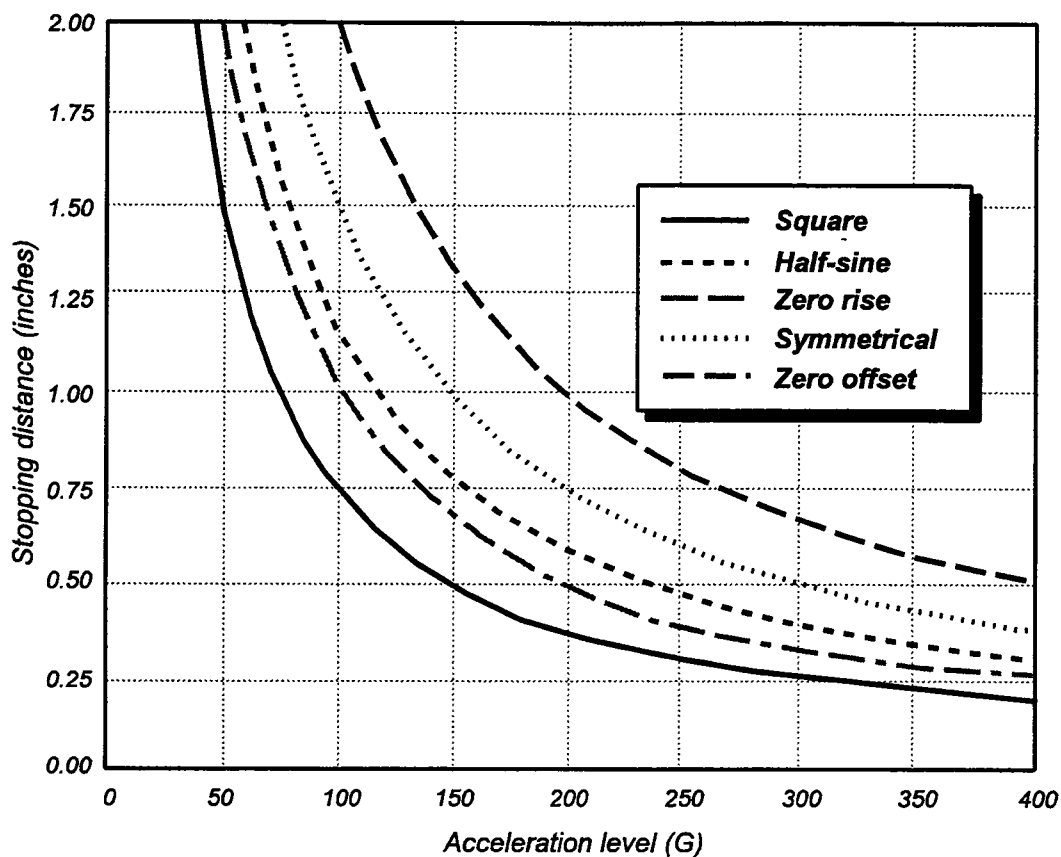


Figure 57. Theoretical stopping distances for various G levels.

crushing process, the material compacts and occupies a percentage of the total thickness. The space required for the compacted material must be considered during the thickness determinations. If not, then a “bottoming out” event is likely to occur, resulting in acceleration spikes being transferred to the head. Energy liner “bottoming out” occurs when the available crushing distance is exceeded and results in a rapid onset of the measured acceleration level.

Contact area and impact surface shapes should also be considered since they will help determine the load level required for the material to crush. Head shapes typically result in large contact areas when the crown or side regions are impacted, and reduced areas when the forehead or rear regions are impacted. To obtain the same energy absorption capability among the various impact sites with a constant liner thickness, the crush load must be increased for those impact sites with reduced surface areas.

For this reason, it is also important to consider the shape of the impacting surface and the ability of the outer shell to distribute the load. The Army aviation community has eliminated the hemispherical impact anvil from the performance requirement and selected the flat anvil only. This decision was based on the fact that in the Army helicopter crash environment, hemispherical impact surfaces were rarely struck while flat surfaces were prominent. The hemispherical impact anvil presents a point loading threat to the helmet. To defeat this threat, the helmet shell must be rigid enough to resist local deformation and distribute the impact load and the energy liner must possess either an increase thickness or an increase crush resistance load. Designing a helmet system to defeat the point loading threat has typically resulted in increased mass.

The impact attenuation material used in Army aviation helmets has been predominantly expanded bead polystyrene. This material and molding process is well known and inexpensive. It also possesses desirable impact attenuation characteristics, such as good energy attenuation and low rebound. This material is also predominant in the motorcycle and bicycle protective helmets. Other impact attenuation materials are available and should be considered. Polyurethane is one such material. Polyurethane has been and continues to be used by military aviators in the United Kingdom.

Frangibility

Frangibility of helmet components is required when the total head supported mass creates an unacceptable risk of neck injury. The purpose of incorporating frangible (automatically detachable) devices into the helmet assembly is to remove the mass from the helmet, thus reducing the risk of neck injury. The AN/PVS-5 NVG, when used by Army aircrew, were attached to the SPH-4 helmet with "hook and pile" fasteners and elastic tubing. This method did not allow the goggles to easily or consistently detach during a crash. During ANVIS development, the attachment mechanism was designed with a spring loaded "ball and socket" engagement which allowed the NVG to separate from the mount when exposed to an 10 to 15 G loading. This mechanism has performed well in the Army helicopter crash environment. The IHADSS HDU, which is a monocular CRT display, is also easily attached and detached from the helmet mount. Mounted on the right lower edge of the helmet shell, the HDU also detaches from the helmet during crash loadings, and actual crash experience has shown it to perform well.

Both, the ANVIS and IHADSS HDU detachment mechanisms operate when the device is exposed to crash loads and its dynamic inertia loads exceed the mechanical retaining forces. The U.S. Navy, with the introduction of Cats Eyes NVG for their fixed-wing community, developed a pyrotechnically activated detachment mechanism. This device was activated when it received an electrical signal at the beginning of an ejection sequence. This signal activated a squib (a small tube filled with fine-grained black powder) which performed the mechanical release of the Cats Eyes goggles.

A device similar to the Cats Eyes automatic release device could be incorporated into the rotary-wing community, but a sensor would have to be used to sense the crash onset and initiate device release. Such a sensor is being developed by the Program Manager-Air Crew Integrated Systems (PM-ACIS) for activation of the helicopter air bag restraint system. Pursuing such an approach to reduce the head borne weight during crashes introduces system complexities, increases technical risk, and raises program costs. The determination of when the device should be detached is not a trivial issue, and actual crash acceleration data are generally not available upon which to base such determinations. Generally, a portion of such an automatic device remains on the helmet. The trade between the amount of weight being removed versus the amount being retained may become negligible if the design is not optimized.

Current frangibility (breakaway) design requirements are that when subjected to an acceleration of 9 G or less in any vector within the limits described in Figure 58, the designed frangible components shall not separate. However, separation must occur for acceleration of 15 G or greater. During breakaway, the frangible components should not come in contact with the wearer's forehead, eye sockets, or facial regions at any acceleration level (Rash et al., 1996a).

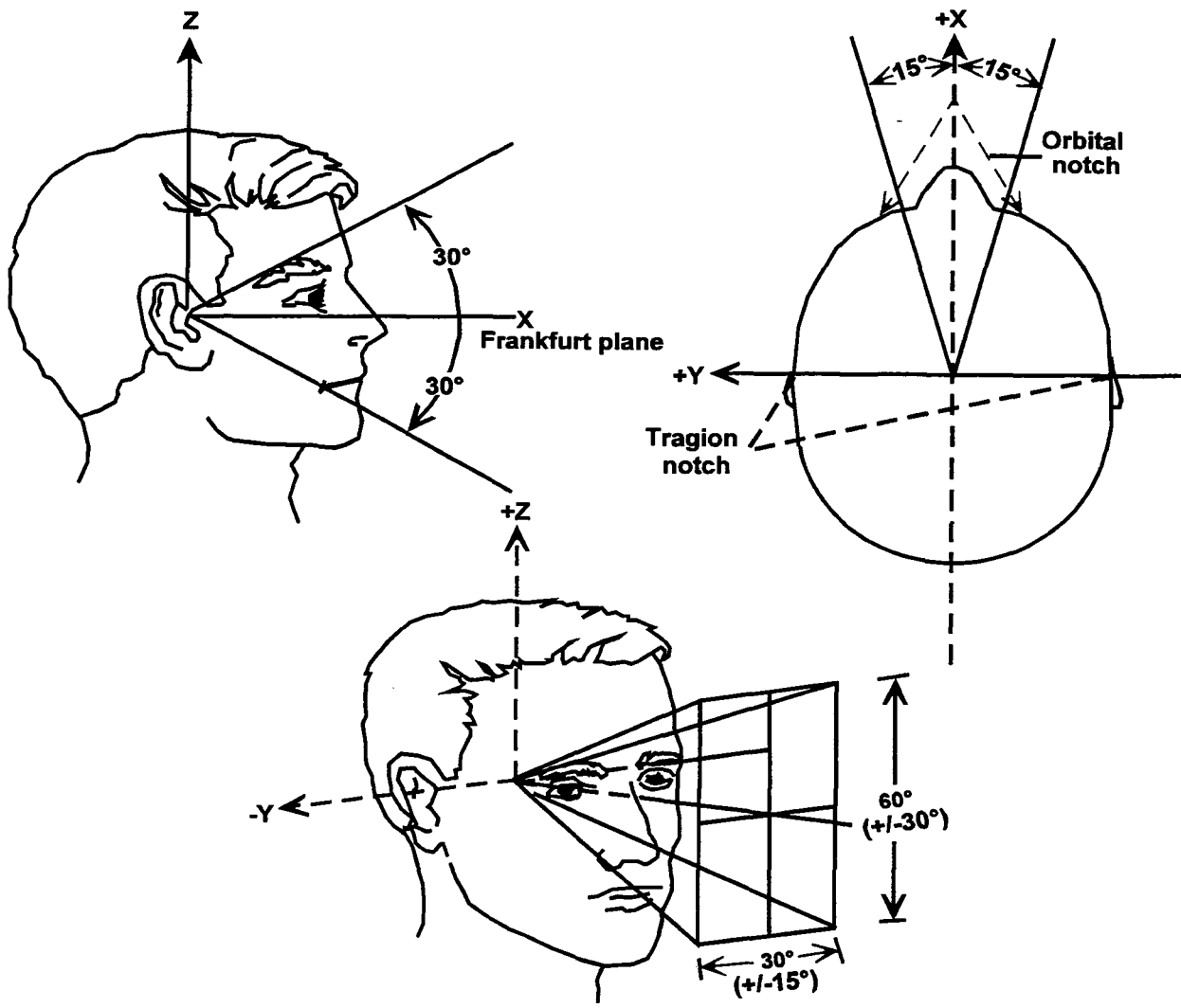


Figure 58. Vector limits for HMD breakaway force.

Individual fitting systems

The selection of a helmet fitting system has become more involved with increased helmet complexity and compatibility requirements. The primary function of the fitting system is to provide a comfortable, stable fit to the wearer. Comfort can be achieved by distributing the helmet weight across the head, thereby preventing or reducing the occurrence of "hot spots" (singular points of increased pressure), and resisting heat buildup. Stability is dependent on both, the helmet's retention and fitting systems.

Numerous fitting methods have been used and devised for aircrew helmets. Listed and described in Table 15 are some of the fitting systems previously used, currently in use, and proposed concepts. This table is not all inclusive, nor does it identify all of the attributes of each system. Some attributes which should be considered when selecting a fitting system include; fitting ease, sanitation, durability, maintainability, comfort, stability, low load deformation, impact attenuation effects, and retention effects. Another parameter is the anthropometric range the system can accommodate and the number of helmet sizes being designed. Fewer helmet sizes suggest the fitting system accommodate a greater anthropometric range. If designing a helmet system with a restricted exit pupil location, numerous helmet sizes may be required with a minimal thickness fitting system. Such design considerations will influence the type and configuration of the selected helmet fitting system.

In the Army's early Aviator Protective Helmet No. 5 (APH-5), multiple leather pads of varying thicknesses were employed. Initially, they were glued to the polystyrene liner; later self-adhesive strips were used. The SPH-3 and SPH-4 helmets initially used a sling suspension system consisting of three nylon cross straps which ran across the top of the head and a leather head band which ran around the circumference of the head, above the brow line. In the center where the cross straps intersected, there was a cushion pad (Figure 59). Both the head band and the cross straps were adjustable.

Formally introduced in the SPH-4 helmet in the mid 1980s, a fitting system design based on thermoplastic liners (TPL™) is used in the SPH-4B and the HGU-56/P helmets. The TPL™ system typically consists of 2 to 5 plies of thermoplastic sheets with 1/4 inch diameter dimples (open cell), covered with a cloth cover (Figure 60). The TPL™ system was adopted to improve comfort and to alleviate fitting problems with the original sling suspension of the SPH-4 helmet brought on by extended mission lengths, the introduction of NVGs, and the increase in the number of female aircrew members with their different anthropometric head dimensions (Barson, Pritts, and Lanoue, 1988). The introduction of the TPL™ solved many of the fitting problems, as well as improving the level of crash protection. The TPL™ suspension method could be considered a custom fit, which overcomes most variations in individual anthropometry, providing a greatly enhanced level of comfort and fit.

The TPLs™ delivered with the HGU-56/P are prefitted to appropriately sized head forms as a part of the manufacturing process. Most aviators can remove the helmet and TPL™ straight from the box and obtain an adequate fit with minor adjustments. If unable to obtain a comfortable fit, custom fitting can be easily accomplished by heating the TPL™ for approximately 10 minutes in a convection oven at a temperature of $200 \pm 5^\circ\text{F}$. The heated TPL™ becomes soft and pliable, retaining its new shape after it cools. The aviator inserts the heated TPL™ into the helmet, which then is placed on the aviator's head for 5 minutes with downward pressure applied. [This is accomplished by having the aviator place his hands over the helmet and pull down towards the crown of his head.] The pressure is released and the helmet worn for an additional 5 minutes. If an optimal fit is not achieved, the process can be repeated, as long as the TPL™ is not overheated.

Another type of fitting system, used primarily in the U.S. Air Force and Navy fixed-wing helmets is based on variations of a custom-fit foam technique. One variation in the foam method involves the mixing of two chemicals which produces a foam liner form-fit to the head; another variation uses a wax mold which is heated and placed on the head. The Army briefly authorized these foam systems during the period when NVGs were first introduced, but withdrew approval due to varying foam density and inconsistent impact protection performance. Thus, they currently are not used in Army aviation.

Table 15.
Helmet fitting systems.

Type	Reference Helmet	Fielding status	Attributes
Foam pads	APH-5 APH-6	No longer used	Various pad thicknesses accommodated variable head sizes. Comfort dependent on user.
Three-strap sling	SPH-3 SPH-4	Some SPH-4 still in use	Individual strap adjustment provided user adjustability. Comfort difficult to achieve, some individuals experience significant discomfort, others had no problems. Attachment clips contributed to SPH-4 impact attenuation.
Thermoplastic Liner (TPL™)	SPH-4 SPH-4B HGU-56/P Others . . .	Currently fielded	Widely accepted in the aviation environment. Can be individually fitted by heating. Can be cleaned. May adversely affect helmet stability. Durable.
Pads, mesh, & drawstring	IHADSS	Currently fielded	Difficult to comfortably fit the IHADSS helmet. May degrade helmet retention if too many pads are used to obtain comfortable fit.
TFL	Various SPH and HGU types	Special cases	Currently used by USAARL when comfortable fits cannot be attained with the standard issue TPL™. Performance still under evaluation.
Foam in place	HGU-33/P SPH-3C	Not used by the Army	Provides an individual fit with little adjustment tolerance. Provides a stable fit, can become uncomfortable if helmet is not repositioned to original fitting location. Difficult to obtain consistent foam density. Could affect impact attenuation performance.
Silicon foam fill	developmental	Proposed	Provides an individual fit. Pliable to relieve pressure points after redonning the helmet. Durability, operational performance, and user acceptability are unknown.
Epoxy coated foam	developmental	Proposed for Comanche helmet	Provides a stable, individual fit. Can become uncomfortable if not repositioned to original fitting location. Durability, operation performance, and user acceptability are unknown.
Custom foam fit	U.S. Navy fixed-wing night attack helmet	Operation	Provides a stable, individual fit. Requires a wax mold of the aviator's head be taken. Liner custom made to casting made from wax mold, at manufacturer's plant. Lengthy time process.

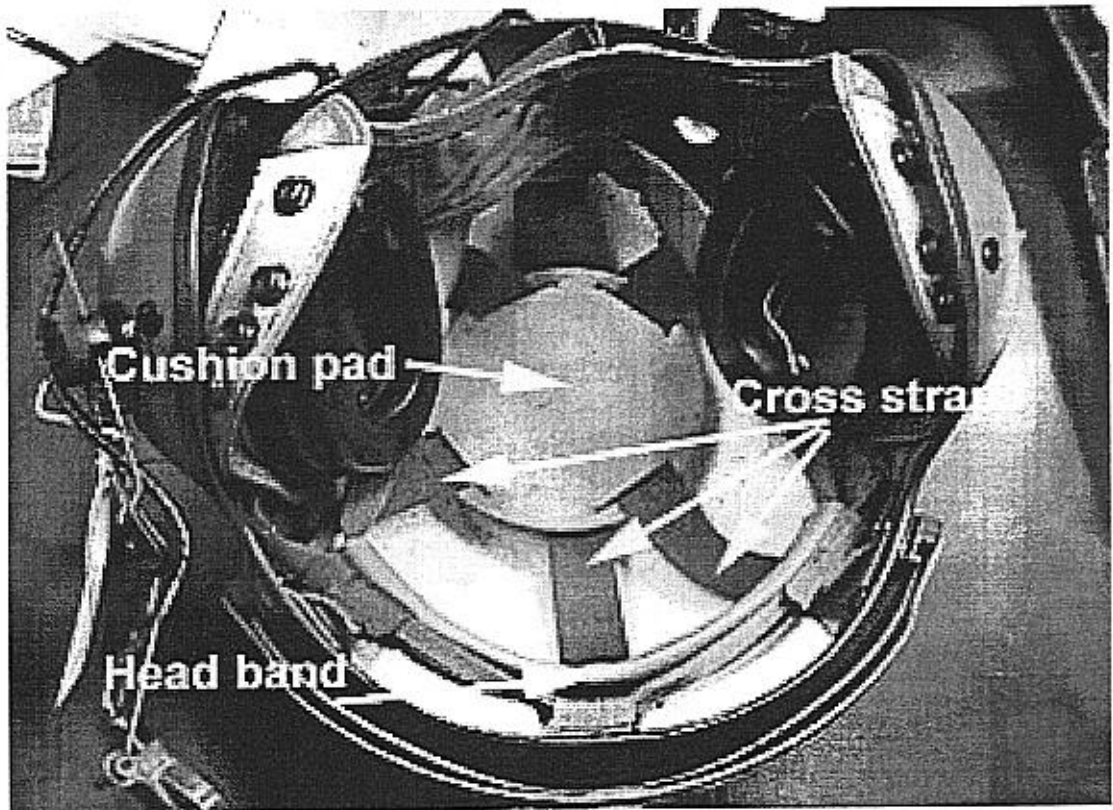


Figure 59. Sling suspension in SPH-4 helmet.

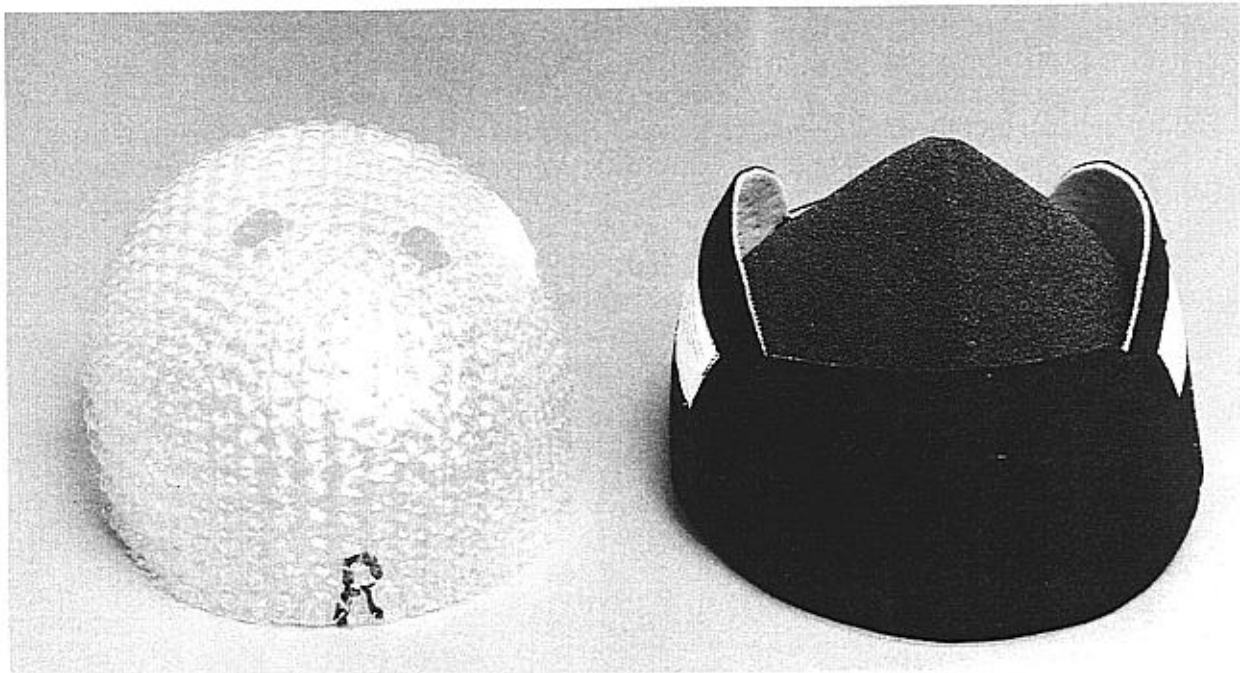


Figure 60. View of a 4-ply TPL™ removed from the foam liner and cloth cover.

Retention

Helmets are unable to provide their impact energy attenuation function if the helmet does not remain on the head during crashes or mishaps. This role is accomplished by the helmet retention system. Reading et al. (1984) showed that helmet retention system failure is a significant factor in mishaps where helmet losses occurred. Typically, modern retention systems consist of an integrated napestrap and a chinstrap. The napestrap runs behind the head just under the occipital region. The chinstrap runs under the chin, being careful to avoid the areas around and about the trachea. A properly designed retention system will prevent the helmet shell from undergoing excessive forward or rearward rotation when the head is exposed to crash induced acceleration(s) (Hines et al., 1990), without introducing potential hazards inherent to its own design. In addition, a positive effect on retention under tangential loads is provided.

In the early SPH-4, the napestrap and chinstrap were separate (although attached) items. The napestrap was part of the earcup retaining fabric, and the chinstrap (with slide-bar adjustment buckle) was attached on each side with single snaps. The use of snaps for the chinstrap was limiting because the snaps were capable of withstanding only approximately 150 pounds of loading force. And, it was found that on the SPH-4, the snaps distorted, the fabric deteriorated with wear, and retention performance was diminished significantly. Another problem associated with the SPH-4 system was chinstrap elongation, which under severe crash loads could be as high as 2 inches. This could result in the helmet rotating off the head during the period of time when its protective characteristics are needed most.

The SPH-4 underwent a number of design modifications during its lifetime. One interim fix applied in the mid 1970's used two snaps on each side (called Y-yoke), which increased the loading force capability to approximately 250 pounds. This was followed shortly thereafter by another change where the chinstrap was permanently attached to one side through a grommet, with the other side fitted with two more closely adjacent snaps. This resulted in an increase to approximately 300 pounds in loading force capability.

As of the mid 1980s, despite the numerous attempts to improve the SPH-4 retention system, investigation of retention system effectiveness showed: a) That double snap fasteners were inconsistent in strength performance (Vrynwy-Jones, Lanoue, and Pritts, 1988), b) that cloth connection between chinstrap/napestrap and the helmet shell allowed excessive helmet displacement, and c) that forward displacement was increased when I² devices were used (Hines et al., 1990). Continuing attempts to improve the SPH-4 retention system included reinforcement of the assembly using tubular nylon webbing. This had a result of increasing chinstrap strength and reducing chinstrap elongation (by as much as 50%), which reduced the upward displacement of the helmet during crash loading (Palmer and Haley, 1988). Using this reinforcement technique as a stepping stone, USAARL, working in cooperation with Gentex Corporation, Carbondale, Pennsylvania, produced a modified yoke harness (Hines et al., 1990) (Figure 61). This harness was a modified universal retention assembly where the forward attachment points of the harness were located 0.9 inch forward and 0.2 inch below the previous attachment points. The rearward attachment point used the headband clip hole which was located 1.1 inches rearward and 0.6 inch below the previous rear attachment point. In addition to the adoption of the double "D" ring adjustment buckle, there were numerous other changes from the then existing assembly. Concurrently, Gentex Corporation developed a swivel yoke harness. Both designs passed the 440 pound load requirement being applied to the then underdevelopment HGU-56/P helmet. The USAARL design demonstrated slightly less chinstrap elongation and subsequently was incorporated into the SPH-4B flight helmet.

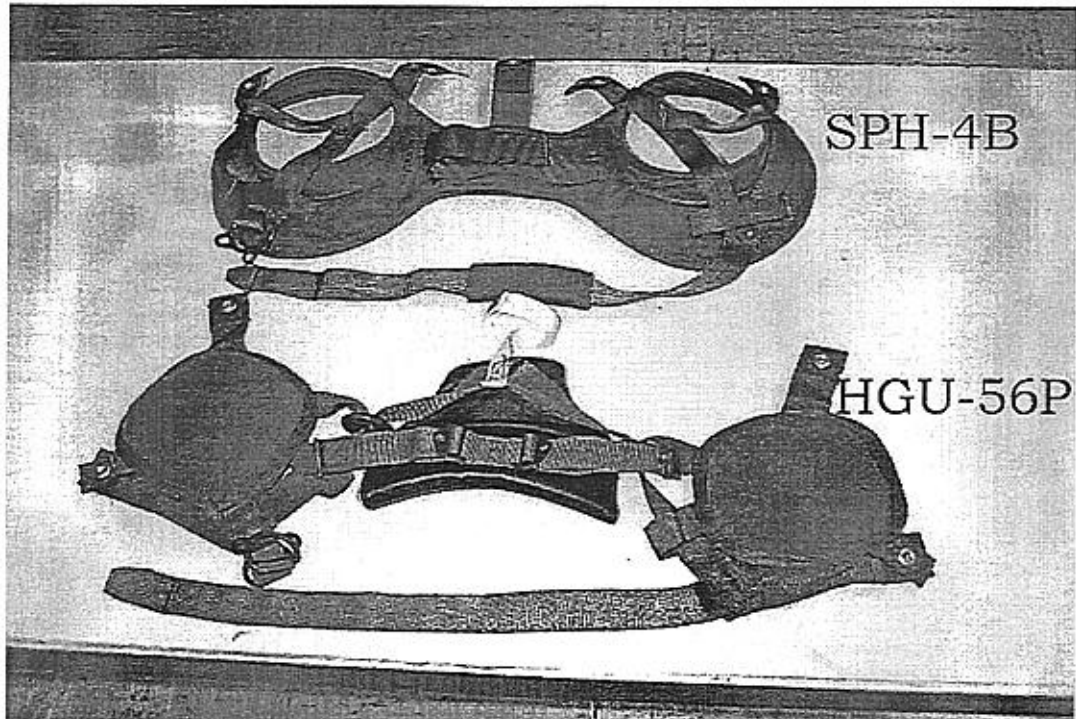


Figure 61. USAARL modified yoke harness, used in the SPH-4B, and the HGU-56/P retention system.

The HGU-56/P is the Army's most recently fielded (1995) aviator helmet. It retained the TPL™ liner and crushable earcups, but the Kevlar™ cloth shell used in the SPH-4B was replaced with a polyethylene and graphite cloth shell. The HGU-56/P replaces the SPH-4B earcup retaining harness with Velcro™ attachments. The two Velcro™ flaps incorporated into the SPH-4B napestrap were replaced with a single piece of cloth-covered foam running horizontally across the back. As in the SPH-4B, the chinstrap load is applied to webbing and then transferred to the helmet shell. A double "D" ring is used, as in the SPH-4B, as the chinstrap buckle. These rings are a special "low slippage" design with one ring slightly smaller than the other. The HGU-56/P retention system is depicted in Figure 61.

As a final note, retention system success is directly related to both proper fit and wear.

Stability

Helmet stability is a measure of the helmet's ability to remain in a constant orientation, with respect to the head, when exposed to low load levels. These loads may be the result of inflight maneuvers and buffeting, vibration transmission from the surrounding structure, inadvertent bumps into cockpit structure during execution of flight duties, rapidly moving the head, and unbalanced helmet systems. Helmet characteristics which effect helmet stability include the fitting system (and the appropriateness of the fit), the retention system (and the appropriateness of the fit), and it's mass properties. Human characteristics which effect helmet stability include individual head shape, quantity and management of hair under the helmet, and looseness of the skin (Neary et al., 1993).

If the helmet position shifts, then: (a) optical field of view reductions may occur, (b) hot spots may develop, and (c) the impact protection zones of the helmet are compromised. For mission

execution, helmet stability is critical when helmet-mounted displays or image intensification devices are used. Excessive helmet slippage could effectively “blind” the aviator from receiving the desired display information for effective aircraft control. Gradual slippage may create pressure points which result in “hot spots” and user discomfort. This can distract aircrew attention away from his primary responsibilities. Additionally, helmet instability is an indicator that the helmet will displace when exposed to high dynamic loads associated with the helicopter crash environment. This compromises the desired impact protection zone of the wearer’s cranium.

Helmet stability is affected by helmet mass and CM placement. High helmet mass and misplaced center of mass locations can result in helmet slippage relative to the aircrew eye location. Flight load exposure typically induces this slippage. Mass moment of inertia (MOI) effects the helmet’s stability when the wearer rapidly moves his head side to side or up and down. The helmet may or may not reposition itself after the motion ceases. This is dependent on the slippage magnitude and the resiliency of the fitting system.

Visors and visor assemblies

Visors are look-through optical media, usually fabricated from polycarbonate materials (and in the past from CR-39 plastic). Polycarbonate is the preferred material due to its enhanced impact protection. The purpose of visors is to provide protection from dust, wind, sun glare, and particle fragments and, in the case of a crash, from tree branches, rocks, debris, and aircraft structural parts. It should be noted that contrary to verbiage in many documents, visors are not designed to provide “ballistic” protection. However, they are expected to provide impact resistance. (To clarify this statement, visors are designed to provide limited protection against shell fragments, but not from direct hits of shells themselves.) In more succinct terms, visors can prevent painful, serious injuries to the head and face (Reynolds et al, 1997).

In U.S. Army aviation, visors are classified as Class I or II. These classes are defined in military specification MIL-V-43511C, “Visors, flyer’s helmet, polycarbonate” (1990). Class I visors are clear, having a photopic (daytime) luminous transmittance of 85% or greater. Class II visors are neutrally tinted, having a photopic luminous transmittance between 12-18%. An exception to the Class II luminous transmittance requirement is granted to the tinted visor used in the IHU of the IHADSS in the AH-64 Apache. The IHADSS Class II visor has a photopic luminous transmittance between 8-12%. This lower range of transmittance is needed to improve visibility of real-time imagery provided on the IHADSS HMD. Regardless, all visors generally are held to the optical specifications for refractive power, prismatic deviation, distortion, haze, impact resistance, etc., cited in MIL-V-43511C. The test for compliance of impact resistance uses a caliber - .22 T37 fragment simulating projectile at an impact velocity between 550 and 560 feet per second. The test is conducted in accordance with MIL-STD-662D, “V50 ballistic test for armor” (1984).

Another deviation from the visor classes above is special purpose visors which are designed to provide protection from lasers. The luminous transmittance of laser visors can vary greatly depending on the wavelengths or combination of wavelengths for which the protection is being provided. Over the years, a number of types of laser visors have been evaluated for use (Rash and Martin, 1990; Bohling and Rash, 1991; Rash, Bohling, and Martin, 1991). However, except for a brief fielding period during the Desert Shield/Desert Storm war, the authors are not aware of any official designation of laser visors. But, in spite of a lack of formal fielding, a number of various types of laser visors are in use among Army aviation units.

Visors are fielded on all current aviator helmets. Issues associated with visors include how frequently they are used, when they are used, whether or not they function as designed, and what problems, mechanical or optical, are typically present. A study of visor use among U.S. Army rotary-wing aviators and aircrewmembers (Rash et al, 1997) found that use of visors improved when a dual visor configuration is available with the flight helmet. Aircrew wearing the SPH-4B and HGU-56/P helmets, which both have a dual visor assembly, report greater usage of visors, especially the clear visor, as compared to wearers of the single visor assembly SPH-4 and IHADSS helmets, who have to overcome the logistics of storage of the alternate visor. Additional problems affecting visor use include the inability to wear a visor when using ANVIS and the custom trimming of the visor needed with the IHADSS helmet to accommodate the helmet display optics.

From the perspective of HMDs, the major contribution of the visors is to attenuate the ambient background luminance in order to improve imagery contrast. The lower the visor transmittance, the more improved the contrast. However, decreased visor transmittance, which may be coupled with the transmittance of a see-through combiner, degrades overall see-through vision. Currently, only three transmittance values can be available at any given time, and this is possible only if a dual visor assembly is available.

The U.S. Air Force (Dobbins, 1974) has investigated the use of variable transmittance visors. Based on liquid crystal or photochromic materials, such visors have the potential to accommodate external luminances over a range greater than 80:1.

An investigation into the effect on visual acuity of visors (sunglasses) of different luminous transmittances has led to a recommendation that a minimum of 30% transmittance is required to achieve the 20/60 high contrast acuity equivalent for the 2nd generation I² systems under brightness conditions of overcast day, twilight, and full moon (Wiley, 1989b). Therefore, the use of visors which produce a combined transmittance of less than 30% will reduce see-through visual acuity below that of 20/60.

Acoustical

Noise levels found in military helicopters exceed noise exposure limits required by Department of Defense Instruction 6055.12 (1991) and Army PAM 40-501, "Hearing Conservation" (1991). Noise consists of a mixture of random broadband noise and periodic harmonic and high frequencies generated by the machinery contained within the helicopter, including impulse noise burst generated by weapons systems (Wiener and Nagel, 1988). Noise levels in helicopters with higher load capacities such as the CH-47 Chinook and the U.S. Air Force CH-53 Pavlow are extremely intense, and under some flying conditions, will exceed the helmet's capability to provide adequate hearing protection for crewmembers. Figure 62 shows a distribution of noise levels found in today's helicopters along with expected noise exposure of individuals wearing normal issue helmets with and without foam earplugs. About 15% of the flight conditions in Army aviation exceed protection limits of 85 dBA that are provided by the HGU-56/P or SPH-4B flight helmets. Wearing foam earplugs in combination with the helmet limits the noise exposure to less than 85 dBA for about 99% of the flight conditions.

Maintaining the necessary hearing protection for the Army noise environments, while providing the highest performance of voice communications for the aviator, has become the central goal of the hearing conservationist. Under conditions presently found in Army aviation, voice communication is reduced because of poor speech signals reaching the ear. Combination protection, earplug in addition to the helmet, is a commonly used technique to provide additional hearing protection, but this technique leads to decreased voice communications capability. The

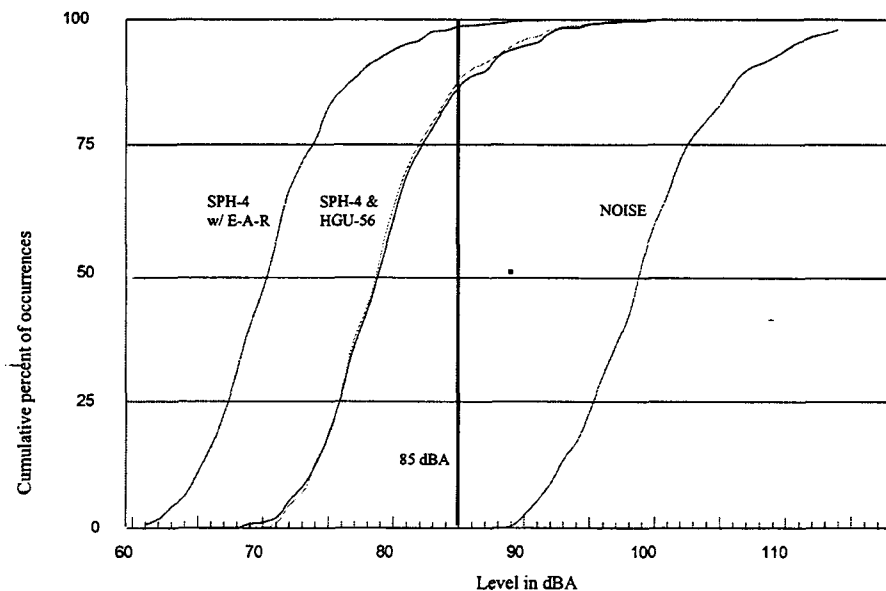


Figure 62. Noise level distribution of U.S. Army helicopters with noise exposure levels for aviators while wearing the SPH-4, HGU-56/P and the SPH-4B with yellow foam earplugs.

combination of less than adequate intercommunications subsystem (ICS) output and the use of earplugs may be responsible for most of the poor speech signal to noise ratio.

Currently, the hearing conservation objective is to increase sound attenuation provided the aviator in order to decrease the noise at the ear, while preserving the communication signal reaching the ear through the hearing protector. Two techniques that may be used to achieve these objectives are being investigated at a number of laboratories around the world. One technique, Active Noise Reduction (ANR), uses electronic circuitry to manipulate and reduce the noise found inside the earcup. The other technique, Communications Earplug (CEP) (Figure 63), uses passive sound attenuation, an earplug in combination with the helmet earcup, to achieve the required noise reduction. To improve speech communications, the earplug is attached to a miniature transducer that delivers the sound signal directly into the occluded portion of the ear canal through a small channel built into the earplug. Both of these techniques have been shown to reduce noise at the wearer's ear and improve the speech intelligibility characteristics of helmet systems. An additional technique that may be available in the near future is an earcup and earseal constructed of a new material recently developed by the U.S. Navy Aerospace Medical Research Laboratory, Pensacola, Florida. Only limited test data based on Acoustical Test Fixtures are available at this time and are insufficient for evaluating its full potential.

While the theory of out-of-phase-cancellation dates back to the 1940s, recent technological advances have made the implementation of ANR possible. ANR is a means of reducing noise levels in a personal hearing protector by measuring noise present inside the earcup and reinserting a processed and out of phase noise signal back into the earcup. The reinserted signal combines with the noise that was originally measured, causing it to be canceled. This out of phase canceling technique is very effective for low frequencies, below 800 hertz, but is generally ineffective for higher frequencies. In some designs, the ANR device actually increases the noise level inside the earcup in the region of 1000 Hertz. Total hearing protection consists of the passive protection provided by the earcup and the ANR component provided by the electronic system. Studies show ANR does improve speech intelligibility when worn alone, but both hearing protection and speech

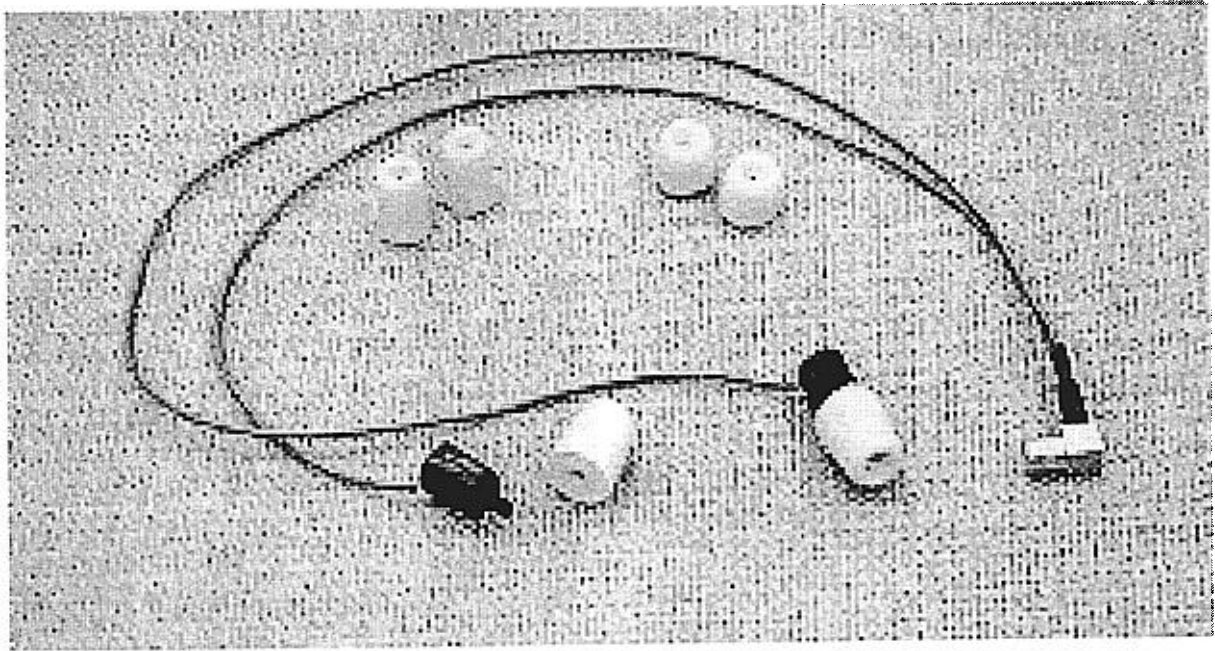


Figure 63. Communications earplug (CEP) (top) and attached to HGU-56/P helmet (bottom).

intelligibility are degraded when worn with ancillary equipment such as spectacles or CB mask (Mozo and Murphy, 1997b).

The CEP, a device that incorporates a miniature earphone coupled with a replaceable foam earplug, can be worn in combination with the aviator's helmet and can provide hearing protection adequate for extremely high noise levels. Donning, doffing and comfort issues for users of the CEP have been examined (Mozo and Murphy, 1997a; Mozo, Murphy, and Ribera, 1995) and have been determined to be within a manageable range. The device also provides voice communication intelligibility that approaches asymptotic limits, near 100%, in those high noise environments.

Protective capability of hearing protective devices which fit around the external ear is reduced whenever the earseal to head interface is broken (Wagstaff, Tvette, and Ludvigsen, 1996). Ancillary equipment such as spectacles and CB protective masks are devices that are commonly used with the aviator helmets and should be evaluated to determine their effects on the protective characteristics as shown in Figure 64. The spectacles were of a type with bayonet temples, which are standard issue for aviators. The CB mask used in the evaluation was the M-45 mask.

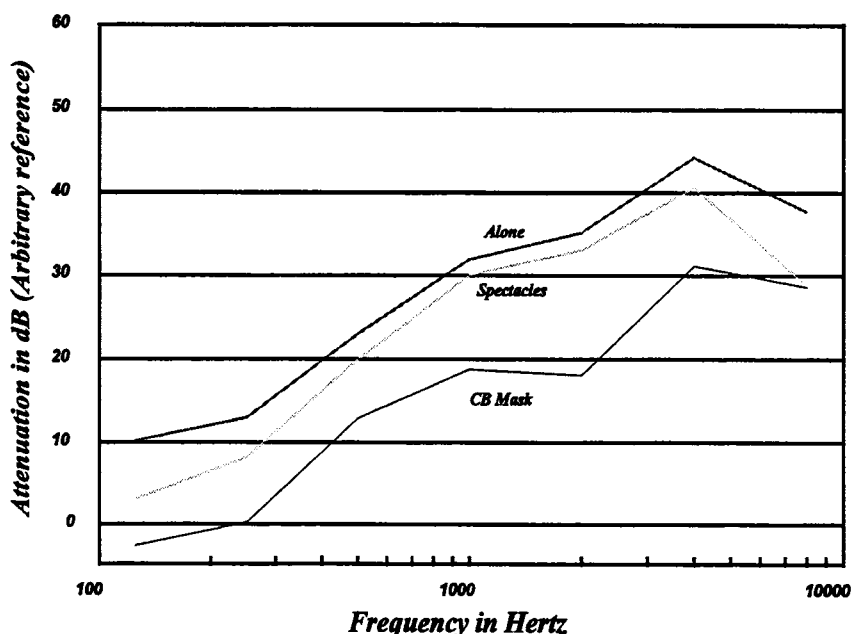


Figure 64. Sound attenuation of the HGU-56/P helmet worn alone, with spectacles and CB mask.

These techniques for providing improved hearing protection, while improving speech intelligibility performance, show promise for near term fielding. Factors that influence which technique is selected are aircraft modification, system cost, lateral impact, weight, and others. These areas should be evaluated carefully when considering the use of ANR or CEP in the helicopter environment.

Sound Attenuation

Sound attenuation and speech intelligibility are the primary quantitative measures of performance used to establish the relative merits of a device. The attributes are usually determined in the laboratory using standardized methodologies (Rash et al., 1996a). Appropriate methods utilize human listeners in the measurement in order to determine effects of head shape and head size on the characteristics of the device.

Sound attenuation measurements utilize a threshold shift method given in the American National Standards Institute (ANSI) standard S12.6, "Method for the Measurement of Real Ear Attenuation of Hearing Protectors" (ANSI, 1984) and an insertion loss method, ANSI S12.42, "Microphone-in-real-ear and acoustic test fixture methods for the measurement of insertion loss of circumaural hearing protection devices" (ANSI, 1995). The attenuation of ANR devices must be measured using the microphone in real ear techniques because of the low-level wide-band noise normally found in ANR systems. Earplug and canal cap type devices are measured using the threshold shift technique, ANSI S12.6, since insertion of a microphone into the canal for the measurement of attenuation is difficult and not generally used to assess devices on human subjects.

Assessment of attenuation differences attained by each of the techniques using the same device and subjects for both measurements show that low frequencies, 125 Hz and 250 Hz, have attenuation values which are slightly lower when using the physical measurement method. The cause of this difference is attributed to the biological noise produced by heartbeat or listeners breathing causing a masked threshold for the lower frequency test signals.

Attenuation results are sometimes difficult to understand in terms of which device provides the best protection. Protection depends on the spectrum of the noise, along with the mean and standard deviation of the attenuation measurement (Mozo and Murphy, 1997a). The measured noise is combined with the measured sound attenuation, standard deviation, and A-Weight factors for each octave band using the following Equation 28. The result is an estimated exposure level (EEL) of A-Weighted noise arriving at the listener's ear while in the noise environment. The Army hazard assessment procedures reduce the mean attenuation value by one standard deviation at each of the test frequencies when calculating the noise exposure level.

$$EEL = 10 \text{ Log} \left(\sum_{125}^{8000} 10^{\frac{\text{Noise Level}_i - A\text{Weight}_i - (\bar{X}_i - 1SD)}{10}} \right) \quad \text{Equation 28}$$

where, Noise Level_i is the measured noise level at the i^{th} frequency, $A\text{Weight}_i$ is the weighting factor at the i^{th} frequency, and $1SD$ is 1 standard deviation.

A group of EELs calculated for flight conditions expected during a mission scenario might be used to estimate the overall noise exposure that an individual may incur during an entire mission. Further, overall noise levels in Army aviation may be used to calculate the sound attenuation required for protection of the aviator population as shown in Figure 62 and Figure 65.

Ambient noise in dBA and estimates of noise levels at the ear shown in Figure 62 provide insight as to the extent of hazard present in the aviation environment and what potential the hearing protection schemes have to adequately protect the aviator. The estimate should include data collected under conditions the hearing protectors are normally used by the aviator. If

spectacles are commonly used, then sound attenuation must be determined while using spectacles as shown in Figure 64 and noise exposure effects as shown in Figure 65.

Speech intelligibility (SI)

Speech intelligibility is generally determined with human listeners evaluating word sets (ANSI, 1989). SI is a measure of one's ability to recognize these words when presented through a system under test. Word sets (Newby, 1972) are standard and comprised of phonetically balanced, monosyllable words that occur often in everyday use of the English language. Tests of communications devices are conducted in sound fields simulating noise found in a helicopter operational environment. Subjects listen and respond to words reproduced through the test system and the device being evaluated with percent of correct responses defined as the SI for that condition. The technique requires considerable time for data collection, but the results provide a reliable estimate of the performance anticipated for a particular field situation.

The Modified Rhyme Test (MRT) is currently the accepted speech material for use in determining the SI of communications devices (Prohaska and Nixon, 1984). Words are presented to listeners through the device under test and the listener responds by selecting one word determined to be correct from a list of similar words. Generally 10 subjects are used in the test to determine the SI of a device.

This Laboratory has evaluated various combinations of helmets with ANR, earplug, and CEP to compare the communications performance under noise conditions (Mozo and Murphy, 1997b). The noise level measured in the UH-60 during level flight at 120 knots is normally used as the noise condition. Speech input levels are defined and correlated with speech intelligibility results to provide insight into operational characteristics of the device under test.

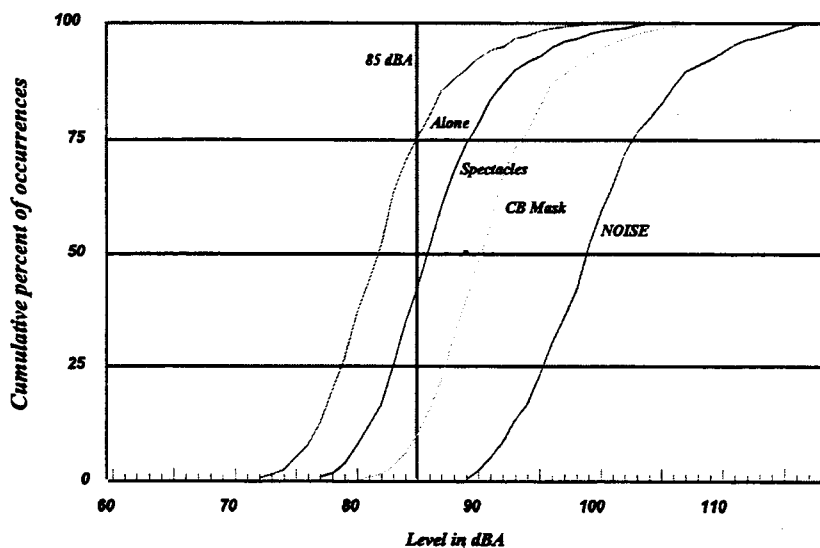


Figure 65. Noise level distribution of U.S. Army helicopters with noise exposure levels for aviators while wearing the HGU-56/P alone, with spectacles and with CB Mask.

A study of the intelligibility of speech when using either ANR or CEP by aviators with noise induced hearing loss demonstrates their usefulness for the helicopter environment (Ribera and Mozo, undated). SI results of SPH-4B with and without ANR and CEP used in the “normal” verses “waivered” study are shown in Figure 66. Curves shown in this figure were developed from SI measurement data using a distance weighted linear smoothing algorithm. The curves show significant differences in the speech level required for the three different devices to perform at the same level of intelligibility. When speech is considered as another source of noise exposure, then lower levels would imply less noise exposure from that source. For example, the estimated speech input level of 82 dBA using the CEP would result in about 80% intelligibility. That level of speech intelligibility would require an input speech level of about 90 dBA for the ANR system and over 100 dBA for the SPH-4B. The net effect should reduce speech levels required for communications and therefore reduce the hazardous effects of the speech signal.

The effect of these techniques on SI for 20 normal and 20 hearing-impaired aviators showed significant improvements over the standard helmet for both sample groups. Results of speech intelligibility of the hearing-impaired aviators wearing CEP or ANR were compared with the 95% confidence interval for the normal aviator wearing the SPH-4 helmet are shown in Figure 67. Only 1% of the hearing impaired aviators were in the 95% confidence interval while wearing the SPH-4, as compared to 65% while wearing the CEP helmet and 40% while wearing the ANR helmet.

Operational assessment

One of the most critical requirements of systems development is to define the worth and acceptability of the system to the user group. User acceptance testing should be performed by the user in the environment or, at a minimum, a high fidelity simulation of the environment. Personal equipment such as communications and hearing protective devices must be assessed during as many user conditions as possible and in as many climatic and environmental conditions as practical (Staton, Mozo, and Murphy, 1997; Mozo and Murphy, 1997a).

A study (Mozo and Murphy, 1997a) comparing the CEP and the HGU-84 using Navy and Marine Corp aviators assigned at Quantico, Virginia, was accomplished over a 4-month period. A preference questionnaire was used to measure the volunteer’s assessment of the CEP when compared to their personal helmet. The areas of interest were comfort, compatibility, communications performance, utility, and overall value added as assessed by each of the individual volunteers. The rating scale used to compare the CEP and the aviator helmet used in CH-46 and CH-53 helicopters was based on the following 7-point scale:

7	6	5	4	3	2	1
Significantly better	Moderately better	Slightly better	Same	Slightly worse	Moderately worse	Significantly worse

A numerical rating of "7" indicated the user’s highest preference value for the CEP while a rating of "1" indicated the users highest preference value for the helmet. If the user perceived no difference between the CEP and the helmet then the volunteer indicated a rating of "4."

Results of the questionnaire responses were analyzed to determine the overall acceptability of the CEP for use in the H-53 missions when compared to the HGU-84 helmet. Table 16 shows the results of questionnaires administered at the mid-point of the study and again at the end of the study. For most of the questions, results showed a slightly stronger preference for the CEP at the end of the study, indicating users found the CEP more acceptable with continued use. The fit and comfort of the CEP were judged to be the same as their standard helmet, indicating discomfort

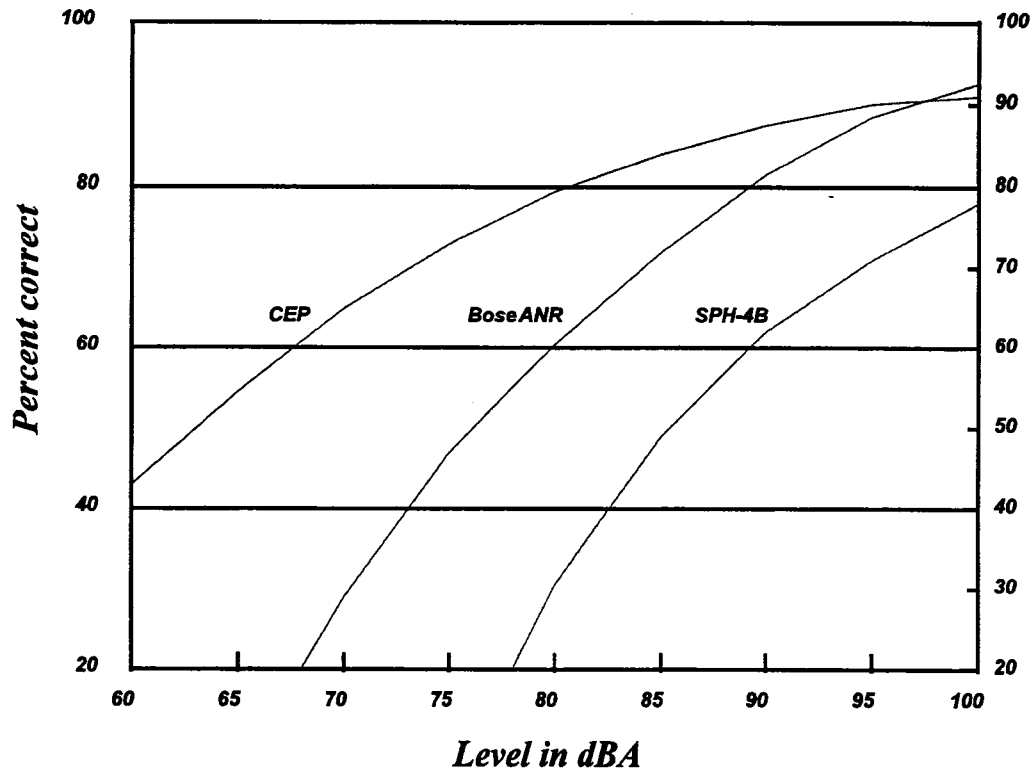


Figure 66. Speech intelligibility versus speech level in UH-60 noise for three devices.

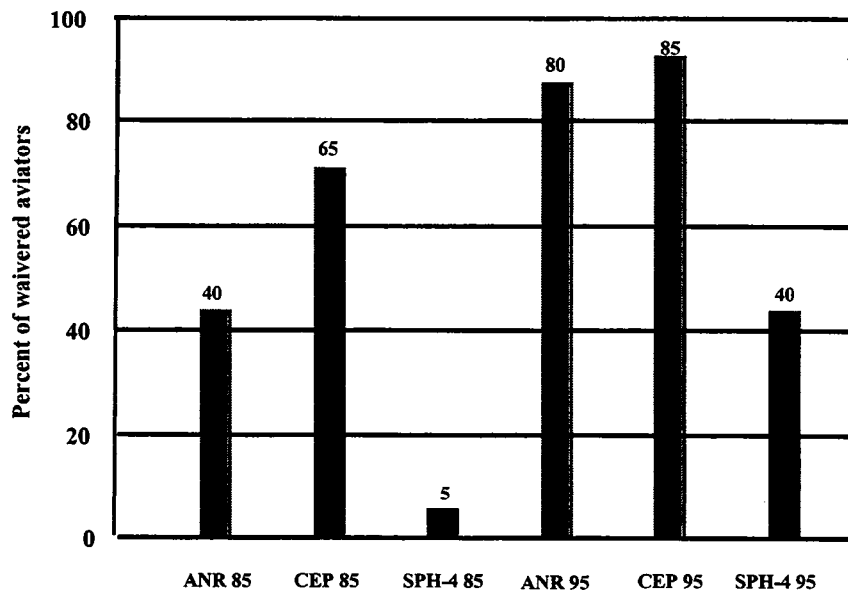


Figure 67. Speech intelligibility improvement for hearing impaired aviators when compared with normal aviators at 95% confidence interval using SPH-4.

was not considered a factor by the user after 4 months of use. There was a difference in favor of the standard helmet in the donning/doffing process because of the extra step required to install the CEP. (It is the authors' opinion that the user will become more proficient in the procedure with continued use of the CEP. Proper planning of events that take place in the donning process will limit or eliminate problems for even the most time critical mission start.) All of the noise reduction and speech clarity responses indicated a strong preference for the CEP over the standard helmet.

Table 16.
Results of midpoint and final questionnaire assessments (15 subjects).

Question	Midpoint score	Final score
Average number of flight-hours using CEP	30.5	40.7
Fit and comfort of CEP	4.2	4.1
Donning/doffing	3.5	3.5
ICS clarity	6.3	6.5
Radio communications clarity	6.3	6.6
Gender clarity (male)	6.1	6.6
Gender clarity (female)	6.0	6.6
Overall clarity	6.3	6.6
Noise reduction	6.3	6.4
Ability to hear warning signals	6.0	6.6

Weight (mass) of helmet/communications

The weight (mass) of the helmet is critical when considering the ultimate effectiveness when used in today's military environment. Individuals riding in aircraft or vehicles are subjected to significant forces on the head and neck system because of head supported mass. These forces become critical during high accelerations of the head caused by rough terrain, direction changes to evade and escape, or mishaps. The weight of the communications system portion of the helmet, as shown in Figure 68, is about 25% of the total weight. Table 17 shows the mass of each communications component of the CEP, the HGU-56/P and an ANR earcup system. Considering the limit in terms of weight (mass) savings, the use of the CEP as a complete replacement of the earcup system would result in saving about 198 grams for the HGU-56/P or about 290 grams for the ANR communications system.

It is the authors' opinion that the earcup performs a significant role in providing comfort for the user and for improving user acceptance of the helmet system as a protective device and mounting platform. The earcup is a very useful feature of the helmet system because it maintains stability of the helmet/head relationship that would otherwise result in significant degradation of the visual performance of the user when using displayed image systems. The earcup also acts to isolate the external ear from pressure of the helmet that would result in causing discomfort to the user. The CEP will provide the major portion of hearing protection and the voice communications signals while the earcup will supplement the protection, resulting in adequate protection for any noise environment found in Army aviation.

Lateral impact has been shown to cause significant injuries that have on occasion resulted in fatalities (Shanahan, 1985). Research efforts to reduce the potential of lateral impact injuries have resulted in the energy absorbing earcup found in current Army helmets. Maintaining the standoff and energy absorbing capability of the helmet is important to the safety of the aviator who may be

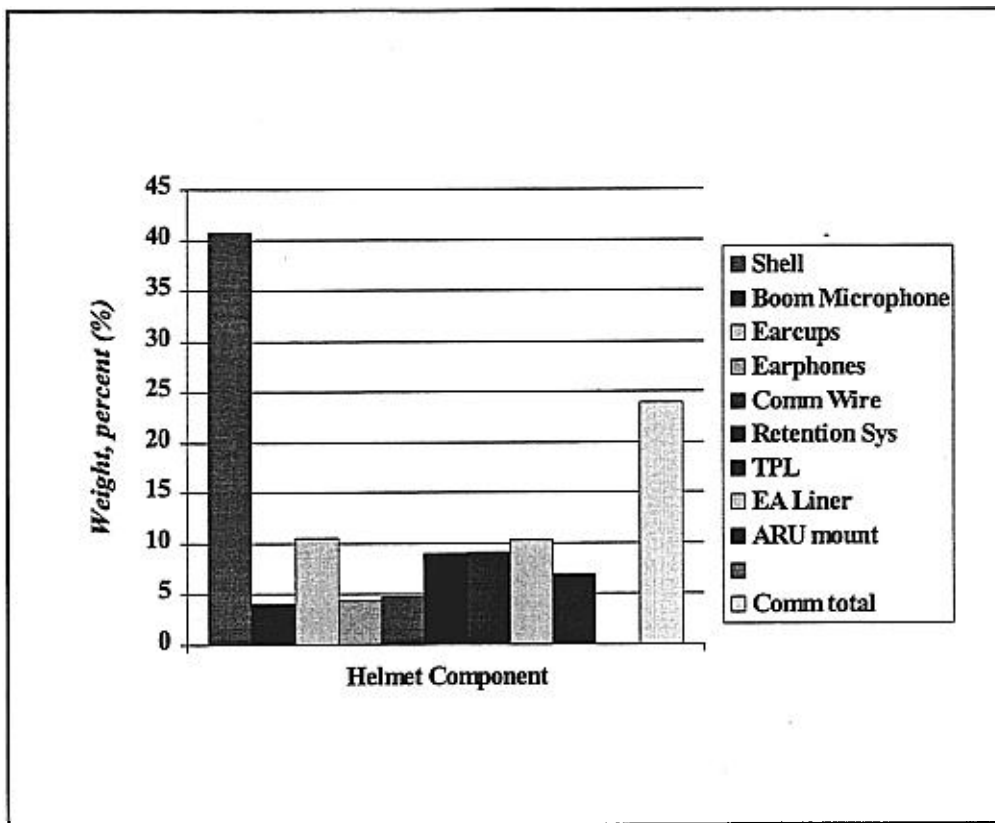


Figure 68. Percent of weight of components in the prototype Comanche helmet.

Table 17.
Mass of the CEP and helmet communications components.

Item	Mass (grams)
CEP with HGU-56/P interface cable and blown-air port adapter	18.8
-CEP	8.0
-Interface cable	5.0
-Blown-air port adapter	5.8
HGU-56/P earcup w/ foam inserts, #2990 earseal, and #996 earphone - X2	215.0
HGU-56/P earcup with foam inserts and #2990 earseal - X 2	175.0
Earphone (Model #996)	19.8
ANR earcup and earseal - X2	308.4

involved in a rotary-wing mishap. Reduction of the earcup weight (mass), by reducing the wall thickness and redesigning the flange may serve to increase the lateral impact protection while maintaining the hearing protection and speech intelligibility provided the user.

3-D audio

Auditory signals input through earphones are now capable of simulating open field signals and are very good at providing the listener information needed to localize a sound source. The auditory signal coupled with visual signals combine to enhance the aviator's ability to localize and detect targets at smaller subtended angles (McKinley, Erickson, and D'Angelo, 1994). Helicopters like the LongBow AH-64 and Comanche can benefit from the 3-D technique since radar signals are available as to locations of targets relative the aviator. Parameters provided by the radar can be used to place an auditory cue at the relative target orientation and direct the head position to the proper location, thus increasing probability of visual detection.

Locations of radio receivers may be distributed around the auditory space of the aviator in a manner that will enable selective attention based on the position perceived by the listener. ICSs may be adapted to provide the listener with information as to the talker's location and again allow for selective attention that may be based on mission requirements at that particular time. There are indications in the literature that the 3-D audio approach may improve the speech intelligibility of information received over the ICS (McKinley, Erickson, and D'Angelo, 1994). Currently, helmet/communications systems in the aircraft are designed for monaural operation. In the advent of 3-D audio, the system will require redesign to accommodate binaural input.

Human factors engineering (HFE) issues

While the physical performance of an HMD system is important, of equal importance are those issues involving user interface with the HMD. These issues include, but are not limited to, the identification of specialized skills and training for operation and maintenance, user adjustments, health and safety issues, anthropometry, fit, ingress and egress, and compatibility with other required man-mounted and aircraft systems.

Manpower and Personnel Integration (MANPRINT) program

To emphasize the integration of human considerations into the design and development of HMDs and all other materiel systems, the Army has implemented the MANPRINT program. This program addresses manpower, training and personnel requirements; health and safety issues; and human factors issues. Safety issues are identified through a Systems Safety Assessment (SSA); health hazards are identified through a Health Hazard Assessment (HHA); and human factors issues are identified through an Human Factors Engineering Assessment (HFEA).

Manpower and personnel requirements

It is necessary to identify early on if the HMD system requires unique or unusual human skills or abilities for either operational use or maintenance. Also, in view of the Army's current reduction of manpower assets, it behooves an HMD developer to minimize such restricting requirements. And, as the Army has a philosophy of not excluding personnel from specific assignments due to anthropometric considerations, the HMD helmet dimensions must not exclude any significant portion of the aviator population. Anyone involved in the evolution of HMD systems in the past have found fitting to be a very soft skill that is perishable if not repeated on a semi-routine basis. Knowledge of head and face anthropometry must be gained before proper articulated fitting can be accomplished. Fitting requirements, to include specialized skills and

equipment, must be minimized as the Army has resisted the establishment of a full time military occupational specialty for aviation life support equipment (ALSE) personnel. Under the existing system of an additional skill identifier, ALSE personnel routinely only spend one assignment in ALSE, then return to their primary military occupational specialty to maintain currency for advancement in the ranks. This severely affects fitting skill quality and, invariably, the quality of provided fits.

Maintenance

Because advanced HMDs incorporate potentially fragile optical and electronic components and require that an optical alignment, needed for viewing and targeting, be maintained, they require increased care in their day to day handling (Rash and Martin, 1988). The field environment in which they operate, coupled with their constant daily usage, subject them to normal wear and tear and occasional abuse. The normal field operational environment experience by Army aviators may be much harsher than that of any of the other military services. Keep in mind that all Air Force and Navy/Marine assets operated from fixed sites or airfields during our last conflicts. The U.S. Army aviation units were forward deployed out of desert sites with no fixed base support to allow for general environmental protection of equipment. Today, in the Bosnian operation, Army aviation assets do not enjoy the same fixed base facilities of the sister services. In order to be acceptable to the military aviation community, HMDs must be able to perform their intended functions without being degraded by normal usage. When failure does occur, repairs need to be accomplished at the lowest maintenance level possible. Where feasible, modular replacement as a maintenance approach is critical.

A formal field maintenance program is essential for the fielding of sophisticated HMDs. Developers must identify critical components and alignments which require periodic checks to ensure optimal daily performance.

Due to the lack of dedicated ALSE personnel, maintenance in the field traditionally suffers from a lack of repair and replacement parts during unit deployments. Such items are not placed on the highest priority/minimum essential equipment lists. For IHADSS, repair has been extremely effective through the modular design approach. An excellent example is the modular electronic cans used in the head tracking system. Historically, the helmet has not been a high maintenance concern, but the visionics has.

Training

Technology is a two-edged sword. While supposed to make tasks and equipment designed to aid tasks easier, technology can result in a system which requires extensive training, either in its operation, maintenance, or both. System designers must provide training packages which provide both the users and maintainers with specific instructions in system use. The Army has the responsibility to ensure the use of such packages in aviator training. And, this training should be introduced as early as possible in the basic training program. It is imperative that the understanding and use of HMDs not be left to the aviator on his own (Newman, 1995).

In a look at lessons learned with the IHADSS HMD in the Apache (Newman and Haworth, 1994), it was reported that student aviators typically require approximately 25 hours of training to learn the IHADSS.

A final point relating to training is that sophisticated systems inherently require more careful handling, which can only be achieved through ruggedized designs and aviator training/education.

System safety assessment

Safe and effective operation of the HMD is an important goal. The SSA is intended to identify system and personnel factors which potentially may result in injury or death to the user or maintenance personnel under normal or nonroutine (e.g., alert, emergency, combat, etc.) operating conditions. It serves to establish safety requirements and training recommendations for operational and maintenance personnel. In addition, the SSA documents the occurrence, investigation, and proposed correction of mishaps or possible safety concerns associated with the system. The SSA is conducted using the guidance provided in Army Regulation, AR 385-16, "System safety engineering and management" (1985) and Military Standard, MIL-STD-882B, "System safety program requirements" (1984). During the SSA, all safety related issues should be documented in a Safety Hazard Log, maintained for this purpose.

Every system will pose safety issues. However, the best safety approach is to design safety into the system. Wiener and Nagel (1988) summarize a 4-step approach to minimize safety issues as derived from MIL-STD-882B (1984). These steps are presented in Table 18.

Table 18.
An order of precedence for satisfying system safety concerns.
(Wiener and Nagel, 1988)

Step	Description
Design for minimum risk	Eliminate hazards through selection of alternate designs.
Incorporate safety devices	Include hardware/software failsafe mechanisms which prevent hazard from leading to mishap.
Provide warning devices	Including visible or audible displays when alert user to hazard.
Develop procedures and training	Provide instruction and training to enhance user understanding of potential hazards and possible means of circumvention.

Health hazard assessment

Every system by virtue of its physical and chemical characteristics has the potential of exposing the user or maintainer to hazards. The HHA should be conducted in general accordance with AR 40-10, "Health hazard assessment program in support of the Army acquisition decision process" (1983). The primary process of the HHA is the analysis of the system under evaluation, including subsystems and components, for the purpose of identifying potential health hazards (Leibrecht, 1990). These hazards generally are classed into six major hazard categories: Mechanical forces, chemical substances, biological substances, radiation, electricity, and environmental extremes.

Following identification of potential hazards, an assessment of each hazard should be performed. This assessment may involve testing of the hazard parameter and consequent data analysis to establish the level of the hazard. In some cases, this assessment may be based on historical data acquired through an established history of the use of a specific device or material.

Based on the hazard analyses, recommendations of actions to eliminate, reduce, or control them should be presented. During the early phases of system development, where insufficient data or hardware are available, an Initial Health Hazard Assessment Report (IHHAR) may be prepared.

HMDs introduce several potential hazards by virtue of their mechanical and electrical design. These hazards may be grouped into others associated with the presence of add-on relay optics and of the image sources themselves (e.g., CRTs and FPDs).

Besides the additional head-supported weight and associated torque about the head and neck CM, the presence of the relay optics just millimeters away from the face and eye(s) increases the potential for facial lacerations and ocular injury during mishaps.

The image source, usually helmet-mounted, can introduce electrical, radiation, and chemical hazards. All image sources require electrical voltages which can result in electrical shock. While voltages associated with most FP technology displays are within the range of 20-200 volts, miniature CRTs use operating voltages in the order of 7-10 kilovolts. It is important that the design of wiring harnesses, electronic assemblies, and the display modules themselves minimize the possible exposure to electrical shock during normal operation, maintenance, and mishaps (MacMillan, Brown, and Wiley, 1995). When CRTs are used as the image source, the presence of the high voltage (at the anode) increases the potential of radiated electromagnetic fields. At a minimum, the HMD should meet ANSI C95.1, "Radio frequency protection guide" (1991).

Inadvertent hazardous voltage release due to an emergency (no hands) disconnect, such as a cockpit emergency egress, is an issue that must be addressed in basic design along with the hazards associated with the multiple disconnects for communications and visionics. Single-point disconnects have become the required standard in designing such systems.

User adjustments

On electro-optical HMD devices, both monocular and binocular, there may be mechanical, electronic, and/or optical adjustment mechanisms available for the user to optimize the attributes of the imagery. The mechanical adjustments are used primarily to align the optical axes and exit pupils of the device to the entrance pupils and primary lines of sight of the user. The electronic adjustments may include display brightness, contrast, electronic focus, sizing, sensor sensitivity characteristics (gain and off-set for FLIR), etc. The optical adjustments may include the focus adjustments for the eyepieces and sensor objective lens, and magnification selection for targeting and pilotage sensors.

Mechanical adjustments

Except for some early hand-held HUDs used in helicopter gun ships for rocket and minigun alignment, the fixed HUDs have no mechanical user adjustments except for seat height. For HMD types, the mechanical adjustments may include IPD, fore-aft, vertical, tilt, roll, yaw, etc. The mechanical adjustment components may range from fine-threaded individual adjustments for one axis or plane to friction locks with ball-joints that include all axes and planes. The mechanical range of adjustments have typically been based on the 1th to 99th percentile male user.

Each mechanical misadjustment affects some visual characteristic, but the adjustments are interrelated (King and Morse, 1992; McLean et al., 1997). For example, with the nonpupil forming ANVIS, when the fore-aft adjustment is set exactly at the optimum sighting alignment point (OSAP) which is the maximum viewing distance that provides a full FOV, increasing the fore-aft distance from the eye along the optical axis proportionally decreases the ANVIS FOV

(Kotulak, 1992; McLean, 1995). From the OSAP, misalignment of the IPD will decrease the FOV in the opposite direction of display movement for each ocular, thereby reducing the binocular FOV, but will not reduce the total horizontal FOV.

Misalignment of the IPD of the NVGs has been blamed for disrupting depth perception (Sheehy and Wilkinson, 1989) and inducing vergence errors (Melzer and Moffitt, 1997). However, when the eyepieces are adjusted to infinity, vergence changes do not occur (McLean et al., 1997).

For a pupil forming system, when the pupil is moved forward or aft of the eye box that is formed around the exit pupil location along the optical axis, the FOV will be reduced. If the pupil of the eye is moved laterally from the edge of the eye box, the full FOV of the image will be extinguished within the distance of the width of the eye pupil.

For NVGs, the displacements of the right and left oculars together or relative to each other around the roll, tilt, and yaw axes will not displace the viewed image when focused at infinity, since the sensor and display are physically bound together and located near the eye. The individual FOV will be displaced in the direction of movement, but not the image. However, for HMDs with remote sensors, any relative movement between oculars around the axes will displace the images and change the convergence, divergence, or cyclo-rotation to the eyes. For the monocular HDU of the IHADSS, the mechanical adjustments are fore-aft and roll. The combiner can be moved up and down for eye alignment with the optical axis of the HDU, but most of the alignment is obtained with proper helmet fit to keep the combiner at the lowest position to obtain the maximum eye clearance and FOV. Misalignment of the HDU and IHADSS helmet outside a specific value will not allow a proper boresight with the total system.

Activation, adjustment, or movement of any mechanism on the HMD must be accomplished by the user through tactile identification and activation through the aviator's flight gloves, as well as, the chemical protective over-glove currently used. Removing gloves for adjustments is not a viable option.

Electronic adjustments

On present night vision imaging systems such as ANVIS, there are no user electronic adjustments provided. The tube amplification and automatic brightness control (ABC) level are set at the factory according to specifications. Since the 2nd and 3rd generation intensifier tubes are basically linear amplifiers with a gamma approaching unity (Allen and Hebb, 1997; Kotulak and Morse, 1994a), the imaged contrast should remain constant for changes in light level and between right and left tubes. A field study at a U.S. Army NVG training facility measured the differences in ANVIS luminance output between the right and left tubes for 20 pairs of ANVIS and found 15% of the sample had luminance differences greater than 0.1 log unit (30%) below the ABC level and none had differences greater than 0.1 log unit above the ABC level (McLean, 1997). The recent AN/PVS-14 monocular night vision device for ground troops has a user adjustable gain control, which may be incorporated in future aviation NVG designs.

For HMDs with remote sensors, both the displays in the HMD and sensor usually have user adjustments for optimization of the image. For the monocular HDU with the IHADSS, the pilot can adjust the contrast and brightness of the CRT display with the aid of a grey scale test pattern. The thermal sensors can be optimized by adjusting the gain and bias levels, where the gain refers to the range of temperatures, and the bias the average or midpoint temperature. The sensor can electronically transmit approximately 30 grey levels, where the HDU can only show about 10 grey levels (Rash, Verona, and Crowley, 1990). This means that scenes containing objects with

large temperature differences would either cause loss of details from the saturation of hot objects and/or no contrast for cooler objects from the background. Thermal sensors are used for both pilotage and target detection. The gain and bias adjustments to optimize the contrast between the trees and sky for pilotage are considerably different than the "hot spot" technique used for the copilot/gunner for target detection. Therefore, the user will desire both manual and automatic sensor adjustment options to obtain specific information for a given scene. Thermal sensors also have an option to electronically reverse the contrast (polarity) from either white hot or black hot to either improve target detection or provide a more natural visual scene for pilotage.

Optical adjustments

For NVGs, the user has both eyepiece and objective lenses to adjust for optimum resolution. The objective lens focus is independent of the eyepiece focus and is similar to the focusing of a camera lens. The eyepiece focus adjusts the spherical lens power to compensate for the user's refractive error (hyperopia or myopia) and/or induced accommodation. The standard objective lenses for ANVIS and the AN/PVS-5 NVGs adjust from approximately 10 inches (4.0 diopters) to infinity for the AN/PVS-5s and slightly beyond infinity for the ANVIS. This 4-diopter objective lens adjustment range is obtained with approximately a 1/3 (120-degree) rotational turn of the focusing knob. This means 1 degree of objective lens rotation equates to approximately 0.03 diopter. With the very fast objective lens for ANVIS (f/# 1.2), detectable blur was found with as little as 0.05 diopter of objective lens misfocus (McLean, 1996). The latest fielded I² version (ANVIS-9) incorporates a fine focus objective lens where 2 turns (720 degrees rotation) change the focus from infinity to 1 meter (1 diopter). Objective lens focus with the ANVIS-9 or the Air Force 4949 is both more precise and much more stable during flight.

Eyepiece diopter focus fixed or adjustable? The most controversial subject for night imaging devices has been the eyepiece focus for I² devices and HMDs. Previous literature has suggested that dark focus, instrument myopia, and night myopia could play a significant part in determining the optimum lens power for night vision devices. A study by Kotulak and Morse (1994b) includes an extensive review of this literature. One group of visual scientists (Moffitt, 1991; Task and Gleason, 1993) suggests using fixed focused systems with a diopter value from 0.00 to -1.00 (infinity to 1 meter). Using aviators labeled emmetropic, other researchers have found better visual resolution with user focus adjustable eyepieces than with infinity fixed focused eyepieces (Kotulak and Morse, 1994a; Task and Gleason, 1993). Using the most plus lens power focusing monocular technique, Kotulak and Morse (1994b) reported that 13 aviator subjects had adjusted the eyepiece focus an average of -1.13 diopters (0.63 SD) with a mean difference between right and left eye focus of 0.57 diopters (0.47 SD). Using the same focusing technique with 12 subjects, Task and Gleason (1993) found an average eyepiece setting of -1.05 diopters (0.24 SD) and with a mean difference between right and left eye focus of 0.40 diopter (0.29 SD).

With the HDU monocular system of the IHADSS, Behar et. al (1990) found the average diopter eyepiece setting by 20 Apache pilots was -2.28 diopters, range 0 to -5.25 diopters. The frequently reported symptoms of asthenopia and headaches were attributed to over stimulating accommodation. [This was attributed to the failure of the IHADSS to provide a zero diopter detent or marking on the HDU focus knob.] However, CuQlock-Knopp et al. (1997) found an average diopter setting for a monocular NVG and the biocular AN/PVS-7 for 22 subjects to be 1.47 diopters and -1.54, respectively, with standard deviations of approximately 1 diopter. CuQlock-Knopp et al. (1997) also evaluated the relationship between the value of the eyepiece diopter setting and the reported eyestrain, and found no significant correlations with either the monocular or the biocular NVG.

For the classical HUD that is mounted on the glare shield and used for an aiming device, the crosshair or pipper must be collimated at infinity to retain alignment with small head and eye movements. For the monocular and binocular night imaging devices, the infinity eyepiece focus will result in some nonspectacle wearing users having less than optimum resolution. Several visual scientists (e.g., Task, Gleason, McLean, et al.) believe that some of the so-called emmetropic aviators that do not wear corrective lenses are actually low myopes (-0.25 to -0.75 D) (Kotulak and Morse, 1994b) that will show reduced resolution with decreasing light levels which increase the pupil size and blur circle on the retina. The eyepiece lens power that provides most users with the best resolution with NVGs and HMDs appears to be slightly minus power between approximately -0.25 and -0.75 diopter. To ensure that optimum resolution is obtained by the aviation population of all of the nonspectacle wearing and spectacle wearing personnel using night imaging devices, a small range of adjustment would be desired, and better training in focusing procedures, to include a binocular focusing method to control accommodation with vergence. A problem found with some fixed-focused viewing devices such as the "Cats eyes NVGs" has been the ability of the factory to precisely set the eyepiece focus within a 0.12 diopter tolerance. The zero position on the diopter scale of newly received ANVIS was found to vary by up to 1.25 diopters on 10 sets of NVGs. The military specification for the zero scale tolerance for NVGs is 0.50 diopter, which would result in blurred vision for emmetropic users if the error were on the plus lens power side. With the newer generation of image intensifiers and thermal sensors, the resolution has improved to approximately 20/25 for optimum conditions. Therefore, the focus adjustments for both the objective and eyepiece will be more critical than previous night imaging devices. Therefore, we recommend a small range of user adjustable eyepiece and objective lens focus for the image intensifier systems and for the eyepieces of HMDs.

Anthropometry

Since the head is being used as the basic support for the HMD, it is important to understand its anthropometry. This point was well illustrated in the initial fielding of the IHADSS. The helmet and fitting system were designed to the parameters of the SPH-4 series helmet. The fit of the SPH-4 to the Army aviator population had been proven satisfactorily. This is attributed to the fact that the manufacturer deliberately built a helmet which exceeded the basic sizing requirements. When the IHADSS helmet was built to specifications, the Army test pilots found the helmet to be "tight" to "unacceptable." A quick survey (Sippo, Licina, and Noehl, 1988) of 500 Army attack helicopter aviators revealed head sizes exceeding existing design specifications. These data, coupled with continuing fielding fit problems, led to a follow-on \$1.6 million effort in the design and fielding of an extra-large IHADSS helmet size. Subsequent helmet designs, such as the HGU-56/P, have taken into consideration and accommodated the small evolving female aviator population of the Army as well as the large male population.

Defining head anthropometry requires an understanding of the basic head parameters and how they are measured (Table 19). While not fully defining the head and articulating all measurements that may be required for head-mounted systems, these are the basic design parameters currently used. Additional considerations may include: Bizygomatic breadth (the maximum horizontal breadth of the face (between the zygomatic arches), menton-sellion length (the distance between the top of the nose and the bottom of the chin, necessary for oxygen and protective mask nose cups), eye inset (the distance between the supraorbital notch (eyebrow) and the cornea of the eye, as well as the distance from the most forward point of the zygomatic process (cheekbone) to the cornea), the disparity between eye inset for the two eyes, the disparity between the vertical positions of the two eyes, and the disparity between the vertical and horizontal positions of the two ears. In addition, neck circumference could become an issue when sizing between the large male and small female.

Anthropometric measurement is a difficult skill to develop and maintain. Accuracy and repeatability of measurements are difficult challenges to the trained anthropometrist. Statistically reliable measurements require a complex sampling plan, including measurement methodologies, instrumentation, personnel qualification and currency, and measurement validation. Recent advances in 3-D anthropometric imaging/mapping techniques show great promise for future assessments (Brunsmann, Daanen, and Files, 1996; Whitestone, 1994). However, current limitations include mapping bony landmarks, hair, and tissue compression as a function of planned fit.

The Army standard for head anthropometry is the 1988 Anthropometric survey of U.S. Army personnel: Pilot summary statistics (Donelson and Gordon, 1991). The survey represents the most recent analysis of the combined U.S. Army and Army aviator populations, both male and female. However, the 500 attack pilot head anthropometry survey (Sippo, Licina, and Noehl, 1988) revealed a head size disparity within the male attack helicopter subpopulation. This disparity is that Army attack aviators tend to have larger head dimensions than the general aviator population. Requirements for additional (under the helmet) equipment (e.g., protective masks and hoods) add a delta to the required head sizing considerations. With these deltas, the largest helmet size should fit a head length dimension of 8.75 inches (22.25 cm), a head breadth dimension of 6.90 inches (17.53 cm), and a head trignon-vertex height dimension (the distance from the trignon to the top of the head with the head in the Frankfurt plane) of 6.15 inches (15.62 cm) (Rash et al., 1996b). However, these ranges do not address nonaviator maintainers (e.g. general Army or civilian populations).

Table 19.
Head anthropometry parameters.

Measurement parameter	Measurement definition (Donelson and Gordon, 1991)
Head breadth	The maximum horizontal breadth upon the attachment of the ears, measured with spreading caliper.
Head circumference	The maximum circumference of the head above the attachment of the ears to the head, measured with a tape passing just above the ridges of the eyebrows and around the back of the head.
Head length	The distance from the glabella landmark between the two browridges to the most posterior point on the back of the head, measured with a spreading caliper.
Interpupillary breadth	The distance between the two pupils, measured with a pupillometer.
Bitrignon coronal arc	The surface distance between the right and left trignon landmarks across the top of the head, measured with a tape. The head is in the Frankfurt plane.

Although not initially included as a requirement for the RAH-66 Comanche HIDSS design, by congressional mandate, all future systems must accommodate an anthropometric range of a minimum of the 5th percentile female. This requirement has since been addressed by the Comanche program.

Fitting

The success or failure of any HMD system is reliant upon an articulated and repeatable fit. Historically, helmet fit has been a function of comfort and maintenance of designed protection through the retention system. As use evolved, placement of communication systems required increased stability and a general repeatability of fit. With the advent of visionics, stability and an articulated fit were required to maintain an acceptable exit pupil for optimized FOV. The process of helmet fitting began with tightening a chinstrap on a "one size fits all" helmet to the present, where we are able to independently adjust chinstraps, nape straps, earcups, microphones, visors, and display optics (monocular or biocular).

As each new capability (e.g., communications, visionics, etc) has been added, stability has become an increasing priority. Not only is stability a function of the retention system and head interface, but it is subject to degradation through outside factors such as stiffness of electronic cabling connecting the helmet to the aircraft and/or aircraft vibration as it relates to the mass and inertia of the headborne system. The resultant comfort of the above integrated systems can not be taken for granted. A recent example is the discomfort caused by the chinstrap of the IHADSS helmet. Although a design acceptable from a crashworthiness, stability, and valid engineering standpoint, interference with the motion of the aviator's laryngea (Adam's apple) during swallowing necessitated a complete redesign of chinstrap placement within the retention system prior to final acceptable fielding..

Directly related to stability is adjustment and sizing. The addition of the female population has demanded an expansion in size accommodation requirements. Numerous studies articulate the extreme difficulty in correlating the independent variables of head anthropometry for purposes of helmet design and sizing. Percentile intervals can describe the limits of fit only through multidimensional distributions. Sippo and Belyavin (1991) sufficiently described a method of this process based upon generalized distances from the means to define the population to be covered. Their model included fitting schema in 8, 9, 15, and 27 sizes. The 9-sized scheme provided a 93.9% acceptable fit, while the 15-sized scheme only increased the acceptable fit to 97.6%. The IHADSS helmet is fielded in three sizes (medium, large, and extra-large). The IHADSS does not accommodate the small female, and even for the male population requires custom fitting, taking 2 hours for an initial fit with subsequent fittings the norm. The HGU-56/P, the current primary candidate for Comanche, has 4 shell sizes (S, M, L, and XL) with 6 impact liner sizes. This system is designed and has been fielded as a system requiring minimal fitting skill and time.

Support equipment required for the basic helmet fitting processes can include screwdrivers, Velcro™ attachments, and/or special tools to remove interior liners, communication assemblies, etc. Visionic alignment and validation can expand the list of support equipment to in excess of \$30,000 (in the case of the early IHADSS fitting kits).

The Army's first experience with custom fitting HMDs was with the IHADSS and resulted in a number of lessons learned (Rash et al.,1987). First was the difficulty in overcoming the Army's decision not to identify specialized personnel to serve as dedicated fitters due to personnel constraints. Second was the reluctance to invest in the specialized visionics support alignment and validation equipment initially recommended by the manufacturer. A scaled down equipment

kit was purchased and found to be inadequate. Third was programming the needed time within the compressed class schedule for the fitting and alignment process prior to first flight. Fourth was the initial resistance to expending resources on a specialized padded helmet bag, which provided greater protection for the delicate relay optics during storage and use in the field. Fifth was the extent of modularity/breakdown of subassemblies for the purpose of reducing replacement costs. For example, in IHADSS, one of the most common items for replacement was visors. However, visor replacement required replacement of the entire visor assembly including the visor housing, visor cover, and visor track and spring assembly. [Note: This issue has been resolved by a parts breakdown and individual component procurement.]

While quality of fit is subjective by nature, Stiffler and Wiley (1992) have attempted to loosely quantify fit using a “fit equation” which addresses three areas of fit: comfort, optical adjustment, and stability. The equation is expressed as:

$$\text{FIT} = (\text{comfort}) + (\text{optical adjustment}) + (\text{stability}) \quad \text{Equation 29}$$

Comfort is a critical factor because discomfort, which can manifest itself as areas of increased pressure or “hot spots,” can result in headaches or general discomfort which distracts, degrading performance. The optical adjustment factor represents the ability of the wearer to adjust the optics to achieve full FOV. The last factor, stability, addresses the ability to maintain the exit pupil(s). A displacement of the exit pupil(s), with the accompanying reduced FOV, due to helmet slippage or transmitted vibration reduces mission effectiveness. However, a deficiency of the model is the failure to provide any numerical values for these factors.

Egress

In general, normal ingress and egress from the aircraft cabin is becoming more of a challenge as we further encumber the aircrew and shrink the entry access, as through the canopy doors of the AH-1 Cobra, AH-64 Apache, and RAH-66 Comanche. Aviators first started doffing equipment, e.g., NVGs on the SPH-4, to avoid inadvertent release and damage during entry and exit. AH-64 aviators rarely enter or exit the cockpit wearing the IHADSS helmet, primarily to prevent damage to the head tracking photosensors mounted on the helmet. Once inside and secured, the helmet communication assembly and video cables are plugged in, and the HDU can be attached; upon exit, the HDU must be first removed. In the event of emergency egress, the three attached cables are each provisioned with a hands-free release. If mission scenarios dictate, the M-43 protective mask and blower assembly also possess a separate hands-free release capability. The RAH-66 Comanche program is engineering a single-point release of all head attached cables for emergency egress.

Equipment compatibility

All HMD designs must be physically and functionally compatible with all existing aviation life support and mission equipment. Examples include corrective/protective eyewear, protective masks, oxygen masks, shoulder harnesses, survival vests and flotation equipment and components, body armor, aircraft seat armor, and cabin interior structures and systems. Figure 69 shows a frontal view of an Apache aviator wearing a full ALSE ensemble with M-43 mask. Figure 70 shows the potential for interior aircraft compatibility by, depicting an aviator in the Apache front seat with the IHADSS HDU attached. Potential compatibility problem areas with the Comanche HIDSS were found with body and seat armor, shoulder harness and buckles, and survival vest and flotation equipment due to the low mounting of the miniature CRTs.



Figure 69. A frontal view of an Apache aviator wearing a full ALSE ensemble with M-43 mask



Figure 70. An aviator in the Apache front seat with the IHADSS HDU attached.

In the past, attempts have been made to integrate and achieve compatibility with protective masks and visual correction/protection. With often different manufacturers for each component, this has been a formidable task. A fairly recent example of the integration process is the IHADSS helmet. The helmet was intended to be fitted while wearing the M-43-A1 protective mask (designation changed to M-49 after 1996). When the mask was not being worn, a custom skull cap was to have been used to replicate the thickness and bulk of the protective mask. However, Apache aviators are not using the skull caps, so the helmet doesn't fit properly when the M-43 (M-49) mask is needed. The mask itself was designed to minimize the adverse effects with the HMD.

The small bubble lenses of the M-43 mask were designed to fit very close to the eyes to minimize eye clearances with the HMD. However, since many IHADSS users can not obtain a full FOV even without the mask, the addition of the mask further increases the distance between the HDU and the eye, reducing the FOV. The close fitting eye lenses can fog within a minute unless sufficient air is artificially circulated within the mask. The over pressure and additional air is provided by a battery powered blower when outside the aircraft and by aircraft power when inside the aircraft. The batteries are lithium with no readily available commercial equivalent, and have a duration of approximately 8 hours with use.

To provide lens correction for distant vision, contact lenses are used for Apache aviators since any corrective lens outsert would increase the eye clearance and further reduce compatibility with the HDU. For presbyopic Apache pilots, the bifocal contact lenses have not been approved. Also, fitting one contact for near and the other for far vision has also not been approved for Army aviation. The use of contact lenses by other than Apache pilots has not been approved due to the lack of adequate logistics and visual support (optometrists and ophthalmologists) to fit the lenses and to follow-up with periodic examinations.

Under certain conditions, NVGs provide information the FLIR cannot. Using only the FLIR, Apache pilots have difficulty in detecting other aircraft at night with covert lighting that is only visible to NVGs. Also, under any moon illumination, the ANVIS resolution is greater than the first generation FLIR. Therefore, the gunner co-pilots (front seat) were authorized to use ANVIS. The IHADSS visor would not support the ANVIS mounting bracket, so a custom visor bracket kit was developed to mount the standard ANVIS SPH-4 visor assembly on the IHADSS helmet. The available mounting points on the IHADSS helmet for the ANVIS visor produces a downward tilt of the ANVIS such that the pilots have to constantly tilt their head backwards for straight ahead viewing with the ANVIS even with the ANVIS tilt adjustment in the maximum up position. The guidance for the use of ANVIS in the AH-64 is to mount either the ANVIS or the HDU on the helmet, but not both. However, many of the Apache aviators mount both, which increases the head supported weight to > 6.5 lbs.

The Apache helicopter uses a near infrared laser range finder and designator that is not eye safe. To initially protect the Apache crewmembers, laser protective spectacles, plano or with correction with KG-3 glass were fielded. The KG-3 glass appears slightly grey tinted and with 3-mm thickness provides approximately 80% visual transmittance with > 4.0 optical density (O.D.). To interface with the HDU, the right lens of the standard aviator frames was reduced in size and reshaped. To further reduce the effect on the FOV of the HDU, the right lens of this modified spectacle was typically increased in pantoscopic tilt (i.e., pitched down). At the same time, a development program was initiated to produce visors with laser protection to replace the spectacles. Unfortunately, the only suitable technology was dye or absorptive materials which may affect the ballistic protection of polycarbonate, and significantly reduces visual transmittance and induces color properties. Because of the proliferation of ruby lasers for range finders and designators by the former communist block, the laser protective spectacles and visors included dyes to absorb red wavelengths. The visible transmittance was further reduced to less than 40%

with a green tint. With the possibility of using laser wavelengths that match the sensitivity wavelengths of the eye, the absorptive dye technology for laser protection produces visible transmittance that are both unacceptable to the aviator for night flight and block the wavelengths emitted from the instrument panel, head down displays and aircraft position lights.

Limited ballistic protection for the eyes has been available with the initial fielding of the SPH-4 aviator helmet with the polycarbonate visors in 1970. The visors will not stop bullets, but will reduce the injuries from spall and flash fires. At present, no other clear optical material provides the degree of ballistic protection for a given thickness as polycarbonate. Therefore, we anticipate that polycarbonate visors will be used for future HMD systems.

USAARL evaluated a nuclear flash blindness protective device with the initial development of the HGU-56/P helmet program in the early 1980's. A certain material of lead, lanthanum, zirconate, and titante (PLZT) could be electronically switched rapidly in polarity, such that when sandwiched with a near infrared blocking material and a fixed polarizing material, the visual transmittance could be varied from full open state (approximately 20%) to a full off (OD >3.0) in approximately 150 microseconds (McLean & Rash, 1985). The original PLZT goggles were developed for nuclear bombers such as the B-52 and B-1 in the Strategic Air Command (SAC), where the crewmembers would hopefully be just outside the blast, radiation, and/or heat damage radii of the weapon. Tactical fighters could also deliver smaller nuclear weapons, but the evaluation of the PLZT goggles for the fighter aircraft was not favorable, due to the weight and visual transmittance (Templin, 1978). Also, the tactical fighters would probably have delivered the weapons in the daytime during this era and the effects of temporary flash blindness in the daytime would be minimal for the smaller nuclear weapons.

USAARL also found that the PLZT electronics, which detected a certain increase in ambient luminance in approximately 4 microseconds, could be accidentally activated by the rotor blades and when near a radar station. The designers of the PLZT goggle had found that the material could be discharged quicker than when charged to change the transmittance. Unfortunately, in order to obtain the desired switching speed, this meant that when the nuclear flash protective goggle failed, it was basically opaque. Other materials such as liquid crystals have also been evaluated for an electronic shutter and variable visual attenuator, but switching speed and minimum transmittance values have been of concern. With the electronics in the lens materials, it was questionable how the lenses or the electronic drive circuitry could be shielded from the effects of electromagnetic pulse (EMP) from a nuclear explosion. However, the real problem with the nuclear flash blindness protective device requirement is the concept for helicopter operations. Unless the nuclear device was delivered by the helicopter on an enemy not having a nuclear capability, the visual trade-off, even if the device worked, would not be logical. One of the most dangerous places a pilot could be during a nuclear attack would be in a helicopter near the ground. In the European scenario with a tactical nuclear war with the former Warsaw pact, the very basic unclassified war game models showed that the only helicopters that could survive were the ones hidden in bunkers. Therefore, we do not recommend the need for a nuclear flash blindness protective device for Air Warrior or Army aviation with the known technology.

Test and evaluation

Inherent to any design program is the need to test and evaluate operational performance. Such testing should begin during the easiest phases of development. The end goal should be that of the system being fully qualified at first flight. Unfortunately, in many past programs, waivers were requested for performance failures which were identified and known for some time. Despite the

belief of program managers, the easiest, most cost-effective time to solve a problem is when it is first discovered.

At the very least, testing and evaluation should be a required action at all major program milestones. Detailed test plans should be predeveloped but be flexible enough to accommodate the recognized complexity of HMD systems. It is not to be expected that one grand HMD test and evaluation plan will serve for all HMD designs. However, there are some basic testing tenets and systems parameters which should be considered, if not required, for a thorough testing plan.

As applicable, testing should consist of a bench (laboratory) phase and a field phase. Also, as applicable, testing should be at the subsystem, as well, as the system level. For the Army aviation HMD design, the basic subsystems are: image source, display optics, helmet, and tracker.

Laboratory

Testing for most, if not all, subsystems can be performed in a laboratory environment. Such testing allows for controlled conditions and produces the most repeatable data. For image source evaluation, CRT techniques are well established and can be found in a number of sources (Verona, 1992; Anstey and Dore, 1980; Verona et al., 1979; Task and Verona, 1976). Quast and Marticello (1996) have developed a test and evaluation plan for flat panel displays intended for military applications. This plan emphasizes the need for continuous testing, identifies test categories (Table 20), and suggests appropriate test equipment and facilities.

Table 20.
Recommended FPD image source evaluation program.
(Quast and Maricello, 1996)

Test category	Test issues
Photometric, radiometric, colorimetric	Luminance, contrast, uniformity, viewing angle performance, reflectance, transmittance, color gamut, response, dimming range
Environmental	Temperature, vibration, shock, chemical exposure, water/salt exposure
Qualitative	Readability, legibility, image quality
Mechanical, physical, and electrical	Weight, CG, volume, power consumption, efficiency, heat generation

Rash et al. (1996a) present an extensive assessment methodology for testing rotary-wing HMDs. It provides recommended test parameters (at system and subsystem level), equipment, techniques, and criteria. A summary of recommended tests are provided in Table 21.

In-flight

Laboratory evaluations, no matter how thorough, can not fully assess the performance of an HMD system. An in-flight evaluation is required to assess performance under actual operating conditions. As in the laboratory evaluation, tests should include operational parameters, potential

Table 21.
Recommended integrated HMD test parameters.
(Adapted from Rash et al., 1996a)

Optical/Visual	Biodynamic	Acoustical
<u>System</u> Visual field Spectral transmittance Physical eye relief Interpupillary distance range Luminous transmittance Chromaticity Neutrality Prismatic deviation Refractive power Cockpit display emission transmittance <u>Display</u> Field-of-view Image overlap Resolution (visual acuity) Extraneous reflections Luminance range Grey levels Chromatic aberration Contrast ratio Exit pupil size Focus range Spherical/astigmatic aberration Image rotation Image luminance disparity Vertical/horizontal alignment Distortion Luminance uniformity Static/dynamic uniformity	<u>System</u> Mass properties Impact attenuation Stability Dynamic retention Anthropometric fit/comfort Ballistic protection HMD breakaway force <u>Protective helmet</u> Shell tear resistance Chin strap assembly integrity <u>Head tracker/aiming system</u> Motion box size Update rate Jitter Pointing angle accuracy Pointing angle resolution	<u>System</u> Real-ear attenuation Physical-ear attenuation Speech intelligibility <u>Earphone/earcup</u> Sensitivity Distortion Frequency response

health hazards, safety issues, and human factors concerns. A comprehensive in-flight assessment plan, developed specifically for HMDs by the U.S. Army Aviation Technical Test Center, Fort Rucker, Alabama, is provided in USAARL Report No. 96-1, "Assessment methodology for integrated helmet and display systems in rotary-wing aircraft" (Rash et al., 1996).

Comprehensive testing should look at reliability, logistic supportability as well as an HHA and SSA, which addresses the identification of potential health hazards and safety concerns. In addition, HFE problems should be noted, thereby emphasizing the integration of human performance and system performance.

Reliability testing provides the opportunity to identify subsystems or components which exhibit a short mean time between failure (MTBF). The frequency of failure of specific items allows early estimation of logistical support requirements. During the SSA, all safety related incidents should be documented in a Safety Hazard Log, maintained for this purpose. During the HHA, present or potential hazards should be identified, along with proposed corrective actions.

Perhaps the most important result which can be obtained from the in-flight testing and evaluation is achieved by means of the HFEA, which identifies issues which may impact the user's ability to perform the designed mission while wearing the HMD system. Issues include generalized and specific parameters relating to controls, connectors, cables, fit, comfort, anthropometry, etc. The U.S. Army Aviation Technical Test Center includes in its in-flight HFEA the areas presented in Table 22 (Rash et al., 1996a):

Table 22.
Recommended in-flight HFEA areas.
(Rash et al., 1996a)

Helmet fit, comfort, range of adjustment, and fit retention for the anthropometric range of aviators
Donning and doffing procedures
Boresight requirements/retention
Sensor image quality
Symbology
Field-of view
Sensor/pilot offset and sensor slew rate
Sensor image quality during day, night, and adverse weather operations
Integration with the target acquisition system
Integration with the aircraft navigation system
Integration with the aircraft survivability equipment
Compatibility with life support systems
Compatibility with nuclear, biological, and chemical equipment
Compatibility with AN/AVS-6 night vision goggles
Registration/magnification

Summary and recommendations

The HMD concept seems to be entrenched in military aviation. Every military aircraft, current and future, does or is striving to incorporate an HMD system in their approach to information display (Bull, 1990). This is especially true in Army aviation. ANVIS and IHADSS are the currently fielded Army HMD systems. The Army's next helicopter, the RAH-66 Comanche, incorporates a binocular, wide FOV HMD, the HIDSS.

Aircraft are representative of the most complex systems built by man (Newman and Greeley, 1997). The presence and use of HMDs in the cockpit adds further to this complexity, with add-on systems being worse contributors than integrated systems. This continued introduction of technology has the potential to create human factors problems, which include workload and sensory overload. This paper has attempted to provide a broad overview of physical and human performance issues which must be addressed during the design of HMD systems. Areas which have been addressed include the physical parameters of optics, acoustics, and biodynamics; the human performance parameters of vision, hearing, and survival, and basic HFE issues.

While it is not feasible to design a “one design fits all” HMD based on the myriad of issues discussed in this report, it is possible to provide some global recommendations. In general, these recommendations for the next generation HMD support optimizing and integrating known or near-term technologies over the pursuit of “futuristic” technologies. The following is a list of the recommendations for basic HMD components:

Helmet - HGU-56/P with improved sectional TPL liner for better NBC compatibility. Other possible improvements are a quick release chinstrap without reducing helmet retention, communications earphones (CEPS) with smaller and/or lighter microphones and ear cups.

HMD - binocular/biocular with monocular operation capability. Unless alignment tolerances can be well controlled, two-eyed designs may be found to be untenable under certain conditions (especially those aggravated by stress and fatigue). In such cases, monocular operation must be available. The selection of an optical design is best made on the basis of mission objectives. In general, optical design performance parameters are not independent. Therefore, the question of which parameter(s) to optimize should be based on intended use.

Visors - dual visor configuration. The ability to attenuate all potentially eye damaging laser wavelengths and still allow any useable see-through vision has not been achieved to date. It is recommended that the basic laser visor configuration attenuate only wavelengths the U.S. and its allies use for designators and range finders. Research and development should continue to pursue improved laser protective systems, but should only be fielded if there are no adverse effects with normal vision. A requirement for nuclear flash protection is not conceptually sound or technologically possible without adversely affecting see-through vision or compatibility with HMDs and NBC equipment.

Night imaging system - I² and FLIR combination. For the head-borne component, the direct view with no see-through vision night vision I² technology such as the advanced ANVIS provides the best resolution and FOV under most conditions compared to any potential infrared sensor and helmet mounted display system. The prototype panoramic I² system with 100° horizontal FOV may provide an approach for Army application, but with a smaller FOV and more eye relief. FLIR imagery can also be valuable for both flight and target detection. However, it is recommended that the FLIR imagery only be provided in a head down display, with selectable flight path following mode. The FLIR should also be coupled with automatic target detection software to provide potential target locations using symbols.

Targeting system - Magnified optics. The one to one magnification used for day or night imagery with the unaided eye, NVGs, or PNVs from aircraft is not sufficient for target detection and survivability with modern warfare. Image magnification with visible, near infrared and far infrared spectrum, radar warnings, and/or data linked information is required to remain outside the effective lethal range of even unsophisticated anti-aircraft weapons for helicopters. If the information is data linked, symbology could be used to provide information for both target engagement or avoidance. The FLIR has proven very successful in aiding target detection, but with magnification using a head-down or direct view optical system such as the Targeting Sight Unit (TSU) in the Apache or its equivalent in the M1 tank. FLIR on a head-down display with several magnification settings that can be positioned in the fixed forward, flight path following, and steerable modes can also be helpful for flight and navigation.

NBC protective mask - Stand alone protective system. The Joint Service General Purpose Mask (JSGPM) should be available in the near- to mid-term time frame. The JSGPM should replace the M49 and M45 masks. The concept of the integrated NBC mask with the helmet was tried in the HGU-56/P aviator helmet program and found to be unacceptable. The protective

mask should not require blown air (batteries and aircraft power) for protection. Protection is needed by the aviator both inside and outside the aircraft, with and without the helmet. An integrated system would require the user to wear the helmet at all times. Although, the aviator would like to eliminate the NBC hood inside the helmet to improve comfort and compatibility, no other alternative has been shown to provide an acceptable level of protection.

Acoustics - CEP. The CEP performs as well as, or better than, any other system and does not involve modification of the aircraft. If a new airframe is being developed, then ANR techniques should be incorporated. If the performance and utility of the 3D-audio concept continues to be validated by ongoing research, then it is recommended that it be implemented.

In conclusion, the design of an HMD system is a formidable task involving the need to balance requirements for head, hearing, and eye protection; and visual and acoustical performance. In addition, sound HFE practices must be followed, and a concerted effort must be made to minimize health hazards and safety concerns.

References

- Adam, E. C. 1995. Head-Up Displays versus Helmet-Mounted Displays—The Issues. Helmet- and Head-Mounted Displays and Symbology Design Requirements II, Proceedings of SPIE, Vol. 2465, pp. 175-183.
- Alam, M. S., Zheng, S. H., Iftekharuddin, K. M., and Karim, M. A. 1992. Study of field-of-view overlap for night vision applications. Proceedings of the IEEE National Aerospace and Electronics Conference, NEACON, Vol. 3, pp. 1249-1255.
- Allen, P. C., Barnes, A. D., Davidson, C., Gibb, I. G., Goddard, R. W., and Trimble, F. R. 1995. High performance backlights: A new approach. Cockpit Displays II, Proceedings of SPIE, Vol. 2462, pp. 309-313.
- Allen, J. H., and Hebb, R. C. 1997. Determining the gamma of a night vision device. Orlando, FL: Naval Air Warfare Center. Report No. NAWCTSD-TR-95-003.
- Allen, J. H., and Hebb, R. C. 1983. Helmet mounted display feasibility model. Orlando, FL: Naval Training Equipment Center. NAVTRAE-QUIPEN IH-338.
- Altadonna, L. 1996. LCD backlight manufacturing development program. Cockpit Displays III, Proceedings of SPIE, Vol. 2734, pp. 283-292.
- American National Standards Institute. 1984. Method for the measurement of the real-ear attenuation of hearing protectors. ANSI 12.6-1984.
- American National Standards Institute. 1989. Method for measuring the intelligibility of speech over communications systems. ANSI S3.2-1989
- American National Standards Institute. 1995. Microphone-in- real-ear and acoustic test fixture methods for the measurement of insertion loss of circumaural hearing protection devices. ANSI 12.42-1995.
- American National Standards Institute. 1991. RF protection guide. ANSI C95.1-1991.
- Anstey, G., and Dore, M. J. 1980. Automatic measurement of cathode ray tube MTFs. Royal Signals and Radar Establishment.
- Arbak, C. J. 1989. Utility evaluation of a helmet-mounted display and sight. Helmet-Mounted Displays, Proceedings of SPIE, Vol. 1116, pp. 138-148.
- Armbrust, J., Ros, N., Hale, S., and Rabin, J. 1993. Final report, developmental test (DT) of the Night Vision Pilotage System. Fort Rucker, AL: U.S. Army Aviation Technical Test Center. TECOM Project No. 4-AI-100-RAH-008.
- Armstrong Aerospace Medical Research Laboratory. 1989. Subjective Workload Assessment Technique (SWAT): A user's guide. Dayton, OH: Armstrong Aerospace Medical Research Laboratory. AAMRL-TR-89-023.
- Bachman, W. G. 1988. Extended-wear soft and rigid contact lenses: Operational evaluation among Army aviators. Fort Rucker, AL: U.S. Army Aeromedical Research Laboratory. USAARL Report No. 88-17.

- Barnes, G. R., and Sommerville, G. P. 1978. Visual target acquisition and tracking performance using a helmet-mounted sight. Aviation, Space, and Environmental Medicine, Vol. 49, pp.565-572.
- Baron, P. C. 1994. Display Systems. Proceedings of SID, Vol. II, pp. F-5/1-69.
- Barrette, R. E. 1992. Wide-field-of-view full-color high-resolution helmet-mounted display. Proceedings of SID, Vol. XXIII, pp. 69-72.
- Barson, J. V., Pritts, D. P., and Lanoue, B. A. 1988. TPL...Installation, fitting, and maintenance for the SPH-4 helmet. Fort Rucker, AL: U.S. Army Aeromedical Research Laboratory. USAARL Report No. 88-18.
- Barten, P. G. J. 1993. Effects of quantization and pixel structure on the image quality of color matrix displays. Journal of SID, Vol. 1, No. 2, pp. 147-153.
- Barten, P. G. J. 1991. Resolution of liquid-crystal displays. Proceedings of SID, Vol. XXII, pp. 772-775.
- Beasley, J. H., Martin, J. S., Klymenko, V., Harding, T. H., Verona, R. W., and Rash, C. E. 1995. A characterization of low luminance static and dynamic modulation transfer function curves for P-1, P-43, and P-53 phosphors. Fort Rucker, AL: U.S. Army Aeromedical Research Laboratory. USAARL Report No. 95-29.
- Beaton, R. J. 1988. Linear systems metrics of image quality for flat-panel displays. Image Processing, Analysis, Measurement, and Quality, Proceedings of SPIE, Vol. 901, pp. 144-151.
- Behar, I., Wiley, R.W., Levine, R. R., Rash, C. E., Walsh, D. J., and Cornum, R. L. S. 1990. Visual survey of Apache aviators (VISAA). Fort Rucker, AL: U.S. Army Aeromedical Research Laboratory. USAARL Report No. 90-15.
- Belt, R. A., Knowles, G. R., Lange, E. H., and Pilney, B. J. 1997. Miniature flat panels in rotary-wing head mounted displays. Head-Mounted Displays II, Proceedings of SPIE, Vol. 3058, pp. 125-136.
- Bennett, C. T., and Hart, S. G. 1987. PNVS related visual problems: Pilot's reflections on visually coupled systems, 1976-1987. Working paper. Moffett Field, CA: NASA-Ames Research Center.
- Benson, A. J. 1978. Spatial disorientation: general aspects. Aviation medicine. London: Tri-Med Books.
- Bernard, E. 1996. Novel LED backlights for small-aperture LCDs. Information Display, Vol. 12, No. 3, pp. 16-18.
- Berry, J., Dyer, R., Park, R., Sellers, A., and Talton, M. 1984. PNVS Handbook. Fort Rucker, AL: U.S. Army Training and Doctrine Command.
- Biberman, L. M., and Alluisi, E. A. 1992. Pilot errors involving head-up displays (HUDs), helmet-mounted displays (HMDs). Alexandria, VA: Institute for Defense Analysis. IDA Paper P-2638.

- Biberman, L. M., and Tsou, B. 1991. Image display technology and problems with emphasis on airborne systems. Alexandria, VA: Institute for Defense Analysis. IDA Paper P-2448.
- Biocca, F. 1992. Will simulation sickness slow down the diffusion of virtual environment technology? Presence, Vol. 1, pp. 334-343.
- Bitzakidis, S. 1994. Improvements in the moving-image quality of AMLCDs. Journal of SID, Vol. 2, No. 3, pp. 149-154.
- Blackwell, H. R. 1946. Contrast thresholds of the human eye. Journal of the Optical Society of America, Vol. 36, p. 624-643.
- Blackwell, O. M., and Blackwell, H. R. 1971. Visual performance data for 156 normal observers of various ages. Journal of the Illuminating Engineering Society (IES) of North America, October, p. 3-13.
- Boettcher, K., Schmidt, D., and Case, L. 1988. Display system dynamics requirements for flying qualities. Wright-Patterson AFB, OH: Wright Aeronautical Laboratory. AFWAL Report No. TR-88-3017.
- Boff, K. R., and Lincoln, J. E. 1988. Vibration characteristics of rotary-wing aircraft. Engineering Data Compendium: Human Perception and Performance. Wright-Patterson Air Force Base, OH: Armstrong Aerospace Medical Research Laboratory. pp.2072-2136.
- Bohannon, W. K. 1997. Scanning laser projectors. Information Display, Vol. 13, No. 8, pp. 32-36.
- Bohm, H. D. V. and Schrammer, R. 1990. Requirements of an HMS/D for a Night-Flying Helicopter. Helmet-Mounted Displays II, Proceedings of SPIE, Vol. 1290, pp. 93-107.
- Bohling, J. H., and Rash, C. E. 1991. Optical evaluation report: AH-64 triple-notch laser protective visors (LPV), preproduction samples. Fort Rucker, AL: U.S. Army Aeromedical Research Laboratory. USAARL LR 91-7-2-7.
- Braithwaite, M., Groh, S., and Alvarez, E. 1997. Spatial disorientation in U.S. Army helicopter accidents: An update of the 1987-92 survey to include 1993-1995. Fort Rucker, AL: U.S. Army Aeromedical Research Laboratory. USAARL Report No. 97-13.
- Brickner, M. S. 1989. Helicopter flights with night-vision goggles - Human factors aspects. Moffett Field, CA: Ames Research Center. NASA Technical Memorandum 101039.
- Brindle, J. H. 1996. Advanced helmet tracking technology: Developments for Naval aviation. Head-Mounted Displays, Proceedings of SPIE, Vol. 2735, pp. 27-38.
- Brindle, J. H., Marano-Goyco, J., and Tihansky, P. M. 1995. Helmet-mounted sight display system (HMD/DS) technology development status/vision. Warminster, PA: Naval Air Warfare Center.
- Brunsmann, M., Daanen, H., and Files, P. 1996. Earthquake in anthropometry: The view from the epicenter. CSERIAC Gateway, Vol. VII, No. 2, pp. 1-6.

- Buchroeder, R. A. 1987. Helmet-mounted displays, Tutorial Short Course Notes T2. SPIE Technical Symposium Southeast on Optics, Electro-optics, and Sensors, Orlando, FL.
- Bull, G. C. 1990. Helmet Display Options - A Routemap. Helmet-Mounted Displays II, Proceedings of SPIE, Vol. 1290, pp. 81-92.
- Butler, B. P. 1992. Helmeted-head and neck dynamics under whole-body vibration. Ph.D. Dissertation, University of Michigan, Ann Arbor, MI.
- Butler, B. P., Maday, R. E., and Blanchard, D. M. 1987. Effects of helmet weight and center-of-gravity parameters on head tracking performance in a vibration environment. Fort Rucker, AL: U.S. Army Aeromedical Research Laboratory. USAARL LR-97-12-4-5.
- Caldwell, J. L., Cornum, R. L. S., Stephens, R. L., and Rash, C. E. 1991. Visual processing: Implications for helmet mounted displays. Helmet-Mounted Displays II, Proceedings of SPIE, Vol. 1290, pp. 165-172.
- Calves, J. P., and Brun, J. 1978. Colour and brightness requirements for cockpit displays: Proposal to evaluate their characteristics. Presented at the 29th AGARD Avionics Meeting, Paris.
- Cameron, A. A. 1997. VISTA/NF-16D Programmable Helmet Mounted Display System. Head-Mounted Displays, Proceedings of SPIE, Vol. 3058, p. 339-350.
- Cameron, A. A and Steward, D.G. 1994. The Viper HMD - from design concept to flight test. Helmet- and Head-Mounted Displays and Symbology Design Requirements, Proceedings of SPIE, Vol. 2218, p. 137-148.
- Cameron, A. A., Trythall, S., and Barton, A. M. 1995. Helmet trackers - The future. Helmet- and Head-Mounted Displays and Symbology Design Requirements II, Proceedings of SPIE, Vol. 2465, p. 281-295.
- Campbell, F. W., and Green, D. G. 1965. Monocular versus binocular visual acuity. Nature, Vol. 208, pp. 191-192.
- Castellano, J. A. 1992. Handbook of display technology. San Diego: Academic Press, Inc.
- Cathey, D. A. 1995. Field emission displays. Information Display, Vol. 11, No. 10, pp. 16-20.
- Charman, W. N. and Olin A. 1965. Tutorial: image quality criteria for aerial camera systems. Photographic Science and Engineering, 9:385-397.
- Cheng, R., Yang, K. H., Levine, R. S., King, A. I., and Morgan, R. 1982. Injuries to the cervical spine caused by a distributed frontal load to the chest. Proceedings of the 26th Stapp car crash conference. Warrendale, PA: Society of Automotive Engineers. SAE paper No. 821155. October. pp. 1-40.
- Clark, M. G. 1992. Flat panel displays. Color in electronic displays. Widdel, H., and Post, D. L. New York: Plenum Press. p. 257-277.
- Clarke, T. D., Smedley, D. C., Muzzy, W. H., Gragg, C. D., Schmidt, R. E., and Trout, E. M. 1972. Impact tolerance and resulting injury patterns in the baboon: Air Force shoulder harness-

- lap belt restraint. Proceedings of the 16th Stapp car crash conference. Warrendale, PA: Society of Automotive Engineers. SAE paper No. 720974.
- Cohen, B. J. 1979. Helmet-mounted displays: A computer assisted analysis of day-night visual requirements. Wright Patterson Air Force Base, OH: Aerospace Medical Research Laboratory. AMRL-TR-79-62.
- Coleman, H. S. 1947. Stray light in optical systems. Journal of the Optical Society of America, pp. 434-451.
- Conticelli, M., and Fujiwara, S. 1964. Visuo-motor reaction time under differential binocular adaptation. Atti Della Foundizione, Giorgio Ronchi.
- Cornsweet, T. N. 1970. Visual perception. New York: Academic Press.
- Cornum, R. L. S., Caldwell, J. L., and Ludwick, B. S. 1993. Factors influencing success or failure in the AH-64 course. Aviation, Space, and Environmental Medicine, Vol. 64, No. 12, pp.1120-1124.
- Craig, I. R., Marshall, A. A., and Jordan, C. S. 1997. Attitude symbology for helmet-mounted displays: lessons learned. Head-Mounted Displays II, Proceedings of SPIE, Vol. 3058, pp. 105-1114.
- Crane, D. F. 1980. The effects of time delay in man-machine control systems: Implementations for design of flight simulator-display-delay compensation. Williams AFB, AZ: Air Force Human Resources Laboratory. Proceedings of the Image III Conference, pp. 331-343.
- Crane, H. D. 1994. The Purkinje image eye tracker, image stabilization, and related forms of stimulus manipulation. Visual Science and Engineering: Models and Applications. New York: Dekke, pp. 15-89.
- Critchley, B. R., Blaxtan, P. W., Eckersley, B., Gale, R. O., and Burton, M. 1995. Picture quality in large-screen projectors using the digital micromirror device. SID Journal, Vol. XXVI, pp. 524-527.
- Crook, M. N., Hanson, J. A., and Weisz, A. 1954. Legibility of type as a function of stroke width, letter width, and letter spacing under low illumination. Dayton, Ohio: U.S. Air Force. WADC Technical Report 53-440.
- Crookes, T. G. 1957. Television images. Nature, V. 179, pp. 1014-1025.
- Crowley, J. S. 1991. Human factors of night vision devices: Anecdotes from the field concerning visual illusions and other effects. Fort Rucker, AL: U.S. Army Aeromedical Research Laboratory. USAARL Report No. 91-15.
- Crowley, J. S., Haworth, L., Szoboszlay, Z., and Lee, A. 1997. Helicopter pilot estimation of self-altitude in a degraded visual environment. Presented at the Aerospace Medical Association Annual Scientific Meeting, Atlanta, GA.
- CuQlock-Knopp, V. G., Sipes, D. E., Torgerson, W., Bender, E., Merritt, J. O., McLean, W., and Myles, K. 1997. Extended use of night vision goggles: An evaluation of comfort for monocular

and biocular configurations. Aberdeen Proving Ground, MD: U.S. Army Research Laboratory. Report No. ARL-TR-1427.

Davidoff, J. 1991. Cognition through color. Cambridge, MA: The MIT Press.

Defense Supply Agency. 1962. Military standardization handbook 141, optical design. Washington, DC: Defense Supply Agency.

DeMars, S. A. 1975. Human factors considerations for the use of color in display systems. Cape Kennedy, FL: NASA. NASA TR-1329.

Department of the Army. 1988. Night flight techniques and procedures. Washington, DC: Department of the Army. TC1-204.

Department of the Army. 1985. System safety engineering and management. Washington, DC: Department of the Army. AR 385-16.

Department of the Army. 1983. Health hazard assessment program in support of the Army materiel acquisition decision. Washington, DC: Department of the Army. AR 40-10.

Department of Defense. 1981. Military standard: Human engineering design criteria for military systems, equipment, and facilities. Washington, DC: Department of Defense. MIL-STD-1472C.

Department of Defense. 1984. System safety program requirements. Washington, DC: Department of the Army. MIL-STD-882B.

Department of Defense. 1984. V50 ballistic test for armor. Washington, DC: Department of the Army MIL-STD-662D.

Department of Defense. 1986. Seat system: Crashworthy, nonejection, aircrew, general specification for. Washington, DC: Department of Defense. MIL-S-58095(AV).

Department of Defense. 1989. Military specification: Aviator's Night Vision Imaging System AN/AVS-6(V)1, AN/AVS-6(V)2. Washington, DC: Department of Defense. MIL-A-49425 (CR).

Department of Defense. 1990. Visors, flyer's helmet, polycarbonate. Washington, DC: Department of Defense. MIL-V-43511C.

Department of Defense. 1991. Hearing conservation. Washington DC: Department of the Army. DA PAM 40-501

Department of Defense. 1991. Hearing conservation program. Washington, DC: Department of Defense. DOD Instruction 6055.12, 26 Mar 91.

Desjardins, S. P., Zimmermann, R. E., Bolukbasi, A. O., and Merritt, N. A. 1989. Volume IV - Aircraft seats, restraints, litters, and cockpit/cabin de-lethalization. Fort Eustis, VA: Aviation Applied Technology Directorate. USAAVSCOM TR 89-D-22D.

- DeVilbiss, C. A., Ercoline, W. R., and Antonio, J. C. 1994. Visual performance with night vision goggles (NVGs) measured in U.S. Air Force aircrew members. Helmet- and Head-Mounted Displays and Symbology Design Requirements, Proceedings of SPIE, Vol. 2218, pp. 64-70.
- Dobbins, J. P. 1974. Variable-transmittance visor for helmet-mounted display. Wright-Patterson AFB, OH: Aerospace Medical Research Laboratory. AMRL-TR-74-28.
- Donelson, S. M., and Gordon, C. C. 1991. 1988 Anthropometric survey of U.S. Army personnel: Pilot summary statistics. Natick, MA: U.S. Army Natick Research, Development, and Engineering Center. Technical report No. TR-91/040.
- Drewery, C. C., Davy, H. J., and Dudfield, H. J. 1997. Evaluation of a methodology to develop future helmet-mounted display symbology. Head-Mounted Displays II, Proceedings of SPIE, Vol. 3058, pp. 97-104.
- Droessler, J. G., and Rotier, D. J. 1989. Tilted Cat helmet mounted display. Head-Mounted Displays, Proceedings of SPIE, Volume 1116, pp. 19-26.
- Dudfield, H. J. 1991. Colour head-up displays: help or hindrance? Proceedings of the Human Factors Society 35th Annual Meeting.
- Durnford S.J., DeRoche S., Harper J., Trudeau L.A. 1996. Spatial disorientation: A survey of U.S. Army rotary-wing aircrew. Fort Rucker, AL: U.S. Army Aeromedical Research Laboratory. USAARL Report No. 96-16.
- Edgar, G. K., Carr, K. T., Williams, M., and Clark, A. L. 1991. The effect upon visual performance of varying binocular overlap. AGARD Proceedings 517, pp. 8-1 to 8-15.
- Edwards, K. L., Buckle, J. w., Dotherty, M. J., Lee, L. J., Pratty, A. C., and White, J. F. 1997. An operationally-applicable objective method for the analysis and evaluation of the flights of helicopter mission task elements during field-of-view trials. Head-Mounted Displays II, Proceedings of SPIE, Vol. 3058, pp. 235-251.
- Eggleston, R. G. 1997. User-centered design in the trenches: Head-mounted display system design and user performance. Head mounted displays: Designing for the user. New York: McGraw-Hill. p. 17-54.
- Electronic Industries Association (EIA) Tube Engineering Advisory Council (TEPAC). 1980. Optical characteristics of cathode ray tube screens. Washington, D.C.: Electronic Industries Association. TEPAC Publication No. 116.
- Ewing, C. L., Thomas, D. J., Sances, A., Jr., and Larson, S. J. 1983. Impact injury of the head and spine. Springfield, IL: C. C. Thomas.
- Farrell, R. J., and Booth, J. M. 1984. Design handbook for imagery interpretation equipment. Seattle: Boeing Aerospace Company.
- Feltz, J. C. 1990. Development of the modulation transfer function and contrast transfer function for discrete systems, particularly charge-coupled devices. Optical Engineering, Vol. 29, No. 8, pp. 893-904.

- Fernie, A. 1995. Helmet-mounted display with dual resolution. SID Digest of Application Papers, Vol. XXVI, pp. 37-40.
- Ferrin, F. J. 1997. Selecting new miniature display technologies for head mounted applications. Head-Mounted Displays II, Proceedings of SPIE, Vol. 3058, p. 115-124.
- Fischer, R. E. 1997. Fundamentals of HMD optics. Head mounted displays: Designing for the user. New York: McGraw-Hill, pp. 83-116.
- Foyle, D. C. and Kaiser, M. K. 1991. Pilot distance estimation with unaided vision, night-vision goggles, and infrared imagery. SID International Symposium Digest of Technical Papers, XXII, pp. 314-317.
- Foret-Bruno, J. Y., Tarriere, C., LeCoz, J. Y., Got, C., and Guillon, F. 1990. Risk of cervical lesions in real world and simulated collisions. 34th annual proceedings of the Association for the advancement of automotive medicine, pp. 373-389.
- Furness, T. A. 1981. The effects of whole-body vibration on the perception of the helmet-mounted display, Unpublished Doctoral Thesis, University of South Hampton.
- Genco, L. V. 1983. Optical interactions of aircraft windscreens and HUDs producing diplopia. Wright-Patterson, AFB: Air Force Aerospace Medical Research Laboratory. AFAMRL-TR-83-095.
- Gillingham, K. K., and Wolf, J. W. 1985. Spatial orientation in flight. Fundamentals of aerospace medicine. Philadelphia: Lea and Febiger.
- Giri, R. 1995. Field emitter display (FED) technology. Cockpit Displays II, Proceedings of SPIE, Vol. 2462, pp.67-74.
- Girolamo, H. J., Rash, C. E., and Gilroy, T. D. 1997. Advanced information displays for the 21st-century warrior. Information Display, Vol. 13, No. 3, pp. 10-17.
- Glick, D. D., and Moser, C. E. 1974. Afterimages associated with using the AN/PVS-5, night vision goggle. Fort Rucker, AL: U.S. Army Aeromedical Research Laboratory. USAARL LR 75-1-7-1.
- Godfrey, G. W. 1982. Principles of display illumination techniques for aerospace vehicle crew stations. Aerospace Lighting Institute: Tampa, FL
- Gold, T. 1971. Visual disparity tolerances for head-up displays. Electro-Optical System Design Conference, Anaheim, CA.
- Gold, T., and Hyman, A. 1970. Visual requirements for head-up displays, final report, Phase I. Washington, DC: Office of Naval Research. JANAIR Report 680712.
- Gray, H. 1993. The field emitter display. Information Display, Vol. 9, No. 3, pp. 9-14.
- Greene, D. A. 1988. Night vision pilotage system field-of-view (FOV)/resolution tradeoff study flight experiment report. Fort Belvoir, VA: U.S. Army Night Vision Laboratory. NV 1-26.

- Hale, S., and Piccione, D. 1990. Pilot performance assessment of the AH-64 helmet display unit. Aberdeen Proving Ground, MD: U.S. Army Human Engineering Laboratory. Technical Note 1-90.
- Harding, T. H., Beasley, H. H., Martin, J. S., and Rash, C. E. 1998. Optical and biodynamic evaluation of the Helmet Integrated Display Sight System (HIDSS) for the RAH-66 Comanche development and validation program phase. Fort Rucker, AL: U.S. Army Aeromedical Research Laboratory. In preparation.
- Harding, T. H., Beasley, H. H., Martin, J. S., and Rash, C. E. 1995. Physical evaluation of the Integrated Hemet and Display Sighting System (IHADSS) helmet display unit (HDU). Fort Rucker, AL: U.S. Army Aeromedical Research Laboratory. USAARL Report No. 95-32.
- Harding, T. H., Martin, J. S., Beasley, H. H., and Rash, C. E. 1996a. Figures of merit and performance specifications for the IHADSS and ANVIS. Fort Rucker, AL: U.S. Army Aeromedical Research Laboratory. USAARL Report No. 96-13.
- Harding, T. H., Martin, J. S., Beasley, H. H., and Rash, C. E. 1997. A visual evaluation near the threshold of acuity of five color liquid-crystal flat-panel displays. Fort Rucker, AL: U.S. Army Aeromedical Research Laboratory. USAARL Report No. 97-29.
- Harding, T. H., Martin, J. S., Beasley, H. H., Rash, C. E., and Garrard, J. A. 1996b. A survey of flat panel technologies. Fort Rucker, AL: U.S. Army Aeromedical Research Laboratory. USAARL Report No. 96-19.
- Hart, S. G. 1988. Helicopter human factors. Human factors in aviation. San Diego, CA: Academic Press, pp. 591-638.
- Hart, S. G., and Brickner, M. S. 1989. Helmet-mounted pilot night vision systems: Human factors issues. Spatial Displays and Spatial Instruments. Moffett Field, CA: NASA
- Harvey, L. O. 1970. Survey of visual research literature on military problems during World War II. Arlington, VA: Institute for Defense Analysis.
- Haworth, L. A. 16 Dec 97. Conversation (telephone communication) concerning roll compensation, Aeroflightdynamics Directorate, Ames Research Center, Moffett Field, CA.
- Haworth, L. A., Szoboszlay, Z. P., Kasper, E. F., DeMaio, J., and Halmos, Z. L. 1996. In-flight simulation of visionic field-of-view restrictions on rotorcraft pilot's workload, performance and visual cuing. 52nd Annual Forum of the American Helicopter Society, Washington, DC.
- Hearon, B. F., and Brinkley, J. W. 1985. Psychomotor performance after forward-facing impact. Aviation, space, and environmental medicine, Vol. 56, No. 11, pp. 1043-1051.
- Hericks, J., Parise, M., and Wier, J. 1996. Breaking down the barriers of cockpit metal in magnetic head tracking. Head-Mounted Displays, Proceedings of SPIE, Vol. 2735, pp.150-155.
- Hershberger, M. L., and Guerin, D. F. 1975. Binocular rivalry in helmet-mounted display applications. Dayton, OH: Armstrong Aerospace Medical Research Laboratory. AMRL-TR-75-48.

- Hettinger, L. J., and Riccio, G. E. 1992. Visually induced motion sickness in virtual environments. Presence, Vol. 1, No. 3, pp. 306-310.
- Hines, R. H., Palmer, R. W., Haley, J. L., and Hiltz, E. E. 1990. Development of an improved SPH-4 retention assembly. Fort Rucker, AL: U.S. Army Aeromedical Research Laboratory. USAARL Report No. 90-9.
- Home, R. 1984. Binocular summation: A study of contrast sensitivity, visual acuity, and recognition. Vision Research, Vol. 18, pp. 579-585.
- Hopper, D. G., Dolezal, W. K., Schur, K., and Liccione, J. W. 1994. Draft standard for color AMLCDs in U.S. military aircraft. Cockpit Displays, Proceedings of SPIE, Vol. 2219, pp.230-241.
- Human Factors Society, Inc. 1988. American National Standard for Human Factors Engineering of Visual Display Terminal Workstations. ANSI/HFS 100-1988. Santa Monica, CA: Human Factors Society, Inc.
- Illuminating Engineering Society (IES) of North America. 1984. IES Lighting Handbook. New York: Illuminating Engineering Society of North America.
- Imbeau, D., Wierwille, W. W., Wolf, L. D., and Chun, G. A. 1989. Effects of instrument panel luminance and chromaticity on reading performance and preference in simulated driving. Human Factors, Vol. 31, No. 2, pp. 161-166.
- Infante, C. 1993. On the modulation transfer function of matrix displays. Journal of SID, Vol. 26, pp. 449-450.
- ISO. 1987. Ergonomics of office VDUs: Visual requirements. Geneva: International Organization for Standardization. Draft DP 9241, Part 3.
- Jacobs, D. H. 1943. Fundamentals of optical engineering. New York: McGraw-Hill. Pp. 211-213.
- Jiang, J. C. 1996. New flat type fluorescent lamp for military LCD backlight. Cockpit Displays III, Proceedings of SPIE, Vol. 2734, pp. 277-282.
- Johnston, R. S., and Willey, S. R. 1995. Development of a commercial retinal scanning display. Helmet- and Head-Mounted Displays and Symbology Design Requirements II, Proceedings of SPIE, Vol. 2465, pp. 2-13.
- Jones, S. K., and Jones, G. W., Zimmermann, S. M., Fowler, C. W., Prache, O., Blazewski, E. R. 1996. Field emitter displays for future high performance applications. Cockpit Displays III, Proceedings of SPIE, Vol. 2734, pp.66-74.
- Jones, S. K., and Jones, G. W. 1995. Field emitter displays for future avionics applications. Cockpit Displays II, Proceedings of SPIE, Vol. 2462, pp.57-65.
- Kaiser, P. K., Herzberg, P. A., and Boynton, R. M. 1971. Chromatic border distinctness and its relation to saturation. Vision Research, Vol. 11, pp. 953.

- Kalawsky, R.S. 1993. The science of virtual reality and virtual environments. Wokingham, England: Addison-Welsey.
- Kalmanask, M., and Sundaresan, G. 1996. Dual backlighting system for avionic AMLCDs. Cockpit Displays III, Proceedings of SPIE, Vol. 2734, pp. 270-276.
- Kanahele, D. L., and Buckanin, B. 1996. CONDOR advanced visionics system. Helmet-Mounted Displays, Proceedings of SPIE, Vol. 2735, pp.192-202.
- Karim, M. A. 1992. Electro-optical displays. New York: Marcel Dekker.
- Kasper, E. F., Haworth, L. A., Szoboszlay, Z. P., King, R. D., and Halmos, Z. L. 1997. Effects of in-flight field of view restriction on rotorcraft pilot head movement. Head-Mounted Displays II, Proceedings of SPIE, Vol. 3058, pp. 34-45.
- Kaufman, L. 1963. On the spread of suppression and binocular rivalry. Vision Research, Vol. 3, pp. 401-415.
- Kenyon, R. V., and Kneller, E. W. 1992. Human performance and field of view. Proceedings of SID, Vol. XXIII, pp. 290-293.
- Kimberly, J. and Mueck, S. 1992. Integrated helmet display system (INVIS) flight assessment. Fort Belvoir, VA: Airborne Electronics Research Detachment. Report No. NV-1-92.
- King, P. 1995. Integration of helmet-mounted displays into tactical aircraft. Proceedings of SID, Vol. XXVI, pp. 663-668.
- King, J. M., and Morse, S. E. 1992. Interpupillary and vertex distance effects on field-of-view and acuity with ANVIS. Fort Rucker, AL: U.S. Army Aeromedical Research Laboratory. USAARL Report No. 93-9.
- Kingslake, R. 1983. Optical system design. New York: Academic Press. p.9, 178.
- Klymenko, V., Harding, T. H., Martin, J. S., Beasley, H. H., and Rash, C. E. 1997. Image quality figures of merit for contrast in CRT and flat panel displays. Fort Rucker, AL: U.S. Army Aeromedical Research Laboratory. USAARL Report No. 97-17.
- Klymenko, V., Verona, R. W., Beasley, H. H., Martin, J. S., and McLean, W. E. 1994a. Factors affecting the visual fragmentation of the field-of-view in partial binocular overlap displays. Fort Rucker, AL: U.S. Army Aeromedical Research Laboratory. USAARL Report No. 94-29.
- Klymenko, V., Verona, R. W., Beasley, H. H., Martin, J. S., and McLean, W. E. 1994b. Visual perception in the field-of-view of partial binocular overlap helmet-mounted displays. Fort Rucker, AL: U.S. Army Aeromedical Research Laboratory. USAARL Report No. 94-40.
- Klymenko, V., Verona, R. W., Martin, J. S., Beasley, H. H., and McLean, W. E. 1994c. The effects of binocular overlap mode on contrast thresholds across the field-of-view as a function of spatial and temporal frequency. Fort Rucker, AL: U.S. Army Aeromedical Research Laboratory. USAARL Report No. 94-49.

- Klymenko, V., Verona, R. W., Martin, J. S., Beasley, H. H., and McLean, W. E. 1994d. Factors affecting the perception of luning in monocular regions of partial binocular overlap displays. Fort Rucker, AL: U.S. Army Aeromedical Research Laboratory. USAARL Report No. 94-47.
- Kollin, J. 1993. A retinal display for virtual-environment applications. SID Proceedings, Vol. XXIV, p. 827.
- Kotulak, J. C. 1992. In-flight field-of-view with ANVIS. Fort Rucker, AL: U.S. Army Aeromedical Research Laboratory. USAARL Report No. 93-8.
- Kotulak, J. C., and Morse, S. E. 1994a. Factors that determine visual acuity through night vision goggles for emmetropes. Fort Rucker, AL: U.S. Army Aeromedical Research Laboratory. USAARL Report No. 94-16.
- Kotulak, J. C., and Morse, S. E. 1994b. Relationship among accommodation, focus and resolution with optical instruments. Journal of the Optical Society of America, Vol. II, pp. 71-79.
- Kotulak, J. C., and Rash, C. E. 1992. Visual acuity with second and third generation night vision goggles obtained from a new method of night sky simulation across a wide range of target contrasts. Fort Rucker, AL: U.S. Army Aeromedical Research Laboratory. USAARL Report No. 92-9.
- Krieg, J. C., Rodgers, A. G., Jones, H. R., and Schneider, M. R. 1992. A 4-msec low-latency 120-Hz electromagnetic tracker for virtual reality applications. Proceedings of SID, Vol. XXIII, pp. 77-79.
- Kruk, R., and Longridge, T. M. 1984. Binocular overlap in a fiber optic helmet-mounted display. Proceedings of Image 3, Vol. 363, pp. 363-377.
- Landau, F. 1990. The effect of visual recognition performance of misregistration and overlap for a binocular helmet mounted display. Helmet-Mounted Displays II, Proceedings of SPIE, Vol. 1290, pp. 173-184.
- Larder, D. R., Twiss, M. K., and MacKay, G. M. 1985. Neck injury in car occupants using seat belts. American association for the advancement of automotive medicine. Des Plaines, IL: AAAM. Pp. 153-168.
- Larson, W.L. 1985. Does the Howard-Dolman really measure stereoacuity? American Journal of Optometry and Physiological Optics, Vol. 62, pp. 763-767.
- Lattimore, M. R. 1990. Military aviation: A contact lens review. Aviation, Space , and Environmental Medicine, Vol. 59, No. 2, pp.125-128.
- Lattimore, M. R., and Cornum, R. L. 1992. The use of extended wear contact lenses in the aviation environment. Fort Rucker, AL: U.S. Army Aeromedical Research Laboratory. USAARL Report No. 92-35.
- Laycock, J., and Chorley, R. A. 1980. The electro-optical display/visual system interface: Human factors considerations. Advancements on Visualization Techniques, AGARD, pp. 3/1- 3/15.

- Lehrer, N. H. 1985. The challenge of the cathode-ray tube. Flat-panel displays and CRTs, Tannas, L. E. New York: Van Nostrand Reinhold. pp. 138-176.
- Leibrecht, B. C. 1990. Health hazard assessment primer. Fort Rucker, AL: U.S. Army Aeromedical Research Laboratory. USAARL Report No. 90-5.
- Leroux, T. 1989. Response time of active-matrix LCDs. Proceedings 9th International Display Research Conference, pp. 416-419.
- Levi, L. 1968. Applied optics. New York: John Wiley and Sons. Vol. 1, pp. 394-395.
- Levinsohn, R., and Mason, R. 1997. Advances in helmet mounted display technology. Head-Mounted Displays II, Proceedings of SPIE, Vol. 3058, pp. 219-230.
- Lewis, J. G. 1979. Helmet mounted display and sight system. Proceedings of the 35th Annual National Forum of the American Helicopter Society. Pp. 79-17-1 to 79-17-13.
- Lewis, C. H., and Griffin, M., J. 1979. The effect of character size on the legibility of a number display during whole-body vibration. Journal of Sound Vibration, Vol. 67, pp. 562-565.
- Lippert, T. M. 1990. Fundamental monocular/binocular HMD human factors. Helmet-Mounted Displays II, Proceedings of SPIE, Vol. 1290, pp. 185-191.
- Lippert, T. M. 1986. Color-difference predictions of legibility performance for CRT raster imagery. Society of Information Display Digest, pp. 86-89.
- Lohmann, R. A. and Weisz, A. Z. 1989. Helmet-Mounted Displays for helicopter pilotage: design configurations tradeoffs, analysis, and test. Helmet-Mounted Displays, Proceedings of SPIE, Vol. 1116, pp. 27-32.
- Lovasik, J. V., Matthews, M. L., and Kergoat, H. 1989. Neural, optical, and search performance in prolonged viewing of chromatic displays. Human Factors, Vol. 31, No. 3, pp. 273-289.
- MacMillan, R. T., Brown, R. W., and Wiley, L. L. 1995. Safety of flight testing for advanced fighter helmets. Helmet- and Head-Mounted Displays and Symbology Design Requirements II, Proceedings of SPIE, Vol. 2465, pp. 122-129.
- Markey, W. P. 1988. Preliminary findings - Night vision goggle distortion measurements and specifications. Fort Belvoir, VA: Center for Night Vision and Electro-Optics. Memorandum for record.
- Marshall, G. F. 1989. The helmet integrated system of Albert Bacon Pratt (1916). Helmet-Mounted Displays, Proceedings of SPIE, Vol. 1116, pp. 2-11.
- Marticello, D. N., and Hopper, D. G. 1996. Insertion of field emission displays into high performance cockpits. Cockpit Displays III, Proceedings of SPIE, Vol. 2734, pp. 32-37.
- Masterman, H., Johnson, C., Silverstein, M. F. 1990. How to Select a CRT Monitor. Medfield, MA: Beta Review, Inc.
- McElhanney, J. H. 1993. Biomechanical aspects of cervical trauma. Accidental injury: Biomechanics and prevention. New York, NY: Springer-Verlag.

- McKinley, R. L., Erickson, M. A., D'Angelo, W. R. 1994. 3-Dimensional auditory displays: development, applications, and performance. Aviation, Space, and Environmental Medicine. Vol.67, No. 11. May 1994. 65(5, Suppl.): A31-8.
- McLean, W. E. 1990. Eye dominance tests and PNVS training. Unpublished data.
- McLean, W. E. 1995. Video method of measuring field-of-view of electro-optical devices versus eye clearance. Fort Rucker, AL: U.S. Army Aeromedical Research Laboratory. USAARL Report No. 95-30.
- McLean, W. E. 1996. ANVIS objective lens depth of field. Fort Rucker, AL: U.S. Army Aeromedical Research Laboratory. USAARL Report No. 96-17.
- McLean, W. E. 1997. An assessment of luminance imbalance with ANVIS at an Army helicopter training airfield. Fort Rucker, AL: U.S. Army Aeromedical Research Laboratory. USAARL Report No. 97-21.
- McLean, W. E., and Rash, C. E. 1984. The effect of modified spectacles on the field of view of the helmet display unit of the Integrated Helmet and Display Sighting System. Fort Rucker, AL: U.S. Army Aeromedical Research Laboratory. USAARL Report No. 84-12.
- McLean, W. E., and Rash, C. E. 1985. U.S. Army aviation concept evaluation of the PLZT nuclear flashblindness protective goggles. Fort Rucker, AL: U.S. Army Aeromedical Research Laboratory. USAARL LR-85-11-2-7.
- McLean, W. E., Rash, C. E., McEntire, J., Braithwaite, M. G., and Mora, J. C. 1997. A performance history of AN/PVS-5 and ANVIS image intensification systems in U.S. Army aviation. Helmet- and Head-Mounted Displays II, Proceedings of SPIE, Vol.3058, pp.264- 298.
- McLean, W. E., and Smith, S. 1987. Developing a wide field of view HMD for simulators. Display System Optics, Proceedings of SPIE, Vol. 778, pp. 79-82.
- McMillan, G. 1995. Brain-actuated control: Thinking ahead to "Firefox." CSERIAC Gateway, Vol. VI, No. 5, pp. 8-9.
- Melvin, J. W., and Alem, N. M. 1985. Analysis of impact data from a series of UH-60 "Black Hawk" pilot seat tests. Columbus, OH: Battelle Columbus Laboratories, Contract No. DAAG29-81-D-0100.
- Melzer, J. E. and Larkin, E. W. 1987. An integrated approach to helmet display system design. Display System Optics, Proceedings of SPIE, Vol. 778, pp. 83-88.
- Melzer, J. E., and Moffitt, K. 1989. Partial binocular-overlap in helmet-mounted displays. Display System Optics II, Proceedings of SPIE, Vol.1117, pp. 56-62.
- Melzer, J. E., and Moffitt, K. 1997. Head mounted displays: Designing for the user. New York: McGraw-Hill.
- Mertz, H. J. 1993. Anthropomorphic test devices. Accidental Injury: Biomechanics and prevention. New York, NY: Springer-Verlag.

- Michael, P. R., Jardine, T. E., and Goom, M. K. 1978. Visual effects of helicopter manoeuvre on weapon aiming performance. Operational Helicopter Aviation Medicine, AGARD, pp. 25/1-25/15.
- Moffitt, K. 1991. HDU image focus and visual accommodation. San Jose, CA: Kaiser Electronics. Position paper, dated 7 Oct 1991.
- Moffitt, K. 1997. Designing HMDs for viewing comfort. Head mounted displays: Designing for the user. New York: McGraw-Hill. pp. 117-145.
- Moffitt, K., Rogers, S. P., and Cicinelli, J. 1988. Chromatic aftereffects associated with a night vision goggle simulation. Aviation, Space, and Environmental Medicine, Vol. 59, No. 2, pp.125-128.
- Mon-Williams, M., Wann, J. P., and Rushton, S. 1995. Design factors in stereoscopic virtual-reality displays. Journal of SID, Vol. 3, No. 4, pp. 207-210.
- Morse, S. E. and Reese, M. A. 1997. The use of bifocal soft contact lenses in the Fort Rucker aviation environment. Ft. Rucker, AL: U.S. Army Aeromedical Research Laboratory. USAARL Report No. 97-27.
- Mozo, B. T., and Murphy, B. A. 1997b. The assessment of sound attenuation and speech intelligibility of selected active noise reduction devices and the communications earplug when used with the HGU-56/P aviator helmet. Fort Rucker, AL: U.S. Army Aeromedical Research Laboratory. USAARL Report No. 97-08.
- Mozo, B. T., and Murphy, B. A. 1997a. Evaluation of the communications earplug in the H-53 and CH-46 helicopter environments. Fort Rucker, AL: U.S. Army Aeromedical Research Laboratory. USAARL Report No. 97-36.
- Mozo, B. T., Murphy, B. A., and Ribera, J. E. 1995. User acceptability and comfort of the Communications Earplug (CEP) when used in the UH-1 helicopter. Fort Rucker, AL: U.S. Army Aeromedical Research Laboratory. USAARL Report No. 95-17.
- Murray, J. 1997. Content and media analysis for intelligent helmet-mounted displays. Head-Mounted Displays II, Proceedings of SPIE, Vol. 3058, pp. 86-96.
- Murry, H. F. 1995. Recent advances in AC magnetic helmet tracking. Proceedings of SID, Vol. XXVI, pp. 655-662.
- Nakamura, T., and Mohri, J. 1995. New materials realize color VFD tubes, expand horizons. Journal of Electronic Engineering, Vol. 32, No. 348, pp. 23-25.
- Naor, D., Arnon, O. and Avnur, A. 1987. A lightweight innovative helmet airborne display and sight (HADAS). Display System Optics, Proceedings of SPIE, Vol. 778, pp. 89-95.
- National Research Council. 1997. Tactical display for soldiers: Human factors considerations. Washington, DC: National Academy Press.
- Neary, C., Bate, I. J., Heller, L. F., and Williams, M. 1993. Helmet slippage during visual tracking: The effect of voluntary head movements. Aviation, Space, and Environmental Medicine, Vol. 64, No. 7, pp.623-630.

- Nelson, S.A. May 1996. Personal communication concerning temporal issues of displays. Honeywell, Inc.
- Nelson, S.A. 1994. CVC HMD – next generation high-resolution head-mounted display. Helmet- and Head-Mounted Displays and Symbology Design Requirements, Proceedings of SPIE, Vol. 2218, pp. 7-16.
- Nelson, S. A., and Cox, J. A. 1992. Quantitative helmet mounted display system image quality model. Helmet-Mounted Displays III, Proceedings of SPIE, Vol. 1695, pp. 128-137.
- Nelson, W. T., Hettinger, L. J., Haas, M. W., Russell, C., Warm, J. S., Dember, W. N., and Stoffregen, T. A. 1995. Compensation for the effects of time delay in a helmet-mounted display: perceptual adaptation versus algorithmic prediction. Helmet- and Head-Mounted Displays and Symbology Design Requirements II, Proceedings of SPIE, Vol. 2465, pp. 154-164.
- Newby, H. A. 1972. Audiology. New York: Meredith Corporation. 3rd ed.
- Newman, R. L. 1995. Head-up displays: Designing the way ahead. Hants, England: Avebury Aviation.
- Newman, R. L., and Greeley, E. W. 1997. Integrating head-mounted displays into a cockpit. Head-Mounted Displays II, Proceedings of SPIE, Vol. 3058, pp. 46-56.
- Newman, R. L., and Haworth, L. A. 1994. Helmet-mounted display requirements: Just another HUD or a different animal altogether? Helmet- and Head-Mounted Displays and Symbology Design Requirements, Proceedings of SPIE, Vol. 2218, pp. 226-237.
- Nicholson, B., and Troxel, D. 1996. Update of the AN/AVS-7 head up display program. Helmet-Mounted Displays, Proceedings of SPIE, Vol. 2735, pp.215- 220.
- Onishi, S., Yoshimatsu, H., Kawamura, A., and Ashizaki, K. 1994. An approach to natural vision using a novel head-mounted display. Proceedings of SID, Vol. XXV, pp.28-31.
- Osgood, R. K., and Wells, M. J. 1991. The effects of field-of-view size on performance of a simulated air-to-ground night attack. Helmet mounted displays and night vision goggles, AGARD, Pensacola, FL.
- Palmer, R. W., and Haley, J. L. 1988. SPH-4 helmet retention assembly reinforcement. Fort Rucker, AL: U.S. Army Aeromedical Research Laboratory. USAARL Report No. 88-10.
- Pastoor, S. 1990. Legibility and subjective preference for color combinations in text. Human Factors, Vol. 32, No. 2, pp. 157-171.
- Patel, J. and Werner, K. 1992. Ferroelectric ready for prime time? Information Display, Vol. 8, No. 10, pp. 14-17.
- Perconti, P. 1997. Noise limited resolution of the Advanced Helicopter Pilotage helmet mounted display and image intensified camera. Head-Mounted Displays II, Proceedings of SPIE, Vol. 3058, pp. 254-263.

- Permobil Medtech, Inc. 1997. Comparison of some ways of measuring eye movements. Woburn, MA: Permobil Medtech, Inc. Technical Note TN 13.
- Peterson, W. D., King, B. C., and Hilgendorf, R. L. 1977. Single seat attack-night simulation study phase 1: Target detection/classification. Wright-Patterson AFB, OH: Air Force Aeronautical Systems Division. Report ASD-TR-77-30.
- Post, D. L. 1983. Color contrast metrics for complex images. Doctoral dissertation, Virginia Polytechnic Institute and State University, Blacksburg, VA.
- Post, D. L., Monnier, P., and Calhoun, C. S. 1997. Predicting color breakup on field-sequential displays. Head-Mounted Displays II, Proceedings of SPIE, Vol. 3058, pp. 57-65.
- Post, D. L., Sarma, K. R., Trimmier, J. r., Heinze, W. C., Rogers, J. C., Ellis, R. K., Larson, B. D., and Franklin, H. 1994. A new color display for head-mounted use. Journal of SID, Vol. 2, No. 4, pp. 155-163.
- Proctor, P. 1996. Retinal displays portend synthetic vision, HUD advances. Aviation Week and Space Technology, July 15, p. 58.
- Prohaska, A. M., and Nixon, C. W. 1984. Hearing protection and speech intelligibility of two nonstandard inflight communications headsets. Wright-Patterson AFB: Air Force Aerospace Medical Research Laboratory. AFAMRL-SR-84-504.
- Quast, T., and Marticello, D. N. 1996. Flat panel display test and evaluation for U.S. military applications. Cockpit Displays III, Proceedings of SPIE, Vol. 2734, pp. 305-310.
- Rabin, J. 1995. Two eyes are better than one: Binocular enhancement in the contrast domain. Ophthalmic and Physiological Optics, Vol., pp. 45-48.
- Rabin, J. 1996a. Comparison between green and orange visual displays. Journal of SID, Vol. 4, No, 2, pp. 107-110.
- Rabin, J. 1996b. Image contrast and visual acuity through night vision goggles. Fort Rucker, AL: U.S. Army Aeromedical Research Laboratory. USAARL Report No. 96-26.
- Rabin, J., and Wiley, R. W. 1995. Comparison between helmet-mounted CRTs and LCDs. Journal of SID, Vol. 3, No, 3, pp. 97-100.
- Rabin, J., and Wiley, R. W. 1994. Switching from forward-looking infrared to night vision goggles: Transitory effects on visual illusion. Aviation, Space , and Environmental Medicine, Vol. 65, No. 4, pp.327-329.
- Rash, C. E., and Becher, J. 1983. Preliminary model of dynamic information transfer in cathode-ray-tube displays. Proceedings of IEEE Southeastcon, pp. 166-168.
- Rash, C. E., and Becher, J. 1982. Analysis of image smear in CRT displays due to scan rate and phosphor persistence. Fort Rucker, AL: U.S. Army Aeromedical Research Laboratory. USAARL Report No. 83-5.

- Rash, C. E., Bohling, J. H., and Martin, J. S. 1991. Optical evaluation report: Laser protective visors. Gentex Corporation. Fort Rucker, AL: U.S. Army Aeromedical Research Laboratory. USAARL LR 91-9-2-9.
- Rash, C. E., and Martin, J. S. 1990. Optical evaluation report: AH-64 laser protective device verification testing. Fort Rucker, AL: U.S. Army Aeromedical Research Laboratory. USAARL LR 90-4-2-4.
- Rash, C. E., and Martin, J. S. 1988. The impact of the U.S. Army's AH-64 helmet mounted display on future aviation helmet design. Fort Rucker, AL: U.S. Army Aeromedical Research Laboratory. USAARL Report No. 88-13.
- Rash, C. E., and Martin, J. S. 1987a. A limited user evaluation of the Integrated Helmet and Display Sighting System. Fort Rucker, AL: U.S. Army Aeromedical Research Laboratory. USAARL Report No. 87-10.
- Rash, C. E., and Martin, J. S. 1987b. Effects of the M-43 chemical protective mask on the field-of view of the Integrated Helmet and Display Sighting System. Fort Rucker, AL: U.S. Army Aeromedical Research Laboratory. USAARL LR 87-10-2-5.
- Rash, C. E., and Martin, J. S., Gower, D. w., Licina, J. R., and Barson, J. V. 1987. Evaluation of the U.S. Army fitting program for the Integrated Helmet and Display Sighting System. Fort Rucker, AL: U.S. Army Aeromedical Research Laboratory. USAARL Report No. 87-8.
- Rash, C. E., and McLean, W. E. 1983. Visual and optical evaluations of the XM-40 protective mask. Fort Rucker, AL: U.S. Army Aeromedical Research Laboratory. USAARL LR-83-9-2-6.
- Rash, C. E., McLean, W. E., and Monroe, D. R. 1981. Effects of reduced combiner transmittance in the Integrated Helmet and Display Sighting System. Fort Rucker, AL: U.S. Army Aeromedical Research Laboratory. USAARL LR-81-1-2-1.
- Rash, C. E., Monroe, D. R., and Verona, R. W. 1981. Computer model for the evaluation of symbology contrast in the Integrated Helmet and Display Sighting System. Fort Rucker, AL: U.S. Army Aeromedical Research Laboratory. USAARL Report No. 81-6.
- Rash, C. E., Mora, J. C., Ledford, M. H., Reynolds, B. S., Ivey, R. H., and McGowan, E. 1997. Visor use among U.S. Army rotary-wing aviators. Fort Rucker, AL: U.S. Army Aeromedical Research Laboratory. USAARL Report No. 98-16.
- Rash, C. E., Mozo, B. T., McLean, W. E., McEntire, J. L., and Licina, J. R. 1996b. RAH-66 Comanche health hazard and performance issues for the Helmet Integrated Display and Sighting System. Fort Rucker, AL: U.S. Army Aeromedical Research Laboratory. USAARL Report No. 97-1.
- Rash, C. E., Mozo, B. T., McLean, W. E., McEntire, B. J., Haley, J. L., Licina, J. R., and Richardson, L. W. 1996a. Assessment methodology for integrated helmet and display systems in rotary-wing aircraft. Fort Rucker, AL: U.S. Army Aeromedical Research Laboratory. USAARL Report No. 96-1.
- Rash, C. E., and Verona, R. W. 1987. Temporal aspects of electro-optical imaging systems. Imaging Sensors and Displays II, Proceedings of SPIE, Vol. 765, pp. 22-25.

- Rash, C. E., Verona, R. W., and Crowley, J. S. 1990. Human factors and safety considerations of night vision systems flight using thermal imaging systems. Helmet-Mounted Displays II, Proceedings of SPIE, Vol. 1290, pp. 142-164.
- Reading, T. E., Haley, J. L., Sippo, A. C., Licina, J. K., and Shopper, A. W. 1984. SPH-4 U.S. Army flight helmet performance 1972-1983. Fort Rucker, AL: U.S. Army Aeromedical Research Laboratory. USAARL Report No. 85-1.
- Reinhart, W. F., and Post, D. L. 1996. Human factors of two-primary color AMLCDs. Head-mounted Displays, Proceedings of SPIE, Vol. 2735, pp. 105-114.
- Reynolds, B. S., Rash, C. E., Colthirst, P. M., Ledford, M .H., Mora, J. C., and Ivey, R. H. 1997. The role of protective visors in injury prevention during U.S. Army rotary-wing aviation accidents. Fort Rucker, AL: U.S. Army Aeromedical Research Laboratory. USAARL Report No. 98-18.
- Ribera, J. E., and Mozo, B. T. Undated. A comparison of three aviation helmet systems. Fort Rucker, AL: U.S. Army Aeromedical Research Laboratory. USAARL Draft Report.
- Robinson, R. M., and Wetzell, P. A. 1989. Eye tracker development in the fiber optic helmet mounted display. Helmet-Mounted Displays, Proceedings of SPIE, Vol. 1116, pp. 102-108.
- Rogers, S. P., Spiker, V. A., and Fisher, S. C. 1997. Head-Mounted Displays II, Proceedings of SPIE, Vol. 3058, pp. 14-23.
- Rotier, D. J. 1989. Optical approaches to the helmet mounted displays. Head-Mounted Displays, Proceedings of SPIE, Volume 1116, pp. 14-18.
- Sampsel, J. B. 1994. An overview of the performance envelop of digital micromirror device based projection display systems. Proceedings of SID, Vol. XXV, pp. 669-672.
- Sandor, P. B., and Leger, A. 1991. Tracking with a restricted field of view: Performance and eye-head coordination aspects. Aviation, Space , and Environmental Medicine, Vol. 66, No. 6, pp.1026-1031.
- Schall, D. G. 1989. Nonejection cervical spine injuries due to +G_z in high performance aircraft. Aviation, space, and environmental medicine. Washington, DC: Aerospace Medical Association. May 1989. Vol. 60, No. 5, p. 445.
- Schuchrad, R. A. 1990. Evaluation of uniform CRT display scales with visual threshold data. Applied Optics, Vol. 29, No. 4, pp. 570-578.
- Seeman, J., De Maio, J., Justice, S., Wasson, J., Derenski, P., Hunter, M., and Walrath, L. 1992. Advanced helicopter pilotage visual requirements. Proceedings of the American Helicopter Society, Vol. 48, pp. 233-252.
- Self, H. C. 1986. Optical tolerances for alignment and image differences for binocular helmet-mounted displays. Dayton, OH: Armstrong Aerospace Medical Research Laboratory. AAMRL-TR-86-019.
- Shanahan, D. F. 1985. Basilar skull fracture in U.S. Army Aircraft Accidents. Fort Rucker, AL: U.S. Army Aeromedical Research Laboratory. USAARL Report No. 85-11

- Shanahan, D. F., and Shanahan, M. O. 1989. Injury in U.S. Army helicopter crashes fiscal years October 1979-September 1985. Journal of trauma, Vol. 29, No. 4, pp. 415-423.
- Sheehy, J. B., and Wilkinson, M. 1989. Depth perception after prolonged usage of night vision goggles. Aviation, Space, and Environmental Medicine, Vol. 64, No. 6, pp.573-579.
- Shenker, M. 1987. Optical design criteria for binocular helmet-mounted displays. Display System Optics, Proceedings of SPIE, Vol. 778, pp. 70-78.
- Shirachi, D. K., Monk, D. L., and Black, J. H. 1978. Head rotational spectral characteristics during two-dimensional smooth pursuit tasks. IEEE Transactions on Systems, Man, and Cybernetics, SMC-8, pp. 715-724.
- Shontz, W. D., and Trumm, G. A. 1969. Perceptual processes and current helmet-mounted display concepts. Minneapolis, Minnesota: Honeywell Inc. Technical Note TN-1.
- Shurtleff, D. A., and Wuersch, W. F. 1979. Legibility criteria in design and selection of data displays for group viewing. Proceedings of the Human Factors Society 23rd Annual Meeting. Santa Monica, CA: Human Factors Society, Inc., pp. 411-414.
- Silverstein, M. F. 1989. How to Select a Flat Panel Display. Medfield, MA: Beta Review, Inc.
- Sippo, A. C., and Belyavin, 1991. Determining aircrew helmet size design requirements using statistical analysis of anthropometric data. Aviation, Space, and Environmental Medicine, Vol. 66, No. 1, pp. 67-74.
- Sippo, A. C., Licina, J. R., and Noehl, M. J. 1988. Anthropometric considerations of the U.S. Army IHADSS. Fort Rucker, AL: U.S. Army Aeromedical Research Laboratory. USAARL LR 88-10-4-06.
- Smith, W. J. 1990. Modern optical engineering, the design of optical systems. New York: McGraw-Hill, Inc.
- Snyder, H. L. 1980. Human visual performance and flat panel display image quality. Arlington, VA: Office of Naval Research. HFL-80-1/ONR-80-1.
- Snyder, H. L. 1985. Image quality: Measures and visual performance. Flat-Panel displays and CRTs. New York: Van Nostrand Reinhold, pp. 70-90.
- So, R. H. Y., and Griffin, M. J. 1995. Effects of lags on human operator transfer functions with head-coupled systems. Aviation, Space, and Environmental Medicine, Vol. 66, No. 6, pp.550-556.
- So, R. H. Y., and Griffin, M. J. 1992. Phase lead algorithms for head motion position prediction. Southampton, England: Institute of Sound and Vibration. Research Contract Report 92/06.
- Spengelink, G. P. J., and Besuijen, J. 1996. Chromaticity contrast, luminance contrast, and legibility of text. Journal of SID, Vol. 4, No. 3, pp. 135-144.
- Staton, R. N., Mozo, B. T., and Murphy, B. A. 1997. Operational test to evaluate the effectiveness of the communication earplug and active noise reduction devices when used with

- the HGU-56P aviator helmet. Fort Rucker, AL: U.S. Army Aeromedical Research Laboratory. USAARL Report No. 97-09.
- Stiffler, J. A., and Wiley, L. 1992. I-NIGHTS and beyond. Helmet Mounted Displays III, Proceedings of SPIE, Vol. 1695, pp. 13-20.
- Strauss, S. 1995. Cybersickness: The side effects of virtual reality. Technology Review, Vol. 98, No. 5, pp. 14-16.
- Tannas, L. T., ed. 1985. Flat-Panel displays and CRTs. New York: Van Nostrand Reinhold.
- Task, H. L. 1997. HMD image source, optics, and the visual interface. Head mounted displays: Designing for the user. New York: McGraw-Hill. p. 55-82.
- Task, L. T. 1979. An evaluation and comparison of several measures of image quality for television displays. Wright-Patterson AFB, OH: Aerospace Medical Research Laboratory. AMRL-TR-79-7.
- Task, H. L., and Gleason, G. 1993. Eyepiece focus for night vision goggles (NVGS) and helmet mounted displays: Fixed or adjustable? Wright-Patterson AFB, OH: Armstrong Laboratory. Preliminary report of two focus studies prepared for the Fall 1993 TARP Meeting.
- Task, L. T., Hartman, R. T., and Zobel, A. R. 1993. New methods for night vision goggle test and evaluation. Wright-Patterson AFB, OH: Armstrong Laboratory. AL/CF-TR-1993-0177.
- Task, H. L., and Kocian, D. F. 1995. Design and integration issues of visually-coupled systems (VCS). Wright-Patterson AFB, OH: Armstrong Laboratory. AL/CF-SR-1995-0004.
- Task, H. L., Kocian, D. F., and Brindle, J. H. 1980. Helmet mounted displays: Design considerations, Advancement on Visualization Techniques, AGARD, No. 255.
- Task, H. L., and Verona, R. W. 1976. A new measure of television display image quality relatable to observer performance. Wright-Patterson AFB, OH: Aerospace Medical Research Laboratory. AMRL-TR-76-73.
- Templin, P. S. 1978. Flyer's flash blindness goggles (EEU-2/P). Eglin AFB, FL: USAF Tactical Air Warfare Center.
- Thomas, R. M. 1989. Visually Coupled System Integration. Helmet-Mounted Displays, Proceedings of SPIE, Vol. 1116, pp. 33-36.
- Toyama, J., Akatsuka, T., Takano, S., Tadakuma, A., Mori, T., Suga, S., and Sano, Y. 1994. An electrophoretic matrix display with external logic and driver directly assembled to the panel. Proceedings of SID, Vol. XXV, pp. 588-90.
- Travis, D. S., Bowles, S., Seton, J., and Peppe, R. 1992. Reading from color displays: A psychophysical model. Human Factors, Vol. 32, No. 2, pp. 147-156.
- Tsou, B. H. 1993. System design considerations for a visually coupled system. Emerging Systems and Technologies, Vol. 8 of The Infrared and Electro-Optics Systems Handbook, pp. 515-540.

- U.S. Navy. 1966. Optical man 382. Washington, DC: U.S Navy. Navy Training Course NAV Pers 10205.
- Velger, M., Merhav, S., and Grunwald, A. 1986. Adaptive filtering of biodynamic stick feedthrough in manipulation tasks onboard moving platforms. New York: Institute of Aeronautics and Astronautics. AIAA Paper 86-2248CP.
- Venturino, M., and Wells, M. J. 1990. Head movements as a function of field-of-view size on a helmet-mounted display. Proceedings of the Human Factors Society 34th Annual Meeting. Santa Monica, CA: Human Factors Society, Inc., pp. 1572-1576.
- Verona, R. W. 1992. Comparison of CRT display measurement techniques. Helmet Mounted Displays III, Proceedings of SPIE, Vol. 1695, pp. 117-127.
- Verona, R. W., Beasley, H. H., Martin, J. S., Klymenko, V., and Rash, C. E. 1994. Dynamic sine wave response measurements of CRT displays using sinusoidal counterphase modulation. Helmet- and Head-Mounted Displays and Symbology Design Requirements, Proceedings of SPIE, Vol. 2218, pp. 105-118.
- Verona, R. W., Johnson, J. C., and Jones, H. 1979. Head aiming/tracking accuracy in a helicopter environment. Fort Rucker, AL: U.S. Army Aeromedical Research Laboratory. USAARL Report No. 79-9.
- Verona, R. W., and Rash C. E. 1989. Human factors and safety considerations of night vision imaging systems. Display System Optics II, Proceedings of SPIE, Vol.1117, pp. 2-12.
- Verona, R. W., Rash C. E., Holt, W. R., and Crosley, J. K. 1986. Head movements during contour flight. Fort Rucker, AL: U.S. Army Aeromedical Research Laboratory. USAARL Report No. 87-1.
- Verona, R. W., Task, H. L., Arnold, V. C., and Brindle, J. H. 1979. A direct measure of CRT image quality. Fort Rucker, AL: U.S. Army Aeromedical Research Laboratory. USAARL Report No. 79-14.
- Vollmerhausen, R. H., Nash, C. J., and Gillespie, J. B. 1988. Evaluation of pilotage sensors at Reforger '87.
- Vyrnwy-Jones, P. 1988. Disorientation accidents and incidents in U.S. Army helicopters, 1 Jan 1980 - 30 Apr 1987. Fort Rucker, AL: U.S. Army Aeromedical Research Laboratory. USAARL Report No. 98-3.
- Vyrnwy-Jones, P., Lanoue, B., and Pritts, D. 1988. SPH-4 U.S. Army flight helmet performance 1983-1987. Fort Rucker, AL: U.S. Army Aeromedical Research Laboratory. USAARL Report No. 88-15.
- Vos, G. D. and Brandt, G. 1990. Use of holographic optical elements in HMDs. Helmet Mounted Displays II, Proceedings of SPIE, Vol. 1290, pp. 70-80.
- Wagstaff, A. S., Tvette, O., and Ludvigsen, B. 1996. The effect of a headset leakage on speech intelligibility in helicopter noise. Aviation, Space, and Environmental Medicine. Vol.67, No. 11. November 1996.

- Walsh, M. J., and Kelleher, B. J. 1978. Evaluation of air cushion and belt restraint systems in identical crash situations using dummies and cadavers. Proceedings of the 22nd Stapp car crash conference. Warrendale, PA: Society of Automotive Engineers.
- Ward, D. 1992. Matching inverters to CCFT backlight. Information Display, Vol. 8, No. 2, pp. 15-17.
- Warszawski, B. 1993. Matrix addressing and driving in a new electrochemical display technology. Proceedings of SID, Vol. 24, pp.993-96.
- Webb, R. H., Hughes, G. W., and Delori, F.C. 1987. Confocal scanning laser ophthalmoscope. Applied Optics, Vol. 26, No. 8, pp. 1492-1499.
- Wells, M. H., and Griffin, M. J. 1984. Benefits of helmet-mounted display image stabilization under whole-body vibration. Aviation, Space, and Environmental Medicine, Vol. 55, pp. 13-18.
- Wells, M. H., and Griffin, M. J. 1987a. Flight trial of a helmet-mounted display image stabilization system. Aviation, Space, and Environmental Medicine, Vol. 58, pp. 319-322.
- Wells, M. H., and Griffin, M. J. 1987b. Performance with helmet-mounted sights. Institute of Sound and Vibration Research, Technical Report 152.
- Wells, M. H., and Griffin, M. J. 1987c. A review and investigation of aiming and tracking performance with head-mounted sights. IEEE Transactions on Systems, Man, and Cybernetics, SMC-17, pp. 210-221.
- Wells, M. H., and Haas, M. 1992. The human factors of helmet-mounted displays and sights. Electro-optical displays, M. Karim, Ed. New York: Marcel Dekker. p. 743-785.
- Wells, M. J., and Venturino, M. 1989. Head movements as a function of field-of-view size on a helmet-mounted display. Proceedings of the Human Factors Society 33rd Annual Meeting. Santa Monica, CA: Human Factors Society, Inc., pp. 91-95.
- Westerink, J. H. D. M. and Roufs, J. A. J. 1989. Subjective image quality as a function of viewing distance, resolution, and picture size. SMPTJ, 98:113-119.
- Whiteley, J. D., Lusk, S. L., and Middendorf, M. S. 1990. The effects of simulator time delays on a sidestep landing maneuver: A preliminary investigation. Santa Monica, CA: Human Factors Society. Proceedings of the Human Factors Society, Vol. 2, pp. 1538-1541.
- Whitestone, J. J. 1994. Improving total contact burn masks: Three-dimensional anthropometric imaging techniques. CSERIAC Gateway, Vol. V, No. 3, pp. 1-5.
- Widdel, H., and Post, D. L. 1992. Color in electronic displays. New York: Plenum Press.
- Wildjunas, R. M., Baron, T. L., Wiley, R. W. 1996. Visual display delay effects on pilot performance. Aviation, Space, and Environmental Medicine, Vol. 66, pp. 214-221.
- Wiley, R. W. 1989a. Visual acuity and stereopsis with night vision goggles. Fort Rucker, AL: U.S. Army Aeromedical Research Laboratory. USAARL Report No. 89-9.

- Wiley, R. W. 1989b. Unpublished data on visual acuity and tinted lenses. Fort Rucker, AL: U.S. Army Aeromedical Research Laboratory.
- Wiley, R. W., Glick, D. D., Bucha, C. T., and Park, C. K. 1976. Depth perception with the AN/PVS-5 Night Vision Goggle. Fort Rucker, AL: U.S. Army Aeromedical Research Laboratory. USAARL Report No. 76-25.
- Wilkinson, M., and Bradley, A. 1990. Night vision goggles: An analysis of dynamic range and visual performance for the unaided and night vision goggle-aided eye. Presented at the Fifth Annual Joint Service Night Vision Conference, St. Louis, MO.
- Wiener, E. L., and Nagel, D. C. 1988. Human Factors in Aviation. Academic Press, Inc.
- Wolpaw, J. R., and McFarland, D. J. 1994. Multichannel EEG-based brain-computer communication. Electroencephalography and Clinical Neurophysiology, Vol. 90, pp. 444-449.
- Wood, R. B. 1992. Holographic head-up displays. Electro-optical displays, M. Karim, Ed. New York: Marcel Dekker. p. 337-415.
- Worboys, M. R., Day, S. C. M., Foster, S. J., Radcliffe, S., Mitchell, K., Vass, D. G., and Underwood, I. 1994. Miniature display technologies for helmet and head mounted displays. Helmet- and Head-Mounted Displays and Symbology Design Requirements, Proceedings of SPIE, Vol. 2218, pp. 17-24.
- Yaniv, Zvi. 1995. Reflective cholesteric displays. Information Display, Vol. 11, No. 10, pp. 10-14.
- Zangemeister, W. H., and Stark, L. 1981. Active head rotations and eye-head coordinations. Annals of New York Academy of Sciences, Vol. 374, pp. 541-549.
- Zimmermann, R. E., Warrick, J. C., Lane, A. D., Merritt, N. A., and Bolukbasi, A. O., 1989. Volume III - Aircraft structural crash resistance. Fort Eustis, VA: Aviation Applied Technology Directorate. USAAVSCOM TR 89-D-22C.
- Zuckerman, J. 1954. Perimetry. Philadelphia: Lippincott.

Sample calculations for contrast figures of merit in an HMD design

For the HMD scenario depicted in Figure 11, assume a CRT (and optics) luminance of 800 fL and an ambient scene luminance of 3,000 fL. The 3000 fL passes through the aircraft canopy ($T_{\text{Canopy}} = 0.7$), the visor ($T_{\text{visor}} = 0.18$ or 0.85), the spherical combiner ($T_{\text{SpherCom}} = 0.7$), and the plano combiner ($T_{\text{PlanorCom}} = 0.6$). Therefore, the luminance reaching the eye from the outside ambient scene ($L_{\text{Ambient-Eye}}$) is

$$\begin{aligned} L_{\text{Ambien-Eye}} &= (3000 \text{ fL})(T_{\text{Canopy}})(T_{\text{visor}})(T_{\text{SpherCom}})(T_{\text{PlanorCom}}) \\ &= (3000 \text{ fL})(0.7)(0.18)(0.7)(0.6) \\ &= 159 \text{ fL for the shaded visor, and} \\ &= (3000 \text{ fL})(0.7)(0.85)(0.7)(0.6) \\ &= 750 \text{ fL for the clear visor.} \end{aligned}$$

The 800 fL CRT luminance reflects off the plano ($R_{\text{PlanoCom}} = 0.4$) and spherical ($R_{\text{planoCom}} = 0.7$) combiners and passes back through the plano combiner ($T_{\text{PlanorCom}} = 0.6$) to the eye. Therefore, the luminance from the CRT reaching the eye ($L_{\text{CRT-Eye}}$) is

$$\begin{aligned} (L_{\text{CRT-Eye}}) &= (800 \text{ fL})(R_{\text{PlanoCom}})(R_{\text{planoCom}})(T_{\text{PlanorCom}}) \\ &= (800 \text{ fL})(0.4)(0.7)(0.6) \\ &= 134 \text{ fL.} \end{aligned}$$

Since the luminance reaching the eye is a summation of light originating from both the ambient scene and the CRT, then for the purpose of the calculations, the target luminance is the sum of 750 fL and 134 fL for a total of 884 fL when using the clear visor, and the sum of 159 fL and 134 fL for a total of 293 fL when using the shaded visor. For the clear visor, the background luminance is 750 fL. For the shaded visor, the background luminance is 159 fL.

Michelson contrast

Michelson contrast is defined as follows

$$C_m = (L_{\text{max}} - L_{\text{min}}) / (L_{\text{max}} + L_{\text{min}}) \quad (\text{Modulation contrast}) \quad \text{Equation 6a}$$

$$= |(L_t - L_b)| / (L_t + L_b) \quad \text{Equation 6b}$$

For the values above,

$$\begin{aligned} C_m &= |(L_t - L_b)| / (L_t + L_b) \\ &= (884 - 750) / (884 + 750) \\ &= 134 / 1634 \\ &= 0.08 \text{ for the clear visor,} \end{aligned}$$

and

$$\begin{aligned} &= (293 - 159) / (293 + 159) \\ &= 134 / 452 \\ &= 0.3 \text{ for the shaded visor.} \end{aligned}$$

Contrast ratio

Contrast ratio is defined as follows

$$C_r = L_t / L_b \quad \text{for } L_t > L_b \quad (\text{Contrast ratio}) \quad \text{Equation 5a}$$

$$= L_{\max} / L_{\min} \quad \text{Equation 5c}$$

For the values above,

$$\begin{aligned} C_r &= 884/750 \\ &= 1.17 \text{ for the clear visor, and} \\ &= 293/159 \\ &= 1.84 \text{ for the shaded visor.} \end{aligned}$$

Shades of grey

Number of shades of grey is defined as follows:

$$\text{Number of SOG} = [\log(C_r) / \log(\sqrt{2})] + 1 \quad \text{Equation 12}$$

For the values above,

$$\begin{aligned} \text{SOG} &= [\log(1.17) / 0.15] + 1 \\ &= 0.45 + 1 \\ &= 1.45 \text{ for the clear visor, and} \end{aligned}$$

$$\begin{aligned} \text{SOG} &= [\log(1.84) / 0.15] + 1 \\ &= 0.1.76 + 1 \\ &= 2.76 \text{ for the shaded visor.} \end{aligned}$$